Durham University

Durham E-Theses

Identification and molecular characterisation of chemotaxis genes in agrobacterium tumefaciens

Wright, Emma Louise

How to cite:

Wright, Emma Louise (1999) *Identification and molecular characterisation of chemotaxis genes in agrobacterium tumefaciens*, Durham theses, Durham University. Available at Durham E-Theses Online: http://etheses.dur.ac.uk/4307/

Use policy

The full-text may be used and/or reproduced, and given to third parties in any format or medium, without prior permission or charge, for personal research or study, educational, or not-for-profit purposes provided that:

- a full bibliographic reference is made to the original source
- a link is made to the metadata record in Durham E-Theses
- the full-text is not changed in any way

The full-text must not be sold in any format or medium without the formal permission of the copyright holders.

Please consult the full Durham E-Theses policy for further details.

Academic Support Office, The Palatine Centre, Durham University, Stockton Road, Durham, DH1 3LE
e-mail: e-theses.admin@durham.ac.uk Tel: +44 0191 334 6107
http://etheses.dur.ac.uk

Identification and Molecular Characterisation of Chemotaxis Genes in *Agrobacterium tumefaciens*.

by

Emma Louise Wright

A thesis submitted to the Department of Biological Sciences

University of Durham

In accordance with the requirements for the degree of

Doctor of Philosophy

April 1999

The copyright of this thesis rests with the author. No quotation from it should be published without the written consent of the author an information derived from it should be acknowledged.

2 4 AUG 1999

Identification and Molecular Characterisation of Chemotaxis Genes in *Agrobacterium tumefaciens.*

Emma Louise Wright

PhD 1999

Abstract.

Using heterologous probing, with fragments from the *S. meliloti che* operon, putative chemotaxis genes were identified in *A. tumefaciens*. The cosmid pDUB1911, from a representative genomic library of C58C1, was identified and found to contain a cluster of chemotaxis-related genes. A 9.6kb region of pDUB1911 was completely sequenced (GenBank Accession No. AF044495), in both directions, and found to contain an 8kb chemotaxis cluster. The cluster begins with *orf1*, followed by *orf2*, *cheY1*, *cheA*, *cheR*, *cheB*, *cheY2*, *orf9* and *orf10*. All of the identified homologues showed a high degree of sequence conservation with their counterparts in the chemosensory regions of the related bacteria *S. meliloti* and *R. sphaeroides*, and were arranged in a similar order. A homologue of the flagellar gene *fliF* was identified directly downstream of the *che* cluster. This arrangement is similar to that seen in *S. meliloti*, where the *che* operon is followed by a large region containing flagellar/motility-related genes. It was therefore postulated that the region identified in this work could be linked to the cluster of flagellar/motility-related genes previously identified in *A. tumefaciens*.

Mutant strains were created by in-frame deletion of *cheA* and *orf10*, and insertion of a neomycin resistance cassette in *orf1*, *cheA* and *fliF*. The *orf1* and *cheA* mutants showed wild type motility, but impaired chemotactic capabilities. Deletion of *orf10* appeared to have no effect on either motility or chemotaxis, under the conditions studied. Mutation of *fliF* resulted in a non-motile, non-flagellate phenotype. A "gutted" strain was created by deletion of the entire *che* cluster. As with the *orf1* and *cheA* mutant strains, the gutted strain showed severely impaired chemotaxis, but wild type patterns of motility.

Preliminary work was conducted on the construction of a selectively-infective phage (SIP) system for studying biomolecular interactions within, and between, the *che* and *vir* systems of *A. tumefaciens*. A phage vector was constructed, which following further testing, should allow such work to begin.

Probing with a fragment coding for the conserved region of an MCP recently identified in *R. leguminosarum*, suggested that *A. tumefaciens* could contain a number of proteins resembling the classical MCPs of *E. coli*. A putative MCP homologue was also identified in pDUB1911, downstream of the main *che* cluster. Although the *che* cluster was found not to contain a homologue of *cheW*, heterologous probing and PCR using consensus primers indicated that *cheW* maps elsewhere in the *A. tumefaciens* genome.

For My Mum and Dad

Declaration

I declare that the work contained within this thesis submitted by me for the degree of Doctor of Philosophy is my own original work, except where otherwise stated, and has not been submitted previously for a degree at this or any other University.

The copyright of this thesis rests with the author. No quotation from it should be published without prior written consent and the information derived from it should be acknowledged.

Acknowledgements.

I would like to thank my supervisor Dr. C. H. Shaw for allowing me to study for my Ph.D. in his laboratory, and for all the helpful advice and guidance he has given me over the past three years. I am also grateful to the BBSRC for funding my Ph.D. studentship.

Too many thanks to mention (and lots of beers!) to Dr. Bill Deakin for helping me throughout my Ph.D. Whether it be in person, over the phone, by post or e-mail he has always been there to help and given me good advice.

I have enjoyed working in the field of bacterial chemotaxis and would like to thank all the people working in the field who have given me assistance, particularly Dr Paul Hamblin, Viktor Sourjik and Chris Yost for their kind gifts and helpful advice on various aspects of my work.

Thanks to Julia Bartley, Vicky Kelly and Gillian Storey for DNA sequencing work, Christine Richardson for assistance with electron microscopy, and Paul Sidney for his excellent photographic skills! I would also like to thank all the members of the lab. who have made studying for my Ph.D. so much fun, particularly Bill, Danita, Vicky, Hassan, Ana and Behrouz.

Thankyou to my family, who have all always encouraged me throughout my years of studying, and without whom I would not have achieved so much. I would particularly like to thank my mum and dad, and nan and grandad for their most welcome financial support!

Finally, my love and thanks to Kevin, who's always been there for me, providing support and encouragement when I've needed it most, and most importantly for believing in me and teaching me how to believe in myself.

Contents.

Figures.

4.1.1 Diagram outlining the main steps involved in construction of the *orf1* mutant plasmid.

4.1.2 Diagram showing the EcoRI and HindIII band sizes expected for C58C1 and the *orf1* mutant strain (C1-orf1Neo).

4.1.3 0.7% agarose gel and subsequent Southern blot, showing digests of the putative *orf1* mutant strains and hybridisation with the *orf1* probe.

4.1.4 0.7% agarose gel and subsequent Southern blot, showing digests of the putative *orf1* mutant strains and hybridisation with the neomycin probe.

4.2.1.1 Diagram outlining the main steps involved in construction of the *cheA*-Neo plasmid.

4.2.1.2 Diagram showing the *Pst*I and *Hin*dIII band sizes expected for C58C1 and the *cheA* mutant strain, C1-ANeo.

4.2.1.3 0.7% agarose gel and subsequent Southern blot, showing digests of the putative *cheA* mutant strains and hybridisation with the *cheA* probe.

4.2.1.4 0.7% agarose gel and subsequent Southern blot, showing digests of the putative *cheA* mutant strains and hybridisation with the neomycin probe.

4.2.2.1 Diagram outlining the main sub-cloning steps involved in the construction of the *cheA* in-frame deletion plasmid.

4.2.2.2 Primers used for in-frame deletion of *cheA*.

4.2.2.3 Primers used to amplify *cheA*.

4.2.2.4 0.7% agarose gel showing the genotype of the putative *cheA* integrated intermediate strains.

4.2.2.5 0.7% agarose gel showing the genotype of the putative *cheA* in-frame deletion mutant strains.

4.2.2.6 Diagram showing the approximate size of the *Eco*RI and *Hin*dIII hybridising bands expected for C58C1, the two possible mutant intermediate strains and the *cheA* in-frame deletion strain (C1-Adel).

4.2.2.7 0.7% agarose gel and subsequent Southern blot, showing digests of the putative *cheA* in-frame deletion mutant strains and hybridisation with the *cheA* deletion probe.

4.3.1.1 Diagram outlining the main sub-cloning steps involved in the construction of the *orf10* in-frame deletion plasmid.

4.3.1.2 Primers used to delete *orf10*.

4.3.2.1 Primers used to amplify *orf10*.

4.3.2.2 0.7% agarose gel showing the genotype of the putative *orf10* integrated intermediate strains.

4.3.2.3 0.7% agarose gel showing the genotype of the putative *orf10* in-frame deletion mutant strains.

4.3.2.4 Diagram showing the position and approximate size of the main hybridising *Eco*RI (E) and *Hin*dIII (H) fragments expected for C58C1, the two possible intermediates and the *orf10* in-frame deletion mutant strain, C1-del10.

4.3.2.5 0.7% agarose gel and subsequent Southern blot showing digests of the putative *orf10* in-frame deletion mutant strain and hybridisation with the *orf10* deletion probe.

4.4.1 Diagram outlining the main sub-cloning steps involved in construction of the *che* deletion plasmid.

4.4.2.1 Primers used to amplify the *che* region.

4.4.2.2 0.7% agarose gel showing the genotype of the putative *che* mutant strains.

4.4.2.3 Diagram showing the approximate sizes of the hybridising *Eco*RI bands expected for C58C1, the two possible intermediates and the *che* deletion mutant strain, C1-delche.

4.4.2.4 0.7% agarose gel and subsequent Southern blot, showing digests of the putative *che* deletion mutant strains and hybridisation with the *che* deletion probe.

4.5.1 Diagram outlining the main sub-cloning steps involved in construction of the *fliF*-Neo plasmid.

4.5.2.1 Diagram showing the position and approximate size of the hybridising fragments for C58C1 and the *fliF* mutant strain, C1-FNeo.

4.5.5.2 0.7% agarose gel and subsequent Southern blot, showing digests of the putative *fliF* mutant strain and hybridisation with the *fliF* probe.

4.5.2.3 0.7% agarose gel and subsequent Southern blot, showing digests of the putative *fliF* mutant strain and hybridisation with the neomycin probe.

4.6.1 Photographs showing the swarming behaviour of each of the mutant strains created.

4.6.3 Electron micrographs of each of the mutant strains.

4.6.4 Photographs showing complementation of the C1-ANeo, C1-Adel and C1-delche mutant strains by the cosmid pDUB1911.

4.6.5 0.7% agarose gel and subsequent Southern blot, showing digests of the deletion mutant strains containing Ti plasmids and hybridisation with the neomycin probe.

5.1 Maps of fd, fHAGHAG and pAK200, showing the location of the phage genes, and the position of relevant restriction sites.

5.2.1 Diagram outlining the steps involved in construction of the SIPs fHPCR1 and fHPCR2.

5.2.2.1 Primers used to amplify the N-terminal domain of gene III, plus the six H residues, from fHAGHAG.

5.2.2.2 Colony blot of possible positive transformants, probed with PCR1.

5.2.2.3 Primer used to amplify the N-terminal domain of gene III from fHAGHAG.

5.2.2.4 Colony blot of possible positive transformants, probed with PCR2.

5.3 Oligonucleotides used to create a new multiple cloning site, for use in introducing fragments into the SIP fHPCR2.

Tables.

Abbreviations.

Amp	=	ampicillin
ATP	=	adenosine triphosphate
bp	=	base pairs
BSA	=	bovine serum albumin
cAMP	=	cyclic adenosine monophosphate
Cm	=	chloramphenicol
DMF	=	N,N-dimethyl formamide
dNTPs	=	deoxyribonucleoside triphosphates
DTT	=	dithiothreitol
EDTA	=	ethylenediaminetetraacetic acid
Ery	=	erythromycin
Gm	=	gentamycin
IPTG	=	isopropyl-β-D-thiogalactopyranoside
Kan	=	kanamycin
kb	=	kilobase pairs
kDa	=	kilodaltons
MOPS	=	3-(*N*-morpholino)propane sulphonic acid
Neo	=	neomycin
OD	=	optical density
PEG	=	polyethylene glycol
p.s.i	=	pounds per square inch
Rif	=	rifampicin
RNAase	=	ribonuclease
SDS	=	sodium dodecyl sulphate
Strep	=	streptomycin
Tc	=	tetracycline
Tris	=	tris(hydroxymethyl)aminomethane
UV	=	ultraviolet
wrt	=	with respect to
X-Gal	=	5-bromo-4-chloro-3-indolyl-β-D-galactopyranoside
5'	=	5' terminal phosphate of DNA molecule
3'	=	3' terminal hydroxyl of DNA molecule

Abbreviations.

Amp	=	ampicillin
ATP	=	adenosine triphosphate
bp	=	base pairs
BSA	=	bovine serum albumin
cAMP	=	cyclic adenosine monophosphate
Cm	=	chloramphenicol
DMF	=	N,N-dimethyl formamide
dNTPs	=	deoxyribonucleoside triphosphates
DTT	=	dithiothreitol
EDTA	=	ethylenediaminetetraacetic acid
Ery	=	erythromycin
Gm	=	gentamycin
IPTG	=	isopropyl-β-D-thiogalactopyranoside
Kan	=	kanamycin
kb	=	kilobase pairs
kDa	=	kilodaltons
MOPS	=	3-(*N*-morpholino)propane sulphonic acid
Neo	=	neomycin
OD	=	optical density
PEG	=	polyethylene glycol
p.s.i	=	pounds per square inch
Rif	=	rifampicin
RNAase	=	ribonuclease
SDS	=	sodium dodecyl sulphate
Strep	=	streptomycin
Tc	=	tetracycline
Tris	=	tris(hydroxymethyl)aminomethane
UV	=	ultraviolet
X-Gal	=	5-bromo-4-chloro-3-indolyl-β-D-galactopyranoside
5'	=	5' terminal phosphate of DNA molecule
3'	=	3' terminal hydroxyl of DNA molecule

1 Introduction.

1.1 Signal Transduction in Bacteria.

Over the past thirty years, work on signal transduction mechanisms in bacteria has shown there to be a basic system common to many different processes e.g. cell division, virulence, response to environmental stress and tactic responses. This system, known as the "two-component signalling system" [29, 31, 36, 152], consists primarily of a receptor kinase that autophosphorylates at a histidine residue (H), and a response regulator that is phosphorylated by the histidine kinase at a specific aspartyl residue (D) [204]. The histidine kinase detects a specific change, then by phosphorylation transmits this information to the response regulator, which is able to elicit a physiological signal in response to the change:

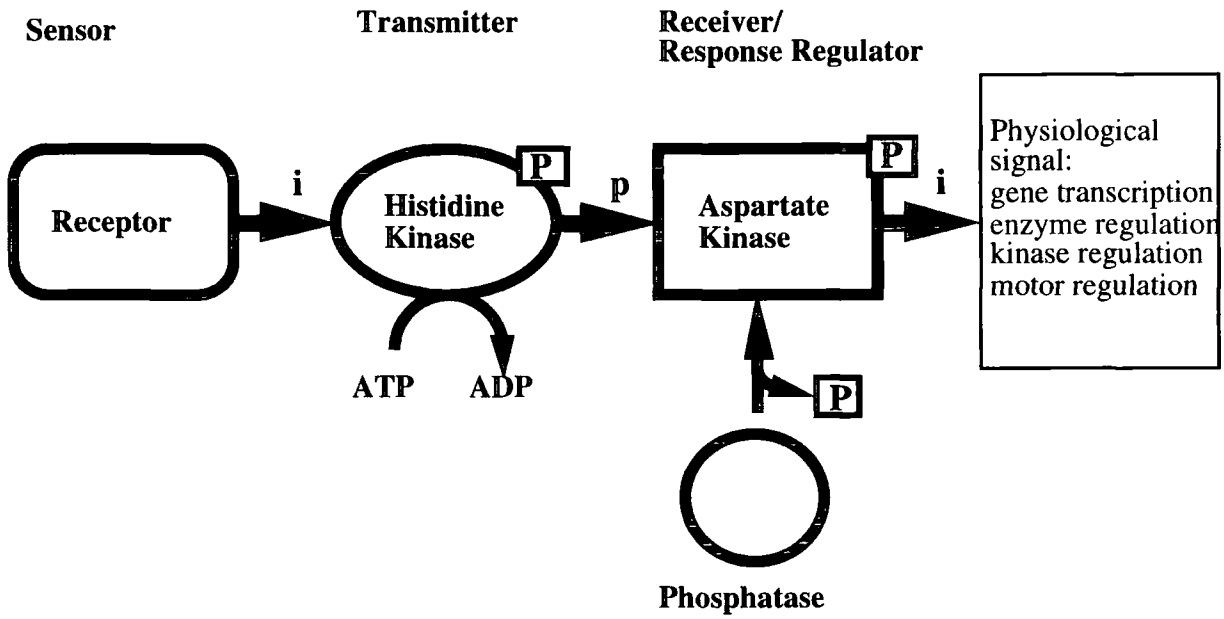

Fig. 1.1 General structure of a two-component signalling pathway. Adapted from [68]. **i** = information transfer, **p** = phosphotransfer. The receptor and phosphatase parts of the pathway can be separate proteins, or "in-built" into either the histidine kinase or response regulator proteins.

Osmoregulation in *Escherichia coli* cells is one of many examples of a two-component signalling system controlling a physiological response. The histidine kinase in this system is EnvZ. It is an inner membrane protein, that is able to sense changes in the osmolarity of the medium the cells are growing in. On detecting a change it is able to autophosphorylate at a specific H residue using cellular ATP. The phosphoryl group is then transferred to a D residue of the response regulator, in this case, OmpR. OmpR is a cytoplasmic DNA-binding protein [99]. It is able to regulate porin gene expression by differentially binding to the promoters of *ompF* and *ompC* [159] which produce porins with different characteristics. The overall result is that at low osmolarity OmpF is

produced, whereas at high osmolarity the major porin in the outer membrane is OmpC. OmpC having a smaller pore and slower flow rate. The bacterium is therefore able to detect and respond to an environmental signal.

As well as its role in osmoregulation it has been shown that the EnvZ - OmpR two component signalling system is able to regulate many other processes in the cell, of particular interest to this work is the effect on flagellar synthesis, which will be discussed later.

To date the best characterised two-component signalling pathway is the chemosensory system of *E. coli* and the closely related bacterium *Salmonella typhimurium.* [25, 68, 105, 151, 202, 203, 205, 208]. More recently however, significant progress has been made in elucidating similar pathways in bacteria such as *Sinorhizobium meliloti* and *Rhodobacter sphaeroides* [6, 9]. These systems will subsequently be discussed in more detail.

1.2 Behavioural Responses in Bacteria.

In a similar manner to the EnvZ - OmpR system many motile bacteria possess specific receptors for detecting external stimuli, and transduction systems to convert this sensory information into signals to effect their locomotory behaviour [123]. Such behavioural responses include chemotaxis, phototaxis [8, 79, 169], aerotaxis and taxis in response to cellular energy changes. In some bacteria these responses are metabolism dependent, in others they are not, and although the resulting responses seen in most motile bacteria are quite similar, the mechanisms used to elicit these responses show a great deal of variation, both between and within different bacteria. The behavioural responses exhibited by *E. coli* will be discussed in more detail, and where relevant, discussions will include consideration of similar processes seen in other bacterial species:

1.2.1 Chemotaxis in *E. coli* - The Model System.

When swimming in an unstimulated liquid environment the pattern of motility of *E. coli* cells can be thought of as a three-dimensional, random walk. Individual cells show forward movement in a given direction, a run, interrupted by brief stops and subsequent changes in direction, or tumbles, which randomly re-orientate the cells, allowing a new run to begin in a different direction. This pattern of runs and tumbles allows the bacteria to move throughout a solution. If a gradient of attractant or repellent is present, the cells can use their chemosensory system to monitor the changes in their external environment with time, and then alter their pattern of motility as necessary. For example, if swimming up a gradient of attractant, by use of their chemosensory system, cells are able to reduce the

probability of a tumble occurring and hence increase the length of the run along the favourable gradient. Conversely in an unfavourable environment e.g. in an increasing gradient of repellent, or decreasing attractant, the cells can increase tumbling frequency and hence shorten the run in that particular direction. The net effect of this altered pattern of runs and tumbles is to convert the random three-dimensional walk, into a biased walk dependent on the external environment encountered. This is chemotaxis in its simplest form.

Chemotaxis in *E. coli* has now been studied in some depth. Although much is known of the process it is still far from being fully characterised and understood. Current research centres on elucidating the structures and molecular interactions of the specific proteins involved. The overall dynamics of the system however are known in quite substantial detail. The basic pattern of signal transduction, during chemotaxis in *E. coli*, consists of interactions between specific membrane bound receptors and components of a cytoplasmic phosphorylation cascade that ultimately dictates the pattern of flagellar rotation:

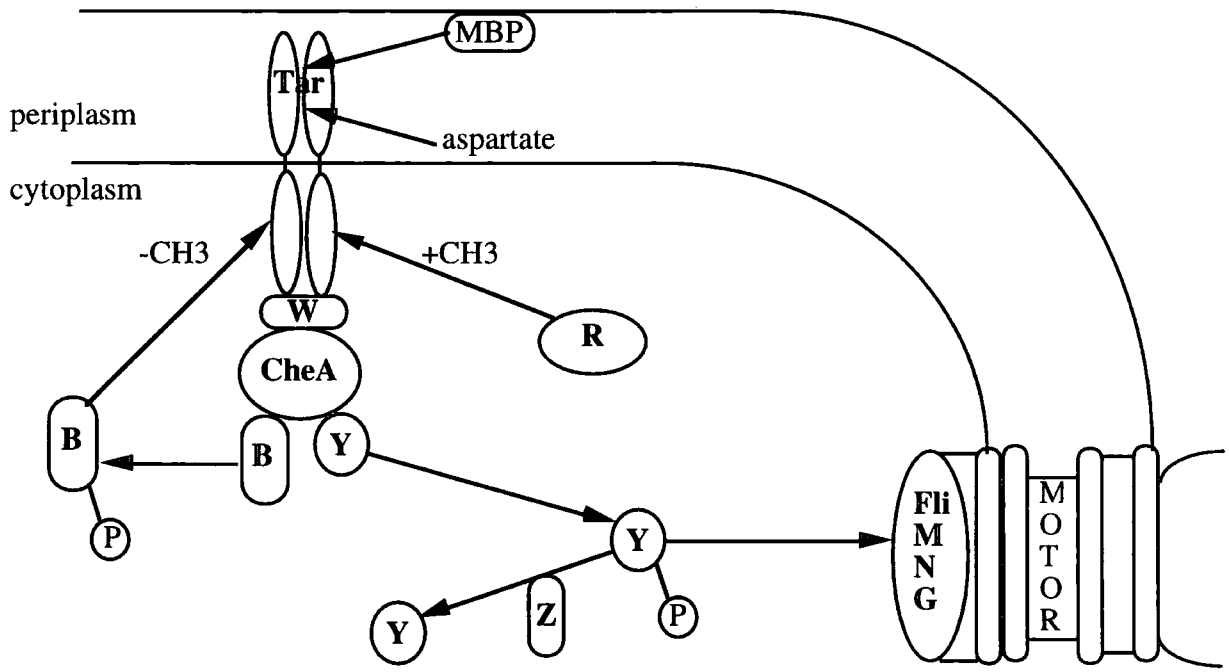

Fig. 1.2 Diagram showing the main proteins involved in the chemotactic response in *E. coli*. Figure adapted from [202].

MBP = maltose binding protein, **W** = CheW, **R** = CheR, **B** = CheB, **Y** = CheY, **Z** = CheZ. Phosphorylated proteins are indicated by an adjoining, encircled letter P.

Specific interactions and details of the proteins are given in more detail in the following text.

1.2.1.1 Transmembrane Signalling.

The detection or receptor part of the pathway consists of a number of components, in particular the periplasmic receptors [162] and specific membrane-bound chemoreceptors. The periplasmic receptors are water-soluble binding proteins, located in the periplasmic space, which recognise certain chemoeffectors. Upon activation by ligand binding the ligand-loaded binding proteins are able to interact with one of five known membrane-bound chemoreceptors and initiate a chemotactic response, e.g. the maltose binding protein (MBP), when loaded with maltose, is able to stimulate the chemoreceptor Tar [38, 45] (shown in **Fig. 1.2** and explained in more detail in the following text). The different chemoreceptors show a high degree of sequence homology and all are approximately 60kDa in size.

The classical chemoreceptor consists of four distinct domains; an amino-terminal transmembrane helix (TM1), a periplasmic ligand interaction domain of approximately 150 residues, a second transmembrane helix (TM2) and a large cytoplasmic signalling and adaptation domain of approximately 300 residues. The level of identity between the periplasmic domains of the four different MCPs in *E. coli* (see below) is very low, but there is almost 60% identity between the cytoplasmic domains. Specifically, the cytoplasmic regions contain a highly conserved signalling domain and methyl-accepting sites. The receptors exist as stable homodimers regardless of their ligand occupancy state. Each receptor interacts at its cytoplasmic domain with the histidine kinase of the system, CheA, by means of an anchoring protein, CheW. These receptor / kinase complexes form large clusters, often oriented at one end of the cell [122], giving the bacteria a so-called "nose". The activity of these inner membrane-bound chemoreceptors is modified both by binding of ligand-loaded binding proteins and by the direct binding of specific attractants.

There are four such types of receptor in *E. coli* which are classified according to the substances they elicit a response from:

Receptor Name	Attractants
Tar	Aspartate & maltose
Tap	Dipeptides
Tsr	Serine
Trg	Ribose, glucose & galactose

Tsr and Tar are found at levels 5- to 10-fold greater than Trg and Tap, and are subsequently known as high abundance receptors. In addition to being of lower abundance, Trg and Tap also have lower activity levels than Tsr and Tar. MCP hybrid

studies have shown this to be because they have lower methylation rates than Tsr and Tar. Tsr and Tar have a specific CheR binding site which aids efficient methylation of the proteins and hence increases their activity [19].

The closely related bacterium *S. typhimurium* lacks Tap, but contains Tcp [227], a receptor that allows response to citrate and the repellent phenol. Serine, aspartate and citrate bind directly to their respective chemoreceptors, while maltose, ribose, galactose, glucose and dipeptides all require interaction with a binding protein.

In addition to responding to attractants, chemoreceptors in *E. coli* are also known to mediate responses to changes in temperature, pH and the presence of various repellents e.g. ethanol, indole and several inorganic acids, such as $Ni^{2+}$and Co^{2+}. The repellent Ni^{2+} acts through a binding protein (*nik*A gene product).

Once activated by either direct or indirect binding of a chemoeffector molecule, the chemoreceptors undergo intramolecular conformational changes. These changes transmit a signal of chemoeffector binding, across the bilayer, to the cytoplasmic face of the proteins and hence to the cytoplasmic signalling proteins of the chemosensory system.

1.2.1.2 Cytoplasmic Signal Transduction.

CheA exists in a ternary complex with the cytoplasmic portions of the chemoreceptors [188], and the coupling protein CheW [73, 74]. CheA is a dimeric protein [206], one monomer of which phosphorylates the other on a specific histidine sidechain (H48). This autokinase activity is reduced when attractant ligand is bound to the chemoreceptor, and stimulated when either no attractant or a repellent is bound.

The phospho-CheA (CheA-P) complex interacts directly with the response regulators CheY [129] and CheB, each of which is an autocatalytic aspartate kinase. Both interactions require the cation Mg^{2+}, and take place at distinct interaction domains on CheA [115, 201]. On interaction with CheY, CheA-P donates its phosphoryl group to aspartate residue 57 in the active site of CheY. This causes conformational changes to occur in CheY [22], which allow the phospho-CheY (CheY-P) to dissociate from the complex. CheY-P acts as a phosphorylation-dependent switch which controls the direction of flagellar rotation [174]. The conformational changes caused by phosphorylation of CheY allow it to interact with other proteins, most notably with the switch protein FliM [16, 17], altering flagellar rotation from the default direction of counter clockwise (CCW) to clockwise (CW), resulting in the bacteria tumbling. CheY-P is therefore called the "tumble factor". The lifetime of specific CheY-P molecules is determined by autophosphatase activity, but also by the effects of the protein CheZ [223] which markedly accelerates dephosphorylation. Like phosphorylation of CheY, dephosphorylation also requires the presence of the cation Mg^{2+} [26]. CheZ is a dimeric protein which undergoes further oligomerization upon interaction with CheY-P [28], this oligomerization is thought

to increase its ability to dephosphorylate CheY-P [27]. CheZ was also thought to affect the activity of CheY-P by interacting with the switch proteins. Work by Bren *et al* however shows this to be false [33], in that FliM-bound CheY-P is protected from CheZ action, CheZ only being able to affect it by shifting the balance between bound and free CheY-P.

A further level of control exists within the chemosensory pathway. An additional pathway exists which allows the cell to adapt to a constant background level of stimulus so that it can still respond to chemical gradients. This is known as the adaptation pathway:

1.2.1.3 The Adaptation Pathway.

Adaptation is effectively a feed-back loop that can further modulate the signalling activity of the chemoreceptors, by covalent modification of their cytoplasmic domains. Each receptor has 4-5 glutamate side chains within their cytoplasmic domain which can be specifically methylated by the methyltransferase, CheR [225, 226]. CheR forms a tight association with the C-terminus of certain chemoreceptors. It transfers methyl groups from methionine, via s-adenosyl methionine [40], to the specific glutamate sidechains in both the chemoreceptor it is bound to and adjacent chemoreceptors. Methylation increases the kinase activaton signal of the receptors and hence facilitates CW rotation of the flagella. The receptor / kinase complexes can also be specifically demethylated at the same sites by the methylesterase, CheB, this therefore has the reverse effect. The receptor / kinase complexes phosphorylate CheB which increases its methylesterase activity, therefore constituting the feedback loop, with the chemoreceptors controlling their own relative rates of methylation and demethylation. This method of adaptation gives the receptors the name methyl-accepting chemotaxis proteins, or MCPs.

The methylation level of the chemoreceptors therefore acts as a simple chemical memory. Methylation levels will be high if attractant concentration was high in the recent past, and low if attractant concentrations were low. "Remembered" methylation levels can therefore be compared with current levels of ligand occupancy of the chemoreceptors, and if the environment has significantly changed the activity of the histidine kinase can be altered as appropriate. Methylation is highly regulated and counterbalances the effects of ligand binding; the multiple methylation sites are thought to allow an adjusted response under different conditions, however it is not yet fully understood how this works. What has been shown is that each site has a different rate of methylation and that the most rapidly methylated sites are the most important for chemotaxis.

Therefore in summary, in *E. coli*, the basic chemotaxis system works so that when there is no attractant ligand bound to the MCPs, CheA autophosphorylates and causes phosphorylation of CheY, which then interacts with the flagellar switch and leads to the

bacteria tumbling. If attractant is bound these processes are suppressed and hence the bacteria continues to run in a favourable direction.

1.2.1.4 Characteristics of the Che Proteins.

CheA - The histidine kinase. The *cheA* gene encodes two overlapping proteins, $CheA_L$ and $CheA_S$, both of which have a common carboxy terminal. $CheA_S$ lacks the first 97 amino acids of $CheA_L$.

The CheA protein consists of three functional domains [30]:

- domain i) (amino acid residues 1 - 260) an N-terminal phosphotransfer domain made up of two regions; P1, containing the autophosphorylation site (lacking in $CheA_S$), [72] joined by a linker region to P2, which contains the sites for CheY and CheB binding [138]. P2 is joined by a second linker region to domain ii)
- domain ii) (amino acid residues 260 - 503) a catalytic transmitter domain required for autophosphorylation to occur [65], and necessary for dimerization
- domain iii) (amino acid residues 503 - 654) a C-terminal regulatory domain required for receptor coupling.

The two different forms of CheA are produced in stoichiometric amounts and are thought to play distinct roles in the chemosensory pathway. $CheA_L$ is the main form involved in the phosphorylation cascade to CheY and CheB. CheY and CheB compete for binding to $CheA_L$ because their specific interaction domains on $CheA_L$ overlap [115]. *In vitro* studies have shown that $CheA_S$ is able to bind to $CheA_L$ and $CheA_L$ / CheW complexes and enhance subsequent phosphorylation reactions [130]. It has also been shown that $CheA_S$ can bind to CheZ and augment its ability to dephosphorylate CheY-P [223]. The *in vivo* significance of these interactions however is still not fully understood.

CheW - The coupling protein. CheW is not known to possess any regulatory or functional domains. It is however essential for activation of CheA by the chemoreceptors [46, 73] and acts as a scaffold protein linking the two together.

CheY - The response regulator. The structure and activation of CheY has been extensively studied [22, 128, 175, 187, 224, 232]. CheY contains five active site residues, which are highly conserved amongst other response regulators [119] : D57 the site of phosphorylation, D12 and D13 required for interaction with Mg^{2+}, K109 involved in phosphorylation induced conformational changes and T87 which is thought to stabilise CheY-P [5].

CheZ - The "phosphatase". The exact mode of action of CheZ on CheY-P is unknown. Although most evidence to date would suggest it to be a specific phosphatase, it is possible

that it could simply be an allosteric activator of the inherent phosphatase activity known to exist in CheY [171].

CheZ is thought to be an essential protein in the chemotactic process as when deleted resulting strains showed a tumbly phenotype, and when overexpressed it caused a smooth swimming phenotype, and in both cases the bacteria were no longer able to respond chemotactically. However, although classical methods of testing (e.g. swarm plate analysis and capillary assays) showed *cheZ*- strains to be non-chemotactic, work by Dowd and Matsumura showed the same strains to be chemotactic to photoreleased attractants [62]. This therefore suggests that CheZ is not always necessary for chemotaxis to occur, and that requirement for CheZ depends on the attractant gradient background experienced by the bacteria.

CheB - The methylesterase. CheB consists of two functional domains; an N-terminal regulatory domain which contains the site of phosphorylation by CheA (D56), joined by a linker to a C-terminal catalytic domain. The N-terminal domain is thought to regulate C-terminal methylesterase activity by physically blocking its active site. X-ray crystal structure determination of CheB interactions, suggests that this inhibition is removed by conformational changes occurring in the CheB structure as a result of its phosphorylation by CheA [59], hence enabling CheB-P to interact with the chemoreceptors.

CheR - The methyltransferase. CheR is a soluble enzyme, which exists free in the cytoplasm. The chemoreceptors Tar, Tsr and Tcp contain a five residue motif (NWET/SF) at their C-terminal which specifically binds CheR [143], therefore CheR can also exist as part of the receptor / kinase signalling complex.

1.2.1.5 Other Factors Affecting the Signalling Process.

The Acetate Effect.

The repellent acetate is able to cause prolonged tumbling in *E. coli* cells that contain only CheY from the chemosensory pathway. This is the acetate effect. Acetate is produced in *E. coli* cells via a constitutive fermentation pathway from acetyl co-enzyme A, via acetyl phosphate, using the enzymes phosphotransacetylase (*pta* gene product) and acetate kinase (*ackA* gene product). The intermediate in this process, acetyl phosphate, is known to phosphorylate several response regulators e.g. OmpR, PhoB and CheY; this phosphorylation event could therefore explain the acetate effect. However recent work by Barak *et al* identifies additional factors active in this effect [15]. Acetate metabolism in *E. coli* occurs by the reverse of the above reactions, and also by the action of acetyl coenzyme A synthetase (*acs* gene product). The intermediates in these reactions, acetyl phosphate and acetyladenylate respectively, are both known to interact with CheY. As

explained above acetyl phosphate is able to phosphorylate CheY, acetyladenylate however can acetylate CheY (at K92); like CheY-P the acetylated CheY moiety is also able to promote CW rotation of the bacterial flagella [163]. It is therefore thought that one or both of these pathways may act to modulate the chemosensory response, according to the metabolic state of the cell.

Intracellular Ca^{2+} levels .

Increased levels of free cytoplasmic Ca^{2+} cause increased tumbling frequencies in chemotactically wild-type *E. coli* cells, and conversely reduced levels lead to smooth swimming behaviour. This effect requires CheY, CheA and CheW, but its precise mode of action is unknown [214]. Specific calcium ion channel blockers have also been shown to inhibit tumbling and hence affect chemotaxis [215].

Intracellular Fumarate Levels .

The ability of fumarate to act as a prokaryotic switch factor was first discovered in *Halobacterium salinarium.* Fumarate is a central metabolic intermediate and as such is thought to signal the metabolic flux, through the cell, to the flagellar motor. Recent work by Montrone *et al* has shown that fumarate is essential for clockwise rotation in *E. coli* [135]. It is thought that CheY and fumarate act additively on the switch complex to bring about the transition from CCW to CW motor rotation. The chemorepellents indole and benzoate are known to inhibit fumarase and hence increase cellular fumarate levels [136], they are therefore able to induce flagellar switching in *che- E. coli* strains.

1.2.2 Chemotaxis in *Bacillus subtilis.*

Chemotaxis in the Gram positive bacterium *B. subtilis* follows the same fundamental system as that seen in *E. coli* [144]. Chemoeffectors stimulate the histidine kinase CheA which then, by means of a phosphorylation cascade, activates the response regulator CheY and alters the pattern of motility. However there are substantial differences between the two systems [23]:

In *B. subtilis* it is thought that when attractant is bound to an MCP, CheA autokinase activity is stimulated, resulting in phosphorylation of CheY and CheB. Increased levels of CheY-P then cause CCW rotation of the flagella resulting in smooth swimming. This is in effect the reverse of the steps seen in *E. coli,* where repellent binding stimulates CheA activity and results in the bacteria tumbling (see section **1.2.1**). However the most obvious difference between the chemotaxis system of *B. subtilis* and that of *E. coli* is in the adaptation pathway. In *B. subtilis* both addition and removal of attractants or repellents causes enhanced methanol production, whereas in *E. coli* only negative stimuli cause increased methanol production. Methanol is produced as a result of

the action of CheB-P on the MCPs and is therefore expected when CheA-P and subsequently CheY-P and CheB-P levels are high. The production of methanol at both high and low levels of CheY-P in *B. subtilis* is thought to constitute part of an additional adaptation pathway [104]. In *B. subtilis* an additional methylation step occurs. Whereas in *E. coli* methanol production comes directly from the MCPs, in *B. subtilis* methyl groups are transferred from the MCPs to a further protein from where they are then converted to methanol. The exact mechanism of adaptation in *B. subtilis* is still not clear, however it is thought to involve CheY and the novel proteins CheC and CheD [166], which are known to interact, and affect methylation of the MCPs.

B. subtilis has a *fla/che* region consisting of over 30 genes required for flagellar synthesis and chemotaxis, in addition it also has a number of smaller regions containing specific motility/chemotaxis-related genes. The *fla/che* region is >26kb in length and under the control of dual promoters [67]. It contains genes homologous to structural components of the flagellar and chemotaxis genes from *E. coli* and *S. typhimurium*. *B. subtilis* contains homologues of the chemotaxis proteins CheA, CheB, CheR, CheW and CheY. It also contains three MCP homologues [83]. In addition *B. subtilis* also contains several unique *che* genes, e.g. *cheV* (encodes CheA/W homologue), *cheC* and *cheD*. The presence of these additional *che* genes most likely reflects the peculiarities of the specific chemotaxis system of *B. subtilis*.

In addition to the methylation-dependent pathway described in the preceeding sections, many bacteria are able to respond to numerous stimuli without the need for interactions with the MCPs. In particular the responses to many primary growth limiting factors, e.g. carbohydrates, light and oxygen, are often mediated by systems other than the methylation dependent chemotaxis pathway described in section **1.2.1**. In order to give a net response from a number of stimuli however, it is likely that these alternative pathways integrate at some point with the MCP system [94, 127, 209].

1.2.3 The Phosphotransferase (PTS) System.

Chemotactic responses to many carbohydrates are mediated through the phosphoenolpyruvate (PEP) : sugar phosphotransferase system (PTS) [158]. This system depends on carbohydrates being transported and phosphorylated through a dual transport / chemotaxis pathway.

In enteric bacteria PTS carbohydrates are translocated through the bacterial membrane via specific, membrane-spanning proteins, enzymes II (EII), in combination with another specific protein, enzyme III (EIII).

Depending on the compound being transported, EIII is either a separate protein e.g. for glucose, or part of a larger EII protein e.g. for N-acetylglucosamine. Whilst being

transported into the cell the substrate is concomitantly phosphorylated by EII/EIII. Phosphorylation of the substrate depends on EII/EIII being first phosphorylated by a non-substrate specific pathway involving transfer of a phosphoryl group from PEP, via a non-specific protein, enzyme I (EI), to a hexose protein (HPr).

The chemotactic response therefore depends on the compound being transported and phosphorylated, however further metabolism of the substrate is not an absolute requirement for chemotaxis to occur.

CheA, CheW and CheY are required for chemotaxis to occur to PTS carbohydrates [168], this system is therefore thought to integrate with the methylation-dependent chemosensory system at the point of CheA. Lux *et al* propose that this integration occurs through EI of the PTS system [120] : during uptake of a PTS carbohydrate the rate of dephosphorylation of EI by HPr was found to be greater than its rate of phosphorylation by PEP, leading to a build up of unphosphorylated EI in the cell. It was therefore proposed that the build up of EI inhibited CheA autophosphorylation and hence also CheY phosphorylation, leading to a swimming response up the gradient of PTS carbohydrate.

Interestingly, it has recently been shown that chemotaxis to PTS carbohydrates in *B. subtilis* also requires one, or more, MCPs [71], hence adding a further dimension to the currently known chemotactic signalling pathways existing in *B. subtilis*.

1.2.4 Aerotaxis / Energy Taxis in *E. coli*.

Methylation-dependent chemotaxis in *E. coli* (as described previously) has been extensively studied for several decades. Recently however a new receptor has been identified in *E. coli*, which has been shown to mediate movement to environments able to support optimal growth of the bacteria. This receptor is responsible for the aerotactic response and hence has been given the name Aer. It is thought not only to respond to oxygen, but also to a variety of other stimuli, all of which cause changes in the energy (redox) levels in the cell [77, 210].

The carboxy-terminal of the Aer protein is similar to that of the MCPs involved in chemotaxis, and as such is thought to constitute the signalling domain of the protein. In contrast to the MCPs however Aer has only one predicted hydrophobic sequence. This is thought to anchor the protein at the cytoplasmic surface of the bacterial membrane, thereby making Aer an intracellular sensor with two cytoplasmic domains. The second cytoplasmic domain, thought to be the sensing domain shows sequence homology with the redox sensing domain of the NifL protein from *Azotobacter vinelandii*. The sensing domain of Aer is associated with non-covalently bound FAD which is thought to sense redox changes in the electron transport chain. Aerotaxis has been shown to require CheA, CheW and CheY [168], it is therefore likely that the signalling domain of Aer integrates

into the chemotactic signal transduction system at CheA and CheW and effects changes in the locomotory behaviour of the cell via CheY.

Aerotaxis is also possible through action of the MCP Tsr. This protein is able to detect both the cytoplasmic pH and the periplasmic pH, it is therefore thought to mediate aerotaxis by detecting changes in the proton motive force of the cell.

Energy taxis in *E.coli* is metabolism-dependent, unlike most chemotaxis responses which have been shown to be metabolism-independent. Chemotaxis in the purple photosynthetic bacterium *R. sphaeroides* however, was thought to be completely metabolism-dependent [7, 157] and therefore due to changes in electron transport (redox) levels, rather than due to direct sensing of the chemical by binding to a specific receptor [92]. Chemotaxis in the soil bacterium *S. meliloti* on the other hand is thought to be intermediate between the two. It is therefore evident that similar behavioural responses exhibited by different bacteria are mediated by quite different, but fundamentally related processes (as was suggested earlier for the chemotaxis system of *B. subtilis*).

Homologues of many of the chemotaxis genes identified in *E. coli* are now being discovered in a wide array of bacterial species. Examples of these genes will be considered in more detail in section **1.7**. Consideration will concentrate on those genes identified in members of the α-subgroup of *Proteobacteria* (see section **1.4**) which contains the bacterium *Agrobacterium tumefaciens* on which this study is based.

1.3 Motility in *E. coli.*

E. coli has a peritrichous flagellation pattern, typically having 6 to 8 flagella arising from random points on the cell surface. Each flagellum consists of a helical filament that rotates at its base. It is rotation of these flagella that allow the bacteria to move. The length of each filament can be up to ten times the cell body length (up to 20μm). Transmembrane proton motive force drives the flagellar rotation.

In *E. coli*, like most enteric species, counter clockwise (CCW) rotation of the flagella causes a run, and clockwise (CW) rotation causes the bacteria to tumble. When rotating CCW, the flagella form a bundle which drives the bacteria forward. When one or more of the flagella then switch to CW rotation the bundle is driven apart and subsequently the bacterium tumbles, hence orienting the bacteria in a different direction. In an unstimulated environment a run typically lasts for 1-2 seconds and is interupted by tumbles, which last for 0.1-0.2 seconds.

1.3.1 Flagellar Structure and Assembly [121].

Microscopic, biochemical and genetical studies of *E. coli* have allowed identification of the proteins involved in flagellar assembly and structure. Approximately 40 proteins are known to play a role in this process.

A diagram showing the generalised structure of a flagellum and the genes which encode the various components can be seen in **Fig. 1.3.1**. The *E. coli* flagellum comprises a thin helical tube, the filament, which is joined via accessory proteins to a hook shaped structure. This in turn is connected to a basal structure imbedded in the cell surface, which consists of a rod surrounded by a number of different rings. The basal structure lies mainly within the cell envelope and the rings are named according to their position relative to it.

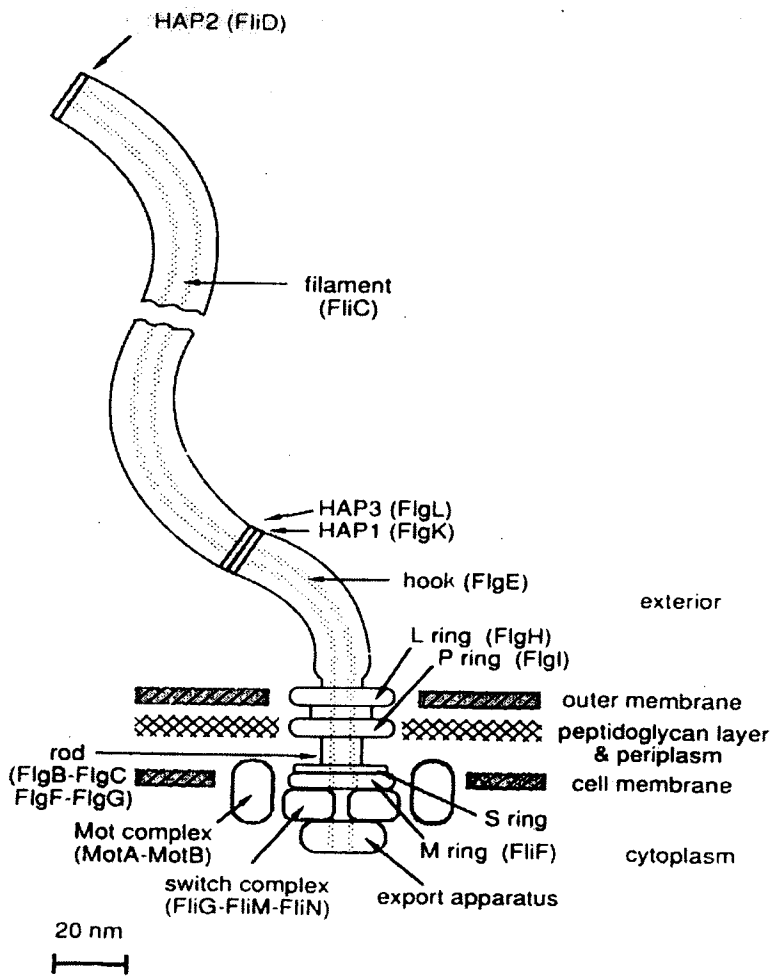

Fig. 1.3.1 Diagram showing the generalised structure of the *E. coli* flagellum. Figure reproduced from [121]. The position of the C-ring is indicated by the switch complex.

Flagellar construction is carefully co-ordinated, construction begins with the innermost proteins, the first being the MS-ring. The MS-ring is made up of a single

protein encoded by the gene *fliF*. It is thought to be a double ring that lies in and just outside the cytoplasmic membrane. As can be seen in **Fig. 1.3.1** the MS-ring forms part of the basal body of the flagella. Also in this region are the C-, L- and P-rings and the rod structure. The basal body is thought to function as a mechanical motor.

The next steps in flagellar assembly require formation of the switch complex consisting of FliG, M and N (FliM and FliN form the C-ring, discussed later) and construction of the basal body rod structure. The rod is made up of four proteins (FlgB, C, F and G), however correct construction also requires other genes, the products of which are thought to be involved in correct functioning of a flagellum-specific export apparatus, through which the rod proteins have to pass.

As most components of the flagellum lie outside the cytoplasm, the correct functioning of the export apparatus plays a pivotal role in flagellar assembly. The shape and exact location of the export apparatus is not known. It is thought to lie at the cytoplasmic face of the MS-ring, possibly forming a component of the C-ring. Export occurs through the hollow centre of the growing structure. Control of this process allows the components to be secreted in the correct sequence and appropriate amounts for assembly in the correct order at the distal point of the structure.

The steps following rod assembly have been better characterised, two proteins, FlgI and FlgH, are secreted across the inner membrane by means of their signal peptide sequences and assemble on the rod, forming the P- and L-rings respectively. Correct assembly of the P-ring requires the protein FlgA, whose exact function is unknown, and also the products of *dsbB* and *dsbA* that allow disulphide bond formation in FlgI. The P-ring lies in the peptidoglycan layer and the L-ring is embedded in the outer membrane.

Next components of the hook are exported through the assembled apparatus and add on to the growing structure. The hook is thought to act as a universal joint (or flexible coupling) between the filament and the cell. During hook construction the protein FlgD remains at the end of the hook and assists in its assembly, once the hook is correctly formed FlgD is discarded. The product of *fliK* controls hook length, although again the exact mechanism of this process is unknown.

The proteins at the hook/filament junction, FlgK and FlgL are then added, followed by FliD which directs filament construction and then the filament protein itself, FliC. Each filament is composed of thousands of copies of the FliC protein, known as flagellin.

1.3.2 Regulation of the Flagellar and Chemotaxis Genes [25].

The genes for flagellation, motility and chemotaxis are arranged in three regions of the chromosome (four regions in *S. typhimurium*), region III is further subdivided into two sections, IIIA and IIIB (see **Fig. 1.3.2.1**).

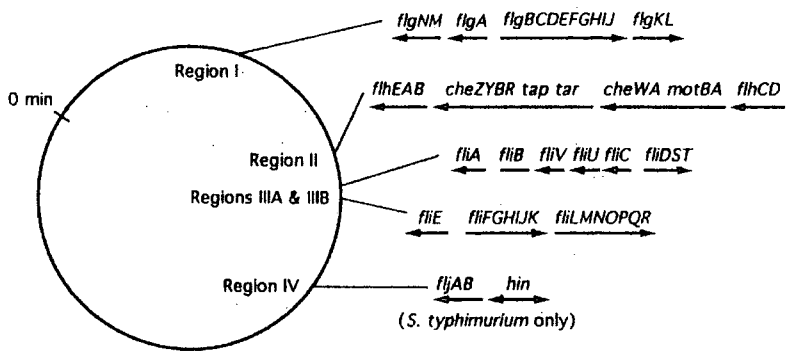

Fig. 1.3.2.1 Organization of the genes for flagellation, motility and chemotaxis in *E. coli* and *S. typhimurium*. Figure reproduced from [25].

In addition the genes within each region are frequently arranged in operons, grouping together genes with similar functions, or those required at a similar step in the overall process. The flagellar genes are named according to the chromosomal region in which they are found; region I = *flg* genes, region II = *flh* genes, region III = *fli* genes and in *S. typhimurium* region IV = *flj* genes. The designation *fl* signifies genes whose products are involved in flagellar structure or assembly, as opposed to the *che* genes required for chemotaxis and the *mot* genes required for motility, but not involved directly in flagellar structure.

Expression of the genes within each of these regions is under the control of a hierarchical system, consisting of three tiers, or levels, of genes. Level two genes requiring those from level one for expression, and level three genes in turn requiring the level two genes. These different levels of expression roughly mirror the stage the gene products are required in flagellar construction or subsequent motility:

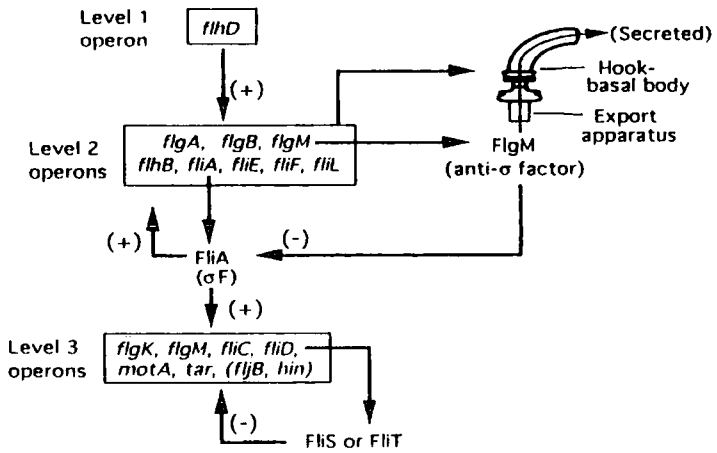

Fig. 1.3.2.2 Regulation of transcription of the flagellar genes. Figure reproduced from [25].

Level one consists of two genes, *flhC* and *flhD*, these are under the control of cyclic-AMP (cAMP) levels in the cell via the regulatory protein CAP. The products of both these genes are required to stimulate transcription of the level two genes.

Level two is made up of the following genes (or operons starting with the named gene); *flgA, flgB, flgM, flhB, fliA, fliE, fliF* and *fliL*, the products from most of which form parts of the flagellum. *fliA* however codes for an alternative sigma factor, that is required for transcription of the level three genes and also aids transcription of the level two genes. In addition *flgM* codes for an anti-sigma factor that binds to FliA and hence inhibits expression of the level three genes. The FlgM protein is also a substrate for the flagellar export apparatus. On correct assembly of the basal body and hook it is actively exported from the cell, hence it prevents the level three genes from being transcribed until the basal parts of the flagella are correctly formed.

Level three genes include *flgK, flgM, fliC, fliD, motA* and *tar* (also *fljB* and *hin* in *S. typhimurium*). The products of *fliS* and/or *fliT* act as negative regulators of the level three genes and are thought to be involved in controlling flagellar length.

Flagellar synthesis is inhibited when cells are grown under stressful conditions e.g. high temperatures or high concentrations of salts or sugars. Expression of the *flhDC* master operon for flagellar synthesis has been shown to be controlled by several different factors. Work by Shin and Park showed that the level of acetyl-P modulated this expression [184], this effect is thought to be mediated by the response regulator OmpR. OmpR-P is proposed to have a negative regulatory role on flagellar synthesis. As explained previously, at high osmolarity the levels of OmpR-P in the cell increase, this would therefore explain how flagellar synthesis is inhibited under such conditions. It is likely that other means of controlling flagellar synthesis exist within the cell. Such regulation could be the result of general cellular mechanisms, as above, or via the action of one or more of the essential flagellar genes already identified, that as yet, have no known function.

1.3.3 Torque Generation [25].

MotA and MotB are thought to be the last components added to the flagellar structure. Together they are believed to form the stator of the motor, surrounding the MS-ring and forming a vital part of the flagella motor. The C-terminal of MotB is anchored to the cell wall. MotA contains four hydrophobic regions which interact with the N-terminal of MotB to form a proton-conducting channel through the bacterial cytoplasmic membrane. Each flagellar motor can contain up to eight independent, associated MotA-MotB complexes, which interact with the motor-switch complex to generate current in response to an inward proton current.

The products of *fliG, M* and *N* form the switch complex. FliG lies at the cytoplasmic face of the MS-ring, and together with the MS-ring forms part of the rotor, its primary role is thought to be in torque generation. FliM and FliN form the C-ring (cytoplasmic ring). They are thought to function together, as a unit, since work using FliM-FliN fusion mutants suggests that they are stationary with respect to one another [101]. It is still not known whether they form part of the rotor, or the stator, of the flagellar motor. Recent work by Toker *et al* proposed FliM to consist of four functional regions [216] : i) the N-terminal involved in switching (where interaction with CheY-P occurs), ii) an extended N-terminal required for switching and flagellar assembly, iii) a middle region for switching and motor rotation which interacts with FliG and iv) the C-terminal required primarily for flagellar assembly. In addition to interactions with CheY-P and FliG, self association of different FliM proteins is thought to occur between regions ii) and iv). FliN is thought to constitute part of the flagellum-specific export apparatus.

Correct flagellar assembly and functioning therefore requires co-ordinate regulation of a large number of genes.

1.4 The α-subgroup of the Class *Proteobacteria*.

Members of the α-subgroup of *Proteobacteria* are characterised by DNA with a high G+C content [137]. The group contains bacteria from a diverse array of environments which exhibit a great deal of variation in their metabolic capabilities. Examples of members of the group are *Agrobacterium*, *Azospirillum*, *Caulobacter*, *Rhodobacter*, *Rhizobium* and *Sinorhizobium* species. In recent years a great deal of work has been carried out on the patterns of motility and chemotaxis systems of *A. tumefaciens*, *C. crescentus*, *R. sphaeroides* and *S. meliloti* from this group. The group is further subdivided into families, of which the family *Rhizobiaceae* is of most relevance to this work.

1.4.1 The Family *Rhizobiaceae*.

The family *Rhizobiaceae* contains soil bacteria that are found in association with plant cells. Within the family *Rhizobiaceae* are the genera *Rhizobium* and *Agrobacterium* which show a great deal of similarity in their behaviour and molecular biology. The classification of *Rhizobium* and *Agrobacterium* species is based on both phenotypic traits and plasmid-encoded characteristics. Both genera contain extra-chromosomal elements [95].

1.4.2 The Genus *Agrobacterium*.

Agrobacteria are Gram-negative, aerobic, soil bacteria. Typically being of 0.6-1.0μm in diameter and 1.5-3.0μm in length (see **Fig. 1.4.3**).

The classification of the genus *Agrobacterium* is traditionally based on the phytopathogenic capabilities of the bacteria [53]. Four different species are recognised; *A. tumefaciens* which causes crown galls, *A. rhizogenes* which causes hairy root disease, *A. rubi* which causes cane galls and *A. radiobacter* which is non-pathogenic. Individual species are then further classified, again according to their pathogenic capabilities. Pathogenic strains that cause the growth of galls or roots induce the infected cells to produce specific chemicals, called opines (see section **1.5.2**). It is therefore possible to classify strains according to the type of opines they cause infected plants to produce.

The phytopathogenicity of Agrobacteria is dependent on the presence of specific oncogenic elements which are known to be easily lost and are transferrable from one strain to another. A classification system dependent on these characteristics has therefore been deemed unreliable and an alternative system suggested.

The alternative system classifies Agrobacteria according to various chromosomally encoded biochemical and physiological differences, and is therefore not reliant on the unstable phytopathogenicity of the organism. Under this classification system the genus *Agrobacterium* is sub-divided into three biovars (biovars 1, 2 and 3). Each biovar contains strains that are genetically and phenotypically distinct from the others. Classification by chromosomal characteristics means each biovar contains both pathogenic and non-pathogenic strains. All Agrobacteria strains possess multipartite genomes, many of which show different topologies i.e. contain both linear and circular chromosomes.

Despite the new classification system the traditional method of classification of Agrobacteria strains is that most used (and will be the method used in this work). The strain used in this work, C58C1, is a derivative of *A. tumefaciens* strain C58, which contains the nopaline-type Ti plasmid pTiC58. C58 is a biovar 1 strain.

1.4.3 *Agrobacterium tumefaciens*.

Morphologically *A. tumefaciens* cells are short, encapsulated Gram-negative rods. *A. tumefaciens* is a motile bacterium and has an unusual flagellation pattern consisting of a polar tuft of two flagella and two to four lateral flagella (see **Fig. 1.4.3**).

Fig. 1.4.3 Electron micrograph of a wild-type *A. tumefaciens* cell (C58C1). Photograph taken by Dr. C. H. Shaw.

The optimum temperature for the growth of *A. tumefaciens* is 28°C. *A. tumefaciens* is a pathogen of most dicot and several monocot plants. It is a natural soil bacterium found worldwide. It is especially prevalent in the plant rhizosphere [100]. Typically the numbers of bacteria found in association with the rhizosphere are a thousand times greater than those in the surrounding soil. Generally the soil contains far more non-pathogenic strains than pathogenic, since the means of pathogenicity is easily lost without selection. Pathogenic strains are usually restricted to the infected plant tissue.

Infection by *A. tumefaciens* causes neoplastic overgrowths of the plant tissue. This can stunt the overall growth of the plant and lead to significant agricultural losses.

1.5 Virulence in *A. tumefaciens.*

A. tumefaciens is the causative agent of Crown Gall disease, so called because of the characteristic tumourous growths (see **Fig. 1.5**) produced at the soil-air junction (crown) of the infected plant.

A. tumefaciens strains are known to respond to specific exudates released by wounded plants into the rhizosphere [11, 197, 198]. Their pathogenicity and competitive advantage in the soil environment are dependent on the presence of a specific plasmid, known as the tumour-inducing (Ti) plasmid [88].

Fig. 1.5 Photograph showing the tumourous growths produced by *A. tumefaciens* on the stem of *Kalanchöe diagremontiana*. Photograph taken from [178].

1.5.1 The Ti Plasmid.

Pathogenic *A. tumefaciens* strains possess a specific Ti plasmid. Although variation exists between different Ti plasmids, all can be seen to have three particular regions that are important to the pathogenic capabilities of the bacteria, i) the *vir*-region, ii) the T-DNA and iii) the opine catabolism region (see **Fig. 1.5.1**).

Ti plasmids are typically 190-240kb in size and are present at a low copy number (1-3 copies per cell). During tumour induction, a specific region of this plasmid DNA, the T-DNA, bounded by 25bp imperfect direct repeats, or border repeats, is transferred to the plant cells. In octopine-type plasmids, the 13kb left T-DNA (T_L) encodes the genes needed for plant transformation and octopine synthesis, whilst different opine biosynthetic genes are encoded by the 7.8kb right T-DNA (T_R) (see **Fig. 1.5.1**). Nopaline-type Ti plasmids have a single 22kb continuous T-DNA.

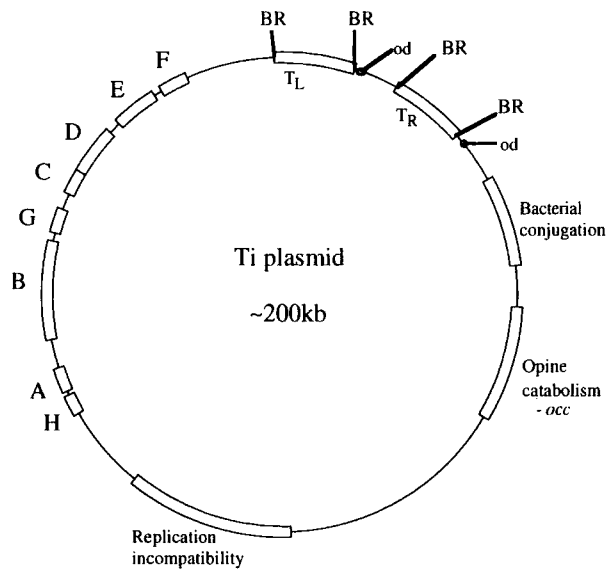

Fig. 1.5.1 Genetic map of an octopine-type Ti plasmid. Reproduced, with permission, from [54]. (The figure is not to scale.)
BR = border repeat, od = overdrive sequence. The figure shows the approximate locations of the *vir* genes, the T-DNA and the opine catabolism region (*occ*). Also shown are the relative positions of the locations of the loci for plasmid replication and incompatibility, and bacterial conjugation.

Attachment of the bacteria to the plant cell is a prerequisite for DNA transfer. The bacteria are thought to initially form a loose binding, mediated by the bacterial Ca^{2+}-binding protein, rhicadhesin, then form a more stable association by producing cellulose filaments [125]. The five genes required for cellulose synthesis (*cel* genes) lie in two operons on the bacterial chromosome [126]. The cellulose fibrils produced, not only bind bacteria to the plant cell surface, but also cause the formation of large aggregates of Agrobacterial cells.

Each plant cell binds a finite number of bacteria suggesting that some sort of receptor on the plant surface is involved in the attachment process. A similar process is seen in the related bacterium *Agrobacterium rhizogenes* which ultimately causes hairy root disease by transfer of part of its Ri (Root-inducing) plasmid. In both cases, transfer and integration of a region of bacterial DNA into plant cells, causes the cells to exhibit several specific responses.

In the case of *A. tumefaciens* expression of the transferred DNA (T-DNA) leads to the production of the plant hormones auxin and cytokinin that cause the plant cells to proliferate autonomously and extensively, hence giving the tumourous phenotype of the infected plants. More interesting however is the biosynthesis of novel amino acid or sugar

derivatives, opines, from the infected cells. The resulting compounds are specifically metabolised by the tumourigenic *A. tumefaciens* strain, but more importantly not by most other soil organisms, hence creating an exclusive energy source for *A. tumefaciens*.

In recent years the value of opines to both the infected plant and other soil micro-organisms has been questioned. It has been shown that opines can be translocated to and exuded from non-infected parts of an infected plant [172]. It has been postulated that this movement of opines may be of benefit to the plant in a insect protection role and may also influence bacterial growth at parts of the plant distal to the infection site.

1.5.2 Opines.

A. tumefaciens strains are classified according to the kind of opines formed in the tumours they induce; to date nine different opine families have been identified which together consist of more than twenty opines [220]. Most opines are secondary amine derivatives, however some are sugar phosphodiesters. The most widely studied opine families are the octopine- and nopaline-types:

The octopine family is made up of the opines octopine, lysopine, histopine and octopinic acid, all of which are formed by the reductive condensation of pyruvate with a basic amino acid, e.g. Octopine (N^2-[1-D-carboxyethyl]-L-arginine) is formed by condensation of pyruvate with L-arginine. Octopine-type Ti plasmids also encode the genes required for the formation and utilisation of the mannityl opines.

The nopaline family consists of nopaline and nopalinic acid. Nopaline (N^2-[1,3-D-dicarboxypropyl]-L-arginine) is similar to octopine, being formed by reductive condensation of 2-ketoglutarate with L-arginine. Nopaline-type Ti plasmids also encode the genes required for the formation and utilisation of the opines agrocinopineA and agrocinopineB [102].

1.5.2.1 Opine Synthesis and Catabolism.

The genes that confer on the plant the ability to synthesise these compounds, the opine synthases, are located on the T-DNA. The originating Ti-plasmid of the T-DNA also encodes corresponding genes that allow the bacteria to utilise the specific opines produced.

For octopine and nopaline plasmids the regions encoding octopine and nopaline uptake and primary catabolism functions are known as *occ* and *noc*, respectively [229]. Each region being made up of a number of different genes. In contrast usually only one gene is required for synthesis of the opines. The genes for uptake and catabolism are specifically induced by their cognate opines and are under the control of a protein with

both positive and negative regulatory functions (known as OccR in octopine strains, and NocR in nopaline strains [222]).

The *occ*, *noc* and similar regions allow the bacteria to transport specific opines [230] and begin catabolism of them, however they do not code for all the components required for complete catabolism of the opines. Work in recent years has identified more of the components required for the complete catabolism of several opines.

Research by Cho *et al* [41] describes the transcriptional regulation and locations of all the genes required for complete catabolism of octopine. The *occ* operon encodes the regulator OccR and the transport proteins OccQ, M, P and J [219]. Complete catabolism of octopine then requires four principal processes:

- i) conversion of octopine to arginine and pyruvate by the enzyme octopine oxidase, which is coded for by *ooxAB* in the *occ* operon on the Ti plasmid
- ii) conversion of arginine to ornithine and urea by arginase, which is encoded by *arcA*
- iii) conversion of ornithine to proline and ammonia by ornithine cyclodeaminase, encoded by both *ocd* in the *occ* operon on the Ti plasmid and *arcB*
- iv) conversion of proline to glutamate by proline dehydrogenase, encoded by *putA*

All of the additional genes required were found to reside on a seperate conjugal genetic element which was not self-transmissible, but could be conjugated into other *A. tumefaciens* strains using the *tra* functions encoded on the coresident Ti plasmid. The *occ* region is known to contain the *traR* gene which is inducible by octopine.

Recent evidence suggests that some opines may also act as chemoattractants [103] and that functions within the relevant opine catabolism region are required for this chemotaxis to take place. The opine utilisation regions of many Ti plasmids have now been sequenced and well studied. Uptake of opines appears to be through ABC-type transporters, consisting of a membrane-associated permease and a periplasmic substrate-binding protein. Mutational studies have shown that it is these binding proteins that facilitate the chemotaxis response to opines. If this is the case it is likely that these proteins interact with specific chemoreceptors, as is seen in binding protein/MCP interactions in the *E. coli* chemotaxis system. The opine transporters therefore appear to have a multi-functional role, as is seen with the sugar transporter ChvE of *A. tumefaciens* (see section **1.5.4**).

1.5.3 The *vir*-Region.

Most important to the functioning of tumour-inducing *Agrobacterium* strains is a region on the Ti-plasmid known as the virulence (*vir*-) region. The *vir*-region is approximately 40kb in size and is located to the left of the T-DNA (see **Fig. 1.5.1**). Different strains of Agrobacteria encode slightly different genes in this region and differences exist between homologous genes from different strains [21, 112]. However

certain gene products can be seen to have a pivotal role in the virulence process and are present in all strains, these are the products of *virA, virB, virC, virD, virE* and *virG*. The VirA and VirG proteins form a two-component regulatory system controlling the expression of the other *vir*-genes [199]. The optimal conditions required for *vir*-induction varies for different Agrobacteria strains [218], however all require particular phenolic compounds and a pH of 5.0-5.8. Monocyclic phenolics, such as acetosyringone, have been shown to be particularly efficient *vir* inducers. Acetosyringone is known to be released naturally from wounds on plants such as tobacco. When low concentrations ($\leq$10μm) of phenolics are present, monosaccharides such as glucose [183] also play a role in the signalling process by enhancing the phenolic perception of the bacteria [3, 191]. The monosaccharides involved in sugar enhancement are all known polymeric components of dicot plant cell walls. Other vir inducers include the lignin precursors coniferyl-alcohol, sinapyl-alcohol [192], ferulic acid and sinapinic acid.

1.5.4 Detection of Wound Exudates.

VirA is an inner membrane protein, it acts as a sensor and detects phenolic compounds either directly [114] or via a binding protein. Sugars which enhance the signalling response have been shown to interact with the chromosomally encoded glucose/galactose binding protein ChvE [14, 90], which then interacts with the periplasmic domain of VirA.

ChvE is a dynamic protein, as well as its role in *vir*-induction it is also required in some species for chemotaxis and maximal growth in certain sugars. In addition it is also known to form part of an ABC-type sugar uptake system [98]. *chvE* transcription is regulated by the gene *gbpR* [60], which lies adjacent to *chvE* on the chromosome but is transcribed divergently to it. It encodes a protein (GbpR) which both positively and negatively regulates *chvE* transcription. This type of regulation is similar to that of OccR, present on octopine Ti plasmids, which regulates the genes required for the breakdown of octopine.

The VirA protein consists of four structural/functional domains [37, 114, 130, 132]; i) an input or receptor domain consisting of an N-terminal periplasmic region and two transmembrane regions (TM1 and TM2), ii) a linker domain iii) a transmitter domain containing the protein kinase function and iv) a receiver domain. The C-terminal region of VirA shows sequence homology with known bacterial sensor proteins e.g. EnvZ, PhoR, NtrB, all of which have both protein kinase and phosphotransferase activities. Plant signals cause VirA to autophosphorylate at residue H474 in the transmitter domain, it is then able to phosphorylate VirG . Phosphorylation of VirG is thought to occur at the conserved residue D52, or possibly at D8, both at the N-terminal of the protein.

Transcription of *virG* is under the control of two promoters, P1 and P2. P1 is induced by acetosyringone and phosphate limitation [4], whereas P2 is responsive to environmental stress e.g. low pH, as such it is thought to be similar to the heat shock promoters found in *E. coli* [124]. A functional copy of the chromosomally-encoded protein ChvD is required for maximal induction of the promoters.

VirG is a cytoplasmic protein, it acts as a transcriptional activator of the other *vir*-genes by binding at its C-terminal to a conserved dodecadeoxynucleotide sequence (TNCAATTGAAPy), the *vir*-box [93, 153], that occurs in the promoter regions of the *vir* operons. For correct VirG functioning, certain nonconserved sequences are also required downstream of the *vir*-box [164]. It has been proposed that requirement for these additional sequences prevents cross-talk from other homologous transducer proteins. It is not known whether phosphorylation of VirG occurs before or after binding to the *vir*-box region. However it is thought that phosphorylation aids DNA binding [82], as is known to occur with the transducer proteins OmpR, PhoB and NtrC in *E.coli*, with which VirG has sequence homology. VirG also regulates *virA* and *virG* transcription and therefore forms a positive feedback loop enhancing the infection process.

The *virA/G* system is thought to have a multifunctional role [11, 86], since at differing phenolic concentrations it is known to affect both chemotaxis [178] and *vir*-induction [63]. Low (nanomolar) concentrations trigger chemotaxis alone, higher (micromolar) concentrations also bring about *vir*-induction and can even suppress chemotaxis, thereby restricting the bacteria to the wound site and hence increasing the likelihood of infection [176].

VirA structurally resembles MCPs and has significant sequence homology to CheA. VirG also shows some similarity to both CheY and CheB. The interactions of CheA, CheY and CheB were shown earlier to involve phosphorylation and subsequent dephosphorylation events, as is seen with VirA and VirG. This, along with the fact that VirA and VirG are known to affect chemotaxis [178], seem to suggest that the pathways for *vir*-induction and chemotaxis interplay with one another, and that VirA and VirG possibly occupy the central role in a bifurcating sensory system responding to plant phenolics (see section **1.9** for further details).

1.5.5 The *vir* Genes.

Different Ti plasmids contain slightly different genes in the *vir*-region: generally, octopine Ti plasmids e.g. pTi15955, contain *virA, virB, virC, virD, virE, virF, virG,virH* (*pinF*) and *virJ*, whereas nopaline-type Ti plasmids e.g. pTiC58, contain *virA, virB, virC, virD, virE, virG* and *tzs*. The total number of *vir* genes is still being determined. Recent work by Kalogeraki and Winans [97] identified a number of additional *vir* genes in both the octopine-type Ti plasmid pTiA6NC and the nopaline-type Ti plasmid pTiC58. These

additional genes were not essential for tumourigenesis, but were postulated to have a more subtle role in the virulence process.

Of the known *vir* genes, *virA, virB, virC, virD, virE* and *virG* are the six key *vir*-regions common to all Ti plasmids. *virA* and *virG* are monocistronic while the other four *vir* loci all encode for more than one transcript and most form operons. Together they form a regulon under the control of the VirA/G two component system. The products of the different *vir* loci play important roles at different stages of tumorigenesis. Upon activation of the *vir*-genes a linear, single-stranded [212] DNA molecule (the T-strand) is formed in a 5' to 3' direction [133], from the right hand border of the T-DNA, following nicking of the border repeats surrounding the T-region.

1.5.6 Generation of the T-Strand.

VirD1 and VirD2 function together as an endonuclease causing site [91] and strand specific nicks between the third and fourth base pairs of the bottom strand of the T-DNA borders. VirD2 attaches to the 5' end of the T-strand at the right hand border nick and to the 5' end of the remaining bottom strand of the Ti plasmid at the left hand border nick. This attachment of VirD2 to the T-strand is thought to be via covalent binding of Y29 [221] of VirD2 to the T-DNA. The presence of VirD1 has been shown to be important in efficient binding. In octopine type Ti plasmids, if VirD1 and VirD2 are limiting, VirC1 aids in T-strand production by binding to the overdrive sequence [217] close to the T-DNA right hand border. This is thought to facilitate nicking of the T-DNA border.

The *virC* and *virD* operons are transcribed divergently under the control of two tandemly arranged promoters. One promoter is responsive to VirG and the other is responsive to the product of the chromosomally encoded gene *ros* [49, 50], which represses the operons. The Ros protein [52] is found in octopine and nopaline strains. It binds to a 40bp sequence bearing a 9bp inverted repeat (TATATTTCA/TGTAATATA), the Ros box, that overlaps the *vir*-box of the *virC* and *virD* loci. It is thought that the action of *ros* is to modulate the amount of T-DNA intermediates formed. Interestingly a *vir*-box-like sequence has been identified upstream of the chromosomal *ros* gene, suggesting that at high levels of induction and hence high levels of VirG, VirG is able to repress transcription of *ros*.

1.5.7 The T-Complex.

The T-strand is transferred from bacterium to plant as a protein-nucleic acid complex, the T-complex, consisting of the T-DNA, bound VirD2 and VirE2. VirE2 is a single stranded DNA binding protein [60]. When bound it renders the ssDNA completely resistant to 3' and 5' exonucleases and endonucleases *in vitro*. It is therefore thought to

have a protection role in the production of the T-strand. The nopaline specific T-complex is 3600nm long and 2nm wide and as such is thought to be made up of 1 T-strand, 1 molecule of VirD2 and approximately 600 molecules of VirE2. It is not known whether the T-strand and VirE2 are transported to the plant cell attached or separately, but both VirD2 and VirE2 are known to be essential for transfer and integration. VirE1 is also involved in T-DNA transfer and has been shown to be essential for the export of VirE2 from the bacterial cell. The export of T-strands however is not dependent on its presence, therefore indicating that separate transfer of VirE2 and the T-strands is likely. Research suggests that VirE2 is a necessary element once inside the plant cells, but is not an absolute requirement in the bacterium [75].

1.5.8 Transfer of the T-Complex [182].

For intercellular transport of the T-complex to occur from the bacterial cell, into the cytoplasm of the plant, it is thought that a channel is formed by the bacterium, although still little is known of the fine details of this process. The channel is likely to be encoded by the *virB* locus, consisting of 11 orfs, the products of all but one (*virB1*) of which are essential for virulence. Evidence suggests that VirB1 is exported through the bacterial membranes and may mediate docking of the *virB* channel at the cell surface. Extensive studies are currently being conducted on the *virB* locus, and it is proposed that the resulting T-DNA transfer machinery is homologous to bacterial conjugal DNA transfer systems. All of the VirB proteins show homology with different Tra proteins of the bacterial conjugal transfer systems of IncN, IncP and IncW plasmids and also of the F plasmid of *E. coli.* Recent work by Lai [119] suggests that VirB2 is a homologue of TraA, which forms the pilin subunits of the F pilus, it being similar in amino acid sequence, protein size and processing. This suggests that a conjugative pilus, the "T pilus", could be encoded by the *vir* genes, primarily *virB2*. Further evidence to support the formation of such a pilus and subsequent conjugation-like transfer of the T-DNA, comes from studies which have shown that elements of the *vir*-system alone are able to bring about transfer of mobilisable, but nonconjugal plasmids, such as RSF1010, between *Agrobacterium* strains.

The products from nine of the *virB* genes are associated with the bacterial membranes. Both VirB9 and VirB10 form separate, membrane-associated complexes, VirB9 is required for formation of the VirB10 complex, probably having a stabilising role. In a similar way VirB7 and VirB8 are required for formation of the VirB9 complex. This co-ordinate synthesis suggests that a multiprotein channel could be formed. Transport of the T-complex through such a channel is likely to be energy dependent, this energy could be derived from the VirB4 and VirB11 proteins located at the inner bacterial membrane.

A third protein from the *virD* locus, VirD4, is essential for virulence [116, 142] and is thought to link the transported T-complex with the *virB* channel. It contains a possible

ATPase consensus sequence and therefore could generate the energy to promote T-complex transport through the channel.

1.5.9 T-DNA Integration.

Many of the processes and genes involved in virulence have been shown to be highly related to the bacterial conjugation system [149, 156]. However, differences occur once the T-complex has entered the plant cell and requires entry into the cell nucleus. It is likely that an endogenous plant cellular pathway is used for this crucial step. The nopaline-type T-complex has a molecular weight of approximately 50,000kDa, while the size exclusion limits of the nuclear pore is about 60kDa [182]. It is therefore obvious that active transport must be involved. In order to be transported into the plant cell, by the plant, the T-complex must contain Nuclear Localisation Signals (NLSs) recognised by the plant [13]. VirD2 contains two such NLSs [167, 213], one, of the monopartite form, at the N-terminal [87] and a second, of the bipartite form at the C-terminal [89]. VirE2 also contains two functional NLSs. Research has shown that all of the identified NLSs are functional [43, 44]. However the extent to which the different signals play a role in nuclear localisation of the T-complex in different plant species is still unknown, and it is possible that they are developmentally regulated [43].

Upon entering the plant cell nucleus the T-DNA has to become integrated into the host cell genome. Sequencing of integrated junctions has shown that the right hand borders show great precision. It is therefore thought that VirD2 is involved in the integration process, perhaps having a ligase function. The omega domain of VirD2, which is a sequence of 5 amino acids (DGRGG) found adjacent to the NLS at the C terminus of VirD2 [186], is thought to be involved in the integration process, although it is not essential for efficient transfer of T-DNA [32]. It is also possible that VirE2 plays a role in T-DNA integration [60]. Also unknown is whether integration precedes synthesis of the second DNA strand or if a double stranded molecule is formed before integration.

For T-DNA insertion into the plant genome to be successful, it is likely to involve proteins transported from the bacterium [106] as well as certain components of the host cell. Work by Escudero and Hohn [66] has shown that T-DNA integration does not necessarily require the triggering, by wounding, of specific DNA metabolic activities in the plant cell, as had previously been postulated. The precise plant mechanisms utilised for T-DNA integration are therefore still ill-defined. Research suggests however that it may be a block in this final integration process that prevents efficient transformation of many monocot plants by *A. tumefaciens* [211].

1.5.10 Chromosomal Virulence Genes [182].

In addition to the Ti-encoded genes required for efficient infection and transformation of plant cells, several loci on the bacterial chromosome are also known to be important for this process to occur. The products of these genes are primarily involved in the initial attachment and *vir* gene induction steps of the infection process. However there are also other genes whose function is as yet unknown, e.g. *acvB* which shows significant homology to the *virJ* gene found on octopine-type Ti plasmids [96] (also of unknown function).

Several chromosomal genes are thought to involved in the attachment process, these include *chvA, chvB, attC43, attC69* and *psca*. Mutants in either of the two constitutively expressed chromosomal virulence genes *chvA* and *chvB* are avirulent. It is known that ChvB is required for the synthesis of cyclic β-1,2-glucan [35], and ChvA is required for its export. Rhicadhesin, the bacterial protein required for attachment, is thought to need β-1,2-glucan for correct functioning, hence explaining the phenotypes of *chvA* and *chvB* mutants. Work by Swart *et al* [207] however showed that the virulence of *chvB* mutants could be restored by growth in a highly osmotic medium. This suggests that cyclic β-1,2-glucan is not required for virulence and attachment, but only indirectly influences these properties through an osmoregulatory effect. The cellulose biosynthesis genes required in the later stages of attachment are also chromosomally encoded [126] (see section **1.5.1**).

The chromosomal genes necessary for *vir* gene induction include *chvD* and *chvE* which were discussed in section **1.5.4**.

In addition to the chromosomal virulence genes thought to be present in all Agrobacteria strains, it is also thought that different strains may contain specific chromosomally encoded genes that enable them to colonise different plant species. Recently a strain of *A. tumefaciens* was identified that was found to naturally infect Alfalfa plants. Alfalfa releases flavanoids into the soil which generally have negative effects on most *A. tumefaciens* species and therefore prevent most strains from being able to infect it. Subsequent study of the new *A. tumefaciens* strain (strain 1D1609) showed it to contain a chromosomal locus absent from other strains. The genes *ifeABR* were identified and proposed to encode an isoflavanoid efflux pump that reduces the cellular accumulation of harmful isoflavanoids [148].

Many of the chromosomal virulence genes of *A. tumefaciens* have homologous and functionally interchangeable counterparts in the related bacterium *S. meliloti.* This fact therefore suggests that members of the *Rhizobiaceae* may have a conserved, chromosomally-encoded, attachment mechanism forming the basis of their pathogenic responses.

1.5.11 Conjugal Transfer of Ti plasmids.

Ti plasmids are transmissible by conjugal transfer between Agrobacteria strains, as well as from Agrobacteria strains to other Gram negative bacteria, such as *E. coli.* Previously it was described that the *vir* system is able to facilitate the transfer between Agrobacteria strains, of IncQ plasmids such as RSF1010 [20]. The *vir* proteins could therefore be involved in the conjugal transfer of Ti plasmids between Agrobacterial hosts [200]. Mutations in the *vir* genes however do not affect interbacterial conjugation, a distinct conjugation system therefore exists for Ti plasmid transfer [48].

Studies of both octopine- and nopaline-type Ti plasmids have identified the regions required for bacterial conjugation. The nopaline-type Ti plasmid pTiC58 contains three distinct regions all involved in conjugal transfer:

The first region, *tra*, contains the origin of transfer (*ori*T) [47] flanked by two divergently transcribed clusters of three *tra* genes (*traAFB* and *traCDG*). The products from three of which show homology with proteins from other conjugal transfer systems.

The second region, *trb*, which is about 100kb distal to region one, consists of 12 *orf*s, 11 of which show significant homolgy to the *trb* genes of RP4 which are involved in mating pair formation and facilitating DNA transfer from donor to recipient. The twelfth gene in this region, *traI*, encodes production of an N-acyl homoserine lactone [231] called *Agrobacterium* AutoInducer (AAI).

The third region, TraI, encodes *traR*, the product of which is the transcriptional activator TraR [155].

Plant cells infected by *A. tumefaciens* produce specific opines. A subset of these, the conjugal opines, induce *Agrobacterium* Ti plasmid donor strains to produce a diffusable chemical, AAI. This, in conjunction with the transcriptional activator TraR, induces expression of the *tra* and *trb* genes necessary for conjugal transfer to occur.

Ti plasmids can therefore be thought of as possessing two genetically independent conjugal transfer systems, the *tra* system required for bacterial conjugation, and the *vir* system modified for DNA transfer from bacteria to plant cells. As a result several researchers have postulated the idea that Ti plasmids could have evolved from the fusion of two or more plasmids [2, 69], where one has retained its function for bacterial conjugation and the other has been modified to allow inter-Kingdom transfer of DNA.

Recent work by Chumakov and Kurbanov [42] identified two different types of pili involved in conjugal transfer of Ti plasmids between Agrobacterial cells. Initial cell contact was found to be mediated by long pili. Acetosyringone-induced cells however, also produced shorter pilus-like structures, consisting of the protein VirB1, which facilitated closer contact of the cells. It was therefore postulated that there could be some integration of the two transfer systems.

1.6 Flagellation and Motility in *A. tumefaciens* and Related Bacteria.

A. tumefaciens has a polar tuft of two flagella, and two to four lateral flagella (see **Fig. 1.4.3**), which are composed of up to four different types of flagellin [39, 54, 56]. As in *E. coli*, the flagella are often much longer than the cell itself. However unlike enteric species the flagella only rotate in one direction, CW. Rotation of the flagella causes the bacteria to run, often for relatively long distances (frequently in excess of 500μm) [118], hence changes in direction are infrequent. The means of changing direction is still unknown for *A. tumefaciens*. The strain used in this work (C58C1) is known to be an active swimmer [118].

R. sphaeroides has a single lateral flagellum, composed of one type of flagellin, which arises from the middle of the long side of the cell. The flagellum only rotates in one direction, usually CW. CCW variants have been identified, but switching of either type has never been observed. Rather than switching, *R. sphaeroides* cells show a swimming and stopping motility. When the motor stops the flagellum forms into a large amplitude coil close to the cell body which slowly rotates and reorientates the cell. In addition the speed of rotation of the flagellum can also vary [146]; it therefore shows a far more complex pattern of motility to that seen in *E. coli.*

S. meliloti has a bundle of two to six "complex" flagella, which are composed of more than one type of flagellin. The flagella only rotate in one direction, CW. The flagella do not switch direction or stop, but rather the cells are able to reorientate by changing the speed of individual motors, which causes the filaments to separate and hence turns the cell. Recent studies have shown that *S. meliloti* cells are able to respond chemotactically by modulating their rate of flagellar rotation, rather than switching the direction of flagellar rotation [193, 194]. CheYII is thought to be the primary regulator of this process, with possible modulation through CheYI, either by competition for phosphate from CheA or by differential interactions of the two at the flagellar motor. CheYII has been termed the "slow" signal for the motor, rather like the CheY-P "tumble factor" of *E. coli*, and CheYI is thought to act as a signal terminator by serving as a phosphate sink for both CheA-P and CheYII-P. (*S. meliloti* contains two *cheY* genes - see section **1.7**). In addition two novel motor genes, *motC* and *motD* have recently been identified in *S. meliloti*, the products of which are thought to vary flagellar rate at a constant proton motive force.

1.7 Chemotaxis Genes Identified in *R. sphaeroides* and *S. meliloti* .

In recent years there has been intensive study into the chemotaxis systems of *S. meliloti* and *R. sphaeroides.* Results have shown both to contain more complex

chemosensory systems to that seen in *E. coli.* This probably reflects the diverse environments in which they live, as compared with enteric bacteria. Similarities can be seen however between the individual chemotaxis systems of the two bacteria, possibly reflecting conserved patterns of chemotactic signalling within the α-subgroup of *Proteobacteria* as a whole [9].

Two chemosensory regions have been identified in *R. sphaeroides* [81] which contain homologues of several of the chemotaxis genes identified in *E.coli.* Together there are three copies of *cheW* [80] and *cheY*, two copies of *cheA* and *cheR*, and one of *cheB*, as well as five *orf*s of unknown function and three *tlp* (transducer-like protein) genes. It is also postulated that *R. sphaeroides* may contain a third signal transduction pathway [165]. *R. sphaeroides* exhibits two distinct chemoresponses; chemotaxis and chemokinesis [145].

A single chemosensory region has been identified in *S. meliloti* [78], which again contains homologues of known chemotaxis genes. There is one copy of *cheA, cheW, cheD* (*che* gene found in *B. subtilis*), *cheR* and *cheB*, two of *cheY*, one unknown *orf* and one *tlp*.

The gene order in both the regions from *R. sphaeroides* and the region from *S. meliloti* show a high degree of similarity, however the arrangement is very different to that seen in *E. coli*:

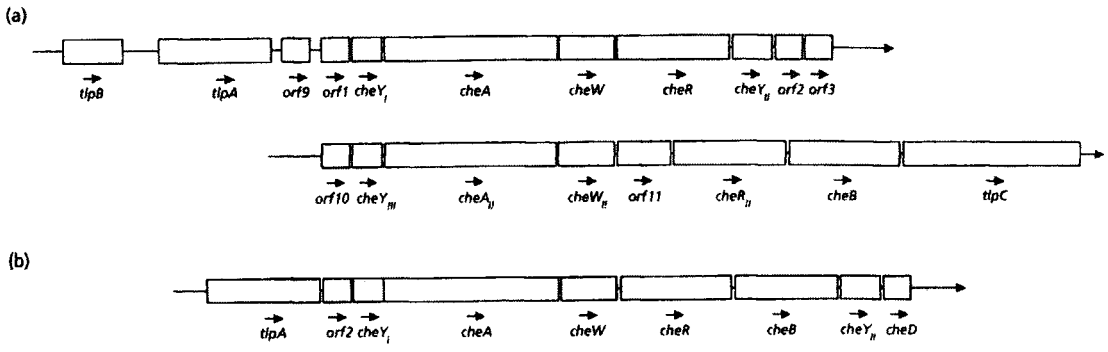

Fig. 1.7 The chemosensory regions identified in a) *R. sphaeroides* and b) *S. meliloti.* Figure reproduced from [9]. In diagram (a) orf11 = $cheW_{III}$.

Most notable in both cases is the lack of a *cheZ* homologue and the presence of at least two copies of the response regulator CheY. Recent work on *E. coli* has shown that the phosphatase, CheZ, is not always essential for chemotaxis. It is therefore possible that *R. sphaeroides* and *S. meliloti* have no requirement for such a protein or that its function is encoded by a different protein.

Multiple copies of *cheY* (and other chemotaxis genes in *R. sphaeroides*) most likely reflect the different patterns of motility and hence the requirement for a more complex regulation of chemotaxis, than is seen in *E. coli.*

Also of interest are the *tlp* genes, which code for transducer-like proteins. All of the identified Tlp proteins show regions of homology at their C-terminal with MCP signalling domains, however they appear to be largely cytoplasmic, unlike the MCPs which are membrane spanning. Therefore due to their apparent lack of a sensing domain it is thought that they may interact with other, probably membrane spanning, proteins through which they can mediate a chemotactic response.

At least four putative MCPs have been identified in *S. meliloti*, one of these, *mcp*C, has been sequenced and appears to more closely resemble the 'classical' MCP configuration, however it is located distally to the other chemotaxis genes identified. It has also recently been reported that *R. sphaeroides* may contain as many as twelve MCP-like genes, expressed under different growth conditions [84].

1.8 Chemotaxis and Motility Genes in *A. tumefaciens.*

It has been shown that *A. tumefaciens* is likely to possess a methylation-dependent chemosensory system [177]. Work by Brown *et al* showed that *A. tumefaciens* requires methionine for chemotaxis to occur. Proteins were identified that were found to be specifically methylated. These proteins were of a similar size (60-65kDa) to the MCPs found in *E.coli.* Western blots using a polyclonal antibody to the *E.coli* MCP Tar also identified proteins of a similar size in *A. tumefaciens.* Furthermore several DNA fragments were identified that hybridised with a synthetic oligonucleotide complimentary to the conserved signalling domain of *E. coli* MCPs.

In addition it has also recently been reported that the Ti-plasmid pTiC58 contains a protein bearing significant sequence homology to known MCPs. The Ti-plasmid pTi15955 also contains a gene (*mcl*) whose product shows significant identity with the C-terminal of known MCPs [141]. Both of the MCP-like genes identified, occur close to opine transport regions.

In order to study the chemotaxis / motility system of *A. tumefaciens* in more detail Tn5 mutagenesis was carried out and resulting behavioural mutants selected [181]. Twenty independent mutants were selected and subdivided into a number of classes. Preliminary phenotypes were assigned to the mutants after analysis on agar swarm plates and viewing by light and electron microscopy. There were 7 non-flagellate (*fla)* mutants, 7 flagellate but non-motile (*mot)* mutants, 1 non-chemotactic (*che*) mutant, 4 mutants with impaired swarming ability and 1 mutant that displayed an unusual pattern of polar cell pairing.

A library of C58C1 genomic DNA was created in the cosmid pLAFR3. A total of 1200 seperate clones were created, each containing an insert of approximately 20-25kb of *A. tumefaciens* genomic DNA. Due to the method of construction of the Tn5 mutants (described by Shaw in [176]) it was possible to isolate the flanking sequence from the Tn5 mutants and use it as a radiolabelled probe to the *A. tumefaciens* cosmid library. Hybridising cosmid clones were then used in complementation studies on the relevant mutant strain and any other strains that hybridised with the cosmid.

One clone, pDUB1900, was found to either complement, or hybridise to, eight of the Tn5 mutants.

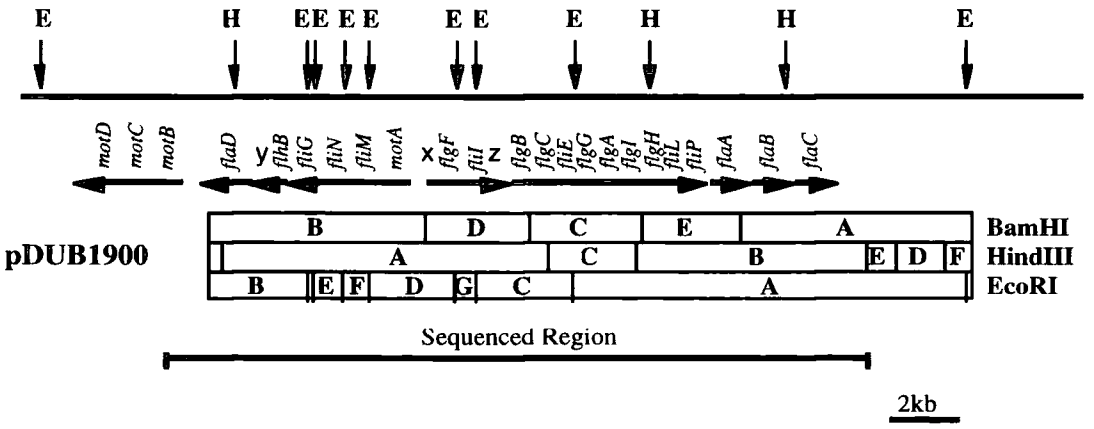

Fig. 1.8 ***A. tumefaciens fla-mot*** **cluster 1.** Figure adapted from [56].
The *Eco*RI (**E**) and *Hpa*I (**H**) sites within the cluster are indicated on the top line. Boxes denote the *Bam*HI, *Eco*RI and *Hin*dIII sites within the chromosomal insert of cosmid pDUB1900.

pDUB1900 contains a 25kb region of the *A. tumefaciens* chromosome. The nucleotide sequence of approximately 22kb of this cosmid has been fully characterised and found to contain homologues of genes primarily involved in flagellar structure and asssembly (see **Fig. 1.8**) [55, 57].

A further clone, pDUB1905, was found to complement three of the remaining Tn5 mutants. Initial sequencing work identified homologues of *fliR* from *E.coli* and *cheL* from *C. crescentus i*n the cosmid pDUB1905.

Analysis of both these and other identified cosmid clones has shown that the organisation of flagellar operons in *A. tumefaciens* is significantly different from that of the enteric bacteria, but shows significant homology with that of the closely related bacterium *S. meliloti.*

1.9 The Significance of Chemotaxis in *A. tumefaciens*.

A great deal is known about the molecular events involved in the *Agrobacterium*-plant interaction process. In particular much is known about the genes involved and how the gene products interact to bring about transfer of the T-DNA to plant cells [182]. Furthermore in recent years there has been a great deal of interest in the genes involved in opine synthesis and catabolism. Less, however, is known about the chemosensory system of *A. tumefaciens,* the fundamental system underlying virulence.

Work by Loake *et al* [118] showed C58C1 to have a highly sensitive chemotaxis system that responded to micromolar concentrations of plant sugars. The greatest response seen was to sucrose. This gave a maximal chemotactic response at a concentration of 10^{-6}M, some 1000-fold lower than the concentration required for a maximal response in *E. coli.* ChvE is known to be required for chemotaxis to certain sugars [34]. In its role in sugar enhancement of phenolic perception by virulent strains of *A. tumefaciens*, ChvE has been shown to interact with the Ti-encoded VirA protein. The studies by Loake *et al* used the avirulent strain C58C1, chemotaxis requiring ChvE is therefore likely to be mediated by a chromosomally encoded chemoreceptor, possibly with similarity to the MCP Trg. Indeed as mentioned in section **1.8** there is significant evidence to suggest that *A. tumefaciens* may contain such proteins.

A. tumefaciens is known to accumulate within and around the plant rhizosphere. This ability to accumulate and maintain position within the rhizosphere, whilst also competing with other root-colonising organisms, is most likely due to the highly sensitive chemotactic responses exhibited by *A. tumefaciens.*

Although a ubiquitous soil organism, the relative numbers of pathogenic *A. tumefaciens* strains, as compared with non-pathogenic strains, is often very low (pathogenic strains often constitute <1% of the *A. tumefaciens* strains within a given area of soil). This therefore raises the question whether the presence of a Ti plasmid offers pathogenic strains any competitive advantage over other strains.

Work by Ashby *et al* [12] showed chemotaxis to the plant phenolic compound acetosyringone (AS) occurred only when a Ti plasmid was present within the bacteria [12]. In addition it was shown that the concentration of acetosyringone required for optimal levels of chemotaxis (10^{-7}M) was some 100-fold lower than that required for maximal induction of the *vir* genes (10^{-5}M). A range of phenolic wound exudates were studied [11] and found to constitute three different groups:

- i) those that were strong *vir*-inducers and required a Ti plasmid for chemotaxis
- ii) those that were weak of non-*vir*-inducers and were attractants with or without a Ti plasmid
- iii) those that were non-*vir*-inducers and non-attractants.

Subsequent work identified VirA and VirG as the Ti-encoded components required for chemotaxis to occur [178]. It is therefore postulated that VirA and VirG are able to mediate two responses according to the concentration of *vir*-inducer encountered. At low *vir*-inducer concentrations the *virA/G* system triggers chemotaxis, whilst at high concentrations of *vir*-inducer it leads to *vir*-induction. The process of *vir*-induction (described in section **1.5**) is known to require VirA and VirG in the form of a two-component signalling system. Chemotaxis to wound exudates also requires phosphorylation of VirA and VirG [147]. The exact mechanism by which phosphorylation of VirA/G is able to mediate two responses to differing concentrations of wound exudates is unknown. It has been shown that the periplasmic domain of VirA is essential for chemotaxis, whereas only the cytoplasmic regions of VirA are required for *vir*-induction. The subtle differences in structural requirements of VirA/G for the two different processes indicate a possible bifurcation in the sensory system. A hypothesis has been proposed to explain this bifurcation in the sensory system [177] (see **Fig. 1.9** and subsequent text).

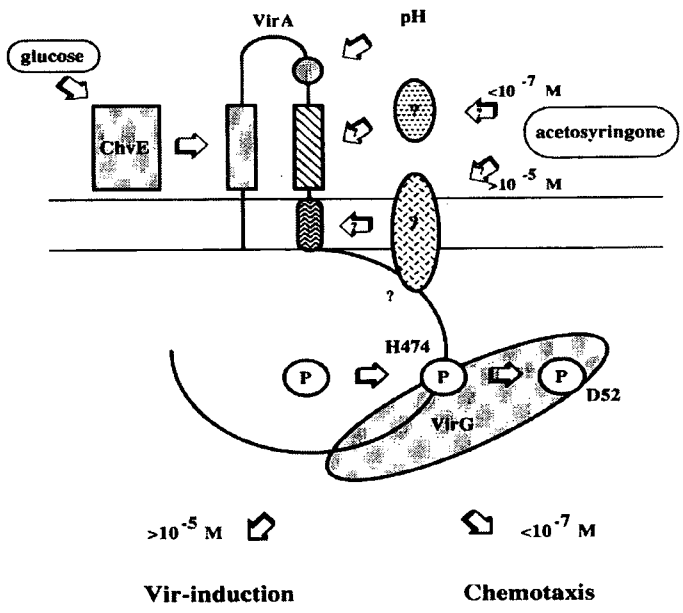

Fig. 1.9 Hypothetical scheme for phenolic sensing in *A. tumefaciens*. Figure reproduced from [177].
Direct sensing domains of VirA are blocked, question marks indicate hypothetical events, those in ovals represent putative PBPs. H474 and D52 are phosphorylated amino acids in VirA and VirG respectively. Upper portion: periplasm; lower: cytoplasm.

Sensing of phenolics is postulated to be mediated by interaction with two distinct types of phenolic-binding proteins (PBPs), each possessing different affinities for specific phenolics. It is suggested that sensing of acetosyringone is by two PBPs. A high-affinity

PBP (possibly periplasmic) that interacts with the periplasmic domain of VirA, and a low-affinity PBP (possibly membrane-bound) that associates with the cytoplasmic linker domain of VirA. At low acetosyringone concentrations the high-affinity PBP could activate VirA and lead to low levels of VirG phosphorylation. The limited phospho-VirG (VirG-P) could have a higher affinity for the chromosomally encoded chemosensory pathway than the *vir* box. Hence mediating a rapid chemotactic response at low acetosyringone concentrations. On encountering higher acetosyringone concentrations, the low-affinity PBP could trigger greater levels of phosphorylation of VirG. Hence resulting in the production of sufficient VirG-P to allow binding to *vir* box regions.

The exact mechanism of phenolic-VirA interaction is still unknown. It is not certain whether phenolics bind directly to VirA or act through specific phenolic-binding proteins. Lee *et al* [111] identified two chromosomally-encoded proteins (p10 and p21) that specifically bound the *vir* gene inhibitor α-Bromoacetosyringone (ASBr). It was therefore postulated that these proteins could act as possible phenolic-binding proteins, mediating the *vir*-induction response to phenolics. More recent work however suggests that phenolics interact directly with VirA [113, 114].

All the work to date has centred on the VirA-phenolic interaction that mediates the *vir*-induction process. None of the work has investigated the ability of VirA to mediate chemotaxis in response to phenolics. To allow detection of phenolics at nanomolar concentrations it seems plausible that a PBP could be involved. Such a protein would constitute a "scavenging" mechanism giving the bacterium a greater likelihood of detecting very low levels of phenolics than would VirA alone. Whether such a protein also mediates the *vir*-induction response seems more questionable, due to recent evidence to the contrary. Work by Lee *et al* [114], involving the transfer of different Ti plasmids into isogenic chromosomal backgrounds, showed that phenolic sensing for *vir*-induction was associated with the Ti plasmid, and in particular with VirA. It is therefore possible that phenolics could be detected by both PBPs and directly by VirA, hence allowing two specific responses to differing concentrations.

Contradictory results have been reported for the requirement of VirA and VirG in AS-mediated chemotaxis [150]. However the use of a less motile strain of *A. tumefaciens* [118] seems to account for this difference of opinion.

Work by Hawes *et al* [85, 86] on the pathogenesis of *A. tumefaciens* on pea plants, demonstrated chemotactic movement in response to specific root exudates. In addition by the use of different growth media the importance of chemotaxis to the pathogenesis of *A. tumefaciens* was demonstrated. In natural habitats it would therefore appear that a loss of chemotactic ability would be a crucial limiting factor in the pathogenesis of *A. tumefaciens*. In support of this idea is the fact that non-chemotactic mutants of *Rhizobium* species have been shown to have reduced nodulation efficiency and overall

competitiveness (the process of nodulation showing a great deal of similarity with the virulence system of *A. tumefaciens*).

A. tumefaciens is known to contain a highly sensitive chromosomally-encoded chemosensory system [118]. The action of which, it is proposed, enables *A. tumefaciens* to localise and maintain in significant populations in the plant rhizosphere. Within the rhizosphere it is then possible that pathogenic strains have a competitive advantage over others due to their enhanced responses to certain wound exudates. Such an enhanced chemotactic response could direct pathogenic strains to possible infection sites and hence ultimately to exclusive carbon and nitrogen sources.

Further support to the importance of chemotaxis in the pathogenicity of *A. tumefaciens* comes from recent work by Kim and Farrand [103]. It has been shown that certain *Agrobacterium* strains are chemoattracted to opines, and that this chemotaxis is Ti-dependent. The chemotactic response to opines was shown to require functions encoded by the opine catabolism operons of the Ti-plasmids. It is thought that chemotaxis does not require transport and catabolism of the opine, as is true for many chemotactic responses. It has therefore been proposed that the periplasmic binding proteins of the ABC-type transport systems of specific opines also act as primary receptors for chemotaxis to their cognate opine. Hence suggesting interaction of these binding proteins with a chromosomally-encoded MCP-like protein. Chemotaxis to opines could therefore be deemed as aiding the pathogenesis of *A. tumefaciens*. Since it could lead to increased accumulation of pathogenic strains at infection sites and therefore enhance the overall infection process.

Sensing and responding to environmental cues is therefore thought to be essential to the pathogenicity and survival of *A. tumefaciens* within the soil [179]. What now remains to be determined is how *A. tumefaciens* is able to respond chemotactically, and how the Ti-encoded *vir* genes are able to integrate with this system.

1.10 Aims of This Work.

The primary aims of this work were to identify and characterise the chromosomally-encoded chemosensory system known to exist in *A. tumefaciens*. Evidence to date, from *A. tumefaciens* and studies on the related bacterium *S. meliloti*, suggested that *A. tumefaciens* may possess a chemotactic system fundamentally related to that of *E. coli.*

Preliminary work by T. Goswami, using *cheA* from the *S. meliloti che* operon as a heterologous probe, identified specific hybridising bands in *A. tumefaciens* genomic DNA. Therefore indicating that *A. tumefaciens* contained genes homologous to the *che* genes identified in *S. meliloti.*

It was planned to use the same probe to identify clones from the *A. tumefaciens* cosmid library that contained possible chemotaxis related genes. Upon identification of possible positive clones, they were then to be studied, initially by sequencing and database analysis, to identify regions bearing significant homology to known *che* genes.

Depending on the number of genes identified, it was proposed to study the function of each gene by site-directed mutagenesis and phenotypical analysis of the resulting mutant strains.

In addition to identifying and characterising the chromosomal chemosensory system of *A. tumefaciens,* if time permitted, it was also hoped to investigate possible interactions of this system with the Ti-encoded virulence system. This was to be done by carrying out tumourigenicity studies and chemotaxis assays on mutant strains with and without Ti plasmids. In addition, to study possible interactions more directly, it was hoped to devise a selectively-infective phage system. Hence enabling studies of interactions between specific proteins, and also possibly for use in screening an *A. tumefaciens* library to identify proteins interacting with specific gene products e.g. CheA or VirA.

2 Materials and Methods.

2.1 Materials.

All inorganic chemicals were of AnalaR quality and purchased from BDH Chemicals Ltd., Poole, Dorset, U.K. unless otherwise specified.

All organic chemicals and enzymes were from Sigma Chemicals Plc., Poole, Dorset, U.K. unless otherwise specified.

Lab M Nutrient Broth (no.2), Lab M Nutrient Agar, nylon hybridisation transfer membranes and radiochemicals were from Amersham Ltd., Bury, U.K..

Agar bacteriological (no.1) and yeast extract were from Oxoid Ltd., Basingstoke, Hants., U.K..

Trypticase Peptone was from BBL, Cockeysville, U.S.A..

Restriction endonucleases, T4 DNA ligase, Klenow enzyme, Taq polymerase, corresponding buffers, DNA markers, X-gal, IPTG and wild type λ DNA were from NBL, Cramlington, Northumberland, U.K., Boehringer Mannheim (UK) Ltd., Lewes, U.K., or Helena Biosciences, Tyne & Wear, U.K..

Agarose was from BRL, Gaithersburg, U.S.A..

Metaphor Agarose was from FMC BioProducts, Rockland, U.S.A..

Ficoll 400 and Sephadex G-50 were from Pharmacia Fine Chemicals, Uppsala, Sweden.

Vacuum grease was from Dow Corning S. A., Seneffe, Belgium.

Fuji RX-100 X-ray film was from Fuji Photo Film Co., Ltd., Japan.

Polaroid film was from Polaroid (UK) Ltd., St. Albans, Hertfordshire, U.K..

Filter paper (3MM) and laboratory sealing film were from Whatman International Ltd., Maidstone, U.K..

Minisart filters were from Sartorius GmbH, Postfach 3243, D-3400 Göttingen, Germany.

Nitrocellulose discs (25 mm, 0.22 μm pore size) for tri-parental matings were from Schleicher and Schuell, Postfach 4, D-3354, Dassel, Germany.

Oligonucleotides for use in sequencing and PCR analysis were from MWG-Biotech, Germany and PE-Applied Biosystems UK, Cheshire, U.K..

Kalanchöe diagremontiana plants for use in tumourigenicity studies were supplied by the Botanic Gardens, Durham, U.K..

2.2 Bacterial Strains and Plasmids.

2.2.1 *E. coli* Strains.

Strain	Characteristics	Resistance	Source
DH5α	F- *supE44 ΔlacU169 (f80 lacZΔM15) hsdR17 recA1 endA1 gyrA96 thi-1 relA1.*		Lab. stock [235]
XL1-Blue	F' *supE44* Tn*10 lacZΔM15 hsdR17 recA1 endA1 gyrA96 thi-1 relA1.*	Tc^R	Lab. stock

2.2.2 *A. tumefaciens* Strains.

Strain	Characteristics	Resistance	Source
C58C1	Ti-cured strain of C58.	Rif^R	Lab. stock [234]
C1-ANeo	Chemotaxis mutant - created by insertion of a neomycin cassette into *cheA.*	Rif^R Neo^R	This study
C1-orf1Neo	Chemotaxis mutant - created by insertion of a neomycin cassette into *orf1.*	Rif^R Neo^R	This study
C1-del10	Chemotaxis mutant - created by in-frame deletion of *orf10.*	Rif^R	This study
C1-Adel	Chemotaxis mutant - created by in-frame deletion of *cheA.*	Rif^R	This study
C1-FNeo	Motility mutant - created by insertion of a neomycin cassette into *fliF.*	Rif^R Neo^R	This study
C1-delche	Chemotaxis mutant - created by deletion of the entire *che* region ("gutted strain").	Rif^R	This study

2.2.2.1 *A. tumefaciens* Mutant Strains Containing Cosmid Clones.

Strain	Characteristics	Resistance	Source
C1-ANeo/1911	C1-ANeo containing pDUB1911.	Rif^R Neo^R Tc^R	This study
C1-Adel/1911	C1-Adel containing pDUB1911.	Rif^R Tc^R	This study
C1-delche/1911	C1-delche containing pDUB1911.	Rif^R Tc^R	This study

2.2.2.2 *A. tumefaciens* Strains Containing Ti Plasmids.

Strain	Characteristics	Resistance	Source
C1del71	C58C1 containing pDUB1003/Δ71.	Ery^R Cm^R Kan^R	Lab. stock
C1del77	C58C1 containing pDUB1003/Δ77.	Ery^R Cm^R Kan^R	Lab. stock
C1/71	C58C1 containing pDUB1003/Δ71.	Rif^R Kan^R	This study
C1/77	C58C1 containing pDUB1003/Δ77.	Rif^R Kan^R	This study
C1-del10/71	C1-del10 containing pDUB1003/Δ71.	Rif^R Kan^R	This study
C1-del10/77	C1-del10 containing pDUB1003/Δ77.	Rif^R Kan^R	This study
C1-Adel/71	C1-Adel containing pDUB1003/Δ71.	Rif^R Kan^R	This study
C1-Adel/77	C1-Adel containing pDUB1003/Δ77.	Rif^R Kan^R	This study
C1-delche/71	C1-delche containing pDUB1003/Δ71.	Rif^R Kan^R	This study
C1-delche/77	C1-delche containing pDUB1003/Δ77.	Rif^R Kan^R	This study

2.2.3 *R.meliloti* Strains.

Strain	Characteristics	Resistance	Source
***R. meliloti* 1021**	Derivative of Su47.	$Strep^R$	Lab. stock

2.2.4 Plasmids.

2.2.4.1 Plasmid Vectors.

Plasmid	Characteristics	Resistance	Source
pBluescriptII SK+	2.96kb *E. coli* vector.	Amp^R	Lab. stock
pUC18	2.69kb *E. coli* vector.	Amp^R	Lab. stock
pJQ200mp18	Suicide vector for *A. tumefaciens* with polylinker of M13mp18 and *sacB*.	Gm^R	Lab. stock [161]

pJQ200uc1	Suicide vector for *A. tumefaciens* with *sacB*.	Gm^R	Lab. stock [161]
pK18*mobsacB*	Allelic exchange vector for *A. tumefaciens*, with *sacB*.	Kan^R	Gift from P. Hamblin [173]

2.2.4.2 Recombinant Plasmids Containing Cloned Chemotactic Genes.

Plasmid	Characteristics	Resistance	Source
pRU1221	10.2kb chromosomal *che* region of *S. meliloti* RU11/101 with Tn5 insertion in *orf1* - cloned into pJOE890.	$Amp^R Kan^R$	Gift from R. Schmitt [78]
pRmelW	1.85kb *Xho*I fragment from *S. meliloti che* operon containing *cheW* -cloned into pIC20R	Amp^R	Gift from V. Sourjik
pMCP3.B	1.8kb *Eco*RI/*Pst*I fragment from *Rhizobium leguminosarum* containing putative MCP gene - cloned into SK+.	Amp^R	Gift from C. Yost
pMCP3.2.7P	*R. leguminosarum* MCP3 subclone in pUC4K derivative.	Amp^R	Gift from C. Yost
pDUB1909	A C58C1 cosmid library clone containing a *Bam*HI chromosomal fragment in the vector pLAFR-3 (carries chemotactic genes).	Tc^R	This study
pDUB1911	A C58C1 cosmid library clone containing a *Bam*HI chromosomal fragment in the vector pLAFR-3 (carries chemotactic genes).	Tc^R	This study
pDUB1913	A C58C1 cosmid library clone containing a *Bam*HI chromosomal fragment in the vector pLAFR-3 (carries chemotactic genes).	Tc^R	This study

2.2.4.3 Recombinant SK+ Plasmids Containing Subcloned *Agrobacterium* Chemotactic Genes.

Plasmid	Characteristics	Resistance	Source
pELW1	pBluescriptII SK+ containing 4.0kb *Hin*dIII fragment from pDUB1911.	Amp^R	This study
pELW2	pBluescriptII SK+ containing 4.0kb *Hin*dIII fragment from pDUB1911.	AmpR	This study

pELW3	pBluescriptII SK+ containing ~5kb *Eco*RI fragment from pDUB1911.	Amp^R	This study
pELW4	pBluescriptII SK+ containing 4.75kb *Eco*RI fragment from pDUB1911.	Amp^R	This study
pELW5	As pELW4 but with fragment in opposite orientation.	Amp^R	This study
pELW6	pBluescriptII SK+ containing 1.7kb *Eco*RI fragment from pDUB1911.	Amp^R	This study
pELW10	pBluescriptII SK+ containing 3.5kb *Hinc*II fragment from pDUB1911.	Amp^R	This study

2.2.4.4 Plasmids Used in Mutant Construction.

Plasmid	Characteristics	Resistance	Source
pRK2013	Helper plasmid for conjugation in *A. tumefaciens*.	Kan^R	Lab. stock [233]
pDUB2033	Neomycin resistance cassette.	$Amp^R Neo^R$	Lab. stock

2.2.4.5 Ti Plasmids.

Plasmid	Characteristics	Resistance	Source
pDUB1003/ Δ71	Deletion mutant of the pTiC58 derivative pGV3105.	Kan^R	Lab. stock [180]
pDUB1003/ Δ77	Deletion mutant of the pTiC58 derivative pGV3105.	Kan^R	Lab. stock [180]

2.2.4.6 Phage / Phagemids / Plasmids used in Selectively-Infective Phage (SIP) Construction.

Plasmid	Characteristics	Resistance	Source
fHAGHAG	SIP construct - Derivative of fd with a gene III antibody-C-terminal fusion and six H residues attached to the N-terminal.	Cm^R Tc^R	[109]
pAK200	Phagemid for the $lacP^{/O}$ controlled expression of proteins as fusions to gene III of fd.	Tc^R	[107]

fHPCR1	SIP construct - Derivative of fHAGHAG minus the antibody fusion to the gene III C-terminal.	Cm^R Tc^R	This study
pAK100Ab	Phagemid containing the antibody from fHAGHAG.	Tc^R	[107]
fHPHCR1Ab	SIP construct - fHPCR1 containing the antibody from fHAGHAG fused to the C-terminal of gene III.	Cm^R	This study
fHPCR2	SIP construct - Derivative of fHAGHAG minus the antibody and six H residue fusions to gene III.	Cm^R Tc^R	This study
pUC18SIP	pUC18 vector containing a modified multiple cloning site.	Amp^R	This study

2.3 Bacterial Growth Media, Conditions and Procedures.

The following media were used in this work:

Lab M nutrient broth no.2 (LM-broth):

25g made up to 1 litre with distilled water gives final concentrations of $10g.l^{-1}$ beef extract, $10g.l^{-1}$ balanced peptone no.1, $5g.l^{-1}$ NaCl, pH 7.5 ± 0.2.

For swarm plates bacteriological agar was added at a concentration of 0.15 - 0.2%.

Lab M nutrient agar (LM-agar):

28g made up to 1 litre with distilled water, gives final concentrations of $5g.l^{-1}$ peptone, $3g.l^{-1}$ beef extract, $8g.l^{-1}$ NaCl, $12g.l^{-1}$ agar no.2, pH 7.3 ± 0.2.

2xYT media:

1.6g trypticase peptone, 1.0g yeast extract, 0.5g NaCl, 1.0g glucose made up to 100ml with distilled water.

If necessary, bacteriological agar was added at a concentration of 1.5% for solid plates.

MinA media:

20ml 5x MinA salts, 2ml 10% glucose, 0.1ml 1M $MgSO_4$ made up to 100ml with distilled water. (5x MinA salts contain 307mM K_2HPO_4, 165mM KH_2PO_4, 7.6mM $(NH_4)_2SO_4$, 8.5mM Na.citrate.$2H_2O$.)

If necessary, bacteriological agar was added at a concentration of 1% for solid plates.

Chemotaxis media:
1ml 0.1M EDTA and 10ml 1M KH_2PO_4 (pH 7.0) made to 1 litre with distilled water.

Antibiotics were added to media after autoclaving, to the following concentrations:

For *A. tumefaciens*; chloramphenicol 25μg.ml^{-1}, erythromycin 100μg.ml^{-1}, kanamycin 50μgml^{-1}, neomycin 100μg.ml^{-1}, rifampicin 100μg.ml^{-1}, spectinomycin 100μg.ml^{-1}, streptomycin 300μg.ml^{-1} and tetracycline 15μg.ml^{-1}.

For *E. coli*; ampicillin 50μg.ml^{-1}, chloramphenicol 34μg.ml^{-1}, gentamycin 10μg.ml^{-1}, kanamycin 50μg.ml^{-1}, neomycin 100μg.ml^{-1}, spectinomycin 50μg.ml^{-1}, streptomycin 20μg.ml^{-1}, and tetracycline 15μg.ml^{-1}.

When selecting for the inactivation of the β-galactosidase gene, by insertion of DNA fragments into the multiple cloning sites of pBluescriptII and other plasmids, 40μl of 20mg.ml^{-1} X-gal (in DMF) were spread over the surface of agar plates.

For *R. meliloti*; streptomycin 100μg.ml^{-1}.

Liquid bacterial cultures were incubated on an orbital shaker at 200rpm at temperatures of 37°C for *E. coli*, and 28°C for *Agrobacterium* and *Rhizobium* strains. Short term (1-2 months) stocks of cultures were kept at 4°C on solid agar plates. Long term stocks were kept in 80% glycerol at -80°C.

Liquid cultures were inoculated with a flamed loop or a sterile cocktail stick. Solutions and bacterial cultures were spread onto agar plates using a glass spreader which had been sterilised in 70% ethanol. Bacterial colonies were inoculated into the centre of swarm plates using a sterile needle.

Aseptic technique was used throughout with bacterial cultures. All glassware, plasticware and other equipment were sterilised by autoclaving at 121°C, 15p.s.i. for 15 minutes. Generally solutions were prepared according to Sambrook *et al.* [170] and autoclaved, as above, if possible. Otherwise solutions were filter-sterilised through a 0.22μm nitrocellulose filter into a sterile container.

2.4 Isolation of DNA.

2.4.1 Alkaline Lysis Plasmid Minipreps.

This method, used to prepare small amounts of relatively pure plasmid DNA, was according to Sambrook *et al* [170].

A single colony of bacteria was grown overnight in 5ml of LM-broth containing the appropriate antibiotic selection. 1.5ml of this culture was pipetted into a sterile eppendorf tube, and the cells harvested by centrifugation for 1 minute in a microfuge. The supernatant was discarded, and a further 1.5ml of the culture pelleted as before. The supernatant was again discarded. The pellet was resuspended in 200µl of ice-cold solution 1 (1% glucose, 10mM EDTA pH8.0, 25mM Tris.HCl pH8.0), 200µl of solution 2 (0.2M NaOH, 1% SDS) was then added and the contents of the tube mixed by gentle inversion. 200µl of ice-cold solution 3 was added to the mixture and the tube inverted ten times to mix the contents. (Solution 3 was prepared by adding 1.15ml of glacial acetic acid to 2.85ml of distilled water and then adding 6ml of 5M potassium acetate. The solution has an overall pH of 4.8 and is 3M wrt potassium and 5M wrt acetate.) The tube was then microfuged for 5 minutes to remove bacterial debris. The supernatant was transferred to a fresh tube, spun down for a further 2 minutes and then pippetted into another fresh tube. The DNA was precipitated by the addition of 1ml of 100% ethanol. The tube was left for 5-15 minutes at -20°C then the DNA collected by centrifugation for 5 minutes. The DNA pellet was washed in 1ml 70% ethanol and air dried for 20-30 minutes. The final pellet was resuspended in 50µl of TE buffer and RNAase A added to a concentration of $20\mu g.ml^{-1}$

When plasmid DNA was to be prepared for sequencing, a QIAGEN QIAprep™ spin plasmid miniprep kit was used according to the manufacturers instructions.

2.4.2 Larger Scale Plasmid Preparation.

Single colonies were inoculated into two 50ml of LM-broth with antibiotic selection and grown overnight with shaking. The cultures were transferred to two 50ml centrifuge bottles and the bacterial cells harvested by centrifugation at 7000g/4°C for 7 minutes in a Beckman J2-HS centrifuge, using a JA-20 rotor. The supernatants were removed and the pellets resuspended in 3.335ml of ice-cold solution 1. 3.335ml of solution 2 was added to each tube and the tubes gently mixed. 3.335ml of ice-cold solution 3 was then added to each tube, and the tubes mixed well. The tubes were centrifuged for 5 minutes, at 4°C and 15000g in a Beckman J2-HS centrifuge, to remove

cell debris. The supernatants were transferred to sterile 50ml Falcon tubes, 20ml of phenol:chloroform:iso-amyl alcohol (25:24:1) were added and the tubes mixed well. The tubes were spun at 3500g for 3 minutes and the aqueous layer transferred to sterile centrifuge tubes. 20ml of ice-cold 100% ethanol was added to each tube and the tubes left on ice for 25 minutes. The DNA was pelleted by centrifugation for 15 minutes, at 4°C and 15000g in a Beckman J2-HS centrifuge. The pellet was then washed in 70% ethanol, dried and resuspended in 500µl of TE.

Solutions 1, 2 and 3 were made as in section **2.4.1**.

2.4.3 Plasmid Minipreps Using Silica Fines.

This method was used to check for the presence of plasmids or cosmids in *Agrobacterium* strains.

A single colony of bacteria was grown overnight in 5ml of LM-broth containing the appropriate antibiotic selection. A 1.5ml aliquot of the culture was pipetted into a sterile 1.5ml eppendorf tube. The cells were harvested by centrifugation for 1 minute in a microfuge, and the supernatant discarded. This procedure was repeated twice and the final pellet (from 4.5ml of culture) resuspended in 350µl of lysis buffer (lysis buffer consists of 8% sucrose, 0.5% Triton X-100, 50mM EDTA [pH 8.0] and 10mM TrisCl [pH 8.0]). 25µl of lysozyme (10mg.ml^{-1} stock) was added to the cell suspension and the tube vortexed for 3 minutes on a whirlimixer. The cells were incubated in a boiling water bath for 90 seconds, then immediately centrifuged for 10 minutes in a microfuge. The resulting pellet was removed with a sterile cocktail stick and discarded. 0.7ml of sodium iodide solution (90.8g NaI and 1.5g Na_2CO_3 dissolved in distilled water, filter sterilised and saturated with 0.5g Na_2SO_3 - stored at 4°C in a light-proof bottle) were added to the supernatant and the tube contents mixed by inversion. 5µl of silica fines were then added and the tube incubated at room temperature for 30 minutes. The silica fines were pelleted by centrifugation for 15 minutes in a microfuge. The supernatant was discarded and the fines washed with 1ml of 70% EtOH. The fines were pelleted by centrifugation for 1 minute in a microfuge, and the EtOH was removed. The fines were then resuspended in 30µl of TE buffer. The tube was incubated at 37°C for 30 minutes to elute the plasmid DNA. Finally the fines were pelleted by centrifugation for 15 seconds in a microfuge and the supernatant, containing the isolated plasmid DNA, removed to a sterile eppendorf tube.

2.4.4 Small Scale Preparation of Bacterial Chromosomal DNA.

A 5ml LM-broth culture of bacteria was grown to stationary phase and 1.5ml of the culture transferred to an eppendorf tube. The cells were spun down for 1 minute in a

microfuge, the supernatant removed and the pellet left at -20°C for 30 minutes. The pellet was then resuspended in 200µl of TE, and the cell suspension incubated with 8µl of lysozyme (10mg.ml^{-1} stock) for 30 minutes at 37°C. The cells were then lysed by the addition of 40µl of 4M sodium perchlorate, 24µl of 10% SDS and 8µl of Proteinase K (20mg.ml^{-1} stock), and incubated at 45°C for 2 hours. The DNA was precipitated by the addition of 2 volumes of ethanol and incubation at -20°C for 30 minutes. The DNA was pelleted by centrifugation in a microfuge for 5 minutes. The pellet was washed with 70% ethanol, dried and resuspended in 500µl of TE buffer. The DNA solution was extracted three times with an equal volume of phenol:chloroform:isoamyl alcohol (25:24:1), the aqueous layer being transferred to a new eppendorf tube each time. The DNA was then extracted once with chloroform:isoamyl alcohol (24:1). The DNA in the final aqueous layer was precipitated by the addition of 2 volumes of ethanol and 0.1 volumes of 3M sodium acetate (pH 4.8), followed by incubation overnight at -20°C. The DNA was pelleted by centrifugation in a microfuge for 5 minutes. The pellet was then washed with 1ml of 70% ethanol, dried and resuspended in 50µl of TE buffer with RNAase A (10mg.ml^{-1} stock) added to a final concentration of 20µg.ml^{-1}.

2.4.5 Small Scale Preparation of Bacterial Chromosomal DNA - 2.

This method was used as a quick preparation of *Agrobacterium* DNA when screening for possible mutant strains.

A 5ml LM-broth culture of bacteria was grown to stationary phase and 1.5ml of this culture transferred to an eppendorf tube. The cells were spun down for 1 minute in a microfuge, the supernatant removed and the pellet resuspended in 200µl of lysis buffer (lysis buffer consists of 40mM Tris-acetate pH7.8, 20mM Sodium acetate, 1mM EDTA and 1% SDS). 82.5µl of 4M NaCl was then added and the tube contents mixed by inversion. The tubes were centrifuged for 10 minutes in a microfuge. The supernatant was then pipetted into a clean eppendorf tube and an equal volume (approximately 250µl) of chloroform:isoamyl alcohol (24:1) added. The tube was inverted 50 times, then centrifuged for 3 minutes in a microfuge. The upper aqueous layer was removed to a clean eppendorf and the DNA precipitated by the addition of two volumes of 100% EtOH and incubation at -20°C for 10 minutes. The DNA was pelleted by centrifugation in a microfuge for 5 minutes. The pellet was then washed with 1ml 70% ethanol, dried and resuspended in 30µl of TE buffer with RNAase A (10mg.ml^{-1} stock) added to a final concentration of 20µg.ml^{-1}.

2.5 DNA Manipulations.

2.5.1 Phenol:Chloroform Extraction of DNA.

A 25:24:1 solution of phenol:chloroform:isoamyl alcohol was equilibrated 3 times with TE buffer and stored, under TE, in a light-proof bottle at 4°C. To remove proteins from DNA solutions an equal volume of phenol:chloroform:isoamyl alcohol was added, the solutions mixed by vortexing for 30 seconds and the phases separated by centrifugation for 2 minutes in a microfuge. The aqueous phase was transferred to a fresh tube. This was repeated until no further protein was visible (as a white precipitate) at the boundary of the two phases.

2.5.2 Restriction Endonuclease Digestions.

Digestions were carried out according to the enzyme manufacturer's instructions. Generally plasmid DNA was digested in a total volume of 10-40µl, with 5 units of restriction endonuclease, 0.1 volumes of the supplied 10x concentrated enzyme buffer, and sterile distilled water to make up the volume. The reaction was incubated at the recommended temperature (usually 37°C) for 1-3 hours. If more than one restriction enzyme was to be used in the same reaction and the buffers supplied differed, the reaction was buffered using one-phor-all buffer PLUS (Pharmacia). Chromosomal DNA was digested in a larger volume, 100-200µl, with 10 units of restriction enzyme added for every microgram of DNA, as well as the appropriate amounts of buffer and sterile distilled water. The reaction mixture was covered with a layer of mineral oil to prevent evaporation and maintain the buffering conditions, before being incubated overnight at the required temperature.

If the digestions were to be analysed by gel electrophoresis, 0.2 volumes of 6x gel-loading buffer were added (6x gel-loading buffer contains 0.25% bromophenol blue, 0.25% xylene cyanol FF and 40% sucrose in distilled water - this was filter sterilised and stored at 4°C).

If the digested DNA was to be used in further subcloning steps, the required fragment was cut out of the gel and purified using silica fines (see section **2.5.4**).

2.5.3 Agarose Gel Electrophoresis.

Gel electrophoresis of DNA samples was carried out with large 180x200mm maxigels (volume 400ml), 100x80mm minigels (volume 50ml) or 77x55mm minigels (volume 35ml). Maxigels were run in a Pharmacia gel apparatus GNA-200 electrophoresis tank. Minigels were run in Pharmacia gel apparatus GNA-100

electrophoresis tanks. The concentration of agarose within a gel could be varied depending on the size of DNA to be separated. Usually a 0.7% agarose gel was used, which efficiently separated linear DNA between 10-0.8kb. The required amounts of agarose and 1x TAE buffer (50x stock - 242g Tris, 100ml EDTA pH8.0, 57.1ml glacial acetic acid per litre) were mixed and the agarose dissolved by microwaving the mixture. The solution was cooled to about 60°C, 10mg.ml^{-1} ethidium bromide was added to a final concentration of 0.2μg.ml^{-1}, and the agarose was poured into a gel mould with a well comb in place. Once the agarose had set the gel was put in a tank and covered with 1x TAE buffer containing 0.2μg.ml^{-1} ethidium bromide. The DNA samples (and size markers) were loaded and electrophoresis carried out at 0.1A for the required amount of time, usually 1 - 1.5 hours. The size markers used were either λ-DNA digested with *Pst*I and/or λ-DNA digested with *Hin*dIII.

When DNA samples less than 1kb in size were to be analysed by agarose gel electrophoresis, Metaphor agarose and TBE buffer (5x stock - 54g Tris, 27.5g Boric acid, 20ml 500mM Na_2EDTA (pH 8.0) made up to 1 litre with dH_2O) were used. Usually 2% Metaphor agarose gels were made with 1x TBE, using the same methodology as above, a 100bp ladder was used as a size marker for these gels.

***Pst*I digested λ-DNA produces DNA fragments of the following sizes (in kb) :**

14.05, 11.49, 5.07, 4.75, 4.51, 2.84, {2.56, 2.46, 2.44}, 2.14, 1.99, 1.70, 1.16, 1.09, 0.81, 0.52, 0.47, 0.45, 0.34...

The fragments enclosed in brackets run together on an agarose gel. Smaller fragments are also produced, but were rarely seen in this work.

***Hin*dIII digested λ-DNA produces DNA fragments of the following sizes (in kb) :**

23.13, 9.42, 6.56, 4.36, 2.32, 2.03, 0.56, 0.13.

DNA within the gel was visualised on a transilluminator (UVP Inc.), and photographed with a Polaroid RP4 Land camera (using a red filter) onto Polaroid 667 film.

2.5.4 Isolation of DNA Fragments from Agarose Gels Using Silica Fines.

The required band was cut out of the gel using a sterile scalpel blade, and placed in a labelled 1.5ml eppendorf tube. 800μl of sodium iodide solution were added to the tube and the tube placed at 70°C for 5 minutes to melt the agarose. Once the agarose had completely melted the tube was mixed by inversion and allowed to cool to room

temperature for 5 minutes. 5µl of silica fines were then added, mixed and the solution left for 10 minutes at room temperature with continuous shaking. The fines were spun down for 30 seconds in a microfuge, the supernatant removed and the fines washed with 70% ethanol. The silica fines pellet was dried with a piece of tissue, then resuspended in 30µl of TE buffer and incubated at 37°C for 10 minutes with occasional shaking. The fines were spun down in a microfuge for 30 seconds and the supernatant, containing the DNA, collected. The fines were then resuspended in 20µl of TE and incubated as before. Further centrifugation and collection of the supernatant gave a total volume of 50µl of DNA.

Preparation of the silica fines:

250ml of silica 325 mesh powder was resuspended in distilled water to give a total volume of 500ml. The suspension was stirred for 1 hour and left to settle for a further hour. The suspension was then centrifuged at 5000g in a Beckman J2-HS centrifuge using a JA-14 rotor. The pellet was resuspended in 150ml of distilled water plus 150ml nitric acid. The suspension was then heated to 98°C and allowed to cool to room temperature. The silica fines were then repeatedly washed with sterile distilled water until the pH was greater than 5.5. Silica fines were stored at 4°C as a 50% slurry in sterile distilled water.

A QIAGEN QIAquick™ Gel Extraction Kit was also sometimes used, according to the manufacturers instructions, for isolating DNA from agarose gels.

2.5.5 Filling in 3'-Recessed Termini.

The DNA fragment (maximum of 500ng) was resuspended in 50µl of TE following isolation from an agarose gel. 7µl of a solution containing all 4 dNTPs (each at 1mM) was added to the DNA. 7µl of Klenow buffer (10x) was added (10x buffer is 0.5M Tris.HCl pH 7.6, 0.1M $MgCl_2$) and the reaction buffer made upto 70µl with sterile distilled water plus 1µl (1 unit) of Klenow fragment. The reaction mixture was left at room temperature for 30 minutes and then the Klenow fragment either inactivated by incubating at 70°C for 5 minutes, or removed using a QIAGEN PCR Purification Kit, according to the manufacturers instructions.

2.5.6 Ligation of DNA.

T4 DNA ligase was used to ligate DNA fragments with compatible cohesive or blunt termini. The fragments of insert and vector DNA were usually mixed at a ratio of 3:1 (insert:vector) with a maximum of 300ng DNA. 0.1 volume of 10x ligase buffer

(0.66M Tris.HCl pH7.5, 50mM $MgCl_2$, 50mM DTT, 10mM ATP) was added and 1 unit of DNA ligase. For cohesive termini the tubes were incubated overnight at 4°C. For blunt-ended termini the reactions were incubated at 16°C overnight. The ligation mix was then used immediately to transform competent *E. coli* cells.

2.5.7 Polymerase Chain Reaction (PCR).

All PCR reactions were performed in a Perkin-Elmer Thermal Cycler. Reactions were usually carried out in a total volume of 25µl, in thin-walled, 0.5ml, PCR tubes. Per reaction tube the following components were added:

10x reaction buffer	2.5µl
dNTPs	2.0µl (each at 1mM)
primer 1	1.0µl (at a concentration of 10pmol/µl)
primer 2	1.0µl (as above)
Taq polymerase	0.25µl (1 unit)
template DNA	1.0µl (see below)
25mM Mg^{2+}	1-4µl (concentration used varied)
dH_2O	appropriate to make final volume 25µl

The amount of template DNA used varied, however it was usually approximately 100ng for plasmid DNA, and 500-1000ng for genomic DNA.

To avoid pipetting very small volumes (<1µl) the 10x reaction buffer, dNTPs, primers and Taq polymerase were made into a "Master mix". For n tubes, the master mix consisted of appropriate volumes of the different components to make up n+1 reaction tubes. The mixture was then dispensed into each of the reaction tubes.

Primer design: Primers used were generally designed so as to contain an equal number of G+C's and A+T's, usually 10 of each pair. Care was taken to ensure the primers would not self anneal or hybridise to each other, as this would reduce the efficiency of the PCR reactions.

PCR Protocol: The temperatures and times used in PCR reactions followed the same basic pattern:

94°C	5 minutes	
94°C	1 minute)	- denature
50°C*1	1 minute) x30	- anneal
72°C	1*2 minute)	- extend
72°C	5 minutes	

- *1 The annealing temperature used varied as it is set by the composition of the primers; the approximate Tm for each primer can be worked out using the following equation:

$$Tm = \{[(\text{no. of G} + \text{C}) \times 4] + [(\text{no. of A} + \text{T}) \times 2]\} - 5\ ^{\circ}C$$

If the annealing temperatures of the two primers differed, the lower temperature was used in the reactions.

- *2 The extension time is set by the length of the largest fragment expected from the reactions, e.g. if expect a 3kb fragment the extension time would be 3 minutes.

2.5.7.1 Hot Start PCR.

Occasionally "hot start" PCR was used, this reduces the amount of non-specific binding of the primers by compartmentalising the contents of the reaction tube until the denaturation temperature is reached. Half the total volume of the reaction (consisting of the 10x buffer, dNTPs, Mg^{2+}, primer 1 and dH_2O) was put in a tube, a wax bead was then added, using sterile forceps, and the tube heated to 70°C for 5 minutes to melt the wax. After heating, the tube was held on ice for 2 minutes to solidify the wax and seal off the bottom half of the tube. The second half of the reaction volume (consisting of the Taq polymerase, template DNA, primer 2 and dH_2O) was then added, on top of the wax seal, and the tubes placed in the thermal cycler.

2.5.7.2 Band Stab PCR [25].

This method was used to reamplify a specific band from a preliminary PCR reaction. When the PCR gave several bands close together, a specific band could be isolated and reamplified by inserting a sterile needle into the relevant area of the agarose gel and then dipping the needle into a reaction tube set up as for hot start PCR.

2.6 Transformation of *E. coli.*

2.6.1 Preparation of Competent Cells.

5ml of LM broth was inoculated with DH5α and grown overnight at 37°C, it was then subcultured 1:100 into fresh LM broth and the cells grown to an OD_{550} of 0.3-0.35.

The culture was chilled for 5 minutes on ice before being spun down in pre-chilled centrifuge tubes at 4000g, 4°C, for 7 minutes. The supernatants were poured off and the cell pellets resuspended in $^{2}/_{5}$ of the original culture volume with solution A (solution A = 30mM potassium acetate, 100mM rubidium chloride, 10mM calcium chloride, 50mM manganese chloride and 15% glycerol. The solution was adjusted to pH 5.8 with 0.2M acetic acid and filter sterilised.) The tubes were held on ice for 5 minutes and spun down as before. The supernatants were poured off and the pellets resuspended in $^{1}/_{25}$ of the original culture volume with solution B (solution B = 10mM MOPS, 75mM $CaCl_2$, 10mM $RbCl_2$ and 15% glycerol. The solution was adjusted to pH 6.5 with KOH and filter sterilised.) The tubes were left on ice for 15 minutes, then 150µl aliquots were added to pre-chilled eppendorfs, frozen in liquid nitrogen and stored at -80°C.

2.6.2 Transformation Procedure.

The cells were thawed by hand and placed on ice for 10 minutes. The DNA to be transformed was added, and the tube held on ice for 30 minutes. The cells were heat shocked at 42°C for 90 seconds, held on ice for 3 minutes and then 800µl of pre-warmed (to 37°C) LM broth were added. The tube was incubated for 1 hour at 37°C, with continuous shaking. Finally appropriate aliquots, usually $^{1}/$10th and $^{9}/$10ths of the tube, were spread onto selective agar plates and incubated overnight at 37°C.

2.7 DNA Hybridisation Procedures.

2.7.1 Radio-Labelling of DNA Fragments.

DNA fragments were labelled with [α-^{32}P] dCTP by the random primer labelling method using an Amersham Multiprime kit. 30-50ng of the DNA to be labelled, in a total volume of 28µl, were boiled for 5 minutes and then held on ice for 2 minutes. 10µl of labelling buffer, 5µl of random hexanucleotide primers, 5µl ^{32}P-dCTP (equivalent to 50µCi) were added, followed by 2µl of Klenow enzyme. The labelling reaction was left to proceed either at room temperature overnight, or for 2-3 hours at 37°C, the probe was then purified through a 10cm Sephadex G-50 column using STE as the elutant. The labelled DNA was collected and stored at -20°C until required. Immediately before use the probe DNA was boiled for 5 minutes.

2.7.2 Southern Blotting.

DNA was transferred to Hybond-N (Amersham) nylon membranes, according to the manufacturer's instructions. Firstly the agarose gel containing the DNA samples was photographed with a ruler down its side. Gels known to have DNA fragments greater than 10kb in size were soaked in 0.25M HCl for 15 minutes, to partially depurinate the DNA, and rinsed twice with distilled water. For blotting the gel was soaked in denaturation buffer (1.5M NaCl, 0.5M NaOH) with occasional shaking for 30 minutes. The gel was then rinsed twice with distilled water and soaked in neutralisation buffer (1.5M NaCl, 0.5M Tris.HCl pH7.2, 0.001M EDTA). After rinsing the gel twice with distilled water, the blot was set up.

For single sided (one-way) blots a reservoir of 20x SSC was set up (20x SSC - 3.0M NaCl, 0.3M Na.citrate pH7.0). A platform was placed over this reservoir and a long piece of Whatman 3MM paper (presoaked in 20x SSC) put on the platform with its ends dipping into the reservoir. The gel was placed, wells uppermost, on the 3MM paper, and a piece of Hybond-N nylon membrane cut to the same size as the gel placed on top of it. Any air bubbles were carefully removed before 3 sheets of Whatman 3MM paper, cut to the gel size and presoaked in 20x SSC, were placed on top. Finally 2 layers of disposable nappies (also cut to gel size) were placed on top, the stack covered with a glass plate and a 1kg weight placed on top.

Double sided (two-way) blots were created by sandwiching the agarose gel between two equivalent stacks of a glassplate, 2 layers of disposable nappies, 3 pieces of Whatman 3MM paper (presoaked in 20x SSC) and a piece of Hybond-N nylon membrane. A 1kg weight was placed on the top glass plate. Liquid retained in the gel transferred the DNA onto both membranes.

Both types of blot were left for at least 16 hours to allow DNA transfer. After which time the apparatus was dismantled, and the positions of the wells marked on the nylon. The nylon filter was washed carefully in 2xSSC, then allowed to air dry for up to 1 hour before being wrapped in clingfilm. It was then exposed to UV light for two minutes each side to fix the DNA to the membrane.

2.7.3 Colony Blotting.

A piece of Hybond-N nylon membrane cut to 6cm x 6cm was carefully placed onto the surface of a prewarmed agar plate containing appropriate antibiotic selection, and allowed to wet from beneath. The membrane and a second agar plate (the master plate) were marked to show correct orientation. Individual bacterial colonies were then inoculated with a sterile cocktail stick onto the membrane and the master plate, as small (~3mm length) streaks, arranged in a grid pattern. Each colony was streaked in an

identical position on both plates and the inoculation procedure was carried out in a lamina flow hood. The plates were incubated overnight at 37°C, the master plate was then stored at 4°C. The membrane was removed from the other agar plate and placed colony side up on a piece of 3MM paper presoaked in denaturing solution, for 7 minutes. The membrane was then transferred to a piece of 3MM paper presoaked in neutralising solution, and left for 3 minutes, this step was then repeated on a fresh piece of 3MM paper. Finally the membrane was washed carefully in 2xSSC, then placed colony side up on a piece of 3MM paper and allowed to air dry for one hour. It was then wrapped in clingfilm and the DNA fixed to the membrane by exposure to UV light for 2 minutes.

2.7.4 Hybridisation of Radio-Labelled Probes to Blots.

Hybridisation reactions were carried out using Techne Hybridisation tubes in a Techne Hybridiser HB-1 oven. The nylon filter was put inside the hybridisation tube and 200µl of pre-hybridisation solution (5x SSC, 5x Denhardt's solution [50x Denhardt's solution is 1% ficoll, 1% polyvinylpyrrolidone, 1% BSA fraction V], 0.5% SDS, 0.1% pyrophosphate and 100mg.ml^{-1} of denatured salmon sperm DNA) added per cm^2 of filter. Any air bubbles were carefully removed and the tube incubated at 65°C, whilst being rotated in the oven. After two hours the labelled probe was denatured, by boiling for 5 minutes, and 100-200 µl added to the tube contents. The tube was replaced in the oven and incubated at 65°C for at least 12 hours. After incubation the pre-hybridisation solution (containing the probe) was poured off and the blots washed.

2.7.5 Washing of Probed Blots.

The nylon filter was washed within the hybridisation tube and was never allowed to dry out. The filter was washed twice in 2x SSC, 0.1% SDS for 10 minutes at room temperature, followed by one wash in 0.1x SSC, 0.1% SDS for 15 minutes at 65°C. After each washing solution was removed, the filter was checked with a Geiger counter and the washing continued until sufficient (apparent) non-specific radio-labelled probe was removed (until a reading of <20cpm was obtained). Finally the filters were wrapped in clingfilm.

2.7.6 Detection of Hybridising Probes.

The wrapped filter was taped onto a larger piece of Whatman 3MM paper in a lead cassette. Radioactive bands could be detected on the filter by exposing Fuji RX-100 X-ray film to the filter. The film sheets were pre-flashed once to sensitise them, and exposure carried out at -80°C, for varying amounts of time. Exposed films were

developed with Ilford Phenisol developer for up to 4 minutes and fixed with Kodak Unifix fixer for 2 minutes. The position of the wells on the filter were marked on the film and the size of any hybridising fragments calculated using the original gel photograph (with ruler included).

2.7.7 Stripping of Probed Blots.

Blots were stripped by pouring a boiling solution of 0.1% SDS over the membrane and allowing the solution to cool to room temperature. Stripping was usually allowed to proceed for a period of at least two hours, after which time the membrane was wrapped in clingfilm and autoradiography carried out for the normal exposure time to check that the probe had been completely removed. The membrane was then pre-hybridised and hybridised with a new probe.

2.8 DNA Sequencing.

DNA sequencing was carried out with an Applied Biosystems 373A DNA Stretch Sequencer and a 377 DNA sequencer, using double stranded DNA templates and dye terminator chemistries. Usually, the universal M13 forward and reverse primers were used, but occasionally custom-synthesised oligonucleotides were also used.

Nucleotide sequence searches were carried out against the GenBank and EMBL databases using the Fasta programme at SEQNET. Putative protein sequences were searched against the Owl database, using the programmes Sooty and Sweep, and BLASTP.

2.9 Conjugation of Plasmids into *Agrobacterium.*

Triparental matings based upon the method of Ditta *et al.*[58] were used to mobilise plasmids into *Agrobacterium* with pRK2013 as a helper plasmid. Cultures of the recipient *Agrobacterium* strain, and the *E.coli* plasmid donor and helper strains were grown to mid log phase. 100µl of each culture were pipetted onto a 0.22µm nitrocellulose filter disc on the surface of an LM-agar plate. This was incubated at 28°C overnight, and the disc then transferred to a universal bottle containing 10ml of 10mM $MgSO_4$. This was vortexed vigorously to wash the bacteria off the disc. Dilutions were made from the resulting cell suspension and plated onto agar plates, with appropriate antibiotic selection.

2.10 Mutagenesis.

2.10.1 Gene Replacement Mutagenesis.

Gene replacement mutagenesis was carried out according to the protocol of Quandt and Hynes [161]. The technique involves replacement of a functional gene with a copy of the same gene interrupted by the insertion of an antibiotic resistance cassette, thereby creating a non-functional copy of the gene in question.

Two vectors were used in this work, pJQ200mp18 and pJQ200uc1, which only differ in the restriction enzymes available in their respective multiple cloning sites. The pJQ200 vectors have gentamycin resistance and a β-galactosidase gene for selection procedures. In addition they have a functional *mob* site which allows conjugation into *A. tumefaciens* strains. They also possess the *sacB* gene from *B. subtilis*, which when activated by sucrose, produces levansucrase, an enzyme whose expression causes the production of toxic compounds that are lethal in Gram negative bacteria. Also crucial to their functioning in this work, is the fact that the pJQ200 vectors are unable to replicate outside of the enterobacteria, they therefore act as suicide vectors in *A. tumefaciens*.

Genes to be mutated were ligated into a pJQ200 vector and correct insertion confirmed by inactivation of the β-galactosidase gene. The neomycin resistance cassette from pDUB2033 was then ligated into the gene and positive constructs obtained by selection on plates containing both gentamycin and neomycin. The final plasmid construct was then conjugated into *A. tumefaciens* C58C1 by tri-parental mating (see section **2.9**).

The pJQ200 constructs are only able to survive in *A. tumefaciens* by integration into the genome via homologous recombination. For correct construction of the mutant strain, a rare second recombination event must occur between the mutated gene and the wild type copy, thus excising the wild type copy of the gene and the plasmid vector from the cells.

After the first recombination and subsequent integration step the entire mutant construct was incorporated into the genome, giving the bacteria both gentamycin and neomycin resistance. Since both intermediate strains and the final mutants possess resistance to neomycin it was not possible to select for correct construction of the mutant by simply growing on plates with neomycin selection alone. The presence of the *sacB* gene on the pJQ200 vector however acts as an additional selectable marker, allowing direct selection of only those strains that have undergone the second recombination event, and contain only the mutated copy of the gene. Selection on sucrose induces the *sacB* gene, thereby killing those strains that still contain the vector sequence.

Tri-parental matings were therefore plated on LM-agar plates containing rifampicin, neomycin and 5% sucrose.

To confirm that gene replacement had occurred, genomic digests and subsequently Southern blots were made of the putative mutant strains and the wild type strain C58C1. The blots were probed with a radioactively labelled copy of both the wild type gene, and the neomycin cassette. Due to the insertion of the neomycin cassette, when digested with the same enzyme, different sized hybridising bands were expected in the mutant strains, as compared to the wild type strain, when probed with the gene in question. The neomycin probe should only hybridise with known sized fragments in the mutants. The differences in band patterns between the wild type strain and the mutant strain therefore confirms gene replacement has occurred.

2.10.2 In-frame Deletion Mutagenesis.

The gene replacement mutagenesis technique described in section **2.10.1**, had one severe disadvantage in this work. The genes under investigation were thought to be under the same regulatory control, forming an operon. If correct, mutation of one gene by insertion of a neomycin cassette would have a polar effect, disrupting any genes downstream of it, and hence not allowing phenotypic studies of the effects of mutating a single gene.

This second mutagenesis method circumvents this problem, by deleting single genes, but leaving all other genes correctly in-frame so they are not affected. It also has the additional advantage of not introducing any additional antibiotic resistance into the final mutant strain, therefore making it more accessible for the introduction of other mutations or specific plasmids e.g. Ti plasmids.

The basic vector used in this work was the allelic exchange vector pK18*mobsacB*, constructed from pK18 and *sacB* by Schafer *et al* [173]. The vector is similar to the pJQ200 vectors in that it contains a β-galactosidase gene for identification of correct transformants, the *sacB* gene for selection purposes and a functional *mob* site for conjugation into Gram negative bacteria. However pK18*mobsacB* is kanamycin resistant.

Generally the gene to be deleted plus 200-500bp of flanking sequence was cloned into SK+. The coding region of the gene was deleted by PCR using specific primers that contained, in addition to flanking sequence, only the first 9bp or the last 3bp of the gene but also had an additional, unique, hexameric restriction site incorporated at their 5' termini. The PCR fragment was then isolated, digested with the restriction enzyme and religated. Sequencing of the fragment was usually carried out to confirm that the PCR reaction and religation had taken place correctly. The insert, containing the specific gene deletion plus flanking sequence, was then isolated using suitable restriction enzymes and cloned into pK18*mobsacB*. Correct insertion of the fragments was selected for by inactivation of the β-galactosidase gene. The final construct was then mobilised into C58C1 by tri-parental mating.

Like the pJQ200 vectors, pK18*mobsacB* is only able to survive in *A. tumefaciens* by integration into the genome via homologous recombination. This first recombination step was selected for by plating of the tri-parental mating mixture on LM-agar plates containing rifampicin and kanamycin. The genotype of resulting colonies was confirmed by PCR analysis and Southern blotting. In order for the, rare, second recombination event to take place a positive colony, previously identified, was grown overnight in LM-broth containing only rifampicin. Neat, 10^{-1}, 10^{-2}, 10^{-3} and 10^{-4} dilutions of the culture were then spread on MinA-agar plates (work using the pK18*mobsacB* vector in *R. sphaeroides* showed that selection at this stage was only possible if sucrose was the only carbon source available to the bacteria, hence MinA-agar plates were used) containing rifampicin and 10% sucrose to force the excision of the vector. Representative colonies were then picked from the lower dilution plates and replica streaked on LM-agar plates containing rifampicin alone, or rifampicin plus kanamycin. Recombinants which were sensitive to kanamycin were checked once again by PCR analysis and Southern blotting. Thus identifying correct in-frame deletion mutants.

Further explanation of the specific mutants created and the exact procedures used, are given in **chapter 4**.

2.11 Complementation Analysis of Mutants.

Wild-type copies of mutated genes (on library cosmids) were introduced into constructed mutants by conjugation. The presence of the plasmid was checked via DNA minipreps (see section **2.4.3**).

2.12 Tumourigenicity Studies.

A. tumefaciens strains containing Ti plasmids were tested for their tumourigenic capabilities by inoculation into the leaves of *Kalanchöe diagremontiana*.

Strains to be tested were grown overnight in 5ml LM-broth cultures with appropriate antibiotic selection. A sterile syringe was used to withdraw a sample of the culture, and a pin-head sized drop was injected into the upper surface of a mature leaf. Plants were selected that contained at least four diametrically opposed leaf pairs, inoculations were then carried out on the central pairs so that neither senescing, nor conversely very immature leaves, were used. Inoculations were usually carried out in duplicate on each leaf (either side of the mid-rib), and at least in duplicate on different

plants, similar patterns of inoculations were also carried out for both positive and negative control strains.

Plants were grown in an incubator at 25°C, under a controlled light regime consisting of eight hours of daylight and sixteen hours of darkness, typically for a period of 4 - 8 weeks. Further details of the work carried out are given in section **4.6.5**.

2.13 Bacterial Growth Measurement.

The optical density of bacteria was measured at 600nm on a Beckman DU7500 spectrophotometer to produce growth curves of the changes in optical density over time.

2.14 Microscopy.

2.14.1 Light Microscopy.

A loopful of bacteria, taken from a fresh swarm plate, was resuspended in 40µl of chemotaxis media and observed under phase contrast optics (using a Nikon Optiphot microscope).

2.14.2 Electron Microscopy.

A loopful of bacteria, taken from a fresh swarm plate, was washed onto a Formvar-coated grid with 100µl of 10mM MgSO4. The bacteria was allowed to settle on the grid for 5 minutes before the excess solution was blotted off. Grids were not allowed to dry out completely at this stage. A drop of saturated aqueous uranyl acetate (pH 4.8) was placed on the grid for 30 seconds, the excess stain was then partially blotted off and the grid allowed to air dry. The grids were viewed and photographed using a Philips EM400.

2.15 Selectively-Infective Phage (SIP) Methods.

2.15.1 Phage Production.

An XL1-Blue bacterial colony, containing the SIP construct, was inoculated into 5ml of 2xYT broth, with appropriate antibiotic selection, and grown overnight at 37°C. 0.5ml of the culture was then inoculated into 25ml of 2xYT broth, containing antibiotic selection, and grown until an OD_{550nm} of 0.5 was reached. The bacterial cells were

pelleted, by centrifugation at 7000rpm for 5 minutes. The pellet was then resuspended in 50ml of 2xYT broth, containing appropriate antibiotic selection and 0.5mM IPTG, and grown overnight, at 26°C, to allow phage production. The phage DNA was then purified by PEG precipitation.

2.15.2 PEG Precipitation of Phage DNA.

Following growth of an overnight culture, 1/6 the culture volume of 20%PEG/2.5mMNaCl was added, and the culture incubated at room temperature for 15 minutes. The culture was then pelleted, by centrifugation at 8000g for 5 minutes. The pellet was resuspended in 1ml of PBS (20mM NaPi, 150mM NaCl; pH7.2), then centrifuged at 13000g, for 2 minutes, to pellet the cell debris. The supernatant, containing phage DNA, was removed to an eppendorf tube, and stored at 4°C.

2.15.3 Testing of Phage Infectivity.

100µl of isolated phage DNA (see section **2.15.2**) was inoculated into 1ml of XL1-Blue culture (previously grown to an OD_{550nm} of 0.5) and incubated at 37°C, for 1 hour, with gentle agitation. Dilutions of the suspension were then plated on 2xYT-agar plates, containing appropriate antibiotic selection, and incubated overnight at 37°C.

Due to the selection contained within the agar plates, colonies should only be produced when the bacteria had been incubated with an infective phage.

3 Identification and Sequencing of Chemotaxis Genes from *A. tumefaciens*.

3.1 Identification of *A. tumefaciens* Cosmid Library Clones Containing Putative Chemotaxis Genes.

Two *Eco*RI fragments from the *S. meliloti* plasmid pRU1221 [78] were used as heterologous probes to identify possible chemotactic genes in *A. tumefaciens*.

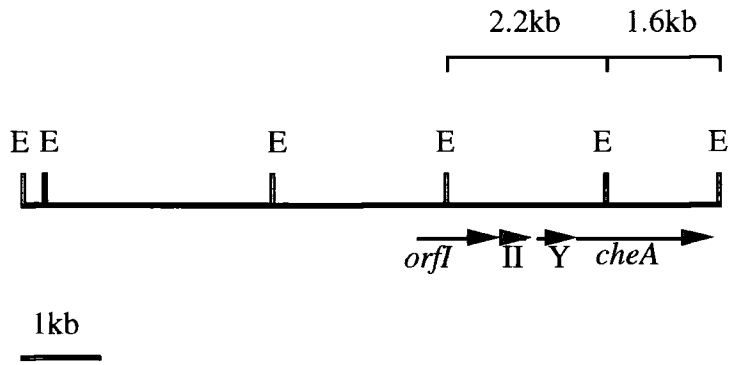

Fig. 3.1.1 Map of pRU1221 showing approximate positions of the *S. meliloti* chemotaxis genes.
E = *Eco*RI, II = *orfII*, Y = *cheYI*.

The 1.6kb *Eco*RI fragment containing the 3' terminal portion of the *S. meliloti cheA* gene was radioactively labelled and used to probe genomic digests of *A. tumefaciens* and *S. meliloti* DNA, plus an *A. tumefaciens* cosmid library DNA mix [181].

The *S. meliloti* acted as a positive control and hybridised to a band of 1.6kb. Three definite hybridising bands were seen with the *A. tumefaciens* digests; a 5kb *Eco*RI band, a 4kb *Hin*dIII band and a 20kb *Bam*HI band, a similar sized *Bam*HI band was also seen with the cosmid library DNA mix digest (see **Fig. 3.1.2**).

The cosmid library DNA mix was transformed into DH5α cells, and the resultant colonies used in a colony blot, using the 1.6kb *S. meliloti cheA* probe. Six colonies showed very strong binding of the probe. DNA was isolated from these colonies, and *Bam*HI digests of each probed with the 1.6kb *cheA* probe. Three of the cosmids gave a hybridising band of 20kb, as was seen with the genomic blot. These cosmids were therefore digested with *Eco*RI and *Hin*dIII and probed once again. All three cosmids gave bands of the expected size for each digest; that is a 5kb *Eco*RI band and a 4kb *Hin*dIII band. The cosmids were named pDUB1911, pDUB1913 and pDUB1909, for use in future work.

Digests of the cosmids gave the same bands for corresponding restriction enzymes, it is therefore likely that they are copies of the same clone. pDUB1911 was used in all subsequent work on cloning and sequencing the putative chemotactic region.

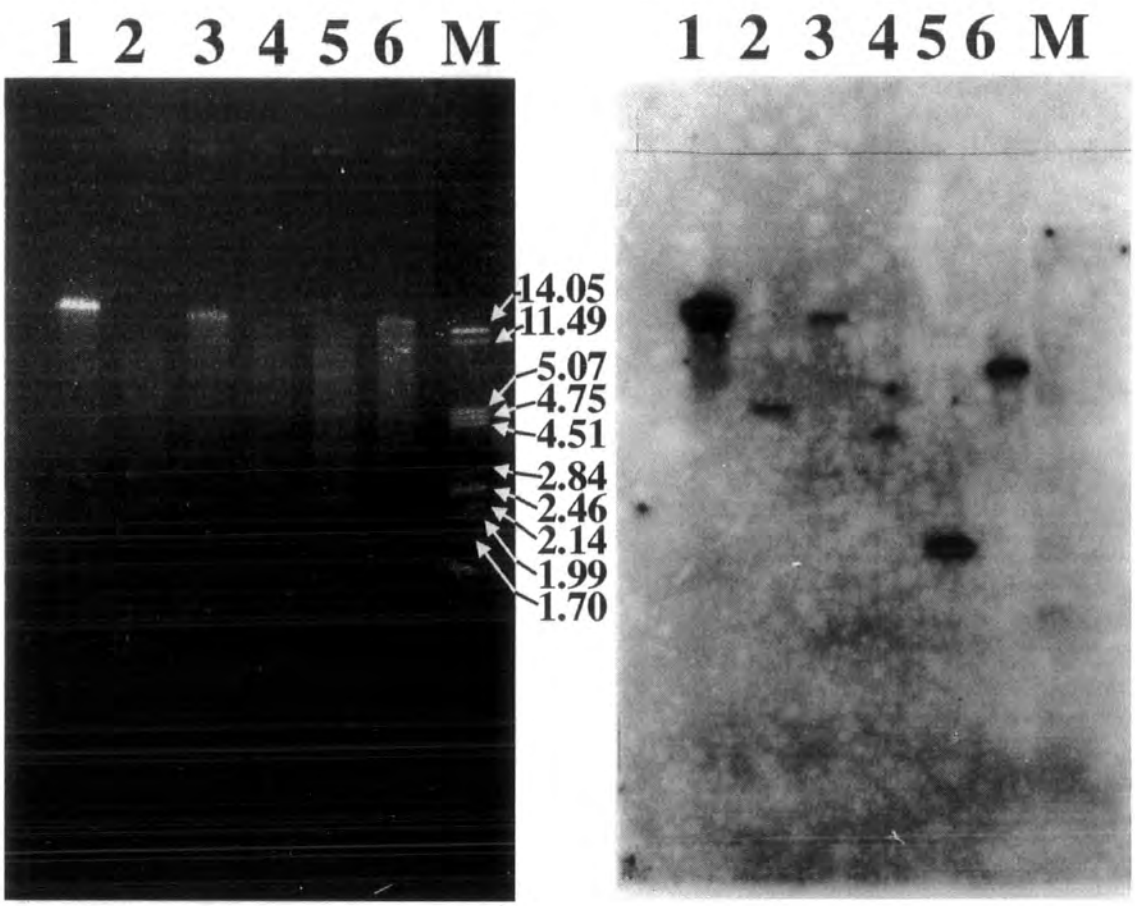

Fig. 3.1.2 0.7% agarose gel and subsequent Southern blot, showing the genomic fragments hybridising with the *S. meliloti cheA* probe.

1 = *A. tumefaciens* cosmid library DNA mix / *Bam*HI, **2** = C58C1 / *Eco*RI, **3** = C58C1 / *Bam*HI, **4** = C58C1 / *Hin*dIII, **5** = *S. meliloti* / *Eco*RI, **6** = *S. meliloti* / *Bam*HI, **M** = λ / *Pst*I.

Further restriction digests of pDUB1911 were carried out and a two-way Southern blot made. One membrane was probed with the 1.6kb *S. meliloti cheA* probe, and the other was probed with the 2.2kb *Eco*RI fragment from pRU1221, which contained the 5' end of the *cheA* gene, *cheY1*, *orfII* and the 3' part of *orfI* (see **Fig. 3.1.1**).

The results of the digests and blots showed pDUB1911 to contain two approximately 4kb *Hin*dIII fragments and two approximately 5kb *Eco*RI fragments that hybridised with the *S. meliloti* probes, and hence were likely to contain possible chemotaxis genes (see **Fig. 3.1.3** and **Fig. 3.1.4**).

3.2 Sequencing of pDUB1911.

11.3kb of sequence from the start of the *A. tumefaciens* cosmid library clone pDUB1911 has been determined. The first 9.6kb of sequence has been fully sequenced in both directions and has been submitted to Genbank under the Accession Number AF044495. A 1.7kb DNA region, directly downstream of this, was partially sequenced by A. McBain (unpublished results).

Both of the 4kb *Hin*dIII fragments and the 5kb *Eco*RI fragments of pDUB1911 were subcloned into pBluescriptII SK+, giving the plasmids pELW1, pELW2, pELW3 and pELW4/5 respectively. Generally sequencing of these plasmids was carried out by further subcloning into pBluescriptII SK+, and using the M13 universal primers forward and reverse. Where there were no convenient sites for restriction digesting custom primers were designed for sequencing.

Sequence data was manipulated and aligned using the Macintosh computer programmes DNA Strider and Sequencher.

The plasmids pELW1, pELW2 and pELW4/5 have been fully sequenced in both directions, pELW3 has only been partially sequenced. The complete sequence of the sense strand of the 11.3kb region from the start of pDUB1911 is listed at the end of this chapter (section **3.9**). A partial restriction map of the region sequenced and the sequencing strategy used can be seen in **Fig. 3.2**.

3.3 Identification of Gene Homologues.

Possible open reading frames, in the complete length of sequence, were identified using the SEQNET programme Testcode (Testcode scores DNA sequences and assesses the likelihood of the sequence to contain coding regions) and the Macintosh programme DNA Strider (see **Figs. 3.3.1** and **Fig. 3.3.2,** respectively). The DNA sequence was compared against the Genbank and EMBL databases using the SEQNET programme

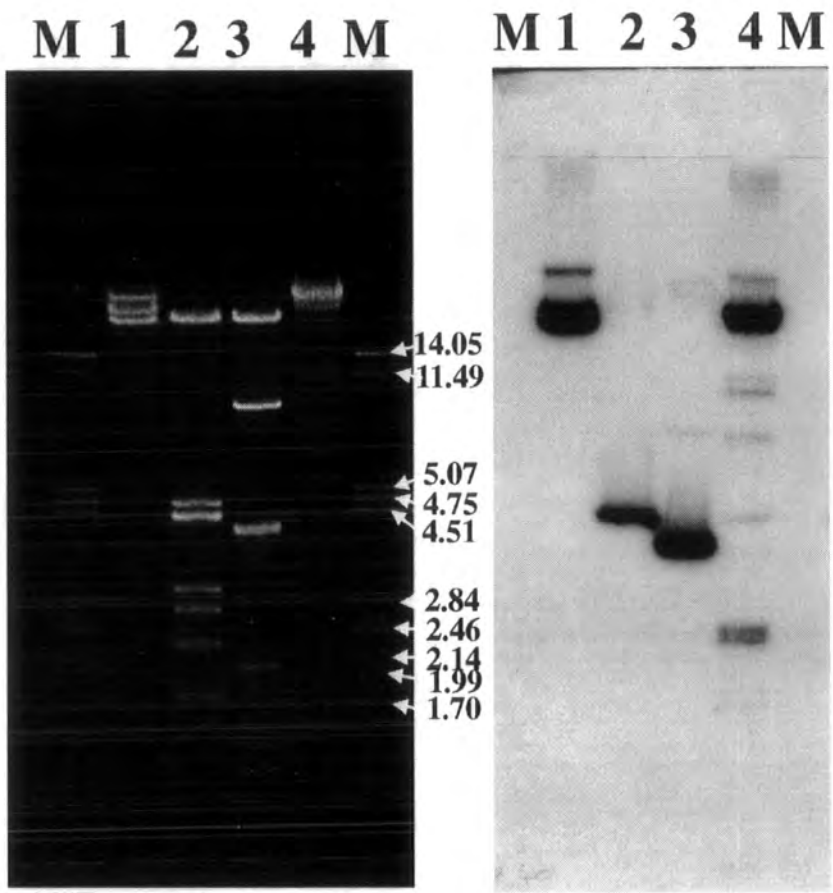

Fig. 3.1.3 0.7% agarose gel and subsequent Southern blot, showing the fragments in pDUB1911 hybridising with the 1.6kb *cheA* probe.

M = λ / *Pst*I, **1** = pDUB1911 / *Bam*HI, **2** = pDUB1911 / *Eco*RI, **3** = pDUB1911 / *Hin*dIII, **4** = pDUB1911 / *Pst*I.

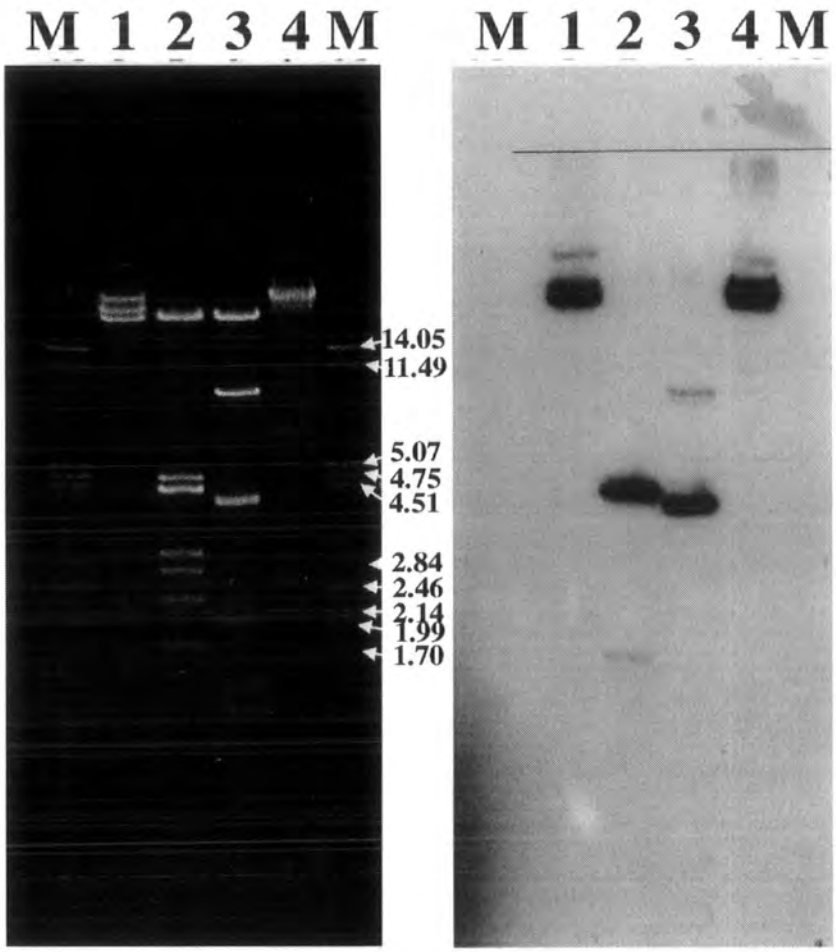

Fig. 3.1.4 0.7% agarose gel and subsequent Southern blot, showing the fragments in pDUB1911 hybridising with the 2.2kb probe.

M = λ / *Pst*I, **1** = pDUB1911 / *Bam*HI, **2** = pDUB1911 / *Eco*RI, **3** = pDUB1911 / *Hin*dIII, **4** = pDUB1911 / *Pst*I.

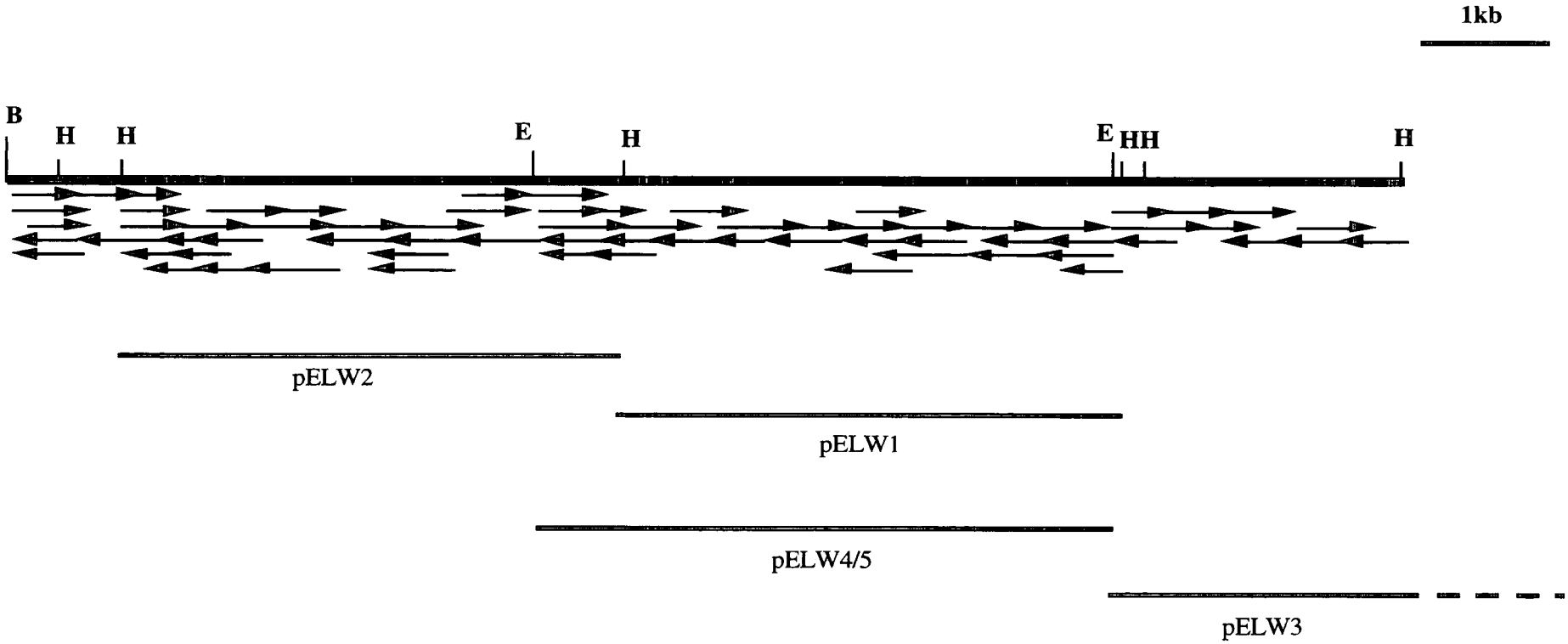

Fig. 3.2 Partial restriction map of the sequenced region of pDUB1911 showing the main subclones used in the sequencing strategy.

B = *Bam*HI, **E** = *Eco*RI, **H** = *Hin*dIII. Arrows represent individual sequencing reactions and the direction of sequencing.

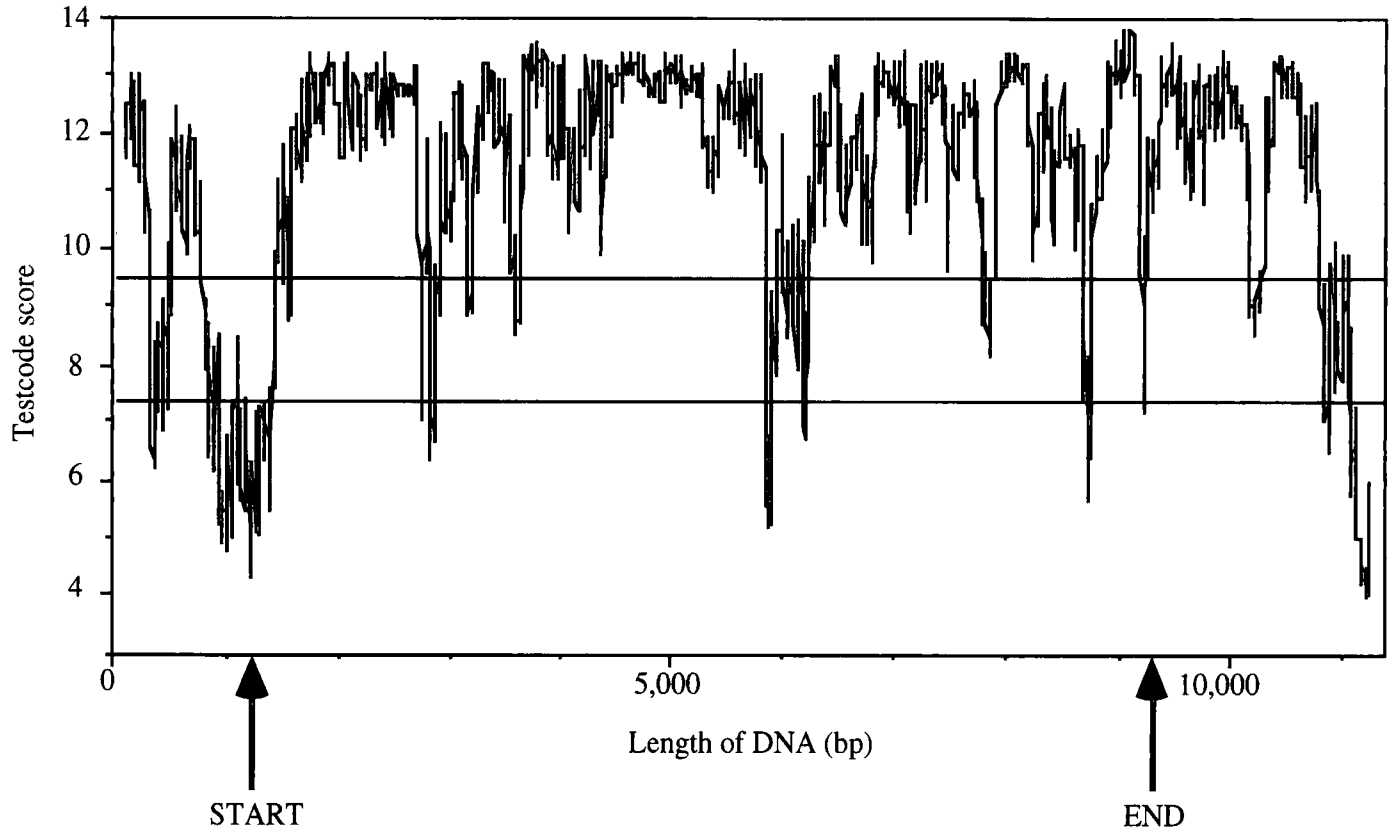

Fig. 3.3.1 Testcode map of the sequenced region of pDUB1911.

Arrows underneath the main figure indicate the limits of the *che* cluster. Regions above the upper horizontal line (9.4) are considered by the programme to have a greater than 95% likelihood of being a coding region. Regions below the lower horizontal line (7.4) are considered to have a greater than 95% likelihood of being a non-coding region. Scores between 9.4 and 7.4 are considered to be equally as likely to be coding or non-coding regions.

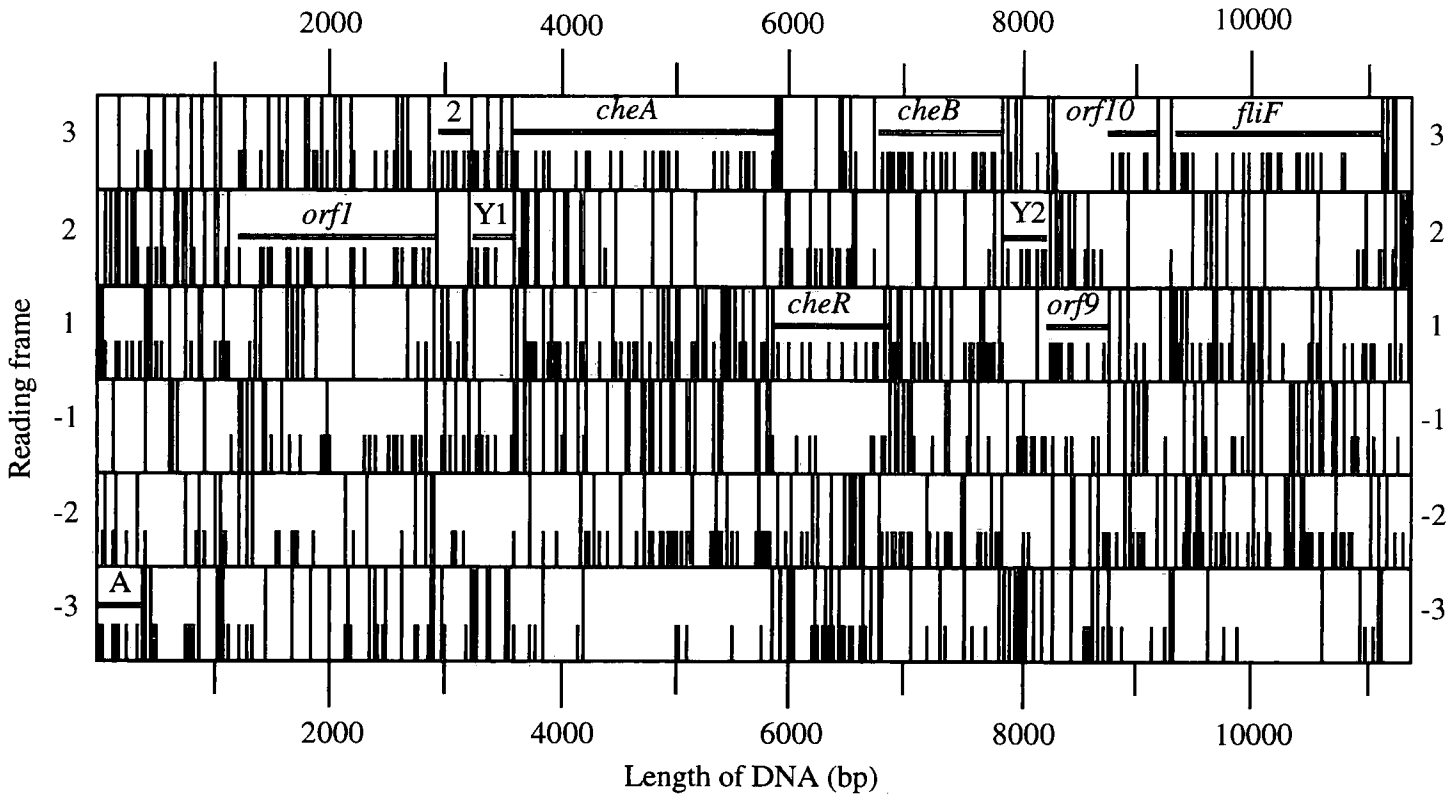

Fig. 3.3.2 DNA Strider open reading frame map of the sequenced region of pDUB1911 showing the location and name given to each identified open reading frame.

A = *phaA*, Y1 = *cheY1*, 2 = *orf2*, Y2 = *cheY2*. Numbers on the vertical axis indicate the three different sense (1, 2 & 3) and antisense (-1, -2 & -3) reading frames. For each reading frame short vertical lines indicate possible start sites (ATG or GTG codons), full length vertical lines indicate possible stop sites (TGA, TAA or TAG).

FASTA, or alternatively regions were translated into their protein sequence and compared against the Owl database using the SEQNET programmes SWEEP and BLASTP.

As can be seen in **Fig. 3.3.1** Testcode analysis gave a large majority of the sequence a score greater than 9.4, suggesting the presence of several open reading frames, only two regions at the start and end of the 11.3kb of sequence gave a significant score below 7.4, suggesting non-coding DNA. Further analysis in DNA Strider (**Fig. 3.3.2**) identified a number of possible open reading frames, in both the sense and antisense directions. Subsequent DNA and protein searches using each of these regions identified eight orfs with homology to known chemotaxis genes, one orf with homology to a known flagellar gene, one partial orf with significant sequence homology to a gene identified in *S. meliloti* and one orf of unknown function. Each orf was subsequently named according to the gene/protein with which it showed greatest homology. **Fig. 3.3.3** shows a partial restriction map of pDUB1911 showing the position of the main subclones created. The sequenced region is shown in more detail; giving the size, polarity and order of the genes identified.

3.4 The Putative *phaA* Homologue.

The start of pDUB1911 contained a partial open reading frame, reading in the antisense direction, which showed significant sequence homology, at the DNA level, with the gene *pha*A from *S. meliloti.* Recent work by Putnoky *et al.* [160] identified a *pha* gene cluster in *S. meliloti,* consisting of seven genes (*phaA, B, C, D, E, F* and *G*), which were shown to be involved in pH adaptation, possibly encoding a novel type of K^+ efflux system. Due to the extensive homology seen previously between the *A. tumefaciens* and *S. meliloti* genomes, it seems likely that a similar cluster of genes may exist in *A. tumefaciens*, upstream of the region studied in this work. Although not directly relevant to this study, the existence of a possible *phaA* homologue, reading in the antisense direction, upstream of the cluster of *che* homologues, confirms that there are no other *che* genes directly upstream of the *orf1* homologue.

3.5 The Putative *che* Gene Cluster.

Approximately 800bp downstream of the supposed *phaA* homologue was the start of an almost 8kb stretch of nine putative chemotaxis genes, reading in the sense direction. The individual genes, gene order and protein translations of the genes in this region showed considerable homology with chemotaxis regions recently identified in *S. meliloti* and *R. sphaeroides* [9, 78, 81]. Names were subsequently given to the identified *A.*

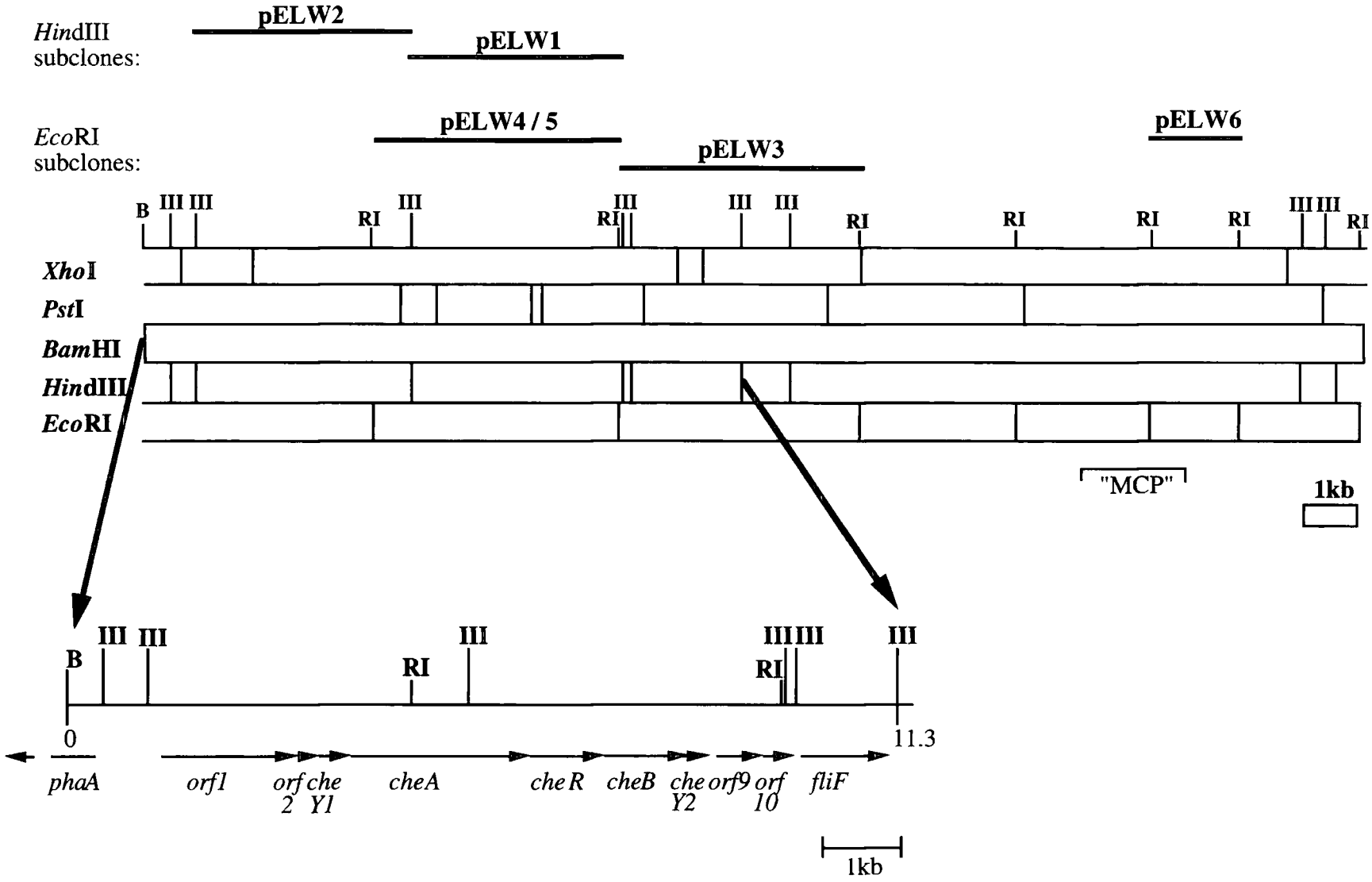

Fig. 3.3.3 Partial restriction map of the cosmid pDUB1911, showing the main subclones created, and in the expanded section, the size, polarity and order of the genes identified. **B** = *Bam*HI, **III** = *Hind*III and **RI** = *Eco*RI.

tumefaciens genes according to the corresponding gene with which they showed greatest homology. The following table shows the principal features of each gene product. Where relevant further details are also given in the subsequent text.

Gene Product	Putative rbs	Start-Stop Sites (bases)	Protein Size (kDa)	Homologues: Closest *E. coli* (% identity)		Conserved Residues
Orf1	GATG	ATG-TGA (1223-2944)	61	*Sm* TlpA (77%)	Tar (25%)	Methylation sites Q295 & E302
Orf2	AGGGAG	ATG-TGA (2922-3221)	10	*Sm* TlpB (59%)		
CheY1	AGGAGA	GTG-TGA (3218-3583)	13	*Sm* $CheY_I$ (90%)	CheY (34%)	Active sites D12, D13, D57, K109, T87
CheA	GGGACA	ATG-TGA (3600-5873)	80	*Sm* CheA (77%)	CheA (39%)	Autophosphorylation site H48
CheR	GAAGG	ATG-TGA (5887-6795)	34	*Sm* CheR (82%)	CheR (37%)	
CheB	GGGAGG	ATG-TAA (6792-7847)	37	*Sm* CheB (80%)	CheB (51%)	Phosphorylation site D56
CheY2	GAAGG	ATG-TGA (7847-8236)	14	*Sm* $CheY_{II}$ (89%)	CheY (34%)	Active sites D12, D13, D57, K109, T87
Orf9	GGATCG	ATG-TAG (8233-8778)	19	*Sm* CheD (71%)		
Orf10	GGAG	ATG-TAG (8793-9176)	13	*Sm* Orf10 (73%)		

Table 3. Characteristics of the genes identified in the *A. tumefaciens che* cluster.
rbs = ribosome binding site [185], *Sm* = *S. meliloti*. The figures for the start and stop sites of each gene relate to their position in pDUB1911. The percent identity figures given are for alignment over the whole length of each protein. The "conserved residues" column indicates those known functional sites in *E. coli* which were also seen in the *A. tumefaciens* homologues.

The start sites of each gene and the putative ribosome binding sites [185] are also marked on the sequence data in section **3.9**. Several of the genes (*orf2/cheY1*, *cheR/cheB* and *cheY2/orf9*) showed overlapping stop/start sites, in an ATGA configuration (GTGA for *orf2/cheY1*). In addition, at the junction of *cheB/cheY2*, there is a one base pair overlap. The ATGA configuration has been seen previously for *A. tumefaciens* flagellar

genes [55, 57], similar overlaps, of one to four base pairs, were also seen for several genes in the *S. meliloti che* operon [78]. This overlapping arrangement of genes suggests that the *che* cluster identified may also be transcribed as an operon.

In enteric bacteria the *che* genes are under the control of class III flagellum-specific promoters [121]. A region of sequence 116bp upstream of *orf1* (see section **3.9**) showed some similarity with the *E. coli* class III consensus promoter, and also with the putative promoters of the *A tumefaciens* genes *flaC* and *flaB* [54] :

	-35		**-10**
E. coli class III consensus promoter	TAAA	N15	GCCGATAA
Putative *A. tumefaciens che* promoter	TAAA	N19	GCGGAATG
Putative *A.tumefaciens flaC* promoter	TAAC	N18	GCGCATCG
Putative *A. tumefaciens flaB* promoter	TAAC	N19	GCTCATCG

In a similar manner to the *flaC* and *flaB* promoter sequences, the putative *che* promoter has a larger gap between the "-35" and "-10" sequences than is seen in the enteric class III consensus promoter. This has also been seen for the putative promoters of several *S. meliloti* flagellar-related genes [54]. The "-10" sequence of the putative *che* promoter shows a low level of homology with the consensus sequence, however it is comparable to that seen for other putative class III promoters in *A. tumefaciens.*

A possible transcription terminator, with a stem-loop motif, was identified directly downstream of *orf10,* using the Macintosh programme DNA Strider and the Terminator programme at SEQNET:

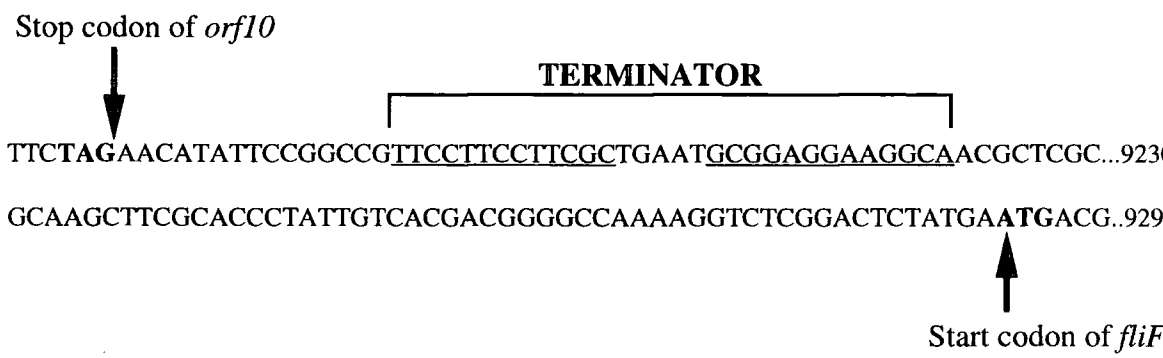

Fig. 3.5 Possible terminator of the *A. tumefaciens che* cluster.
The figures to the right of the sequence indicate the position in pDUB1911. The putative terminator has a 13bp GC-rich stem, with only 2 mismatches, and a 5bp loop. Its position is also marked on the sequence data in section **3.9**.

The presence of putative promoter and terminator sequences flanking the *che* cluster, also indicate that the region may be transcribed as an operon, as is thought for the *che* regions identified in other, closely related bacteria.

3.5.1 Orf1 and Orf2.

Protein homology searches showed Orf1 and Orf2 to have significant homology with TlpA and TlpB, respectively, (previously OrfI and OrfII) from the *S. meliloti che* operon. Over expression and deletion studies of TlpA and TlpB have suggested that they both have an internal sensor role in the chemotactic signal transduction pathway [9]. It is thought they may produce an additive signal, indicating the metabolic state of the cell, and differentially interact with CheA. TlpA bears significant homology with the conserved MCP signalling domain, but lacks the periplasmic receptor domain and the transmembrane domains found in *E. coli* MCPs. It is therefore thought that TlpA is a cytoplasmic sensor. TlpB also has some homology with the classical MCP signalling domain. Homologues of both proteins have been found in the related bacterium *R. sphaeroides*, which also contains a third Tlp; TlpC. A homologue of TlpB has also been identified in *C. crescentus*. The prevalence of these proteins, their presumed cytoplasmic nature and their already proven role in chemosensing suggests they could constitute a new element of the known chemotactic signal transduction pathway.

Orf1 also showed considerable homology with the C-terminal signalling domains of several known MCPs. Kyte / Doolittle analysis of Orf1 from *A. tumefaciens* suggested that it did not contain any transmembrane domains (data not shown). Therefore indicating that, although it may have a chemotactic signalling role, it is unlikely to function in the same manner as the MCPs in *E.coli*. Alignment of Orf1 with Tar (see **Fig. 3.5.1**) confirmed that homology between the two proteins occurs principally at the C-terminal cytoplasmic signalling domain. Orf1 contains two possible methylation sites, assigned according to their homology with the known methylation sites of Tar. It also exhibits significant homology with the conserved region of the signalling domain common to all MCPs found in *E. coli*. It has 81% identity and 90% similarity with the 54 conserved residues in this region, in particular it shows conservation of the residues proposed to mediate interaction with CheW in *E. coli* [117].

In addition to the homology with TlpB, Orf2 also showed homology, at a lower level, with hypothetical protein X (orf2 product) from the *R. sphaeroides che* cluster 1 (31% identity and 49% similarity) and with Orf10 from the start of the *R. sphaeroides che* cluster 2 (35% identity and 51% similarity). (See **Fig. 1.7** for the relative positions of the relevant *S. meliloti* and *R. sphaeroides* genes mentioned.) Alignment of Orf2 with Tar (see **Fig. 3.5.1**) showed that it had 50% similarity with the C-terminal signalling domain,

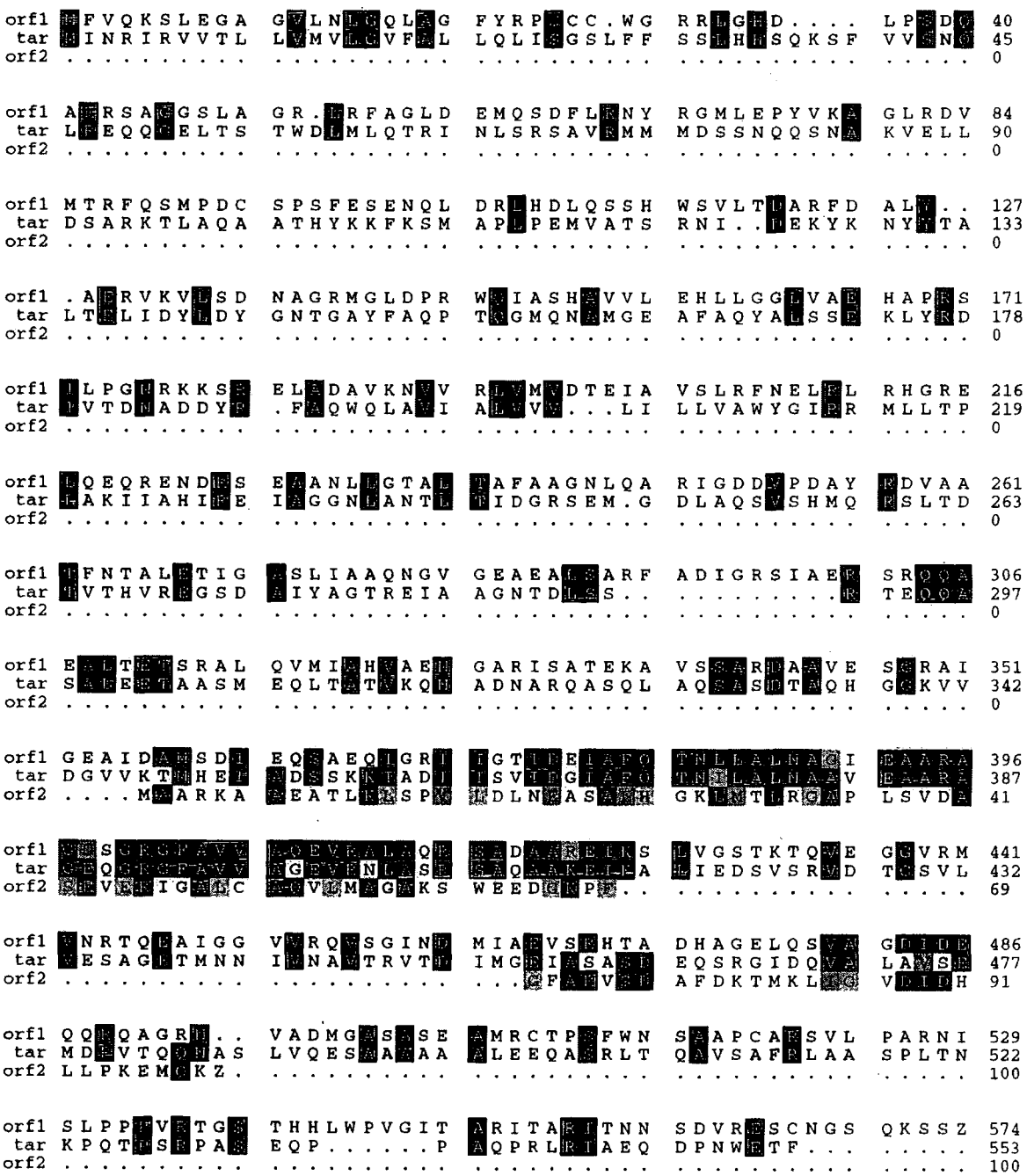

Fig. 3.5.1 Prettybox display of a pileup alignment of Orf1, Orf2 and the *E. coli* MCP Tar.

Black boxes indicate conserved residues, shaded boxes indicate conservative substitutions.

and contained 12 of the 54 residues in the highly conserved region of Tar. Orf2 also showed a similar level of homology with the C-terminal of Orf1.

From homology studies, it therefore appears that both Orf1 and Orf2 are likely to have a signalling role in the chemosensory system of *A. tumefaciens*. In such a role they are likely to either, interact with a membrane-bound sensor protein, which then signals to CheA, or, interact directly with CheA or other Che protein. Mutational studies of both proteins should give a clearer analysis of their function, however it does seem likely that they will have an internal sensor role, possibly detecting the metabolic flux of the cell.

3.5.2 CheY1 and CheY2.

Both CheY proteins showed significant homology to CheY from other bacterial species. However the greatest homology seen was to their counterparts from the *S. meliloti che* operon (see **Table 3**). Gap alignment of CheY1 and CheY2 showed that they have a lower level of homology with each other (59% similarity and 38% identity) than they do with the relevant proteins from *S. meliloti*. This marked difference in amino acid composition seems to suggest that the two proteins have quite different roles in the signalling process. Due to their very high levels of homology with $CheY_I$ and $CheY_{II}$ from *S. meliloti* it seems likely that they will perform similar functions to these proteins. Recent work by Sourjik and Schmitt [194], on phosphotransfer during chemotaxis in *S. meliloti,* has shown that $CheY_{II}$ is likely to be the main regulator of flagellar rotation rate; it has subsequently been termed the "slow" signal. $CheY_I$ however is thought to act as a phosphate sink from both $CheY_{II}$-phosphate and CheA-phosphate, and therefore acts to terminate the slow signal. Whether CheY1 and CheY2 act in the same way in *A. tumefaciens* will only be determined by detailed analysis of each protein.

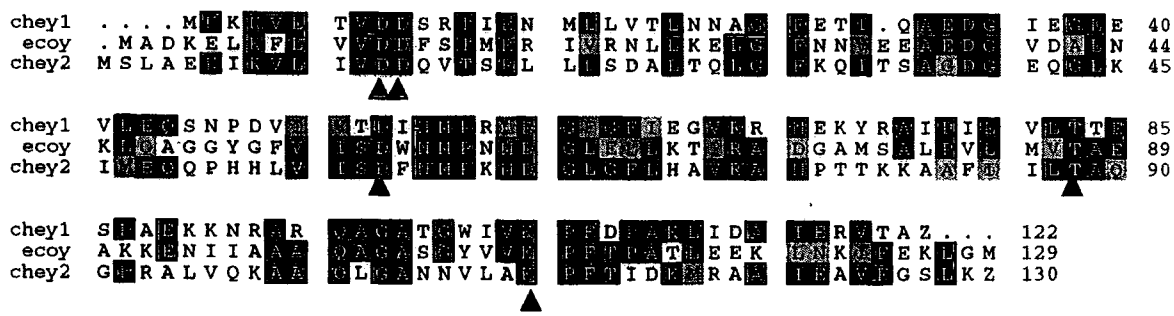

Fig. 3.5.2 Prettybox display of a pileup alignment of CheY1, CheY2 and CheY from *E. coli*.

Black boxes indicate conserved residues, shaded boxes indicate conservative substitutions. Conserved functional residues are denoted by a ▲ .

Alignment of the two CheY homologues showed both to contain the functionally important residues D12, D13, D57, T87 and K109 identified in CheY from *E. coli* (see **Fig. 3.5.2**). Conservation of these residues has also been seen in each of the CheY homologues identified in *S. meliloti* and *R. sphaeroides* [81].

3.5.3 Orf9 and Orf10.

In addition to its homology with CheD (previously Orf9) from the *S. meliloti che* operon, Orf9 also showed homology with CheD from *B. subtilis* (49% similarity and 30% identity). The homology seen was at a level lower than that seen with the *S. meliloti* protein, but at a level comparable to that seen between the other Che proteins identified and those from bacteria other than *S. meliloti.* In *B. subtilis*, CheD is required for methylation of the MCPs by CheR (see section **1.2.2**), it is therefore possible that Orf9 has a similar role in *A. tumefaciens*.

Orf10 occurs in a similar position in both *S. meliloti* and *A. tumefaciens*, that is upstream of *FliF,* but also directly downstream of several chemotaxis genes. Whether it plays a role in chemotaxis or contributes directly to flagellar synthesis is unknown. Identification of a possible terminator downstream of *orf10* in this work suggests that it lies within the *che* cluster. It is therefore probable that Orf10 has a role in chemotaxis rather than flagellar synthesis or assembly.

Orf10 was also found to show homology with hypothetical protein 2 from *R. sphaeroides* (25% identity and 47% similarity), again the function of this protein is unknown.

3.6 The putative *fliF* homologue.

A homologue of the flagellar gene *fliF* was identified downstream of the putative chemotaxis cluster. It showed 81% similarity and 67% identity with FliF from *S. meliloti.* It also showed significant homology with its counterpart from the related bacterium *C. crescentus*, and with that from *E. coli.* FliF forms the MS-ring of the *E. coli* flagellum and is the first protein to be laid down in the construction of a new flagellum (see **Fig. 1.3.1**), the homologue identified in this work is therefore likely to have a similar function in *A. tumefaciens.*

In *E. coli* , transcription of *fliF* is under the control of a class II promoter [121]. The *E. coli* class II consensus promoter has no identifiable "-35" sequence, but has the same "-10" sequence as the class III consensus promoter (see section **3.5**). A putative promoter sequence, which showed three mismatches from the *E. coli* consensus, was identified 141bp upstream of the *fliF* start site. No obvious terminator was identified in the

sequence downstream of *fliF*. The putative promoter is indicated on the sequence data in section **3.9**.

3.7 Positioning of the *che* Cluster in Relation to the Other Flagellar/Motility Genes Identified in *A. tumefaciens*.

Many flagellar/motility-related genes have previously been identified in *A. tumefaciens* (see section **1.8**). The cosmid pDUB1900 contains at least 20 flagellar/motility-related genes grouped into a large cluster (*motA* operon - *motAfliMNG*: 3978bp: accession no. U63290, *fliN* accession no. X65584, *flgB* operon - *flgABCGHIfliELP*: 7205bp; accession no. U39941, 3 flagellins - *flaABC*: 4423bp; accession no. X80701, *flaD*, *flhB*, *flgF* + *fliI* and *MotBCD*. See **Fig. 1.8** for the relative positions of the genes). In addition the cosmid pDUB1905 contains homologues of the flagellar genes *flhA* and *fliR*, as well as a homologue of the *C. crescentus* chemotaxis gene *cheL*. The arrangement of many of the genes identified closely resembles that seen for the corresponding genes in the highly related bacterium *S. meliloti*. Recently Sourjik *et al.* [195] reported that 41 of the chemotaxis, flagellar and motility genes identified in *S. meliloti* mapped to a contiguous 45kb region of the chromosome. Due to the high levels of homology seen between *A. tumefaciens* and *S. meliloti*, consideration must be given to the fact that a similar arrangement may exist in *A. tumefaciens*.

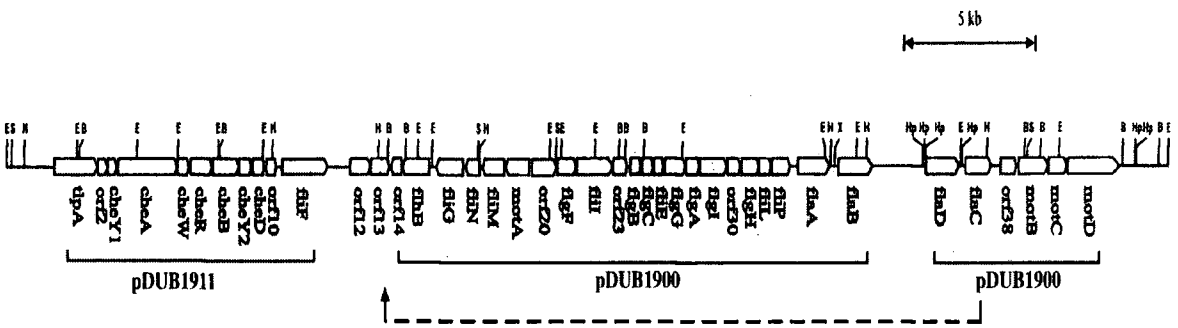

Fig. 3.7 Map showing the position of 41 chemotaxis, flagellar and motility genes in *S. meliloti*, indicating the cosmid location of the corresponding homologues identified in *A. tumefaciens*. Adapted from [195].

As can be seen in the above figure, the chemotaxis cluster identified in this work aligns with the start of the mapped region from *S. meliloti*, up to, and including, *fliF*. Downstream of this point, in *A. tumefaciens*, there is a further 10kb of sequence (identified by mapping the cosmid pDUB1911) which, preliminary sequencing data suggests, does not resemble the corresponding downstream region in *S. meliloti*. In *S. meliloti* the region of

sequence downstream of *fliF* leads into a large group of flagellar-related genes, plus some unknown orfs. A similar group of genes was found in the *A. tumefaciens* cosmid pDUB1900 (see **Fig. 1.8**). There appears to be a conservation of gene order over a large majority of the sequence, with the exception of the *fla* and *mot* genes. These genes occur downstream of the other flagellar genes in *S. meliloti*, but upstream of them in pDUB1900. Since the two bacteria are thought to be closely evolutionarily related it seems likely that there could have been a rearrangement of the sequence in one, or both, of the bacteria. Whether the *A. tumefaciens* library cosmids pDUB1900, pDUB1911 and pDUB1905 are linked awaits further investigation, however the levels of homology seen with corresponding genes in *S. meliloti* would appear to strongly suggest that there may also be a clustering of chemotaxis, flagellar and motility-related genes in the *A. tumefaciens* genome.

3.8 Discussion.

Heterologous probing using a fragment from the *S. meliloti che* operon identified the *A. tumefaciens* library cosmid pDUB1911. Subsequent subcloning and sequence analysis identified a cluster of chemotaxis-related genes. The *che* cluster was flanked upstream by a homologue of the *S. meliloti* gene *phaA*, and downstream by a homologue of the flagellar gene *fliF*.

The *che* cluster contained homologues of the *S. meliloti* genes *tlpA, tlpB, cheY*$_{I}$, *cheA, cheR, cheB, cheY*$_{II}$, *cheD* and *orf10*. Due to the high level of homology and conservation of gene order, of the identified genes, with those from the related bacteria *S. meliloti* and *R. sphaeroides*, it was postulated that the *che* genes were transcribed together, as an operon. In addition, several of the genes exhibited overlapping stop/start boundaries, indicative of coupled transcription. The identification of a putative class III promoter upstream of *orf1*, and a putative terminator downstream of *orf10*, also suggest that the region is transcribed as an operon. At this stage, whether the region is functional, and if it is, how it is transcribed, can not be confirmed without further analysis. This could be done by, for example, site directed mutagenesis of specific genes and identification of any resultant changes in phenotype. The transcription initiation site of the operon could be studied utilising primer extension or S1-nuclease mapping techniques.

The sequences indicated as putative promoters of the *che* region and *fliF* also require further analysis. Although they bear some resemblance to the *E. coli* concensus sequences, if considered statistically, it is possible that many regions could be viewed as putative promoters. Therefore their existence could only be confirmed by carrying out specific experiments that test their functionality.

The products of the *che* genes identified also showed significant sequence homology with their counterparts from numerous other bacterial species, e.g. *E. coli, C. crescentus* and *B. subtilis*; many showing conservation of known functional residues (see **Table 3**). It is therefore possible that they have similar functional roles in *A. tumefaciens*. Once again, this can only be established by further analysis of the proteins.

As with *S. meliloti* and *R. sphaeroides,* no homologue of the chemotaxis gene *cheZ* was identified in *A. tumefaciens*. However, as mentioned in section **1.7**, it is possible that the specific functions of CheZ are encompassed by another protein or that there is no requirement for such a protein in these bacteria. This could be a reflection of the principally unidirectional patterns of flagellar rotation seen in these bacteria.

The main difference between the *A. tumefaciens che* cluster and those from *S. meliloti* and *R. sphaeroides* is the lack of a *cheW* homologue. The precise action of CheW in *E. coli* is still poorly understood (see section **1.2.1.4**). However it is known to be an anchoring protein, required for interaction of CheA with the MCPs. Results to date suggest that the chemosensory pathways of bacteria from the α-subgroup of *Proteobacteria* are likely to be more complex than the basic system found in enteric bacteria. It is possible therefore that the chemosensory system of *A. tumefaciens* represents a more highly evolved version of the basic pathway, and as a result there may be no requirement for a homologue of CheW. Alternatively, as was postulated for CheZ, its function may be contained within another protein. However, homologues of CheW have been found in both *S. meliloti* and *R. sphaeroides*, this therefore suggests that *A. tumefaciens* is likely to possess a CheW homologue. The progress made in identifying CheW is given in section **6.1**.

It is possible that *A. tumefaciens* may possess more than one chemosensory region, as has been found for *R. sphaeroides* [81]. Whether the region identified in this work is functional, and the possible existence of a second *che* region in *A. tumefaciens* will be considered in chapters **4** and **6**.

One further point of consideration, not specifically addressed by the genes identified in the *che* cluster, is the possibility of *A. tumefaciens* utilising MCPs as part of its chemosensory response (see section **1.8**). The presence of homologues of CheB, CheR and CheD, in the *A. tumefaciens che* cluster, suggests that there could also be MCP-like proteins involved in the chemotactic responses of *A. tumefaciens* (as indicated by previous evidence - see section **1.8** and **chapter 6**). However, it is also possible that Orf1, or other, as yet unidentified Tlps, could be the methylation/demethylation targets for these proteins. Whichever, it seems plausible that the process of methylation could constitute part of the chemosensory pathway of *A. tumefaciens*. In mapping the cosmid pDUB1911, several fragments positioned downstream of the *che* region were partially sequenced. One of these fragments, pELW6, was found to show some homology with the *C. crescentus* protein McpA, the significance of this, plus further details, are given in section **6.3**.

3.9 Complete Sequence of the Sense Strand of an 11.3kb Region of the Cosmid pDUB1911.

The first 9.6kb of sequence has been fully sequenced in both directions and has been submitted to GenBank under the **Accession Number AF044495**. The putative promoter sequences of the *che* cluster (bases 1075 - 1105) and *fliF* (bases 9137-9144) are shown in bold type. The putative *che* terminator sequence is double underlined (bases 9192 - 9222). Possible ribosome binding sites for each of the genes are underlined. The position of each gene is marked by its name above the relevant start site and an * underneath the last base of its stop site.

```
        |  10        |  20        |  30        |  40        |  50
    1   GGATCCTTGG   AGGACATGTA   ATAGCGGGCA   TAAAGCACGA   CGAGCAGGCC   50
   51   TATGCCGGTA   ATGAGGATCG   CGAAAATCCA   GGCAAAACCG   TCCAGCCGCA   100
  101   GGGTAAAATT   GAGGCCGAGC   TGCGGAAGCC   ATTCCACATC   ATATTTCAGC   150
  151   ACGCCGCCGC   CGCTGATGGT   GGAATATAAA   AACATGCTGC   TGACGAGGCC   200
  201   GAAGAGGGCG   ACGCCGCCCG   CGACGGAGGC   CGGACCGGCG   GCCGCACCAT   250
  251   CGCGCGGCAT   GAAGGCCGTG   AGGAAAGCGC   CGACAAACGG   CAATGCGACA   300
  301   ATAAATGGGA   GAAGGGTTGC   AAGTGTCATA   TGCGGCGGCG   GTTTTCTTTC   350
  351   TGGAATGGGA   GCCTACGGCG   GGTTTCCGAC   GACTCCGATC   CCTCAAGGTT   400
  401   CACAATGAAC   CCAATGATGA   TGACCGCCGG   ATGACTAATA   CATAATATGC   450
  451   GGAGGCGCGC   GGGGAACCAC   GCTGGCAAAG   TCTCGGAAAG   CTTGTGGCAC   500
  501   GATGGCAACA   GCAACAAGGG   AGGCCTTGGT   ATTTTCGGTA   ATGCTGAGCG   550
  551   CGGGTGAGGG   GAACTCCCCG   TGCTGGAACC   CTCGGCCGGT   ATCGCTGCTC   600
  601   CGGCAGGTGT   AATCGTTGCC   GCTATCGCAA   TCCTTATCGC   GAAGGGAAAG   650
  651   CGAACGGCTG   AGATCGACGG   TCTGTAACCG   CTCGAGGCGG   CTAGCCTTGG   700
  701   AGAGTGCCTT   GACGCCCGAG   GGTACCTGAA   AGCCGATCAT   GACAAGCAGA   750
  751   CTCGCGACCA   CGAGACCGAT   GAGCACTTGC   GGATGGCGCC   TTGAACTGCG   800
  801   GCCTTTCTCC   ATCCGTGGCA   AGTTGGCATC   TCCTTGGTCG   AAAAGGTCTC   850
  851   TCTAAAGCAT   CACCGCTGAG   CGAATATCCC   GTTGATTTGT   TTTAGGGGAA   900
  901   CCCGCACGCG   CTTGTCCAGC   GCGCAGGCCG   GAAAAACCGG   CCGGAGCGTC   950
  951   CGATTCCTTT   TCGTTTTTGC   CCGTTTGCGG   CAAAGTAAGG   GCGACAATGG   1000
 1001   CTAAAAGCTT   TTACAAATTT   TACCGTTTGA   GGCCGGTGCT   TATGTTTCTT   1050
 1051   AACTTTCAAG   CAAGGAATTA   ACCATAAAGA   TTGGTGGTAT   TTCCACGGCG   1100
 1101   GAATGGGGTT   CCTCCCCTTC   CAGGCATGAC   GCCGCACTGC   CGTACCGGGC   1150
 1151   TCGATCCGGT   ATTTTCGTTT   CTTGGTTCAA   GAAGGTCTGG   CAAGCGTCGA   1200
                                 Orf1
 1201   TGCCTCATCG   TCCACGATGG   GTATGTTCGT   TCAAAAATCC   CTGGAGGGTG   1250
 1251   CTGGCGTTTT   GAACCTTGGC   CAATTGGCCG   GGTTTTACCG   GCCATCATGT   1300
```

1301 TGTTGGGGAC GTCGGTTGGG GCACGATTTG CCATCAGATC AAGCGCGTAG 1350

1351 ATCGGCAGGC GGAAGCCTGG CAGGACGGTT GCGCTTTGCC GGCCTTGATG 1400

1401 AGATGCAATC CGATTTCCTG CGCAATTATC GCGGCATGCT GGAGCCTTAC 1450

1451 GTCAAGGCCG GCCTGCGCGA CGTGATGACC CGTTTCCAGT CCATGCCGGA 1500

1501 CTGTTCGCCG TCCTTCGAAA GCGAAAACCA ACTCGATCGC CTGCACGATC 1550

1551 TGCAATCCTC GCACTGGAGC GTCCTGACGG ATGCGCGTTT CGATGCGCTT 1600

1601 TATGCCGAGC GGGTGAAGGT TCTTTCCGAT AATGCCGGTC GCATGGGTCT 1650

1651 CGATCCGCGC TGGCAGATCG CTAGCCACGC CGTCGTTCTG GAGCATCTGC 1700

1701 TCGGCGGGCT GGTGGCTGAA CACGCGCCCC GCTCCATCCT GCCCGGCAAC 1750

1751 CGTAAAAAGA GCCGCGAACT GGCGGACGCC GTGAAGAACG TCGTCCGGCT 1800

1801 GGTGATGGTC GATACCGAGA TTGCCGTGTC GCTGCGCTTC AACGAACTGC 1850

1851 GCCTGCGCCA TGGCCGCGAA CTCCAGGAAC AGCGCGAGAA TGACCGCTCG 1900

1901 GAAGCGGCGA ATTTGCTGGG CACGGCCCTG ACCGCCTTTG CCGCGGGCAA 1950

1951 TTTGCAGGCC CGCATCGGGG ACGATGTGCC CGACGCTTAC AGGGACGTCG 2000

2001 CAGCCACCTT CAACACGGCG CTCGAGACGA TCGGCGCGTC GCTGATAGCC 2050

2051 GCCCAGAACG GTGTAGGCGA GGCCGAGGCG CTGAGCGCCC GCTTTGCCGA 2100

2101 TATCGGCCGC TCGATTGCGG AGCGTTCACG CCAGCAGGCC GAAGCGCTTA 2150

2151 CCGAGACCTC CCGTGCACTC CAGGTGATGA TTGCGCATGT GGCTGAAAAC 2200

2201 GGCGCCCGTA TATCGGCGAC GGAAAAGGCG GTTTCCAGCG CCCGCGACGC 2250

2251 GGCCGTCGAA AGCGGGAGGG CGATCGGCGA GGCGATCGAC GCCATGTCGG 2300

2301 ATATCGAACA ATCAGCCGAA CAGATCGGAC GGATCATCGG CACCATCGAC 2350

2351 GAGATCGCCT TCCAGACCAA CCTTCTCGCC CTCAATGCCG GCATCGAGGC 2400

2401 GGCACGGGCC GGCGACAGCG GACGCGGTTT CGCCGTCGTT GCGCAGGAAG 2450

2451 TCCGGGCATT GGCCCAGCGT TCCGCCGATG CCGCAAGAGA GATCAAGAGC 2500

2501 CTTGTCGGCT CCACCAAAAC GCAGGTCGAG GGTGGGGTGC GCATGGTGAA 2550

2551 CCGCACGCAG GAGGCCATTG GCGGGGTCGT CCGGCAGGTA TCCGGGATCA 2600

2601 ACGACATGAT CGCCGAGGTT TCGCGGCACA CCGCCGACCA CGCCGGAGAA 2650

2651 TTGCAATCGG TCGCCGGTGA TATAGACGAA CAGCAACGGC AGGCCGGGCG 2700

2701 GAATGTCGCC GACATGGGCG CCAGCGCCTC CGAGGCGATG CGCTGCACAC 2750

2751 CGTCATTCTG GAACTCGGCC GCACCGTGCG CGCGTTCCGT ATTGCCCGCC 2800

2801 AGGAACATTT CGCTGCCGCC GCCGGTGCGG ACTGGCAGCA CTCATCATTT 2850

2851 ATGGCCCGTG GGGATAACCG CACGGATAAC AGCCAGAATT ACCAACAATT 2900

Orf2

2901 CAGACGTCAG GGAGTCATGT AATGGCAGCC AGAAAAGCAG CTGAGGCGAC 2950

*

2951 GCTGAAACTG TCACCGGTGC TGGATCTCAA CGAAGCATCG GCTCTGCACG 3000

3001 GCAAGCTGAT GACGCTGAGA GGAGCACCTT TGTCGGTCGA TGCGTCCGAG 3050

3051 GTGGAGCGCA TTGGCGCGCT TTGCGCCCAG GTCCTCATGG CCGGCGCGAA 3100

3101 ATCCTGGGAA GAGGATGGCA AGCCCTTCGG TTTCGCAAGG GTTTCCGATG 3150

3151 CATTCGACAA GACCATGAAA CTGATAGGCG TCGATATCGA CCATTTGCTC 3200

CheY1

3201	CCTAAGGAGA	TGCAAAAGTG	AAGAAAAAAG	TTCTTACCGT	GGATGATTCC	3250
			*			
3251	AGAACGATCA	GGAACATGCT	CCTGGTCACG	CTCAACAATG	CCGGTTTCGA	3300
3301	AACCATTCAG	GCCGAAGACG	GCATCGAGGG	TCTCGAAGTG	CTGGAACAGA	3350
3351	GCAACCCGGA	TGTCATCGTA	ACCGACATCA	ACATGCCGCG	TCTCGACGGT	3400
3401	TTCGGCTTCA	TCGAGGGCGT	GCGGCGCAAC	GAAAAATACC	GTGCGATCCC	3450
3451	GATCCTCGTT	CTGACGACCG	AAAGCGATGC	GGAAAAGAAG	AACCGCGCCC	3500
3501	GCCAGGCCGG	TGCGACCGGC	TGGATCGTCA	AGCCGTTCGA	CCCTGCAAAA	3550
					CheA	
3551	CTCATCGATG	CCATTGAGCG	CGTAACCGCC	TGATACGGGA	CATTTCACGA	3600
				*		
3601	TGGATATGAA	CGAAATCAAG	GAAATCTTTT	TCCAGGAGTG	CGAGGAACAG	3650
3651	CTCGCTGAAC	TGGAATCGGG	GCTTCTTAAA	TTGAATGACG	GGGACCGTGA	3700
3701	TCCGGAAACC	GTCGACGCCG	TTTTCCGTGC	CGTTCATTCC	ATCAAGGGCG	3750
3751	GGGCCGGTGC	CTTTGGTCTC	GATGATCTCG	TGGCCTTCGC	CCACGTTTTT	3800
3801	GAAACGACCC	TCGACTGCGT	TCGCTCCAAC	AAGCTGGAAC	CGACACAGGA	3850
3851	CGTTCTAAAA	GTCATGCTGC	GCTCCGCCGA	TGTGCTGGCG	GATCTGACCA	3900
3901	ACGCGGCCAG	AGACGGCGGC	AGCGTCGATG	AAAGCCGCAC	CCGTGGCCTC	3950
3951	GTCAAGGAAC	TGGAAGCGCT	GGCCAATGGC	GAAGCCGTTC	CGGCATCCGC	4000
4001	GCCGGCTCCT	GTCGCTGTTA	AGGCGCCGGA	ACCCGTCAAG	GCGCCCGCAG	4050
4051	CACCGAAGCC	GACGGATGAA	AGCGGTTTCG	AGCCGATCCC	GTTCTCTTTC	4100
4101	TCCGATTTTG	CCGACGAGAC	GACGCCGCTG	ATGGAGGTGC	CGACCTTCCA	4150
4151	GATTACGTTC	AAGCCGCACG	CCTCGCTTTA	TTCCAAGGGC	AATGAGGCGG	4200
4201	CACTTCTGCT	ACGTGATCTC	TCGCGCATCG	GCGACATGAG	CGTCAATTGC	4250
4251	GACATGTCCG	ACCTGCCGGC	GCTCGACAAG	CTCGATCCCG	AAGCCTCCTA	4300
4301	TCTCTCCTGG	ACGGTTTCCA	TCGCCACCGA	AAAGGGTGAG	GAAGGAATCC	4350
4351	GCAGCGTCTT	CGAATTCGCC	GAATGGGATT	GCGATCTCGA	AATCACCGCA	4400
4401	GTTGTTTCGG	ACGCGTCCGC	GGACGAAGAA	GAACTGCCGA	TGATCCCGGT	4450
4451	TCCGTTCGAT	CTGTCTGCTC	TCGATGGTGA	TGCGCAGGAC	GAACCCGCCG	4500
4501	TCGCGACCCC	CGCGATGGAA	GATGCCTACG	TTGCCGCAAC	CGTCGAAGCT	4550
4551	GCCGTCGCGA	CGACGCAGAT	CGCCCAGAGC	GTCAATGCCG	CTATCGAAAA	4600
4601	GCGCGAGGCG	GCGGCAGCGC	CGGCCGCAGC	GCAGGCGAAC	GCCAATGCCG	4650
4651	CCGCCAATGC	GAGTGCCGGC	CAGACCATCC	GCGTCGACCT	CGATCGCGTC	4700
4701	GACCGCCTGA	TCAATCTCGT	CGGCGAGCTT	GTCATCAATC	AGGCGATGCT	4750
4751	GTCGCAGAGC	GTCATCGAAA	ACGATGCGAG	CGGCACCTCC	GCCGTTAATA	4800
4801	TGGGTCTGGA	CGAGCTGCAG	CAGCTGACGC	GCGAAATCCA	GGACAGCGTC	4850
4851	ATGGCCATCC	GCGCGCAGCC	GGTGAAGCCC	GTCTTCCAGC	GCATGTCGCG	4900
4901	TATCGTCCGC	GAAGTCGCCG	ACATGATCGG	CAAGCAGATC	CGCCTCGTCA	4950
4951	CCGAAGGTGA	GAACACGGAA	GTCGACAAGA	CGGTCATCGA	CAAGCTGGCC	5000
5001	GAACCCCTGA	CCCACATGAT	CCGCAATGCC	GTCGACCATG	GCATCGAGAC	5050

5051 GCCGGAAAAG CGCGAAGCCG CGGGCAAGAA CCCGGAAGGC ACCATCAAGC 5100

5101 TTTCGGCCAA GCACCGTTCG GGCCGTATCC TCATCGAGCT TCAGGACGAT 5150

5151 GGCGCCGGCA TCAACCGTGA GCGCGTCCGC CAGAAGGCGA TCGACAACGA 5200

5201 TCTGATTGCC GCCGATGCGA ACCTGACCGA CGAGGAGATC GACAATCTGA 5250

5251 TCTTCGCGCC GGGCTTCTCG ACGGCAGACA AGATTTCCGA CATTTCCGGC 5300

5301 CGCGGTGTGG GCATGGATGT GGTCAAGCGT TCCATTCAGG CGCTCGGCGG 5350

5351 CCGCATCAGC ATCTCGTCGC GTCCGGGCCT CGGCTCGACC TTCACCATGA 5400

5401 GCCTGCCGCT GACGCTTGCC GTTCTCGACG GTATGGTGGT GACCGTGGCC 5450

5451 GGTCAGACGC TCGTCGTTCC TCTGACGGCA ATCGTCGAAA CCCTGCAGCC 5500

5501 GGAAGCGAAG AACATCCACT CCTTCGGTTC CAACCAGCGG CTGATCTCCA 5550

5551 TCCGCAACTC CTTCTGCCCG CTGGTGGATG TCGGTCGTGT CCTGAACTTC 5600

5601 CGTCCGACCC AGGCCGATCC TGTCGAAGGT GTGGCGCTTC TGGTGGAATC 5650

5651 GGAAGGCGGC GGCCAACGTG CTCTGATGGT CGATGCGATC CAGGGCCAGC 5700

5701 GCCAGGTCGT CATCAAATCT TTGGAAGCCA ACTATACCCA TGTTCCGGGC 5750

5751 ATCGCCGCCG CCACCATTCT CGGTGACGGA CGTGTAGCGC TCATTCTGGA 5800

5801 TGTCGATGCC ATCGTCAGCG CCTCGCGCGG ACAGCCACTG AAACAGGAAA 5850

CheR

5851 TGTCACTCGC GGCGACGGGT TGAAGGCGGA TATCCAATGG CAGCACTTAA 5900

*

5901 TCTCAGCGAT CAGCGACAGT CTCCCGATGA CGTTCTTGCC AGCGGCGAAT 5950

5951 ATCCGCTGAC ACGGCGCGAT TTGTCGGAGA TCGCTGCGAT GATCTATGCC 6000

6001 GATGCGGGCA TCTATCTCAA CGACACCAAG GCGTCGCTGG TCTATTCCCG 6050

6051 CCTCTCGAAA CATATCCGCA ATCTCGGTCT TTCCGGCTTT CGCGAATATT 6100

6101 GCGCACTGGT GTCTTCGTCC GAAGGTGCAC AGCCGCGCCG GGAAATGCTG 6150

6151 TCGCACCTGA CGACAAATTT CACCCGCTTC TTCCGCGAGA ACCATCATTT 6200

6201 CGAACATCTG CGTGACGAGG TCCTGCCGGG CCTCATCGCT CGTGCCAAGA 6250

6251 GTGGCGGGCG TGTCCGCATC TGGTCGGCGG CCTGCTCCGA CGGGCAGGAA 6300

6301 CCCTATTCGA TTGCGCTGAC CGTACTGGCC ATGTTCCCGA ATGCGGCCGA 6350

6351 TTACGATTTC AAGATTCTGG CCACCGATAT CGATCCCAAG ATTCTGGCGC 6400

6401 AGGCCCGTGC CGGCGTTTAC GATGACAACG CGCTTGAAAC CGTGTCTCCT 6450

6451 GCCATGCGCA AGCAATGGTT CACCGAGGTC GATGCCGGCG GTCGCCGCAA 6500

6501 GTTCCGCATC GATGACAAGG TCAAGCGTCT CATCACCTTC AACGAGCTGA 6550

6551 ACCTGATGAC GCAATGGCCC TTCAAAGGCA ATTTCGACGT CATCTTCTGC 6600

6601 CGCAACGTCG TCATCTATTT CGACGAGCCG ACGCAGGTGC GCATCTGGTC 6650

6651 GCGTTTCGCG GGCCTGCTGC CGGAAGGCGG CCACCTCTAT ATCGGCCATT 6700

6701 CCGAACGTGT GTCCGGTGAC GCCAAGAACG TGTTCGACAA TACCGGCATC 6750

CheB

6751 ACCACCTACC GCTTCATCGG TCACGCATCC GGGAGGAAGG CATGAGCGCA 6800

*

6801 CTCGCACGGG TCCTCGTCGT TGACGACTCC CCCACCATGC GCGGCCTGAT 6850

6851 TTCGGCCGTC CTCAAGGCCG ATCCGGAAGT CGAGGTGGTC GGCCAGGCCG 6900

6901 GCAATGCCAT GGAAGCACGT GCCGCCATCA AGCAGCTCAA TCCCGATGTT 6950

6951 GTGACGCTCG ACATCGAGAT GCCCGAGATG AATGGCCTCG AATTTCTCGA 7000

7001 AAAGATCATG CGCCTGCGCC CCATGCCGGT CATCATGGTC TCGTCACTGA 7050

7051 CCCATCGCGG CGCGGATGCA TCGCTTGCCG CGCTTGAAAT CGGCGCTTTC 7100

7101 GACTGTGTCG GCAAGCCGGC TCCCGGTGAC GCGCGCCCCT TCGGCGATCT 7150

7151 GGCCGACAAG GTGAAGGCCG CCGCCCGTTC GCAACATGCC GCCTACCGCG 7200

7201 CCACCCGGCC GGAAACCGCT GCCGCACCGC AGCCGGTTCC GATGAGCGAA 7250

7251 TATCGGGCGG GTCGTAAGGT CGTCGCCATC GGCTCCTCCA CCGGCGGCGT 7300

7301 CGAAGCGCTA ATCGCGGTGC TGCAGAAATT CCCGGCCAAT TGCCCGCCGA 7350

7351 CAGTCATTAC CCAGCACATG CCGCCGACCT TCACCAAGAG TTTCGCGGAG 7400

7401 AGGCTGAACC GCATCTGCGC CCCCGTGGTG GAAGAGGCGA CGGACGGCGC 7450

7451 GCGCCTGCAG ACCGGCAAGA TCTACCTCGC GCCGGGCGGT GAGCGTCATT 7500

7501 TACAGATCGC CAACCGGTCC GCACCCTGCT GCCGGCTTCT GGACCGCGAC 7550

7551 CCCGTCAATG GCCATCGCCC CTCCGTCGAT GTGCTGTTCG ATTCGGTGGC 7600

7601 CGAGCTTGCC GGACGCAACG CCGTCGGTGT CATCTTGACC GGCATGGGCC 7650

7651 GCGATGGCGC GGCCGGGCTT TTGAAAATGC GCCATGCCGG TGCGCGCACC 7700

7701 GTTGGCCAGA ACGAAAAAAC ATGTGTCGTC TATGGCATGC CCCGCGTGGC 7750

7751 CTATGAGCTT GGCGCGGTGG AACAGCAATT GCCGTTGGCC TCCATCGGCG 7800

CheY2

7801 AAGAAATCCT GAAACTAACC ACTGCCCGCA AAGAAGGTGC TGACTAATGT 7850

*

7851 CTCTCGCAGA AAAGATCAAA GTTCTGATCG TCGACGATCA GGTGACCAGC 7900

7901 CGGCTGCTCC TCAGCGATGC GCTGACACAG CTGGGCTTCA AGCAGATCAC 7950

7951 CTCCGCTGGC GACGGCGAGC AGGGATTGAA GATCATGGAG CAGCAGCCCC 8000

8001 ATCATCTCGT CATCTCCGAC TTCAACATGC CGAAGATGGA CGGCCTCGGT 8050

8051 TTCCTGCACG CGGTGCGGGC CAACCCGACC ACCAAGAAGG CCGCCTTCAT 8100

8101 CATTCTCACC GCGCAGGGTG ACCGCGCGCT GGTGCAGAAG GCAGCCCAGC 8150

8151 TCGGCGCCAA CAACGTGCTG GCCAAGCCCT TCACCATCGA CAAGATGCGC 8200

Orf9

8201 GCGGCCATCG AAGCGGTTTT CGGATCGCTG AAATGATGGA AGCTGCGGCC 8250

*

8251 AAGCGCGTAC ATATCATTCA GGGCGAGTAT AAGGTTGTCA GCGATCCCGA 8300

8301 CGTGGTGATG ACGACGATAC TCGGTTCGTG CGTGGCCGCC TGTCTGAGAG 8350

8351 ACCCCGTTGC CGGCCTCGGA GGAATGAACC ACTTCCTGCT GCCGGGAACG 8400

8401 GGCAATGTGA CCGGCGGAGA TGCGACGCGT TATGGCGTGC ATCTCATGGA 8450

8451 GCTGCTGATC AACGGTCTCT TGAAGCAGGG CGCCCGCCGC GACCGGCTGG 8500

8501 AAGCCAAGGT TTTCGGCGGC GCCAAGACGA TCGCCAGCTT CTCGAATGTC 8550

8551 GGCGAGCAGA ACGCCATCTT TGCCATGCAG TTCCTGAAGG ACGAAGGCAT 8600

8601 TCCGGTCATC AGCTCCTCCA CGGGCGGGGA TCATGGCCGC AAGATCGAGT 8650

8651 TCTGGCCGGT CTCTGGACGC GCGCGTCAGC ATCCGCTCAG CGGTGCGGAA 8700

8701 ACCCAGAAGA CGGTTGCCAT GGAAACACGT CCGGTGCCGG CACCCAAACC 8750

Orf10

8751 CGTCGCCAAC GACATCGAAT TTTTCTAGTC ACGGAGTTTC CAATGCAGCT 8800

*

8801 TGCAGAGCAC ACCGCCACCA CTCCGTTCGA AGAAGCCCTG CCGGATGTAC 8850
8851 TGATGCGGGT GGTATCGGAA CTGCACGACG TCGCCTATCT CATCGAGCGC 8900
8901 ATCGAGCCGC AATTGCTTGA TGTGACCAGC GGTCAATTGT CCGCCGAAGG 8950
8951 CGTCAAGCTG TTGCAGGGCA TCGACCTTGC CGTCCAGAAA ACCCGTGGCC 9000
9001 TTGCCGAATT CATCGATACC ATCACCGGCT CCATCCCCGC AGACTGGTTC 9050
9051 GTGGATGTCT CCACCGCACT CAGCCTCGTC AAGCTTGCCG AAATGCAAAA 9100
9101 GGCGCTCGGC GCGGCCTTCC GCCACGGCCA TTCCCA**GCCG** **CTCG**ACAAGG 9150
9151 CTTCCGGCGA CTTCGACCTC TTCTAGAACA TATTCCGGCC GTTCCTTCCT 9200
*
9201 TCGCTGAATG CGGAGGAAGG CAACGCTCGC GCAAGCTTCG CACCCTATTG 9250
FliF
9251 TCACGACGGG GCCAAAAGGT CTCGGACTCT ATGAATGACG GTGCGGAACA 9300
9301 GAATGAATCT GTTAAATCAA ATCCCTCAGG TCTTGAAGAA TGTCGCGGCG 9350
9351 CTGGGCCAGA CGCGGCTGCT GATGCTGGGC GGCGTGGGCG TATTGTCCAT 9400
9401 GGCCATCATC CTGGCTGCAG CGCTTTATGT GAACCGTCCT GCTTACGAGA 9450
9451 CCCTCTATGT GGGTCTTGAA AAAAGTGACC TCAACAAGAT CAGCATTGCA 9500
9501 CTCGCCGAAT CGGGTCTGGA CTTTCAGGTC GGGACCGATG GTTCCAGCCT 9550
9551 TCAGGTTCCG GTCGGGCTCA CCAGCAAGGC ACGGCTGCTT CTGGCTGAAC 9600
9601 GCGGCCTACC CGACAGTGCC AATGCGGGTT ATGAGCTTTT TGACAATGTC 9650
9651 GGCTCCCTCG GCCTGACGTC CTTCATGCAG GAAGTGACGC GCGTTCGTGC 9700
9701 CCTTGAGGGC GAGATCGGCC GCTCCATCCA GCAGATCGAT GGCGTTTCCG 9750
9751 CTGCCCGCGT TCATATCGTC CTGCCTGACG TCGGCAATTT CCGCCGTGGC 9800
9801 GAACAGAAAC CCACGGCATC GGTGATGATC CGCGCGAGCG CATCCGCAGG 9850
9851 CCGCAAGGCC TCCGCCTCCA TTCGCCATCT CGTCGCCTCG GCCGTTCCCG 9900
9901 GTCTCGAAGT CGATGACGTG ACACTGCTCG ATTCGACCGG CCAGCTTCTG 9950
9951 GCCTCCGGCG ATGATGTCAC CAACGCCGCG ATGAACCGGT CGCTGACGCT 10000
10001 GGCCCAAAAT GTTCAGCAGG AAATTACGAC CAATATCGAC AAGGCGCTGG 10050
10051 CGCCTTTCCT CGGCATAGAC AATTTCCGCT CGAGTGTGAC GGCGCAGATC 10100
10101 AATACTGACA GCCGCCAGGT CCAGGAGACC GTTTACGACC CGGAATCGCG 10150
10151 CGTGGAACGC TCCGTTCGCA CGGTGAAGGA AGACCAGAAA TCCCAGGAAA 10200
10201 CGCAGCCGGA TACGGCCGCG ACCGTGGAGC AGAACGTGCC GCAGGCCGCG 10250
10251 CCCCAGGGCG GCGGTGGTGG CCCGCAGTCT TCCGATCAGT CGGCAAAGAA 10300
10301 GGAAGAGCAG ACCAACTACG AGATCAATTC CAAGACGGTT GCCACGGTCA 10350
10351 AGAACGGCTA TACCCTCGAA AAGATTTCGG TTGCCGTGGT CGTCAACAAG 10400
10401 GGCCGTATTG CCAAGATGGT CGGCGAACCG GCCGATCAGG CCAAGATCGA 10450
10451 CGCCTATCTT GCGGAAATGC AGAAGATCGT CACCTCGGCC GCAGGCATTT 10500
10501 CTTCCGATCG TGGCGACATT GTCACCCTGA CGGCGATGGA CTTCCTCGAA 10550
10551 ACGCAGCTGC TTGACGAGGC TGCCAGTGGG CCGGGTGTCA TGGAAGTGCT 10600
10601 GAGCCGAAAT TCCGCCGGCA TCATCAACTC ACTCGCCTTC GTCGCCGTCG 10650
10651 CCTTCCTCGT AGTCTGGCTC GGTGTACGCC CTCTGGTCCG CACGGTCACT 10700

```
10701  GCCAACGGTT  CGGCTGCGGC  TCAGCTCAGC  CAGGAGTCCG  CCGGTCTCGA  10750
10751  ATTGCCGGAC  TTCTCTCCGG  GCATGGAGGC  GGGTGCAGGT  GGTCTCATGG  10800
10801  AAGGTTTCGG  GGCGGATTTC  GGTTTCGACA  GCACCGACGA  TTTTCTGGCT  10850
10851  GGCGGCGATG  GCGAAGGCAC  ATTCAACCGC  CGGTTCGCGA  AGGACCCGAA  10900
10901  CGCAGGTTCT  CCCGCATGGT  GGAAATCAGC  GAGGAGAGAG  CCGCCAAGAT  10950
10951  CCTGCGCAAA  TGGGCGGTGG  AAAAAGCAGC  ATAATGACAA  AAAGGCCGGT  11000
11001  TTTACCCGGC  CTTTTTTCCG  TTTCTGGGGT  TTTTGCTATG  CTTGGCGGGC  11050
11051  ACATCGTGGC  AATCTCGTTT  CGGGACAGTG  TTTACAAAAA  ATTCAGCAAC  11100
11101  GATACAGTTT  GCTGGGAATT  GGCTGAGAAT  GCCGTTTATG  GATTGAACAG  11150
                               *
11151  CTTTTCAGTA  TGTTTTTTTA  GCAATAGACG  AACTGGGAAA  TACGTGGAAA  11200
11201  GGCTGTTGCC  AGGTAATGGC  AAACTCCGGT  CGGTTCCATA  AAATGAAGTG  11250
11251  ATTCGGTCTC  CGGGGGCGCG  CCATTCCGTT  TTGGTAAGCT  TCTTGAATGG  11300
11301  AATGATTCCA  TCCCGAGGTA  TAATCTCCCG  CTGGGAGCAA  GAGGGCGTAG  11350
11351  GCGATTGAAA  GTCGATGTTG  ATATC                             11375
          |    10       |    20       |    30       |    40       |    50
```

4 Mutagenesis of the *che* Genes.

4 Mutagenesis of the *che* Genes.

Two different strategies were employed when creating the *che* mutants; gene replacement mutagenesis and in-frame deletion (see section **2.13**). A total of six different mutants were made; neomycin cassettes were inserted into *orf1*, *cheA* and *fliF*, and in-frame deletions were made of *cheA* and *orf10*, the final mutant was a deletion of the entire *che* gene cluster.

4.1 Mutagenesis of *orf1*.

Several factors implied that the genes identified in the *che* cluster of pDUB1911 may be under the same regulatory control, i.e. form an operon. For example several of the genes in the *che* cluster had overlapping stop/start boundaries, all the genes read in the same direction, and many *che* regions from other bacteria are known to form operons. It was therefore decided to mutate *orf1* by insertion of a neomycin cassette and in doing so possibly disrupt the entire *che* region due to a downstream polar effect, assuming there are no internal promoters.

4.1.1 Construction of the *orf1* Mutant Plasmid.

Sequencing showed *orf1* to lie at the 5' end of the *Hin*dIII subclone pELW2 (see **Fig. 3.3.3**). The steps used in creating the *orf1* mutant construct are outlined in **Fig. 4.1.1** and explained in more detail below:

pELW2 was digested with *Sph*I and *Pvu*II and the 1.5kb fragment containing most of *orf1* from pDUB1911 isolated. The fragment was then blunt-ended and ligated into *Sma*I-cut pJQ200uc1, forming the plasmid pJQorf1. Correct insertion of the fragment was selected for by inactivation of the β-galactosidase gene and confirmed by subsequent restriction digests of the possible positive colonies.

pJQorf1 contains a unique *Xho*I site which cuts approximately in the centre of *orf1*. The 1.2kb neomycin cassette was isolated from pDUB2033 by digesting with *Eco*RI. It was then blunt-ended and ligated into blunt-ended, *Xho*I cut, pJQorf1. Correct insertion of the neomycin cassette was selected for by growth on LM-agar plates containing both

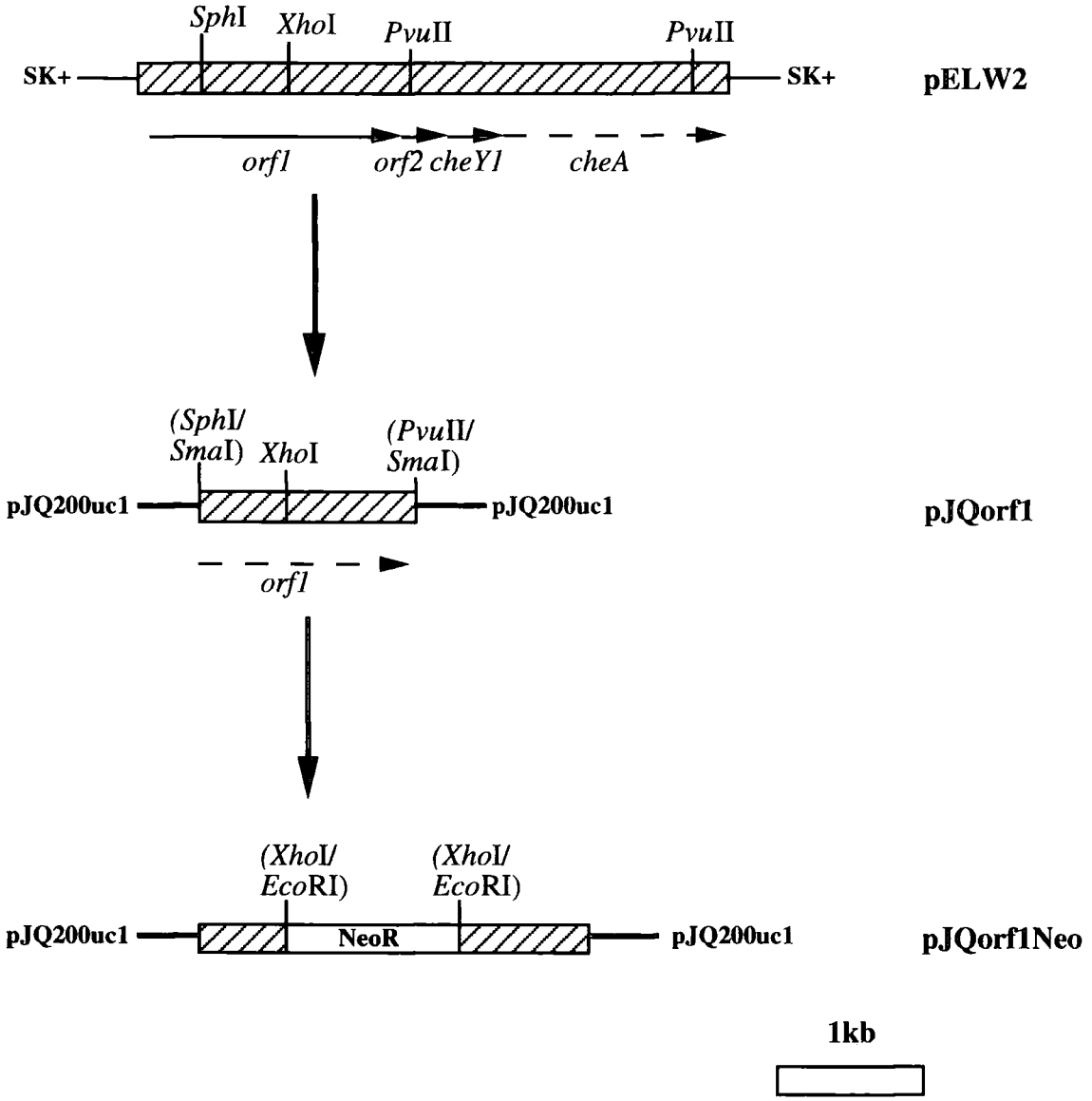

Fig. 4.1.1 Diagram outlining the main steps involved in construction of the *orf1* mutant plasmid.

Approximate sizes and positions of genes are indicated by arrows underneath the main figures. Dashed arrows indicate the presence of only part of a specific gene. Enzymes in brackets indicate restriction sites used in a previous step but no longer existing.

gentamycin and neomycin, and confirmed by restriction digests. The mutant plasmid construct pJQorf1Neo was identified.

4.1.2 Formation of the *A. tumefaciens orf1* Mutant Strain.

The final construct, pJQorf1Neo, was introduced into C58C1 by tri-parental mating (see section **2.9**). The tri-parental mating mixture was plated on LM-agar plates containing rifampicin, neomycin and 5% sucrose. Hence allowing selection of double recombinants that had undergone both gene replacement and excision of the vector. Genomic DNA was isolated from two colonies (Orf1a and Orf1b) selected from the LM-RifNeo5%Sucrose plates. After restriction digests with *Eco*RI and *Hin*dIII, the two possible mutant strains were checked by Southern blotting alongside similarly cut C58C1 DNA. The neomycin cassette and the 1.5kb *Sph*I-*Pvu*II *orf1* fragment (see **Fig. 4.1.1**) were used as radioactively labelled probes. The neomycin probe was expected to hybridise only with the mutant DNA, giving known sized bands. The *orf1* probe was expected to hybridise with both wild type and mutant DNA, giving different sized bands for the two strains. The expected band sizes are given in **Fig. 4.1.2**.

The Southern blot hybridisation results with the *orf1* and neomycin probes can be seen in **Fig. 4.1.3** and **Fig. 4.1.4** respectively. When hybridised with the *orf1* probe the following bands were produced:

	***Eco*RI**	***Hin*dIII**
C58C1	8kb	4kb
Orf1a	9kb	3.8kb+1.5kb
Orf1b	9kb	3.8kb+1.5kb

With the neomycin probe, no bands were seen in the C58C1 lanes, and both of the possible mutant strains gave the same bands as for the *orf1* probe. The bands produced were therefore as predicted in **Fig. 4.1.2**. Orf1a was selected for use in subsequent work and renamed C1-orf1Neo.

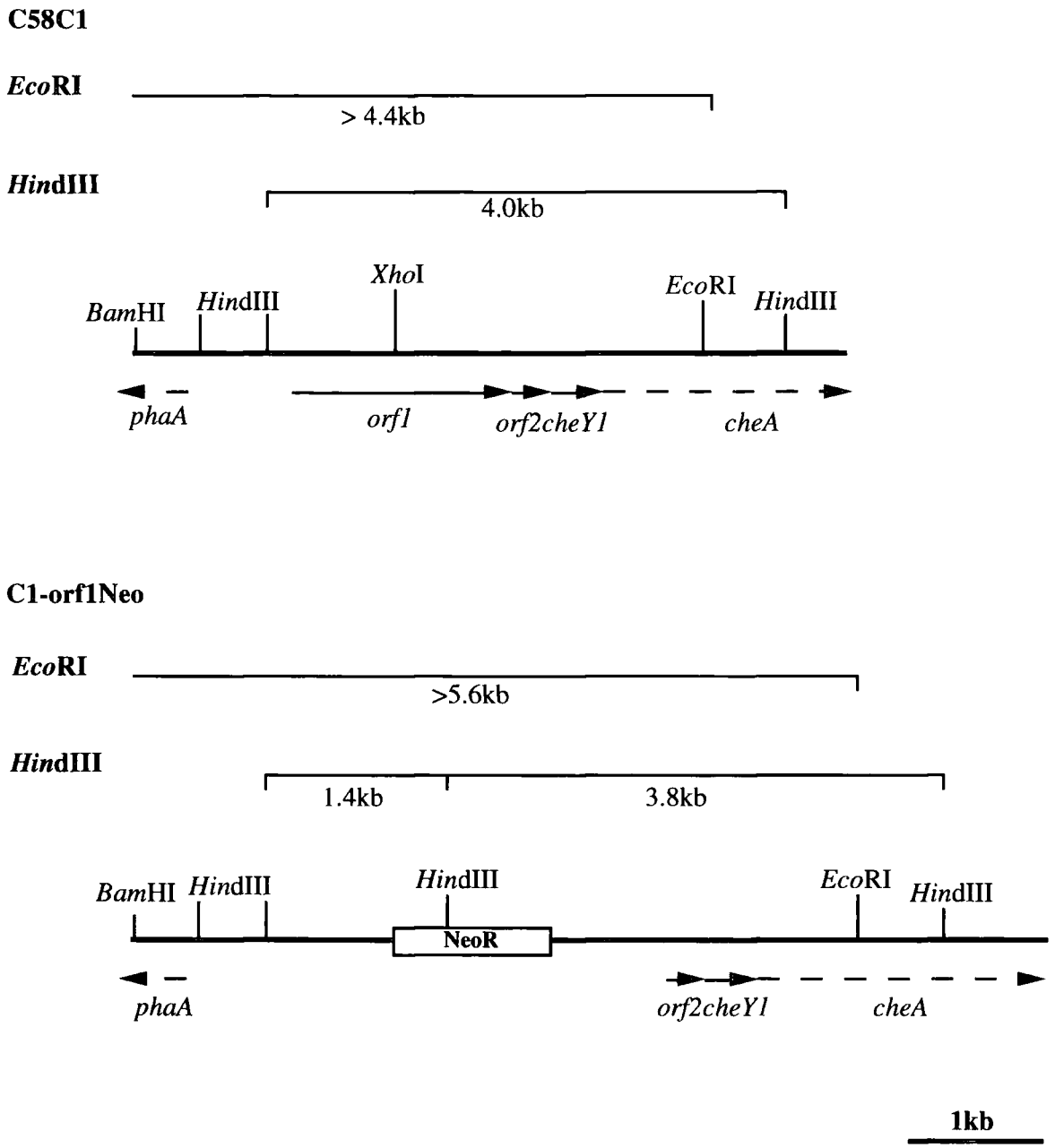

Fig. 4.1.2 Diagram showing the *Eco*RI and *Hin*dIII band sizes expected for C58C1 and the *orf1* mutant strain (C1-orf1Neo).

The figures given for C58C1 are for the *orf1* probe only. The figures for the mutant strain apply for hybridisation with both probes.

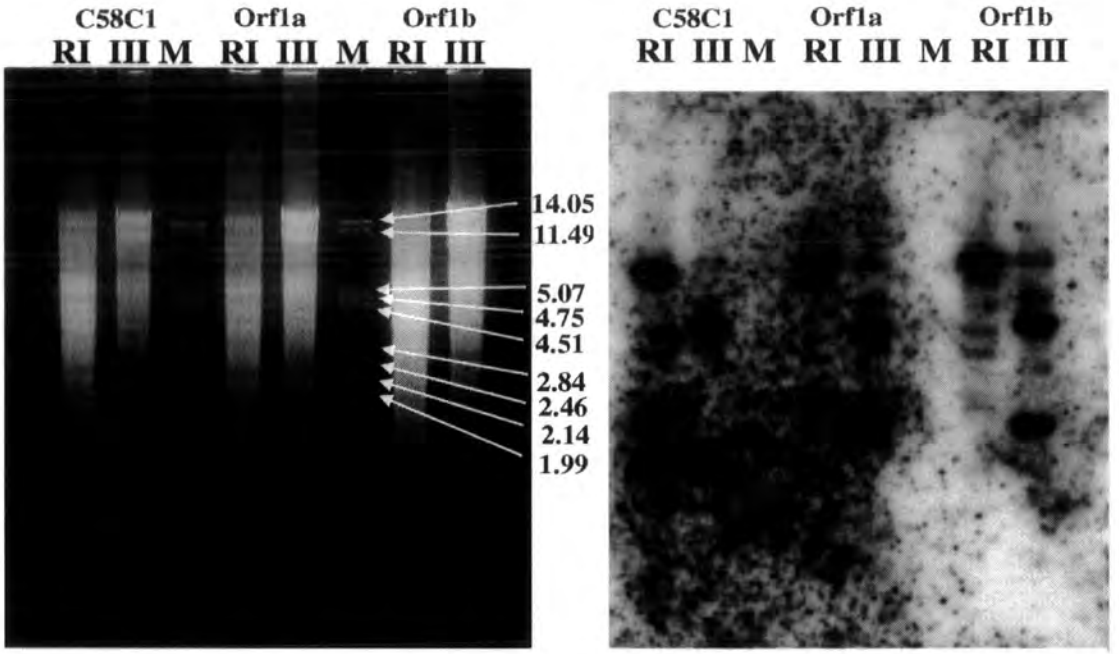

Fig. 4.1.3 0.7% agarose gel and subsequent Southern blot showing digests of the putative *orf1* mutant strains and hybridisation with the *orf1* probe.
RI = *Eco*RI, **III** = *Hin*dIII, **M** = λ / *Pst*I.

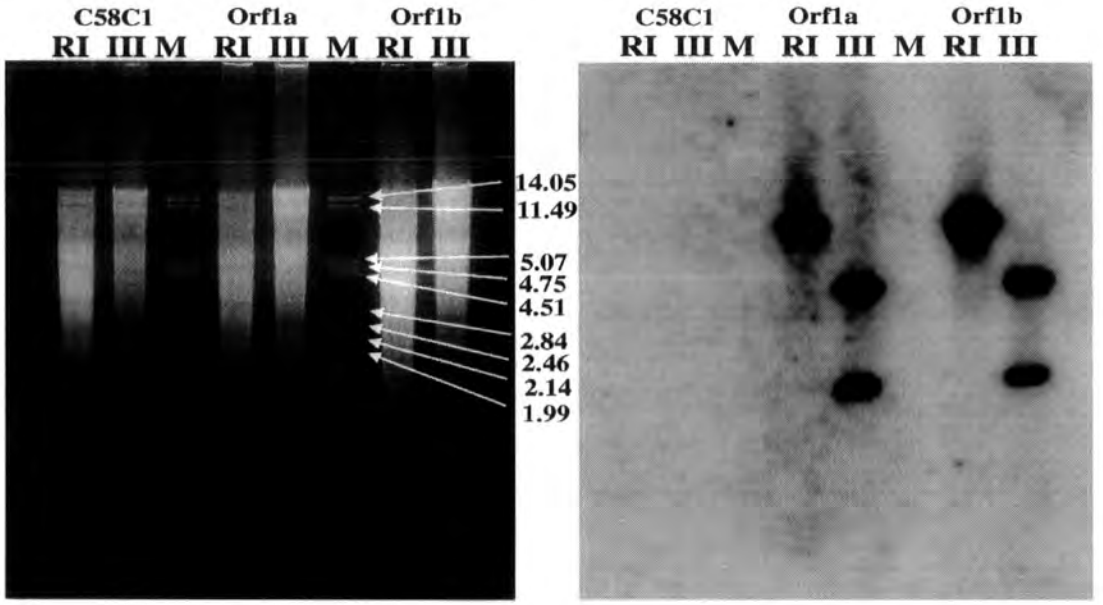

Fig. 4.1.4 0.7% agarose gel and subsequent Southern blot showing digests of the putative *orf1* mutant strains and hybridisation with the neomycin probe.
RI = *Eco*RI, **III** = *Hin*dIII, **M** = λ / *Pst*I.

4.2 Mutagenesis of *cheA*.

Studies on the chemotaxis systems of *E. coli* and other bacteria (see section **1.2.1**) have identified *cheA* as a key component of the overall system. CheA is the histidine kinase that reacts to changes in the sensory proteins and transmits this signal to the response regulators, particularly CheY, which then effects changes in the locomotory behaviour of the cell. Therefore without CheA it is likely that chemotaxis and many other defined responses to specific stimuli will not occur due to the lack of the "mediator" which links the detector and effector parts of these systems. Hence it seemed logical when carrying out mutagenesis work on a chemotaxis cluster, to look at the effects of mutating the *cheA* gene.

Two *cheA* mutants were created. The first was by insertion of a neomycin cassette in the gene, and the second was an in-frame deletion of the gene. Although both essentially *cheA* mutants it was hoped to look at any differences that might arise between the two due to the possible polar effects of the first mutation on downstream genes such as *cheR, cheB* and *cheY2*.

4.2.1 Gene Replacement Mutagenesis of *cheA*.

Although none of the subclones identified from pDUB1911 encompassed the entire *cheA* gene, the *Eco*RI subclone pELW4 contains approximately two-thirds of the gene. It was therefore decided to use pELW4 as the starting point for construction of a *cheA* mutant.

4.2.1.1 Construction of the *cheA*-Neo Plasmid.

The main stages involved in creating the *cheA*-Neo construct are outlined in **Fig. 4.2.1.1**. Initially pELW4 was digested with *Eco*RV, and the 1.5kb fragment containing the 3' section of *cheA* isolated. This fragment was then ligated into *Sma*I cut pJQ200mp18. Correct insertion of the fragment was selected for as described in section **4.1.1**, hence identifying the plasmid pJQcheA.

pJQcheA was digested with *Not*I, which only cut in the *cheA* insert. The resulting fragment was gel isolated and blunt-ended. The neomycin cassette was isolated from pDUB2033 by digesting with *Eco*RI, it was then blunt-ended and ligated into the blunt-

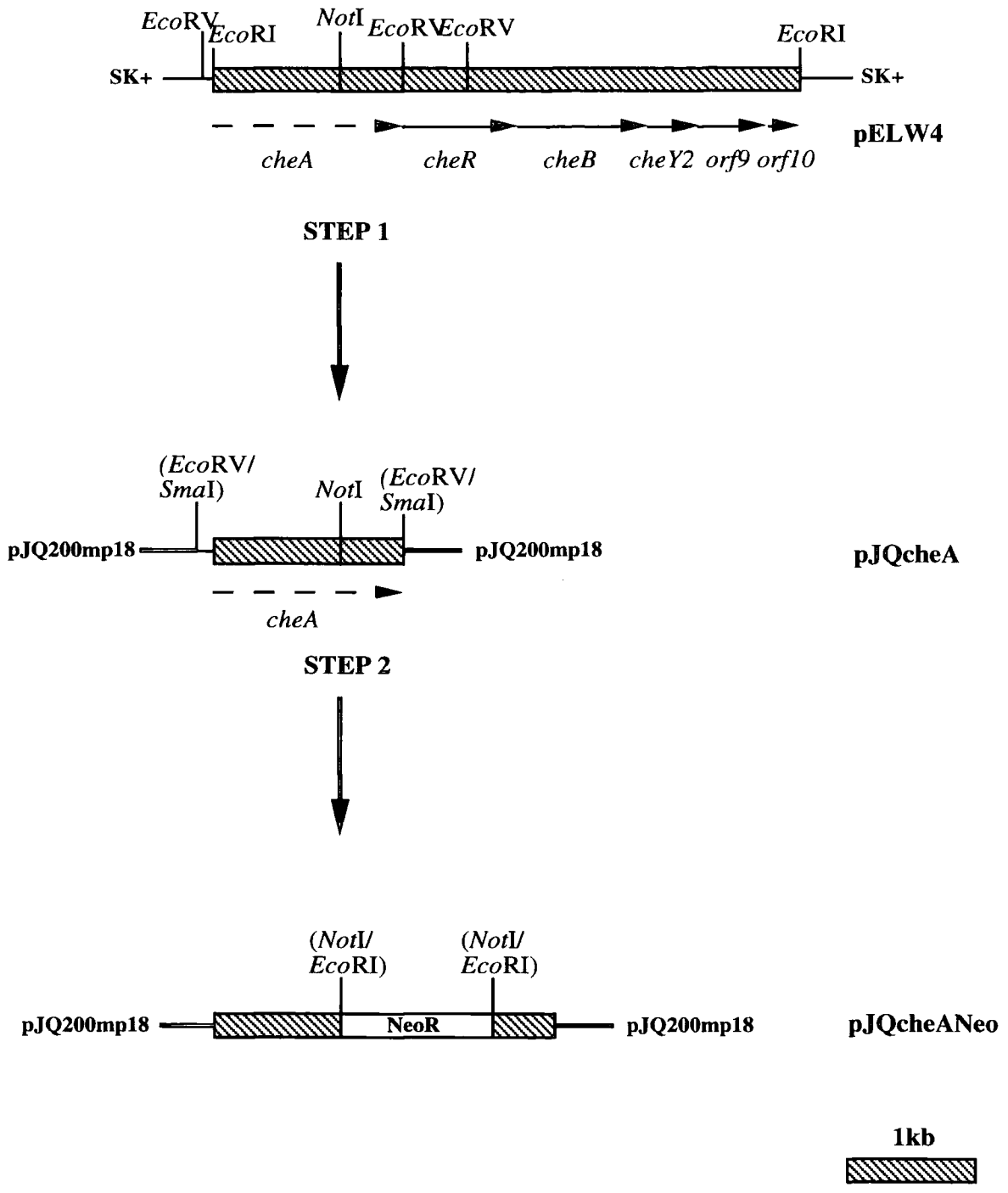

Fig. 4.2.1.1 Diagram outlining the main steps involved in construction of the *che*A-Neo plasmid.

Approximate sizes and positions of genes are indicated by arrows underneath the main figures. Dashed arrows indicate the presence of only part of a specific gene. Enzymes in brackets indicate restriction sites used in a previous step but no longer present.

ended, *Not*I cut, pJQcheA. Correct insertion of the neomycin cassette was confirmed as described previously in section **4.1.1**. The correct subclone pJQcheANeo was therefore identified.

4.2.1.2 Formation of the *A. tumefaciens cheA* Mutant Strain.

The mutant construct pJQcheANeo was conjugated into C58C1 and double recombinants selected by plating on LM-RifNeo5% sucrose plates.

Five colonies were selected from the LM-RifNeo5%sucrose plates and their swarming behaviour assessed by inoculation in 0.2% LM-broth swarm plates. All five strains showed impaired swarming, producing swarms approximately half the size of those produced by C58C1, over the same period of time (see **Fig. 4.6.1**).

Two of the strains (A1 and A5) were checked, along with C58C1, by digesting with *Hin*dIII and *Pst*I, and Southern blotting. The 1.5kb *cheA* fragment and the neomycin cassette were used as radioactively labelled probes to the blots. The band sizes expected for each digest are given in **Fig. 4.2.1.2**.

The Southern blot hybridisation results with the *cheA* and neomycin probes can be seen in **Fig. 4.2.1.3** and **Fig. 4.2.1.4** respectively. When hybridised with the *cheA* probe the following bands were produced:

	***Pst*I**	***Hin*dIII**
C58C1	6.8kb+1.9kb+ <1kb	4.2kb
A1	6.8kb+1.9kb	4.5kb+4.1kb+ <1kb
A5	1.9kb	4.5kb+4.1kb+ <1kb

The lack of the large hybridising fragment in the *Pst*I digest of A5 was probably due to overdigestion of the DNA. With the neomycin probe, no bands were seen in the C58C1 lanes. Both of the possible mutant strains gave a *Pst*I band of 1.9kb and *Hin*dIII bands of 4kb and <1kb. Both of the possible mutant strains therefore produced hybridising fragments as predicted in **Fig. 4.2.1.2** and appeared to be correct. Strain A1 was selected for use in subsequent work and renamed C1-ANeo.

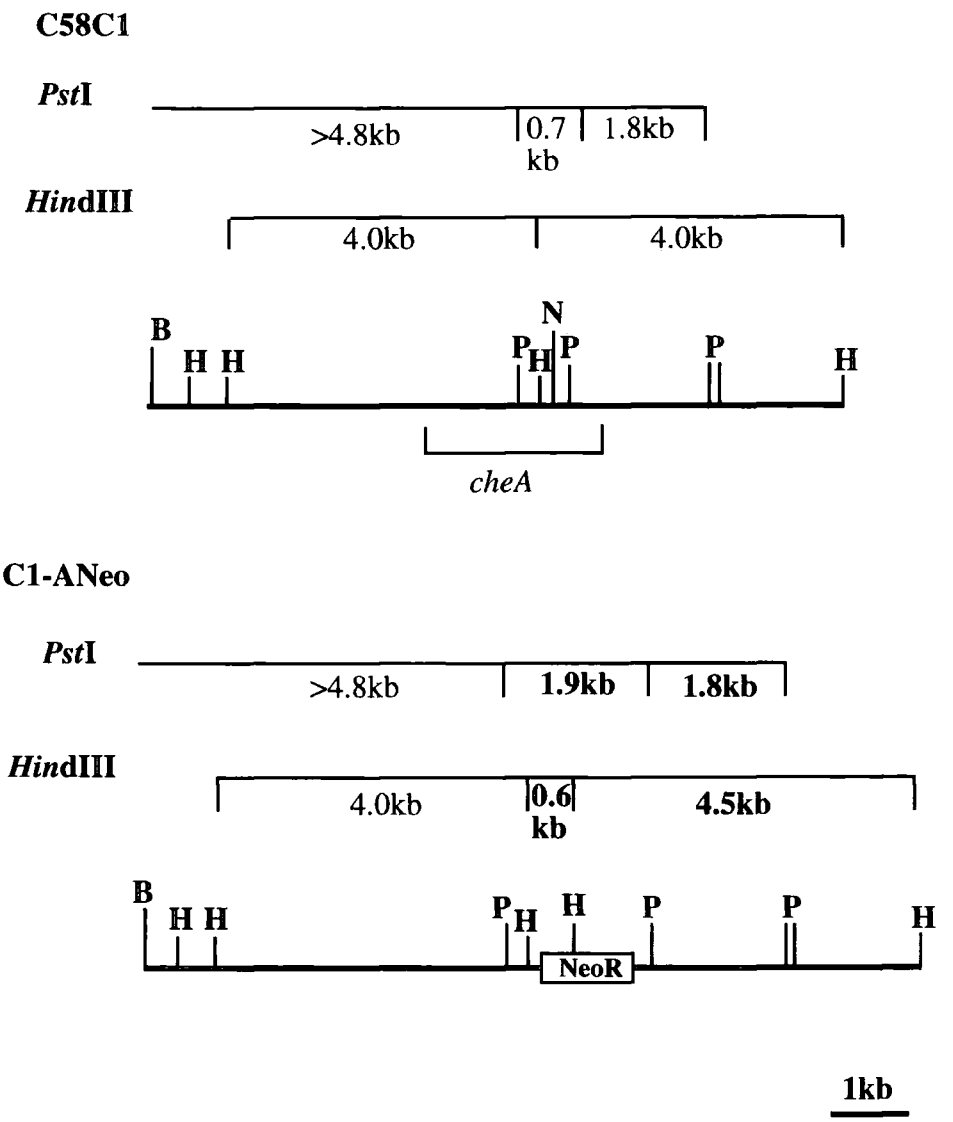

Fig. 4.2.1.2 Diagram showing the *Pst*I and *Hin*dIII band sizes expected for C58C1 and the *cheA* mutant strain, C1-ANeo.

B = *Bam*HI, **H** = *Hin*dIII, **P** = *Pst*I, **N** = *Not*I. The figures given apply for hybridisation with the *cheA* probe. Figures given in bold for the mutant strain are those fragments that would also hybridise with the neomycin probe.

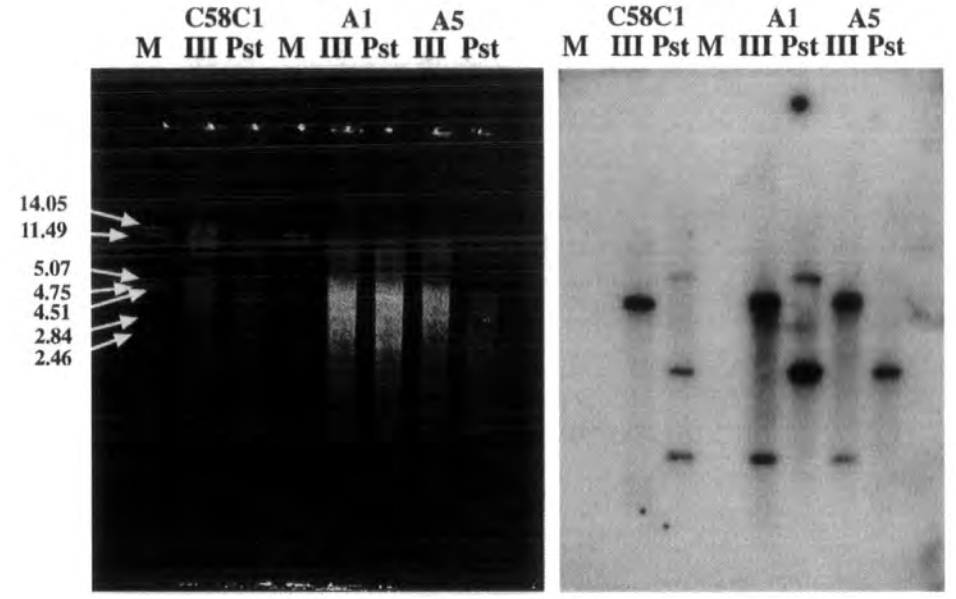

Fig. 4.2.1.3 0.7% agarose gel and subsequent Southern blot showing digests of the putative *cheA* mutant strains and hybridisation with the *cheA* probe.
M = λ / *Pst*I, **III** = *Hin*dIII, **Pst** = *Pst*I.

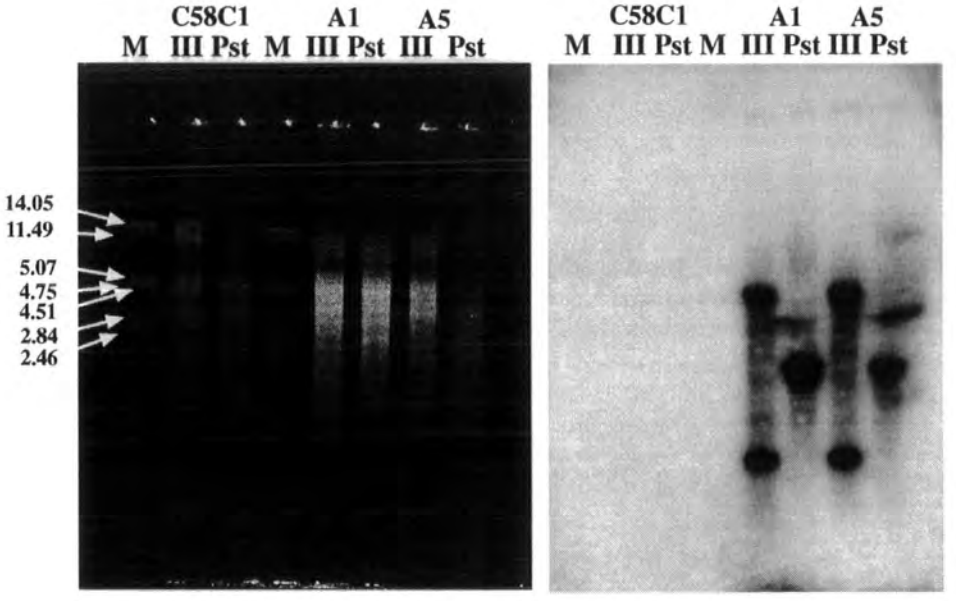

Fig. 4.2.1.4 0.7% agarose gel and subsequent Southern blot showing digests of the putative *cheA* mutant strains and hybridisation with the neomycin probe.
M = λ / *Pst*I, **III** = *Hin*dIII, **Pst** = *Pst*I.

4.2.2 In-frame Deletion of *cheA*.

In order to make an in-frame deletion of *cheA* it was first necessary to construct a subclone containing *cheA* with some flanking sequences. Sequence analysis showed the *cheA* gene to span the two *Hin*dIII subclones, pELW2 and pELW1. During the sequencing process further subclones of these two plasmids had been made. Two in particular, SK+/ELW2RV1 and SK+/ELW1HII2, were found to be suitable for construction of the *che*A subclone. The main steps involved in constructing the *cheA* in-frame deletion plasmid construct are outlined in **Fig. 4.2.2.1**.

4.2.2.1 Construction of the *cheA* Deletion Plasmid.

SK+/ELW2RV1 consists of the 3' *Eco*RV fragment of pELW2 subcloned into *Eco*RV-*Hin*dIII cut SK+, this plasmid was digested with *Eco*RV and *Hin*dIII, and the 1.9kb fragment containing *cheY1* and part of *cheA* isolated. SK+/ELW1HII2 consists of the 5' *Hin*cII fragment of pELW1 subcloned into *Sma*I cut SK+, this plasmid was cut with *Hin*dIII and *Nru*I, and the 0.99kb fragment containing the 3' terminal portion of *cheA* and all of *cheR* isolated.

The two *cheA* fragments were ligated together and into *Sma*I cut SK+ all in one step (see **Fig. 4.2.2.1, step 1**). Resulting colonies were checked by digesting with *Eco*RV. Correct clones were cut twice by *Eco*RV; once in the SK+ vector and once in the *Hin*dIII-*Nru*I fragment, therefore giving bands of known sizes and identifying the new plasmid SK+/cheA.

To delete *che*A, specific primers were designed from *cheA* and the sequence directly flanking it. The approximate positions of the primers are marked on the SK+/cheA diagram in **Fig. 4.2.2.1**. Primer 1 contains flanking sequence and the first 9bp of *cheA* (underlined), plus a 5' *Nco*I site (shown in bold type). Primer 2 contains flanking sequence, the last 3bp of *cheA* (underlined) and again a 5' *Nco*I site (shown in bold type). The sequence of the two primers are given in **Fig. 4.2.2.2**.

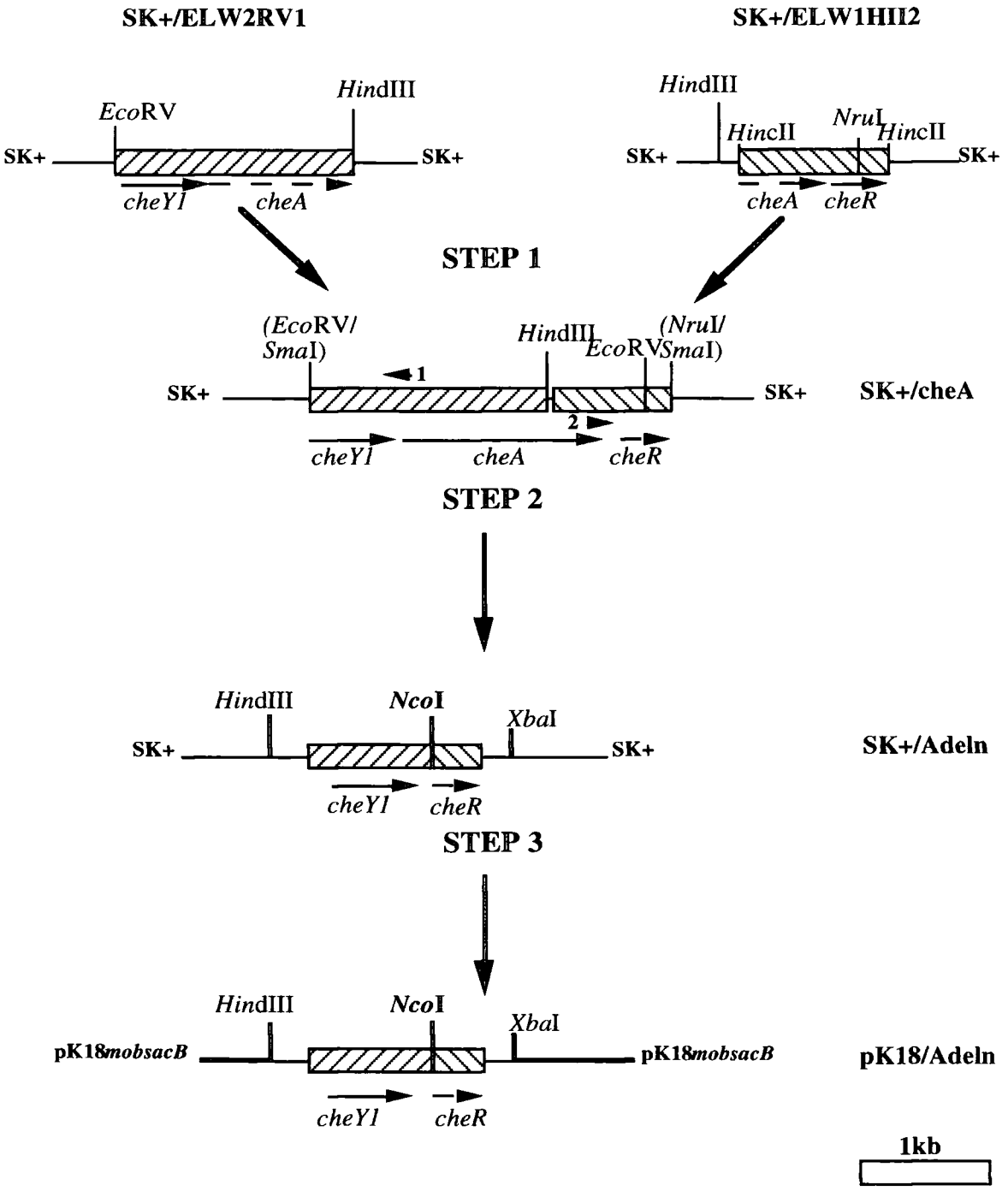

Fig. 4.2.2.1 Diagram outlining the main sub-cloning steps involved in the construction of the *cheA* in-frame deletion plasmid.

Approximate sizes and positions of the *cheA* gene, plus flanking genes, are indicated by arrows underneath the main figures at each stage. Dashed arrows indicate the presence of only part of a specific gene. Enzymes in brackets indicate restriction sites used in a previous step but no longer existing.

Primer 1: 5' *GGA CTC* **CAT GGC** ATA TCC ATC GTG AAA TGT C 3'

3608

Primer 2: 5' *GGA CTC* **CAT GGT** GAA GGC GGA TAT CCA ATG G 3'

5871

Fig. 4.2.2.2 Primers used for in-frame deletion of *cheA*.

Italicised bases are random additions, numbers underneath each primer indicate the map position of the 5' terminus of each primer in the cosmid pDUB1911 (see section **3.9**).

PCR reactions were carried out using SK+/cheA as the template and using the following protocol:

94°C	5 mins
94°C	1 min)
50°C	1 min) x 30
72°C	4 mins)
72°C	5 mins

The PCR reactions gave a product of the expected size (3.6kb). The band was gel isolated, digested with *Nco*I and the resulting cohesive termini ligated together. Possible positive colonies containing the religated fragment were checked by digesting with *Nco*I, and by sequencing in both the forward and reverse directions. The positive clone SK+/Adeln was identified (see **Fig. 4.2.2.1**).

The *cheA* deletion fragment was isolated from SK+/Adeln by digesting with the enzymes *Xba*I and *Hin*dIII, which both only cut in the SK+ multiple cloning site. The isolated fragment was subcloned into similarly cut pK18*mobsacB*. Positive colonies containing the *cheA* deletion fragment were selected for by inactivation of the β-galactosidase gene, and checked by digestion with *Nco*I. In correct clones *Nco*I cut once in the vector and once in the *cheA* deletion insert, giving two bands of known size. The subclone pK18/Adeln was therefore identified.

4.2.2.2 Formation of the *A. tumefaciens cheA* Deletion Strain.

The pK18/Adeln construct was conjugated into *A. tumefaciens* C58C1 by triparental mating as described in section **2.9**. Initially intermediate strains, containing

both the wild type and mutated forms of *cheA*, were selected for by plating the tri-parental mating mixture on LM-agar plates containing rifampicin and kanamycin.

Formation of such an integrated intermediate, containing both the wild type and deleted copies of *cheA*, was checked for by PCR using the primers CheA1 and CheA2. These were designed to amplify *cheA* and some adjacent sequence (see **Fig. 4.2.2.3**).

CheA1 5' ACC GTG GAT GAT TCC AGA AC 3'
3236

CheA2 5' GAC CGA GAT TGC GGA TAT GT 3'
6079

Fig. 4.2.2.3 Primers used to amplify *cheA*.
Numbers below each primer represent the map position of each 5' terminus in the cosmid pDUB1911 (see section **3.9**).

Three colonies were selected from the L-RifKan plates. PCRs were carried out on DNA from each colony and also wild type (C58C1) genomic DNA. The following protocol was used:

94°C	5 mins
94°C	1 min)
55°C	1 min) x 30
72°C	3 mins)
72°C	5 mins

The expected band sizes were 2.84kb for the wild type form of *cheA* and 561bp for the *che*A deletion fragment.

The PCR reactions for each of the three possible mutant intermediates contained a band corresponding to the size of the *cheA* deletion fragment (see **Fig. 4.2.2.4**). As expected this fragment was not seen in the C58C1 PCR. However, neither the possible mutant strains, nor C58C1, produced a band corresponding to the wild type copy of *cheA*.

To investigate why a band corresponding to the wild type copy of *cheA* was not amplified further PCRs were carried out, each time altering a different variable, e.g. the Mg^{2+} concentration, the template concentration or the specific template used, to see if it was possible to amplify the *cheA* fragment. None of the alterations allowed amplification of *cheA*. The primer CheA1 was substituted for a different primer, ELWa, (ELWa is a

primer that was used in sequencing reactions and is known to bind directly downstream of the start of *cheA*, reading in the sense direction). However it was still not possible to amplify *cheA* from genomic DNA. Finally similar PCRs were carried out on pDUB1911. This time the *cheA* fragment was routinely amplified each time.

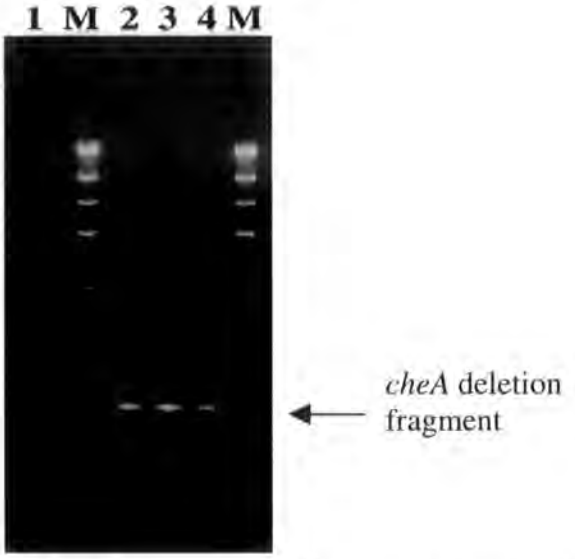

Fig. 4.2.2.4 0.7% agarose gel showing the genotype of the putative *cheA* integrated intermediate strains.

1 = C58C1, **2 –4** = Putative *cheA* integrated intermediate strains, **M** = λ / *Hin*dIII.

It seems likely therefore that the inability to amplify the *cheA* fragment from genomic DNA is due to the primers being unable to bind efficiently because of the specific conformation of the DNA in the genome or possibly because of a contaminant inhibiting the PCR reaction. Therefore although the C58C1 did not act as a positive control, showing the size of the wild type form of *cheA*, it was useful as a negative control element due to the lack of a band of a size corresponding to the *cheA* deletion fragment.

One of the identified mutant intermediates, C1-Adel2 (lane **2**, **Fig. 4.2.2.4**), was selected for use in the next steps of the mutant construction. To force the second recombination event to take place C1-Adel2 was grown overnight in 5ml of LM-broth containing selection for rifampicin only. Recombination should lead to excision of the plasmid and either reversion to the wild type gene or introduction of the deleted mutant form. To force this excision to take place aliquots of the LM-Rif culture were plated on MinA-agar plates containing rifampicin and 10% sucrose.

Neat, 10^{-1}, 10^{-2}, 10^{-3} and 10^{-4} dilutions of the LM-Rif C1-Adel2 culture were plated, in duplicate, on MinA-agar plates containing rifampicin and 10% sucrose in order

to select for colonies that had undergone the second recombination step. After two days incubation at 28°C the plates contained the following numbers of colonies:

	No. colonies / plate	
Dilution	**1**	**2**
Neat	>500	>500
10^{-1}	~200	~200
10^{-2}	~50	~50
10^{-3}	1	4
10^{-4}	1	5

In order to identify colonies that were kanamycin sensitive and hence had excised the pK18/AdeIn plasmid, all of the colonies from the 10^{-4} and 10^{-3} plates were replica streaked on LM-agar plates containing rifampicin alone, or rifampicin and kanamycin. Four of the eleven colonies tested were rifampicin resistant and kanamycin sensitive. Genomic DNA was therefore isolated from these possible mutant colonies. PCR amplifications were carried out using the primers CheA1 and CheA2, and following the same protocol as outlined previously:

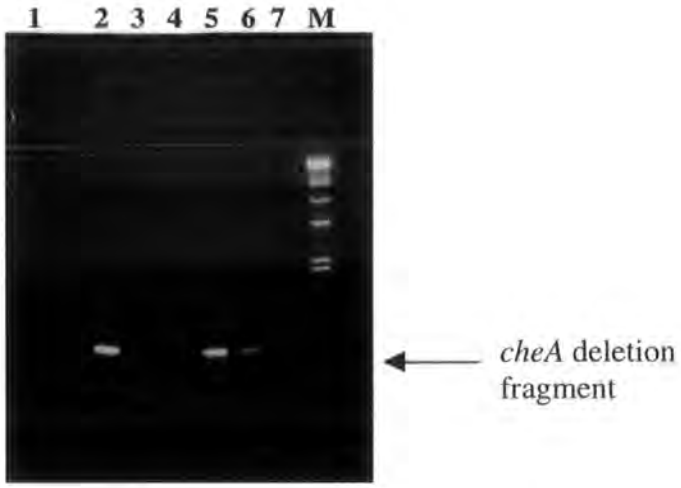

Fig. 4.2.2.5 0.7% agarose gel showing the genotype of the putative *cheA* in-frame deletion mutant strains.

1 = PCR blank, **2** = C1-Adel2, **3 – 6** = putative *cheA* in-frame deletion strains, **7** = C58C1, **M** = λ / *Hin*dIII.

The results of the PCR amplifications showed two colonies, C1-Adel8a and C1-Adel10a (lanes **5** and **6** respectively, in **Fig. 4.2.2.5**), to contain a band corresponding to

the deleted *cheA* fragment. Genomic DNA from the possible mutant strains was digested with *Eco*RI and *Hin*dIII. The strains were then checked by Southern blotting alongside similarly cut DNA from the mutant intermediate, C1-Adel2, and C58C1. The *cheA* deletion fragment was used as a radioactively labelled probe. The hybridising band sizes expected for C58C1, the intermediate strain and a correctly constructed *cheA* in-frame deletion strain are given in **Fig. 4.2.2.6**. C1-Adel2 could have been formed by two possible recombination steps, either recombination of the *cheY1* flanking sequence or recombination of the *cheR* flanking sequence. The band sizes expected for both possibilities are given in **Fig. 4.2.2.6**.

The Southern blot hybridisation results can be seen in **Fig. 4.2.2.7**. The approximate size of the hybridising bands produced are:

	***Eco*RI**	***Hin*dIII**
C58C1	7.0kb+4.5kb	4.4kb
C1-Adel2	7.2kb+3.6kb+ 2.0kb	6.6kb+4.0kb+ 3.7kb
C1-Adel8a		6.0kb
C1-Adel10a		6.0kb+4.0kb

The bands produced correspond well with those predicted in **Fig. 4.2.2.6**. No bands were seen in the *Eco*RI digests of the possible mutants due to the enzyme not cutting properly. The hybridising bands for C1-Adel2 show that the initial integration event had occurred via recombination of the *cheR* flanking sequence i.e. as Intermediate B in **Fig. 4.2.2.6**. C1-Adel10a contained a 4.0kb *Hin*dIII band in addition to the 6.0kb band expected, the most likely explanation for this is that the culture contained a mixture of both wild type and mutant bacteria. C1-Adel8a produced the expected hybridising bands for the *cheA* in-frame deletion mutant, it was therefore renamed C1-Adel and used in all subsequent work.

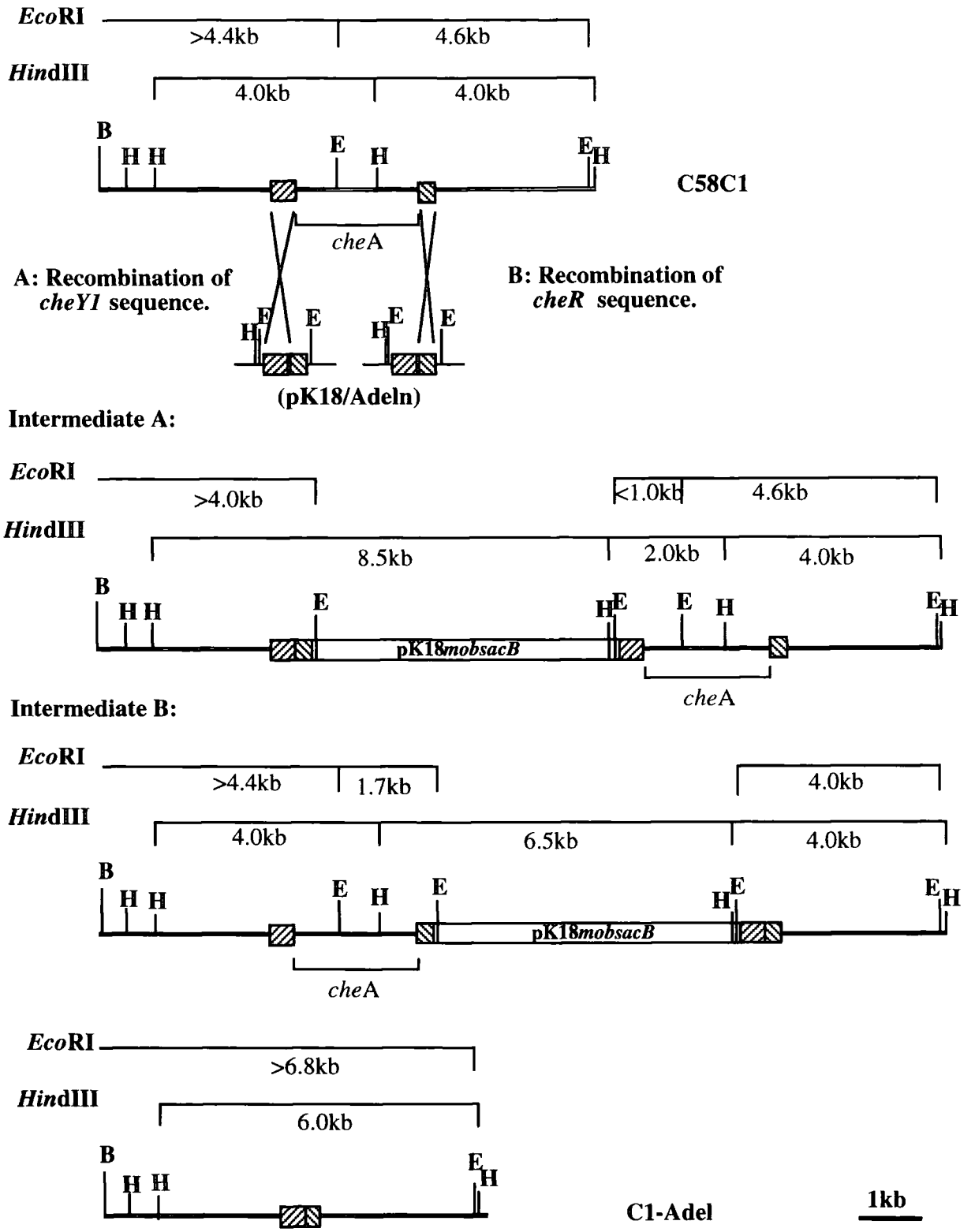

Fig. 4.2.2.6 Diagram showing the approximate size of the *Eco*RI and *Hin*dIII hybridising bands expected for C58C1, the two possible mutant intermediate strains and the *cheA* in-frame deletion strain (C1-Adel).

B = *Bam*HI, **E** = *Eco*RI, **H** = *Hin*dIII.

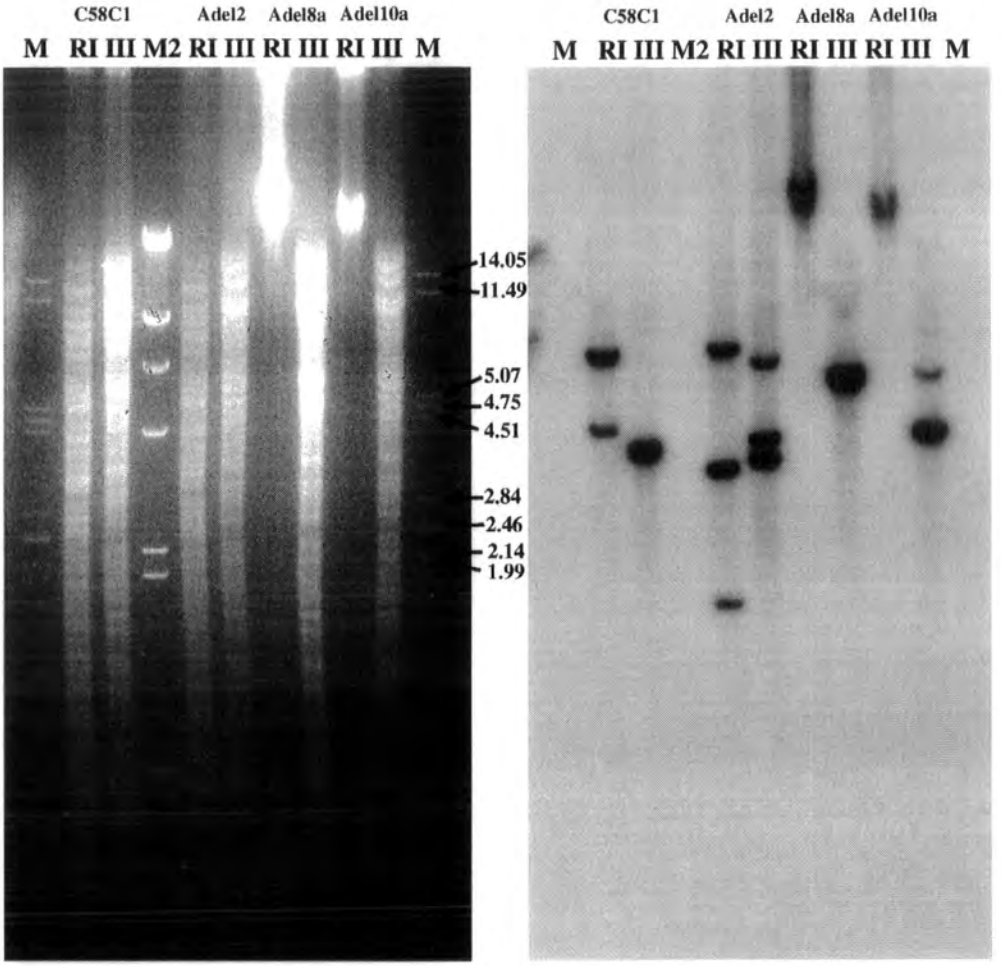

Fig. 4.2.2.7 0.7% agarose gel and subsequent Southern blot showing digests of the putative *cheA* in-frame deletion mutant strains and hybridisation with the *cheA* deletion probe.

RI = *Eco*RI, **III** = *Hin*dIII, **M** = λ / *Pst*I, **M2** = λ / *Hin*dIII.

4.3 Mutagenesis of *orf10*.

Sequencing identified the putative open reading frame *orf10*, which spans the two *Eco*RI subclones pELW4 and pELW3. It was decided to make an in-frame deletion of this *orf* to see if any specific loss of function would result from its removal. As with the *cheA* in-frame deletion, a subclone had to be made which contained the *orf10* gene and flanking sequence. The main steps involved in creation of the *orf10* deletion construct are outlined in **Fig. 4.3.1.1** and explained in more detail below.

4.3.1 Construction of the *orf10* In-frame Deletion Plasmid.

A 1.1kb fragment from pELW4, containing *cheY2, orf9* and part of *orf10*, was isolated by digestion with *Eco*RI and *Hin*cII. The 3' terminal portion of *orf10* and part of *fliF* were isolated from pELW3 by digestion with *Eco*RI and *Pst*I, and isolating the 416bp fragment produced. The two *orf10* fragments were then ligated together and into *Hin*cII-*Pst*I cut SK+ in one step, forming the plasmid SK+/Y2F (**Fig. 4.3.1.1**, steps **1+ 2**). Before deleting the *orf10* gene it was decided to reduce the upstream flanking sequence by digestion of SK+/Y2F with *Hin*cII and *Mlu*I, then isolating, blunt-ending and religating the large fragment produced, thus creating the plasmid SK+/orf10.

To delete *orf10* specific primers were designed from *orf10* and the sequence directly flanking it. The approximate positions of the primers are marked on the SK+/orf10 diagram in **Fig. 4.3.1.1**. Primers **a** and **b** were designed to include only the first 9bp and the last 3bp of *orf10* (underlined) respectively, plus some flanking sequence and each incorporating a 5' terminal *Sph*I site (shown in bold):

Primer a: 5' GCA TGC <u>AAG CTG CAT</u> TGG AAA CTC CG **3'**
8801

Primer b: 5' GCA TGC <u>TAG</u> AAC ATA TTC CGG CCG TT **3'**
9174

Fig. 4.3.1.2 Primers used to delete *orf10*.
Numbers below each primer indicate the map position of each 5' terminus in the cosmid pDUB1911 (see section **3.9**).

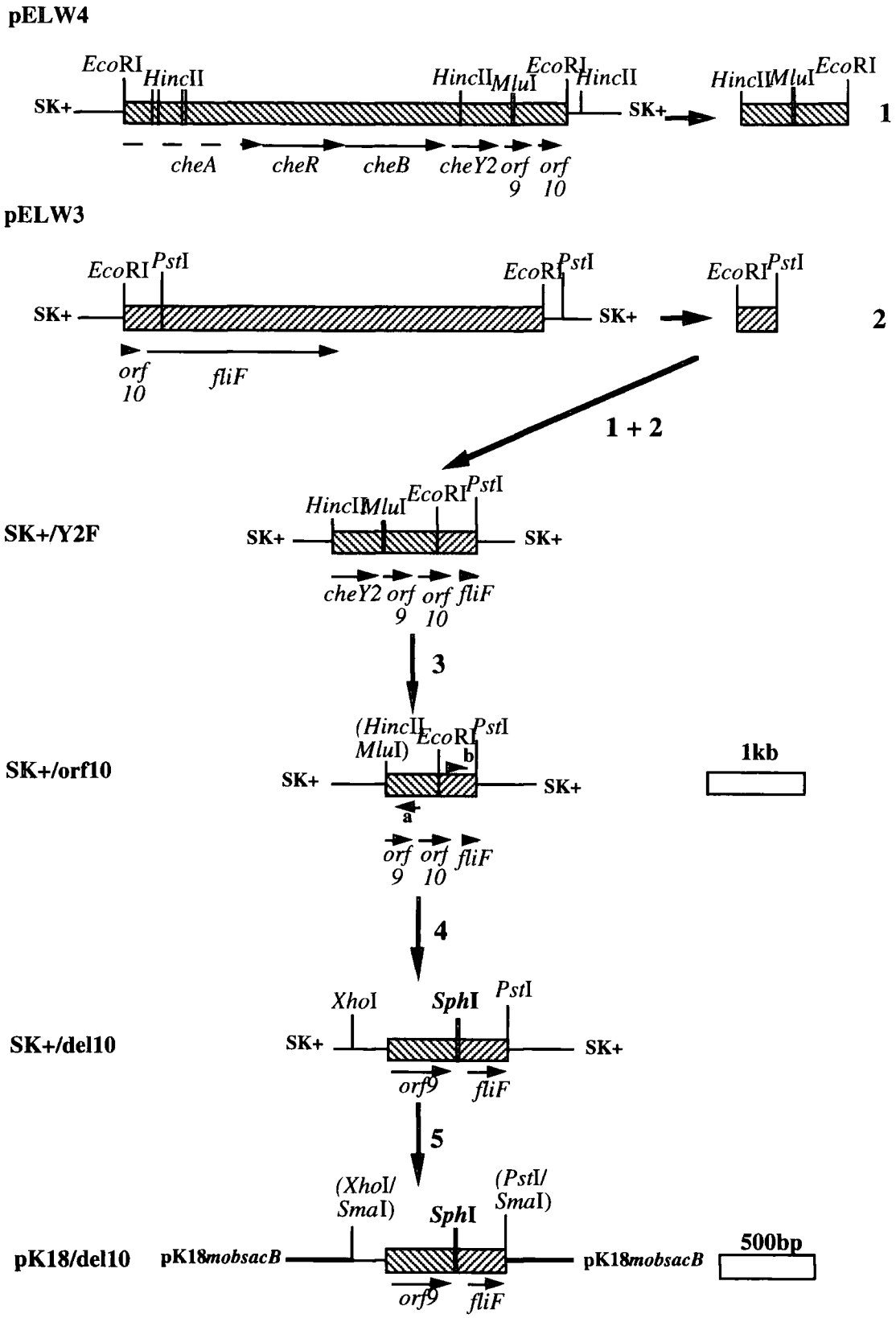

Fig. 4.3.1.1 Diagram outlining the main sub-cloning steps involved in the construction of the *orf*10 in-frame deletion plasmid.

PCRs were carried out using SK+/orf10 as the template and using the following protocol:

94°C	5 mins
94°C	1 min)
50°C	1 min) x 30
72°C	4 mins)
72°C	5 mins

A product of the expected size (3.6kb) was produced. The band was therefore gel isolated, digested with *Sph*I and the cohesive termini ligated together, forming the plasmid SK+/del10 (see **Fig. 4.3.1.1**). Correct formation of SK+/del10 was confirmed by sequencing across the *Sph*I site.

The approximately 600bp *orf10* deletion fragment was isolated using the *Pst*I site which incorporates the fragment in to SK+ and the *Xho*I site in the SK+ multiple cloning site. The *Xho*I-*Pst*I fragment was blunt-ended and ligated into *Sma*I cut pK18*mobsacB*. Correct insertion of the fragment was confirmed as described in section **4.2.2.1**. The mutant construct pK18/del10 was therefore identified.

4.3.2 Formation of the *A. tumefaciens orf10* In-frame Deletion Mutant Strain.

The construct pK18/del10 was conjugated into C58C1 and integrated recombinants selected by plating on LM-RifKan plates. Primers were designed that would amplify *orf10* plus some flanking sequence:

ORF10a 5' GCT GAT CAA CGG TCT CTT GA **3'**
8454
ORF10b 5' GCG ACA TTC TTC AAG ACC TG **3'**
9346

Fig. 4.3.2.1 Primers used to amplify *orf10*.
Numbers below each primer indicate the map position of each 5' terminus in the cosmid pDUB1911 (see section **3.9**).

Five colonies were selected from the LM-RifKan plates, and along with C58C1, checked by carrying out PCR amplifications using the primers **ORF10a** and **ORF10b**.

The PCR protocol used was:

94°C	5mins	
94°C	1min	)
55°C	1min	) x 30
72°C	1min	)
72°C	5mins	

The expected band sizes were 892bp for the wild type form of *orf10* and 520bp for the *orf10* deletion fragment.

The PCR reactions for each of the five possible integrated intermediate strains contained a band corresponding to the *orf10* deletion fragment and a band corresponding to the wild type form of *orf10* (see **Fig. 4.3.2.2**):

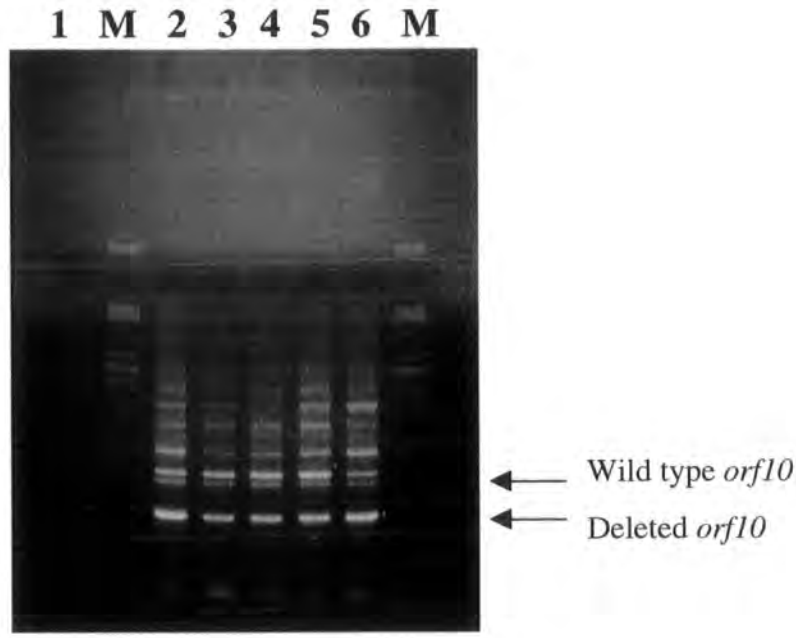

Fig. 4.3.2.2 0.7% agarose gel showing the genotype of the putative *orf10* integrated intermediate strains.

1 = PCR blank, **2 – 6** = putative *orf10* integrated intermediate strains, **M** = λ / *Pst*I.

The C58C1 PCR only contained the larger band corresponding to the wild type form of *orf10* (not shown). All of the tested strains therefore had undergone the first recombination step. One of the strains, C1-orf10del1 (**Fig. 4.3.2.2**, lane **2**), was selected for use in the next stages of the mutant construction and grown overnight in 5ml of LM-broth containing selection for rifampicin alone. As described in section **4.2.2.2** a serial dilution of the LM-Rif culture was plated, in duplicate, on MinA-Rif10% sucrose plates. After three days incubation at 28°C the plates contained the following number of colonies:

	No. colonies / plate	
Dilution	**1**	**2**
Neat	>500	>500
10^{-1}	~100	~100
10^{-2}	9	16
10^{-3}	1	0
10^{-4}	0	0

The nine colonies from the 10^{-2} plate 1 and the single colony from the 10^{-3} plate 1 were replica streaked on LM-Rif and LM-RifKan plates. Four of the ten colonies were found to be rifampicin resistant and kanamycin sensitive. PCR amplifications were carried out on these four strains, along with C1-orf10del1 and C58C1, using primers **ORF10a** and **ORF10b** and the following protocol:

94°C	5mins	
94°C	1min	)
55°C	1min	) x 30
72°C	1min	)
72°C	5mins	

The results of the PCR amplifications can be seen in **Fig. 4.3.2.3**.

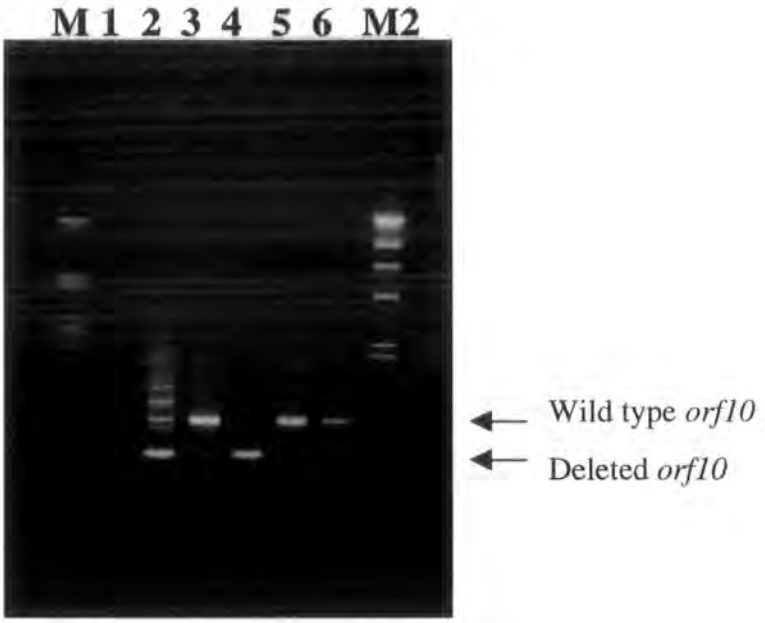

Fig. 4.3.2.3 0.7% agarose gel showing the genotype of the putative *orf10* in-frame deletion mutant strains.

1 = PCR blank, **2** = C1-orf10del1, **3 – 6** = putative *orf10* in-frame deletion strains, **M** = λ / *Pst*I, **M2** = λ / *Hin*dIII.

The kanamycin sensitive colonies were C1-orf10del1a, 2a, 4a and 10a, in lanes 3, 4, 5 and 6 respectively, of these C1-orf10del2a can be seen to contain only the deleted form of *orf10*. This strain, along with the intermediate C1-orf10del1 and C58C1, was digested with *Hin*dIII and *Eco*RI and checked by Southern blotting. The *orf10* deletion fragment was used as a radioactively labelled probe. The hybridising fragments expected for C58C1, the two possible intermediates and a correctly constructed *orf10* in-frame deletion mutant are given in **Fig. 4.3.2.4**. The Southern blot hybridisation results can be seen in **Fig. 4.3.2.5**, the approximate sizes of the hybridising bands produced are:

	***Eco*RI**	***Hin*dIII**
C58C1	5.0kb+4.7kb	4.0kb+2.2kb
C1-orf10del1	6.4kb+5.0kb+ 4.7kb	6.0kb+4.0kb+ 2.2kb+2x<1kb
C1-orf10del2a	9.0kb	3.8kb+2.0kb

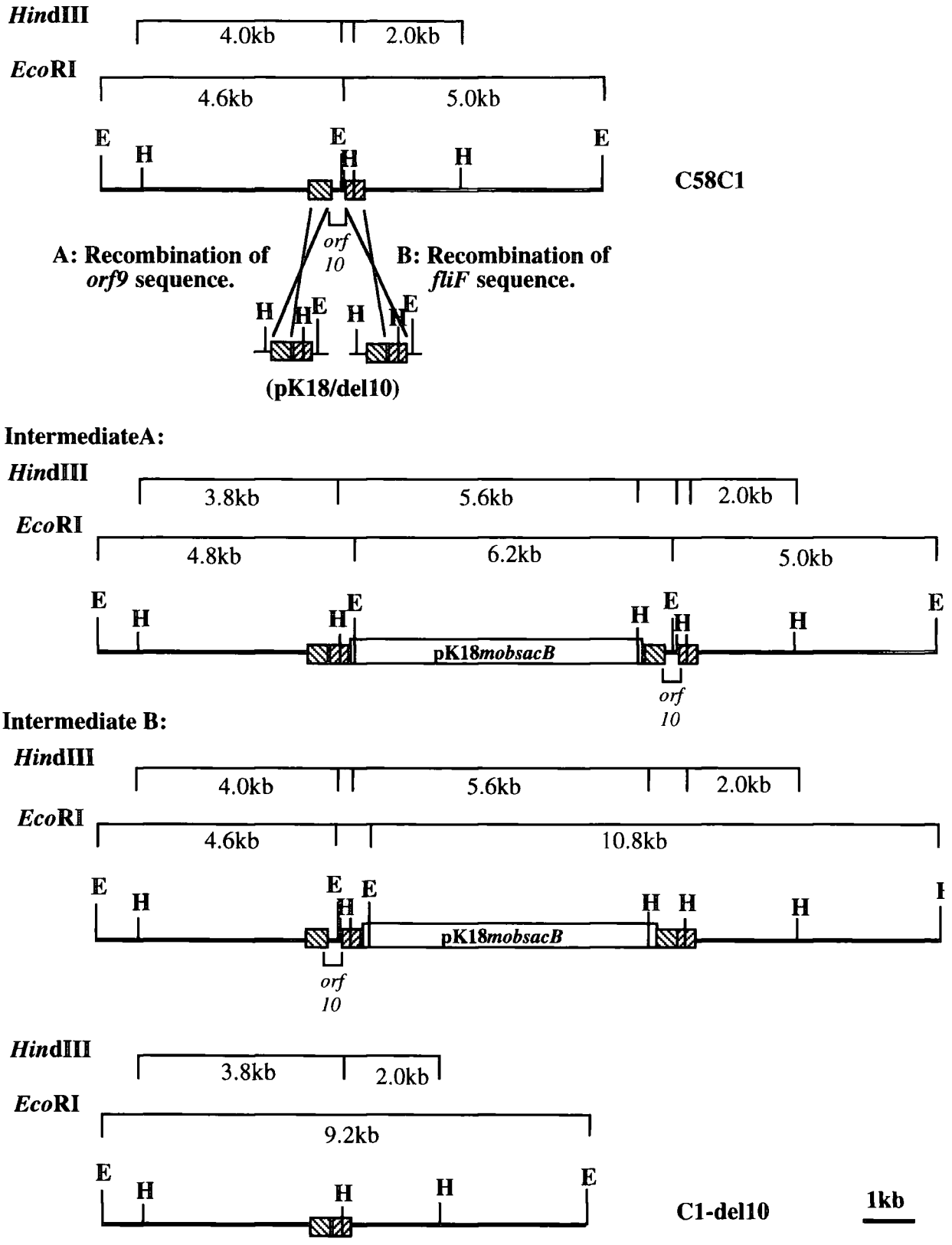

Fig. 4.3.2.4 Diagram showing the position and approximate size of the main hybridising *Eco*RI (E) and *Hin*dIII (H) fragments expected for C58C1, the two possible intermediates and the *orf10* in-frame deletion mutant strain, C1-del10.

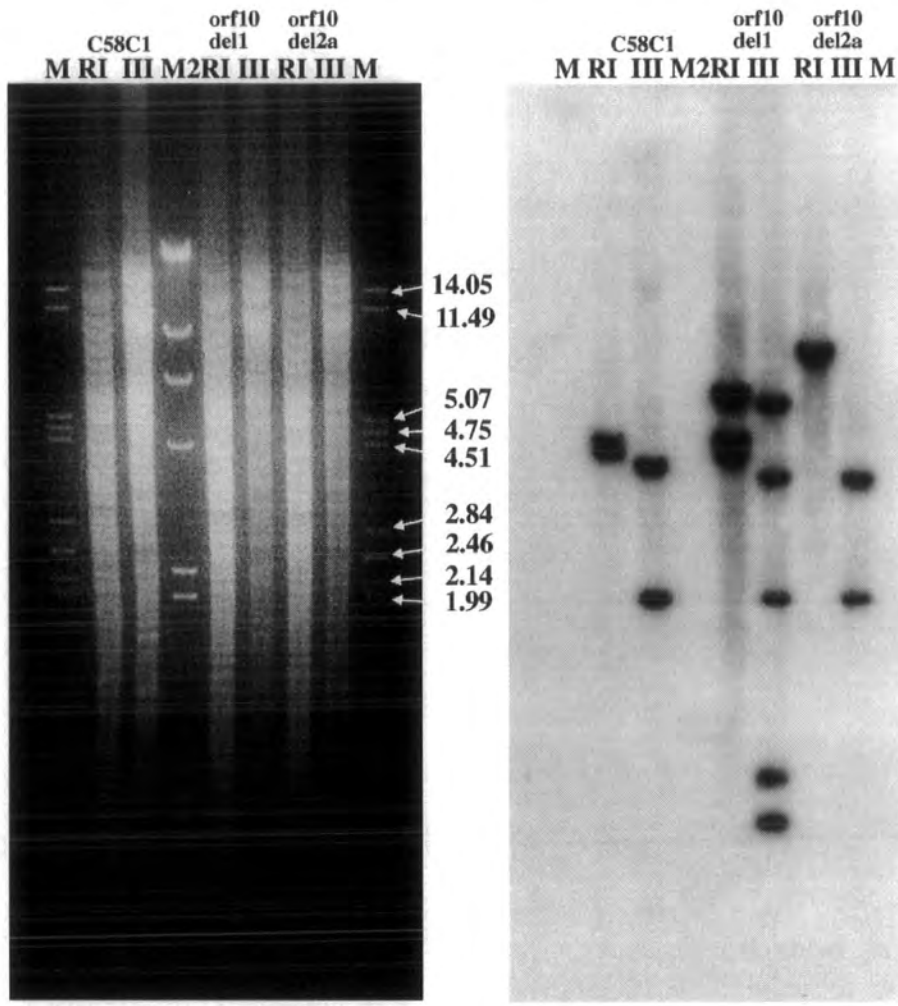

Fig. 4.3.2.5 0.7% agarose gel and subsequent Southern blot showing digests of the putative *orf10* in-frame deletion mutant strain and hybridisation with the *orf10* deletion probe.

RI = *Eco*RI, **III** = *Hin*dIII, **M** = λ / *Pst*I, **M2** = λ / *Hin*dIII.

The bands produced correspond well with those predicted in **Fig. 4.3.2.4** and confirm correct construction of the *orf10* in-frame deletion strain. The hybridising bands for C1-orf10del1 show that the initial integration event had occurred via recombination of the *orf9* flanking sequence, i.e. as Intermediate A. C1-0rf10del2a was renamed C1-del10 and used in all subsequent work.

4.4 Deletion of the Entire *che* Cluster.

After successfully deleting individual genes from the *che* cluster it was decided to make a *che* "gutted" strain with the whole region deleted. The main reasons for creating such a mutant were twofold; i) one of the aims of this work was to investigate possible interactions between the *che* and *vir* genes of *A. tumefaciens*, having a *che*- strain available would greatly aid this work, and ii) recently a second chemotaxis region was identified in the related bacterium *R. sphaeroides* [81], removing the identified *che* region would therefore facilitate investigations into the possible existence of a second *che* region in *A. tumefaciens*.

The method used for creating the *che* deletion was similar to those for the *cheA* and *orf10* in-frame deletions except larger flanking sequences were used.

4.4.1 Construction of the *che* Deletion Plasmid.

Rather than deleting the *che* region by PCR it was found that there were convenient restriction sites in the subclones pELW10 and pELW3 that would allow simple construction of a *che* deletion plasmid. The steps involved in construction are outlined in **Fig. 4.4.1**. For the upstream flanking sequence pELW10 was digested with *Bam*HI and *Nhe*I and the 690bp *Bam*HI-*Nhe*I fragment, containing sequence from the start of pDUB1911, isolated. Downstream flanking sequence was obtained by digesting pELW3 with *Xba*I and *Hin*cII, and isolating the 1.2kb *Xba*I-*Hin*cII fragment produced. *Nhe*I and *Xba*I produce compatible cohesive termini, it was therefore possible to ligate the two fragments together and into *Bam*HI-*Hin*cII cut SK+ all in one step. Insertion of the two fragments was selected for by inactivation of the β-galactosidase gene. Correct insertion of the fragments in to SK+ was confirmed by digesting possible positive colonies with *Hin*dIII. The plasmid SK+/delche was identified and further checked by sequencing in the forward and reverse directions, which confirmed the construct was correct.

SK+/delche was digested with *Bam*HI and *Hin*cII and the 1.9kb *che* deletion fragment isolated. The fragment was blunt-ended and ligated into *Sma*I cut pK18*mobsac*B. Correct insertion of the fragment was confirmed by digesting possible positive colonies with *Hin*dIII. The mutant construct pK18/delche was therefore identified.

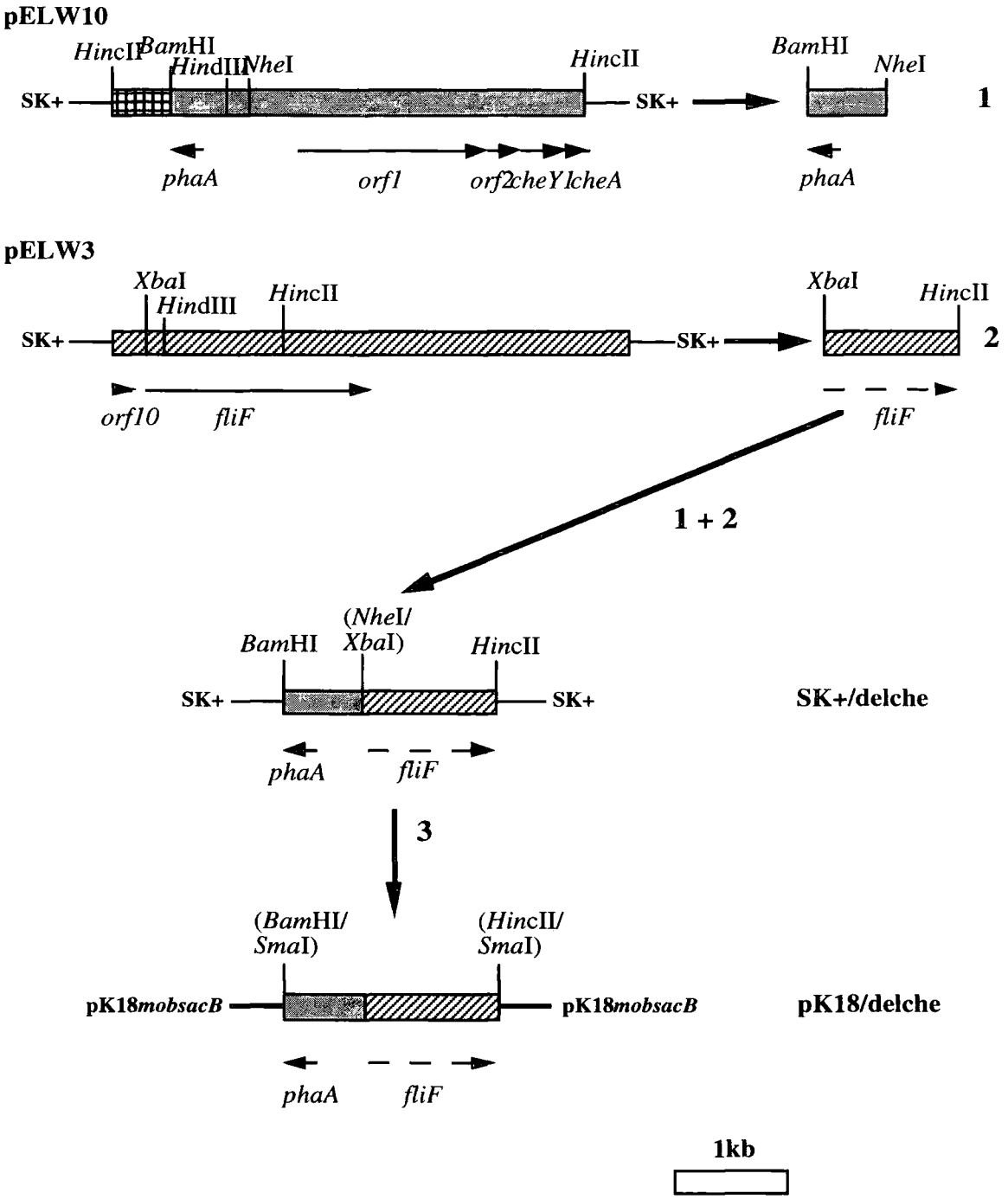

Fig. 4.4.1 Diagram outlining the main sub-cloning steps involved in construction of the *che* deletion plasmid.

Approximate sizes and positions of genes are indicated by arrows underneath the main figures. Dashed arrows indicate the presence of only part of a specific gene. Enzymes in brackets indicate restriction sites used in a previous step but no longer present. The cross-hatched region of pELW10 indicates sequence of the cosmid vector of pDUB1911 rather than *A. tumefaciens* insert sequence.

4.4.2 Formation of an *A. tumefaciens che* "Gutted Strain".

The plasmid pK18/delche was conjugated into *A. tumefaciens* C1-Adel. Integrated intermediate recombinant strains were selected for by plating on LM-RifKan plates.

The primers **delche1** and **ORF10b** were designed from the upstream and downstream flanking sequences of the *che* region:

delche1: 5' CGG AAG CCA TTC CAC ATC AT 3'
123

ORF10b: 5' GCG ACA TTC TTC AAG ACC TG 3'
9346

Fig. 4.4.2.1 Primers used to amplify the *che* region.
Numbers below each primer indicate the map position of each 5' terminus in the cosmid pDUB1911 (see section **3.9**).

PCRs were carried out with four possible intermediate strains from the LM-RifKan plates and C58C1, as a control, using the following protocol:

94°C	5mins	
94°C	1min	)
55°C	1min	) x 30
72°C	1min	)
72°C	5mins	

The expected band sizes were 740bp for the *che* deletion fragment and 9.2kb for the wild type *che* region. Due to the limits of the PCR reaction it was not possible to amplify the large *che* fragment. Using long extension times in an attempt to do this was likely to cause amplification of non-specific products which would confuse the results, it was therefore decided to only carry out extension for 1 minute, allowing amplification of the deleted fragment but not the wild type region. All four possible intermediate strains produced a PCR band of approximately the size of the *che* deletion fragment (740bp). This fragment was absent from C58C1.

One of the strains, C1-delche1, was selected and grown overnight in 5ml LM-broth containing selection for rifampicin alone. To force excision of the plasmid neat, 10^{-1}, 10^{-}

^{2}, 10^{-3} and 10^{-4} dilutions of the LM-Rif culture were then plated, in duplicate, on MinA-Rif10% sucrose plates. After 3 days incubation at 28°C the plates contained the following number of colonies:

	No. colonies / plate	
Dilution	**1**	**2**
Neat	>500	>500
10^{-1}	>500	>500
10^{-2}	~200	~200
10^{-3}	25	22
10^{-4}	1	1

The two colonies from the 10^{-4} dilution plates and the twenty two colonies from the 10^{-3} plate 2 were replica streaked on LM-Rif and LM-RifKan plates. Colonies 3, 8, 14, 15, 19 and 20 were kanamycin resistant and therefore had not excised the plasmid construct, however the other 18 colonies checked were all kanamycin sensitive and therefore possible mutants. Each of the 18 colonies were checked by PCR using the primers **ORF10b** and **delche1** and following the same protocol as before:

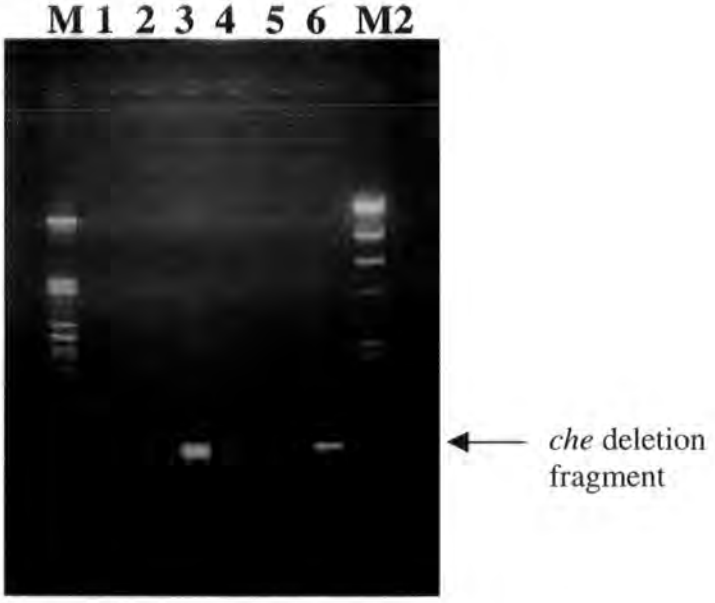

Fig. 4.4.2.2 0.7% agarose gel showing the genotype of the putative *che* deletion mutant strains.

1 – 5 = putative *che* deletion strains, **6** = C1-delche1, **M** = λ / *Pst*I, **M2** = λ / *Hin*dIII.

The results of the PCR reactions showed that most of the colonies checked contained the *che* deletion fragment. The PCR amplifications from five of the colonies are shown in **Fig. 4.4.2.2**. Genomic DNA was isolated from two of the possible mutant strains; C1-delche10a and C1-delche12a (lanes **1** and **3** respectively, in **Fig. 4.4.2.2**), and *Eco*RI digests carried out. The strains were then checked by Southern blotting alongside similarly cut DNA from the mutant intermediate, C1-delche1, and C58C1. The *che* deletion fragment was used as a radioactively labelled probe.

The hybridising band sizes expected for C58C1, the two possible intermediate strains and a correctly constructed *che* deletion strain are given in **Fig. 4.4.2.3**.

The Southern blot hybridisation results can be seen in **Fig. 4.4.2.4**, the approximate sizes of the hybridising bands produced are:

	***Eco*RI**
C58C1	7.0kb+4.8kb
C1-delche1	11.0kb+10.0kb +1.5kb
C1-delche10a	10.0kb+4.5kb
C1-delche12a	7.6kb

The hybridising bands produced by C1-delche10a showed that it was not a correctly constructed *che* deletion strain. However the bands produced in the other lanes corresponded well with those predicted in **Fig. 4.4.2.3** and confirmed that C1-delche12a was a correct *che* deletion strain. The hybridising bands for C1-delche1 showed that the initial integration event had occurred via recombination of the downstream flanking sequence, i.e. as Intermediate B. C1-delche12a was renamed C1-delche and used in all subsequent work.

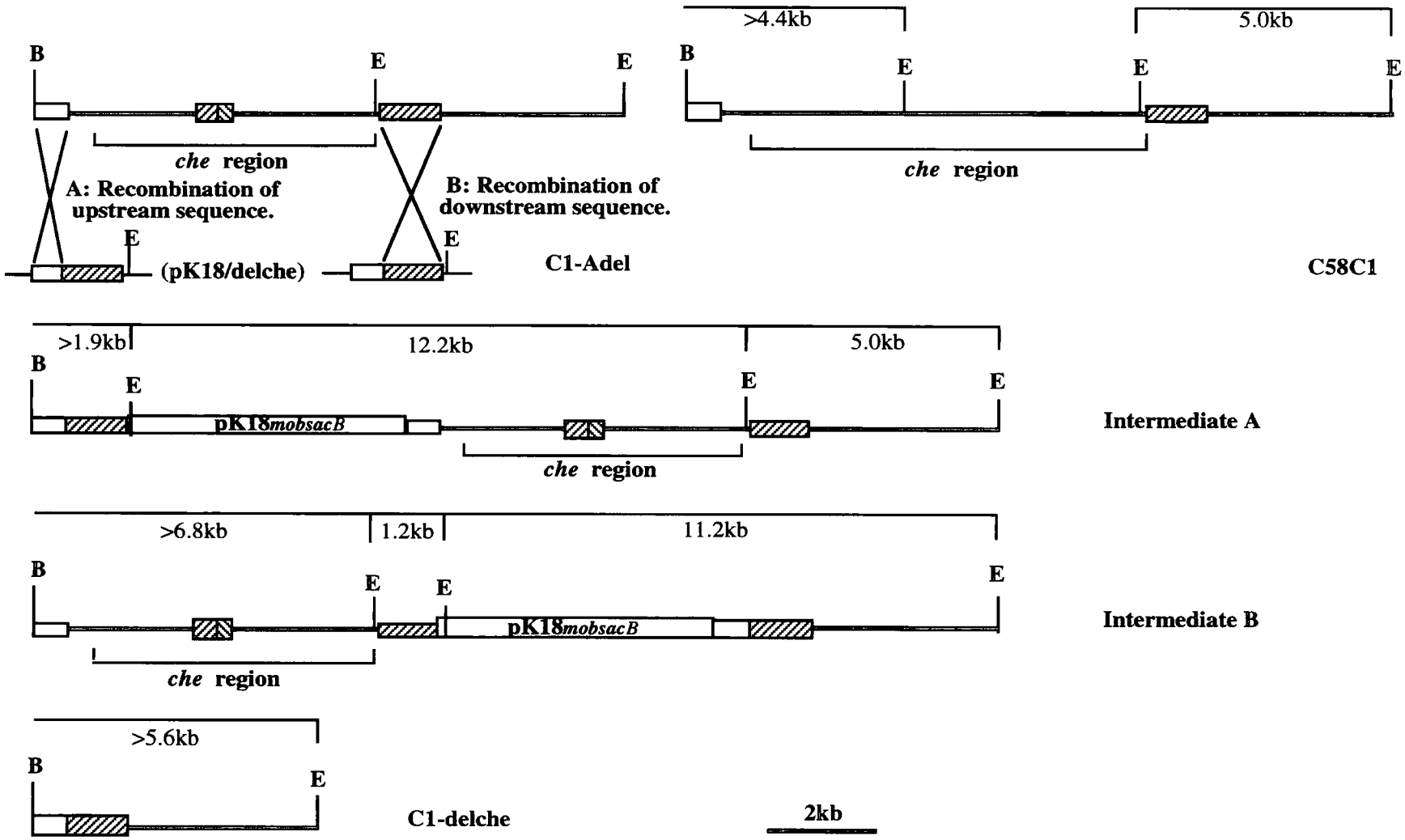

Fig. 4.4.2.3 Diagram showing the approximate sizes of the hybridising *Eco*RI bands expected for C58C1, the two possible intermediates and the *che* deletion mutant strain, C1-delche. B = *Bam*HI, E = *Eco*RI.

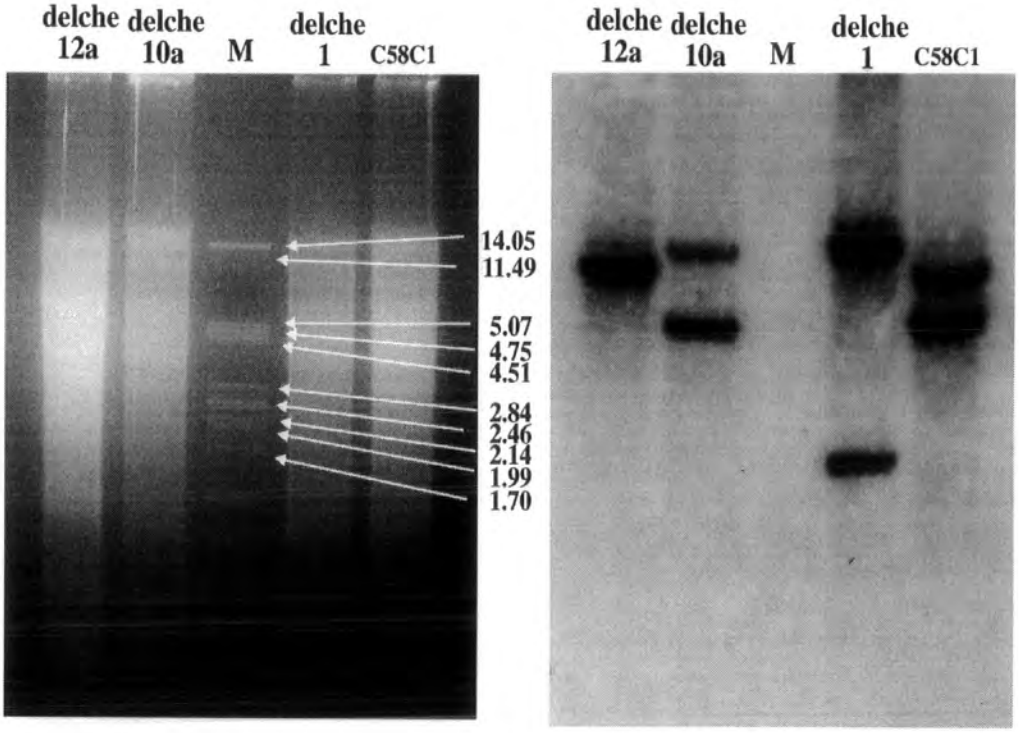

Fig. 4.4.2.4 0.7% agarose gel and subsequent Southern blot showing digests of the putative *che* deletion mutant strains and hybridisation with the *che* deletion probe. M = λ / *Pst*I.

4.5 Mutagenesis of *fliF*.

Although not directly related to the principal aims of this work it was decided to mutate the *fliF* homologue identified directly downstream of the *che* region, to assess whether or not it was a functional copy of the gene. In *E. coli fliF* is transcribed much earlier than the *che* genes (see section **1.3.2**). It was therefore unlikely that the identified homologue was transcribed with the chemotaxis genes identified. Indeed, if it had been, it is likely that the gene replacement mutagenesis work previously carried out would also have affected its transcription, and hence the mutants seen would have been non-motile, rather than chemotactically impaired (described in section **4.6**). Identification of the *fliF* homologue therefore aids this work by delimiting the *che* region identified. If functional it was expected that mutation of the *fliF* homologue would give a different phenotype to that of the *che* mutants (see section **4.6**).

4.5.1 Construction of the *fliF* Mutant Plasmid.

The *fliF* homologue lies at the 5' end of the *Eco*RI subclone pELW3, this was therefore the starting point for construction of the *fliF* mutant. The main steps involved in construction of the plasmid construct are outlined in **Fig. 4.5.1**. First pELW3 was digested with *Eco*RV, and the approximately 2.0kb fragment containing *fliF* isolated. The fragment was ligated into *Sma*I-cut pJQ200uc1, correct insertion of the fragment was confirmed as described in section **4.1.1**. The positive subclone pJQF was identified.

The plasmid pJQF was digested with *Xho*I, which cut approximately 800bp in from the start of *fli*F, the linearised fragment was then gel isolated and blunt-ended. The 1.2kb neomycin resistance cassette was isolated from pDUB2033 by digestion with *Eco*RI, it was then isolated, blunt-ended and ligated into the blunt-ended, *Xho*I cut, pJQF. Correct insertion of the neomycin cassette was selected for by growth on LM-GmNeo plates. Possible positive colonies were checked by restriction digests, the positive clone pJQFNeo was identified.

4.5.2 Formation of the *A. tumefaciens fliF* Mutant Strain.

The plasmid pJQFNeo was conjugated into C58C1 and double recombinants selected by plating on LM-RifNeo5% sucrose plates.

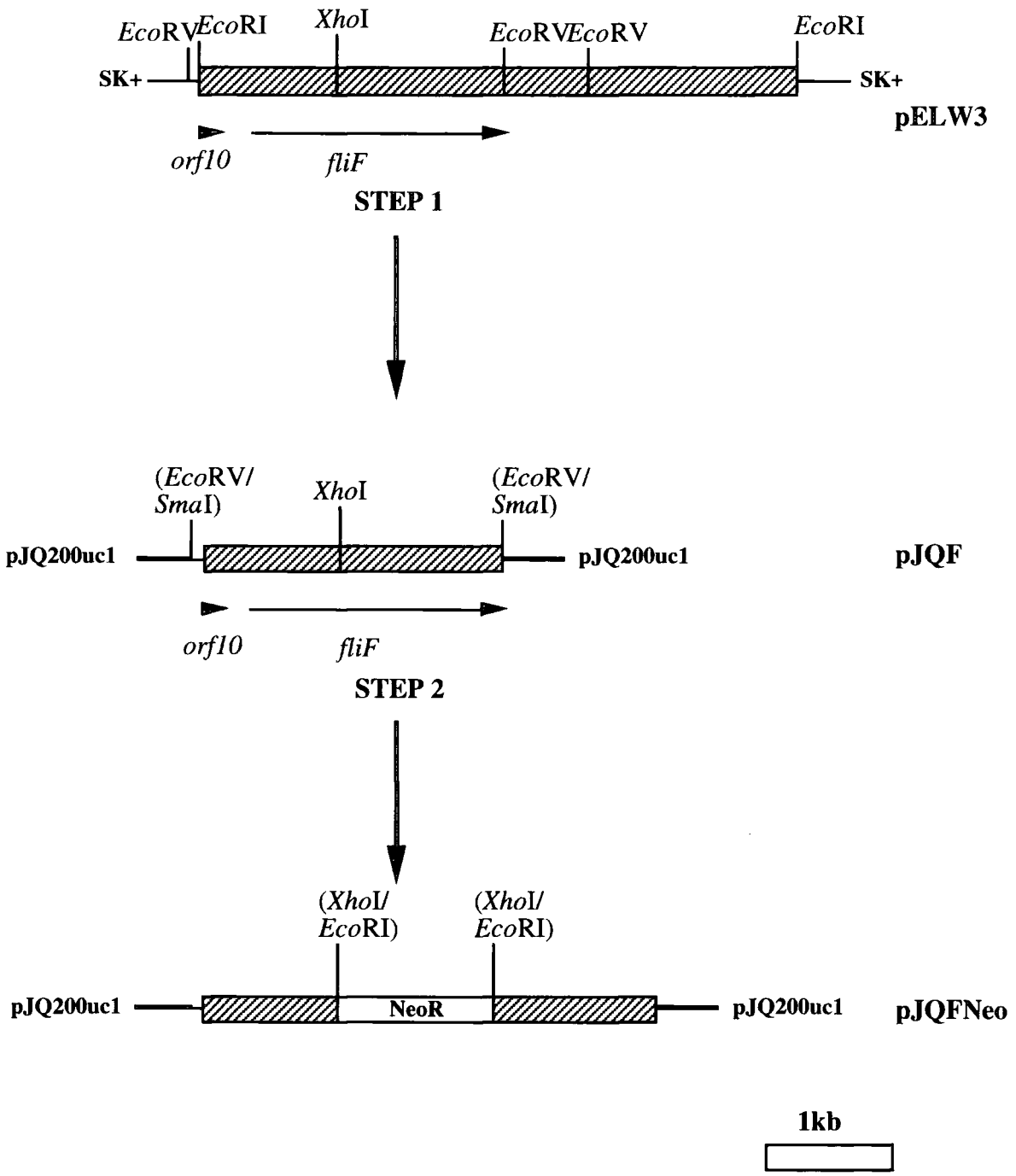

Fig. 4.5.1 Diagram outlining the main sub-cloning steps involved in construction of the *fliF*-Neo plasmid.

Approximate sizes and positions of genes are indicated by arrows underneath the main figures. Enzymes in brackets indicate restriction sites used in a previous step but no longer present.

Four colonies were selected from the LM-RifNeo5% sucrose plates and inoculated, in duplicate, along with C58C1, into 0.2% LM-broth swarm plates. After two days incubation at 28°C none of the possible mutant strains had swarmed. One of the colonies, C1-FNeo2, was therefore selected, digested with *Eco*RI and *Hin*dIII and checked by Southern blotting alongside similarly cut C58C1 DNA. The 2.0kb *fliF* fragment and the neomycin cassette were used as radioactively labelled probes. The hybridising band sizes expected for C58C1 and a correctly constructed *fliF* mutant strain are given in **Fig. 4.5.2.1**.

The Southern blot hybridisation results can be seen in **Fig. 4.5.2.2** and **Fig. 4.5.2.3**. The approximate sizes of the bands produced when hybridised with the *fliF* probe are:

	***Eco*RI**	***Hin*dIII**
C58C1	4.8kb	2.1kb
C1-FNeo2	6.0kb	2.1kb+1.2kb

With the neomycin probe, no bands were seen in the C58C1 lanes, and the possible mutant strain gave the same bands as for the *fliF* probe. The bands produced therefore correspond well with those predicted in **Fig. 4.5.2.1** and confirm correct construction of the *fliF* mutant strain. C1-FNeo2 was renamed C1-FNeo and used in all subsequent work.

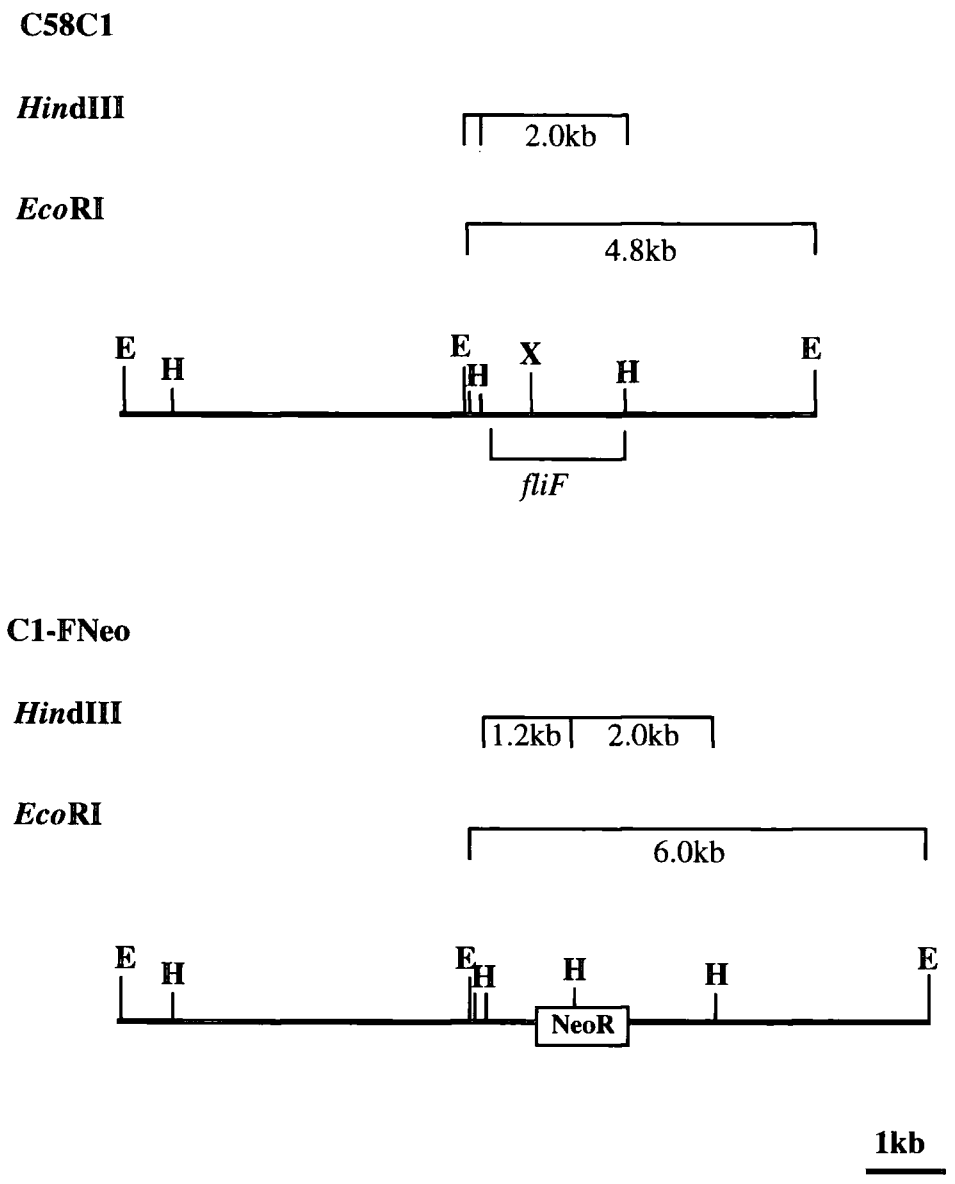

Fig. 4.5.2.1 Diagram showing the position and approximate size of the hybridising fragments expected for C58C1 and the *fliF* mutant strain, C1-FNeo.

E = *Eco*RI, **H** = *Hin*dIII, **X** = *Xho*I. The figures given for C58C1 are for hybridisation with the *fliF* probe only, the figures for C1-FNeo apply for hybridisation with both probes.

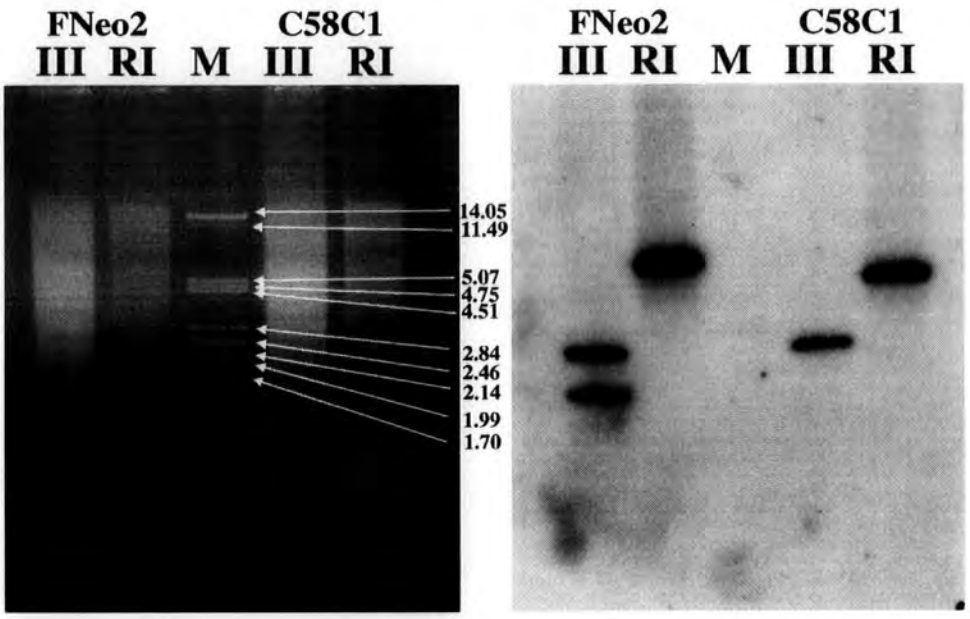

Fig. 4.5.2.2 0.7% agarose gel and subsequent Southern blot showing digests of the putative *fliF* deletion mutant strains and hybridisation with the *fliF* probe.
III = *Hin*dIII, **RI** = *Eco*RI, **M** = λ / *Pst*I.

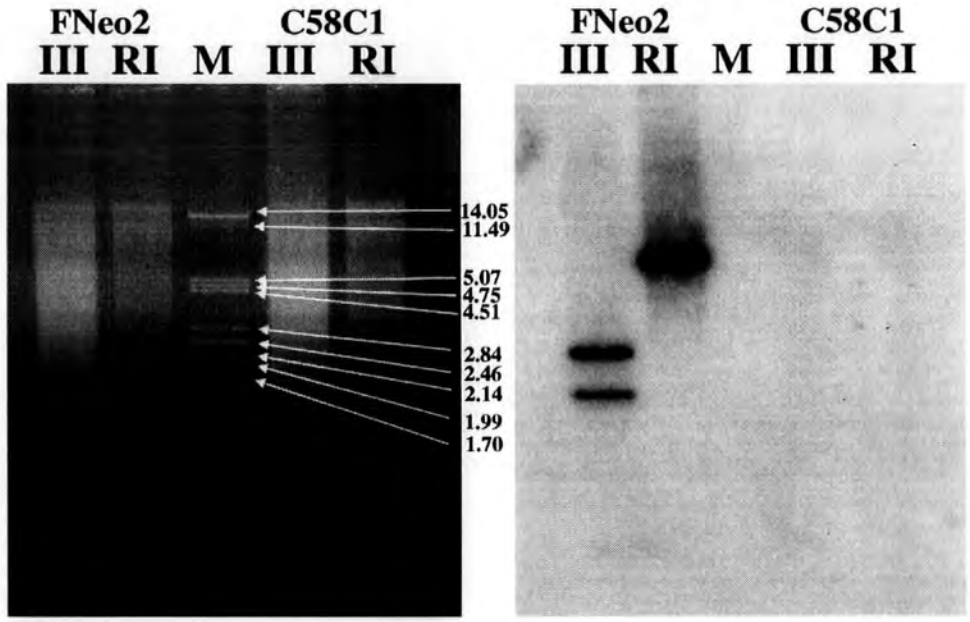

Fig. 4.5.2.3 0.7% agarose gel and subsequent Southern blot showing digests of the putative *fliF* deletion mutant strains and hybridisation with the neomycin probe.
III = *Hin*dIII, **RI** = *Eco*RI, **M** = λ / *Pst*I.

4.6 Phenotypical Analysis of the Mutants.

4.6.1 Swarm Plate Analysis.

To determine whether, when compared to the swarming behaviour of wild type cells, the mutations caused any observable phenotypic effects, the mutant strains and wild type C58C1 were each inoculated into the centre of 0.2% LB swarm plates. The plates were incubated at 28°C, typically for a period of 2-3 days.

When incubated at 28°C for the same period of time C1-orf1Neo, C1-ANeo, C1-Adel and C1-delche formed swarms approximately half the size of those formed by C58C1, but of an equivalent size to each other. C1-del10 produced swarms the same size as those produced by C58C1. C1-FNeo produced "swarms" of approximately 0.5cm in diameter when grown for two days, in comparison the wild type swarms were 5.0cm in diameter after the same length of time. Photographs showing the swarming behaviour of each of the mutant strains, relative to that of C58C1, can be seen in **Fig. 4.6.1**.

4.6.2 Analysis of Growth Rate.

To investigate whether the differences in swarming behaviour were due to a difference in growth rate of the mutant strains, compared to wild type C58C1, the growth rate of each was measured by monitoring the change in OD_{600nm} with time (see section **2.13**).

No discernible differences could be seen in the growth rate of the mutants, compared to C58C1 (data not shown). Therefore confirming that the impaired swarming seen was due to disruption of the chemotactic capabilities of the bacteria.

4.6.3 Microscopic Analysis.

To check whether the differences seen in the swarming behaviour of the mutants was due to a change in the construction or action of the flagellar machinery of the cells, compared to wild type *A. tumefaciens*, each was viewed under light and electron microscopy.

As far as could be determined no discernible differences, to that of wild type *A. tumefaciens* cells, could be detected in the flagellation or patterns of motility of C1-

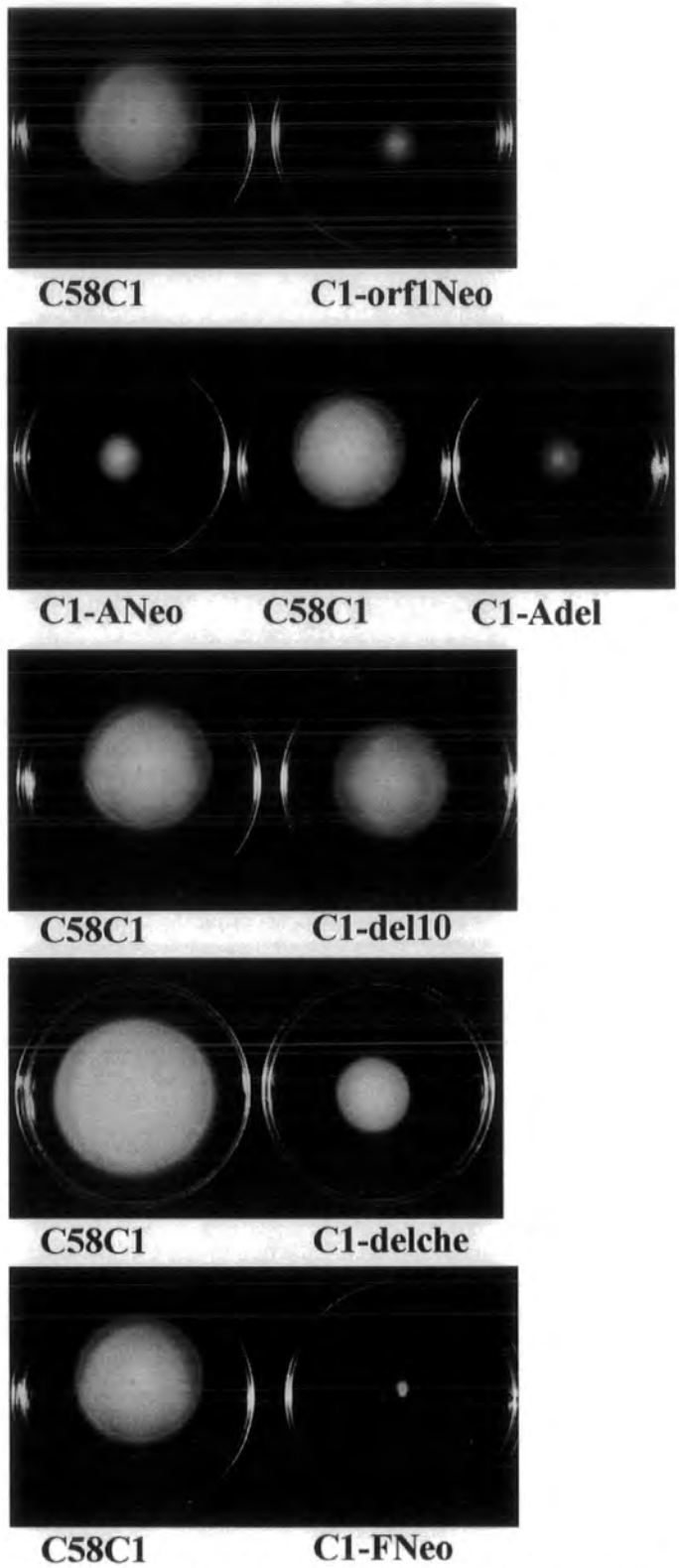

Fig. 4.6.1 Photographs showing the swarming behaviour of each of the mutant strains created.

The plates shown in each panel were incubated at 28°C for the same length of time, typically 48-72 hours.

orf1Neo, C1-ANeo, C1-Adel, C1-del10 and C1-delche. The mutant strains C1-orf1Neo, C1-ANeo, C1-Adel, and C1-delche therefore appeared to have a wild type motility pattern but disrupted swarming capabilities, most likely due to a defect in the chemotactic signalling system. C1-del10 had wild type motility and swarming capabilities, it therefore appears, under the conditions analysed, that deletion of *orf10* had little, if any, effect on the chemotactic behaviour of C58C1. When viewed under light microscopy C1-FNeo was found to be non-motile. Closer examination under electron microscopy showed it to be non-flagellate, therefore explaining the non-motile phenotype seen. An electron micrograph of each of the strains can be seen in **Fig. 4.6.3**.

4.6.4 Complementation Studies.

It was decided to try and complement the *cheA* and *che* deletion mutant strains. This should restore the swarming ability of each mutant to that of wild type C58C1. This was achieved by introduction of the cosmid pDUB1911 into each strain by tri-parental mating (as described in section **2.9**). Introduction of the cosmid pDUB1911 was confirmed by carrying out minipreps using the silica fines method (see section **2.4.3**) and checked by digesting the isolated DNA with *Hin*dIII and *Eco*RI, which both gave a known band pattern for pDUB1911. The correct strains C1-ANeo/1911, C1-Adel/1911 and C1-delche/1911 were therefore identified. To assess whether introduction of pDUB1911 complemented the mutations, each new strain, along with the original mutant strains and C58C1 as reference strains, were inoculated into the centre of 0.2% LM-broth swarm plates.

The swarming behaviour of C1-ANeo, C1-Adel and C1-delche was partially restored by introduction of the cosmid pDUB1911, the new strains showing intermediate swarming between that of the two relevant reference strains (see **Fig. 4.6.4**). The complementation seen, although not complete, was significant. The most likely reason for not seeing complete restoration of swarming behaviour is because of the differences in copy number of plasmid-encoded and genomic forms of the *che* genes. This would disrupt the equilibrium between the *che* gene products and inevitably affect swarming behaviour.

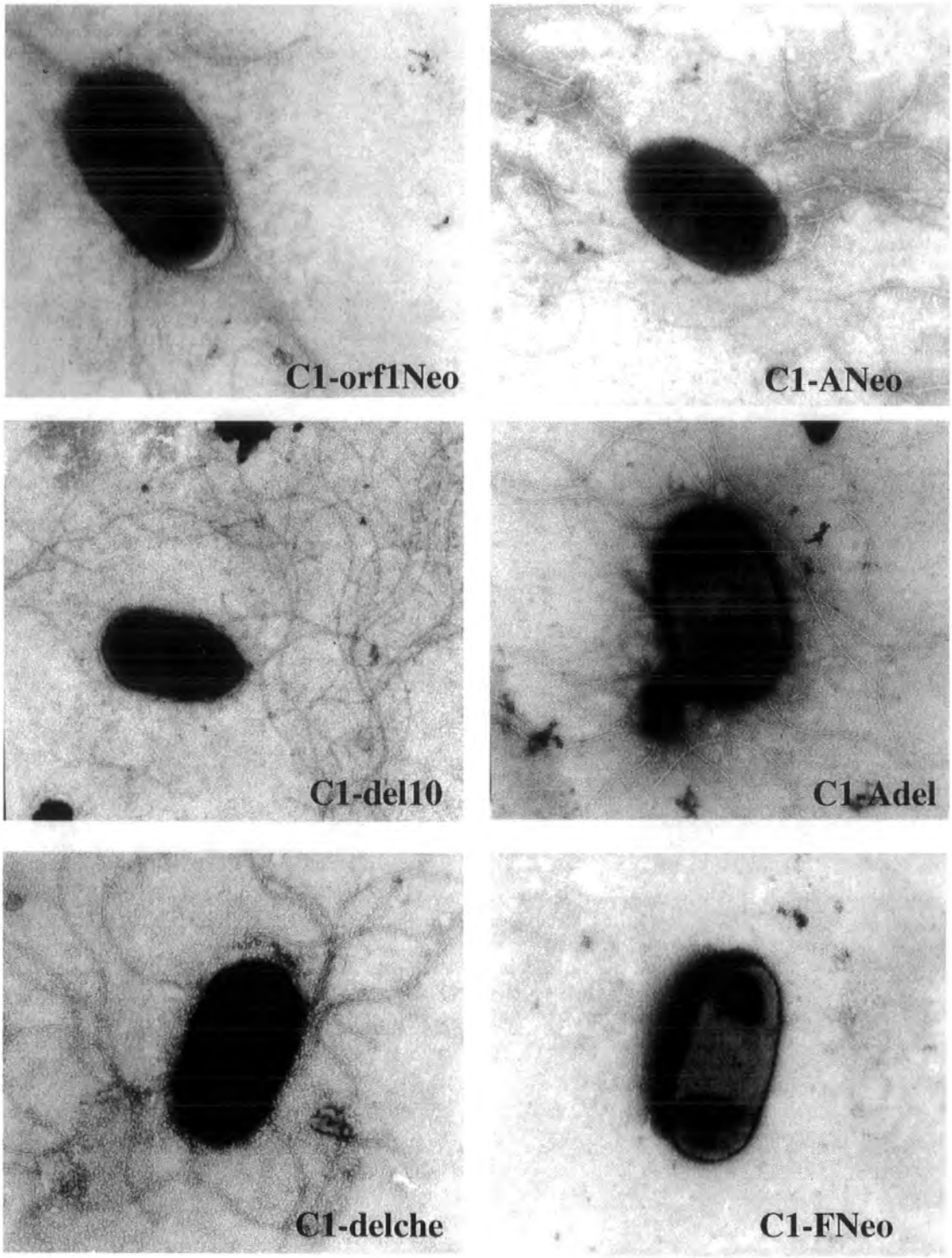

Fig. 4.6.3 Electron micrographs of each of the mutant strains.

For comparison with wild type C58C1 see **Fig. 1.4.3**.

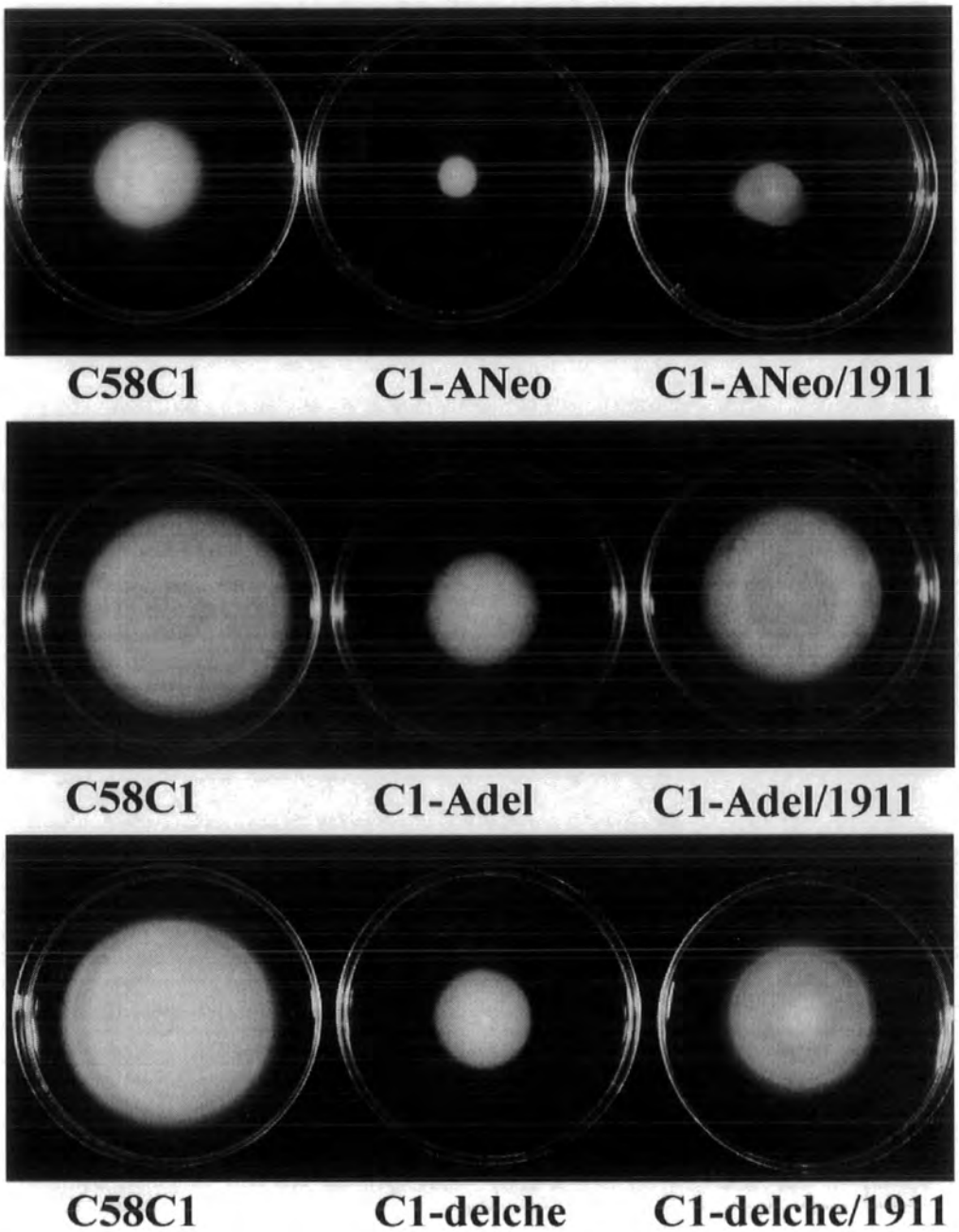

Fig. 4.6.4 Photographs showing complementation of the C1-ANeo, C1-Adel and C1-delche mutant strains by the cosmid pDUB1911.

The plates shown in each panel were incubated at 28°C for the same length of time, typically 48 – 72 hours.

4.6.5 Tumourigenicity Studies.

Since the *cheA*, *orf10* and *che* deletion mutants were created without introducing any additional selectable markers it was possible to easily introduce a Ti plasmid in to each of the strains in order to assess their tumourigenic capabilities.

Two Ti plasmids were used; pDUB1003/Δ71 and pDUB1003/Δ77. These are derivatives of the nopaline-type Ti plasmid pTiC58. They were originally produced in a study of the nopaline synthase (*nos*) promoter region [180], and contain an introduced kanamycin resistance cassette. In the previous study each plasmid was found to be as least as virulent as the wild type Ti plasmid. Therefore the particular manipulations previously carried out were known not to adversely affect their tumourigenicity. The plasmids were maintained in an erythromycin/chloramphenicol resistant strain of C58C1, it was therefore possible to conjugate the plasmids in to the mutant strains by tri-parental mating and selection on L-agar plates containing rifampicin and kanamycin. Introduction of the Ti plasmids was confirmed by isolating total DNA from the bacteria, digesting with *Hin*dIII and Southern blotting using the kanamycin resistance cassette as a radioactively labelled probe. The originating strains of the Ti plasmids (C1del71 and C1del77) were used as positive controls in the Southern blot, and C58C1 was used as a negative control (see **Fig. 4.6.5**).

Each Ti plasmid was introduced into each of the three deletion mutant strains. At the same time each Ti plasmid was also introduced into the, rifampicin resistant, wild type strain of C58C1 used to created the mutants. Eight new strains; C1/71, C1/77, C1-Adel/71, C1-Adel/77, C1-del10/71, C1-del10/77, C1-delche/71 and C1-delche/77, were therefore created. Correct introduction of the Ti plasmids was confirmed as explained above, and shown in **Fig. 4.6.5**.

Plant inoculations were carried out using each of the eight new strains, plus positive and negative control strains. The two EryCmKan resistant strains (originating strains of the Ti plasmids) were used as positive controls and the three original mutant strains, plus the Rif resistant strain of C58C1, were used as negative controls.

The new strains were grouped as 71 or 77 bearing strains, hence giving two groups of four strains. Two different inoculation strategies were used, different strains bearing the same Ti plasmid were inoculated **1)** individually on to different leaves of the same plant and **2)** in groups on to different leaves of the same plant:

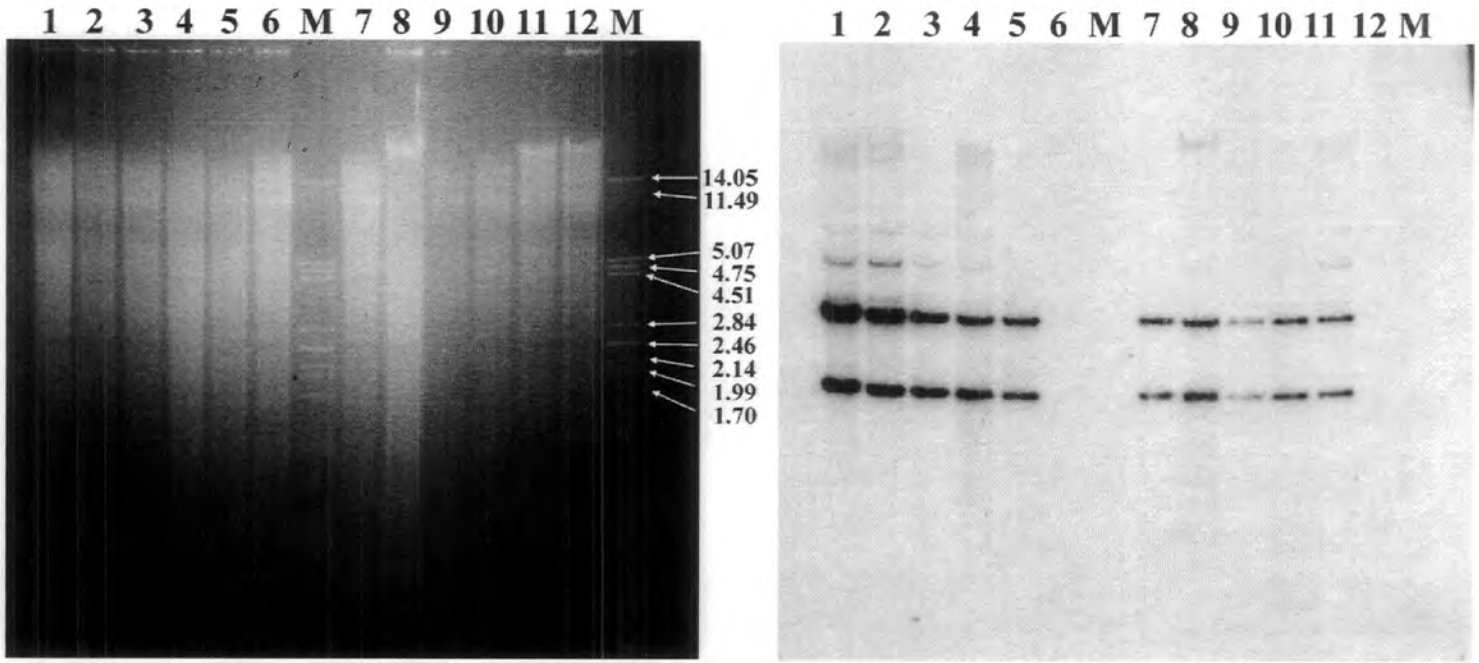

Fig. 4.6.5 0.7% agarose gel and subsequent Southern blot showing digests of the deletion mutant strains containing Ti plasmids and hybridisation with the neomycin probe.

1 = C1del71, **2** = C1-delche/71, **3** = C1-del10/71, **4** = C1-Adel/71, **5** = C1/71, **6** = C58C1, **M** = λ / *Pst*I

7 = C1del77, **8** = C1-delche/77, **9** = C1-del10/77, **10** = C1-Adel/77, **11** = C1/77, **12** = C58C1.

1) Each strain from a group was inoculated (in duplicate, either side of the midrib) on to a different leaf of the same plant, one leaf per strain. This was carried out for both groups, hence giving one plant with leaves bearing strains containing Ti plasmid 71 and another plant with leaves bearing strains containing Ti plasmid 77. This procedure was repeated, giving two plants for each of the two groups. The plants were named 71A, 71B, 77A and 77B.

2) The four strains within a group were inoculated on to a single leaf, two strains either side of the midrib. Similar inoculations were carried out using the other group of strains on the opposing leaf of the plant. The whole procedure was then repeated on a second plant, the plants were named 71+77leavesA and 71+77leavesB.

Two control plants were set up. Each of the four negative and two positive controls were inoculated, either side of the midrib, on to a different leaf of each plant, one leaf per control. The controls were also inoculated on to the experimental plants; the four negative controls were inoculated on to one leaf (two strains either side of the midrib) and the two positive controls were inoculated (in duplicate, either side of the midrib) on a second leaf. This was carried out on plants 71A, 77B and 71+77leavesA.

After eight weeks incubation the tumours produced at the inoculation sites on each plant were scored, according to their size, using the scale given in **Table 4.6.5.1**:

Score	Diameter of tumours (cm)
0	None present
+	<0.5
++	0.5-1.0
+++	1.0-1.5
++++	1.5-2.0
+++++	>2.0

Table 4.6.5.1 Parameters used to score tumour size.

The results of each of the inoculations are given in **Table 4.6.5.2**. Each of the experimental strains were infective and produced small tumours, the mutant strains alone were unable to produce tumours, hence confirming correct introduction of the Ti plasmids

	Experimental Strains								-ve Controls				+ve Controls	
Plant	**C1/71**	**C1/77**	**C1-Adel/71**	**C1-Adel/77**	**C1-del10/71**	**C1-del10/77**	**C1-delche/71**	**C1-delche/77**	**C58C1**	**C1-Adel**	**C1-del10**	**C1-delche**	**C1del71**	**C1del77**
71A	++		++		++		*		0	0	0	0	++++	+++
71B	++		++		+++		+++							
77A		++		++		*		+++						
77B		*		++		++		++	0	0	0	0	++	+++
71+77 leavesA	+++	+++	+++	++	+++	++	+++	++	0	0	0	0	+++	+++
71+77 leavesB	++	++	++	++	++	++	++	++						
Control 1									0	0	*	0	+++++	++++
Control 2									0	0	0	0	+++++	+++++

Table 4.6.5.2 Scores for the tumours produced on each of the inoculated plants.

* indicates the relevant leaf had died prior to scoring, blank cells indicate no inoculation.

into the strains. The positive controls produced large tumours on the control plants; the tumours produced on the experimental plants were of a smaller size, comparable to those produced by the experimental strains. The formation of larger tumours on the control plants is probably because there were less sites of infection and hence the plant would be under less cumulative stress. The inherent differences between, and within, individual plants will lead to differences in tumour size, even when infected with the same bacterial strain. This can be seen by the different scores in **Table 4.6.5.2** for inoculation of the same strains in different plants, thus reinforcing the need for multiple inoculations in such investigations.

Although this work simply confirmed that a Ti-plasmid had been introduced into each of the strains, and that as a result the strains became infective (causing Crown Galls on Kalanchöe plants), it was an essential precursor to further studies. Knowing that the tumourigenic capacity of the strains is equivalent to that of wild type C58C1 will allow the strains to be used in assays which require chemotaxis prior to infection, hence aiding studies into the possible interactions between the chemotaxis and virulence systems of *A. tumefaciens*.

4.7 Discussion.

Mutations were made in three of the nine genes identified in the *che* cluster (*orf1*, *cheA* and *orf10*) and the entire *che* region was deleted. Preliminary studies of the mutants (detailed in section **4.6**) showed each, except that in *orf10*, to produce a defined phenotype. Further analysis confirmed that the phenotypes seen were the result of disruption to the chemosensory pathway. Deletion of *orf10* caused no obvious alteration in the cells chemotactic responses, motility or flagellar structure. Insertion of a neomycin cassette into the *fliF* homologue produced a non-flagellate phenotype. This would be expected if, as in *E. coli*, FliF forms the MS-ring of the flagellar structure and is one of the first proteins to be laid down in the process of flagella construction.

The *orf1*, *cheA* and *che-* mutant strains all showed impaired chemotactic capabilities, but interestingly each also exhibited wild type patterns of motility. This retention of wild type patterns of motility, in each of the mutants studied so far, suggests that there may be an additional level of control of the flagellar motor, independent of that

from the chemosensory system. Further investigations are required to fully assess the extent of the phenotypes seen. The next step in analysing the mutants created would be to carry out chemotaxis assays, using defined chemoattractants, to study the extent of chemotactic impairment. The simplest way of testing chemotactic capabilities would be to perform specific swarm-plate or plug-plate assays on each of the mutants, using the compounds identified by Loake *et al* [118] as specific chemoattractants for *A. tumefaciens* C58C1, as the chemoattractants. In addition either Blindwell or Capillary assays could be performed using a similar range of compounds, hence giving a more quantitative assessment of the chemotactic responses of the strains. This should define whether there is a total loss of chemotaxis, or if loss is limited to a certain range of chemoeffectors. Chemotactic responses could also be studied, on a finer scale, using tethered cells and computerised motion analysis, which would allow a more refined study of the specific responses of each strain.

The phenotype of the *cheA* mutant is similar to that seen for deletion of $cheA_{II}$ from *R. sphaeroides*, which also results in a loss of chemotactic function but wild type patterns of motility [9]. Deletion of *cheA* from *S. meliloti* however causes a "smooth-swimming" phenotype, which more closely resembles the phenotype seen when *cheA* was deleted from *E. coli.* In fact in-frame deletion of each of the *che* genes from *S. meliloti* causes deficient chemotaxis and a direct effect on the pattern of motility. If, as might be expected, *A. tumefaciens* and *S. meliloti* have related chemosensory transduction systems, similar phenotypes may be seen in corresponding mutants in *A. tumefaciens*. Since little is known about the exact mode of action of the flagella in *A. tumefaciens*, without further investigation, it is not possible to state definitively that the *che* mutants created to date have no effect on motility. Ideally each of the mutants should be studied using a computer-linked tracking system that would statistically analyse the motion of the bacteria and compare it to that of the wild type, therefore identifying any differences in motility patterns.

In order to study the chemotactic response of *A. tumefaciens* in more detail, in-frame deletions should be made of the remaining *che* genes thus far identified. This would then allow studies to be conducted on the effects of deleting each of the genes from the chemosensory network. In addition to simply deleting the *che* genes, further analysis of their function could come from performing over expression studies of each of the proteins.

Using specific expression vectors it would be possible to look at the effects of each protein on both wild type and specific *che* mutant strains of, not only *A. tumefaciens,* but also other bacteria e.g. *E. coli* and *S. meliloti.* It would then be possible to begin to understand the functioning of each of the proteins in *A. tumefaciens.*

The above ideas represent general chemotaxis experiments, previously performed in many bacterial species. However, *A. tumefaciens* also offers a unique perspective on which further investigations could be carried out. This is the putative integration of the Ti-encoded virulence system with the chromosomally-encoded chemotaxis system (see section **1.9**). Chemotaxis to plant wound phenolics has been shown to require phosphorylation of VirA and VirG from the Ti plasmid [147]. It is therefore likely that one, or both, of these proteins interacts with one, or more, elements of the chromosomally-encoded chemotaxis system identified in this work. The most obvious point of integration would be at CheA, since studies in other bacterial species have shown CheA to be the likely point of integration for responses to, for example, PTS carbohydrates and the aerotactic response. A rudimentary way to investigate interactions between the *che* and *vir* systems would be to use the Ti-containing *che* mutant strains produced in this work (see section **4.6.4**), in chemotaxis assays, using wound exudates known to require a Ti-plasmid for chemotaxis to occur, as the chemoattractants [11]. Similar work could then be performed on deletion mutant strains of each of the *che* genes, hence giving a crude indication of interactions between the Che and Vir proteins. To look at interactions in more detail, the *che* gutted strain could be used as a basal strain into which defined sets of *che* and *vir* genes could be reintroduced to try and reconstitute the chemotaxis pathway for plant wound phenolics. On identification of the requirements for chemotaxis to phenolics, finer scale mutagenesis of both the *che* and *vir* genes, and then subsequent chemotaxis studies could be carried out to allow a more detailed understanding of the processes involved. An alternative way of studying possible interactions between the *che* and *vir* systems would be to directly investigate phosphotransfer between specific proteins. Sourjik and Schmitt [194] studied phosphotransfer between CheA, CheY1 and CheY2, in *S. meliloti,* using an *in vitro* radiolabelling technique. Similar methods could be employed to establish whether phosphotransfer occurs, for example, between VirA/G and CheA, or other chemotaxis proteins. In addition to studying direct interactions between the two systems, it would also be interesting to study the overall effect mutating the *che* genes has on virulence. When directly inoculated into test plants the *che* mutant strains exihibited

wild type levels of infectivity. However, the methodology used did not address the requirement for the bacteria to sense and respond to specific chemical stimuli, as is presumed to occur within their natural environment. If the strains were tested in an assay that required directed movement, prior to infection, it is possible that quite different levels of infectivity would be seen. Thus demonstrating the importance of the chemotactic response in *A. tumefaciens* biology.

Due to the time constraints of this study, it was not feasible to expect to carry out all the mutagenesis and assay work required to understand the possible interactions of the *che* and *vir* genes. It was therefore decided to attempt to construct a Selectively Infective Phage (SIP) system that would allow easy and reliable investigation of the possible interactions within, and between, the Che and Vir proteins. The progress made on this work is given in the following chapter.

In addition to the work outlined above, future work on chemotaxis in *A. tumefaciens* would also require investigations into the possible existence of additional pathways within the chemosensory network, and the putative involvement of MCPs in the chemotactic response. These possibilities will be considered in more detail in **Chapter 6**.

Mutagenesis of the *fliF* homologue identified in this work, resulted in a non-motile, non-flagellate phenotype. This phenotype is markedly different to those seen for the *che* mutants created. Although not expected, it was possible that *fliF* could have been transcribed along with the *che* cluster, however this difference in phenotype confirms separate transcription. Since, if they were linked, the interruption mutants created in *orf1* and *cheA* would have been expected to have downstream polar effects on *fliF* resulting in non-motile, rather than chemotactically impaired, phenotypes.

5 Construction of a Selectively-Infective Phage (SIP) for Investigating Protein-Protein Interactions Within, and Between, the Che and Vir Proteins of *A. tumefaciens*.

5.1 Phage Display and SIP Technology.

The principle of using phage techniques to study protein interactions was first conceptualised in 1985 [189]. In recent years there has been a wealth of study into this subject, and as a result there have been numerous reports of potential applications of the basic concept (for review see [190]). Most applications are based on the notion of "phage display" [64, 134, 140]. Phage display involves expressing a library of proteins, or peptides, on the surface of phage particles, and detecting those which bind a specific ligand with greatest affinity. The proteins binding to the specific ligand can then be amplified, and characterised by sequencing of the relevant region of the phage genome. Hence facilitating the screening of a large number of potentially interacting partners, using a relatively straightforward procedure.

Most work on phage display has utilised filamentous phage strains e.g. M13, f1 and fd. The filamentous phage genomes have a simple composition e.g. the fd genome is a circular, single stranded DNA (ssDNA) entity, of 6408bp, which is divided into two transcription units of six and four genes, identified as genes I, through to X. Five of the ten gene products subsequently form the structural components of the phage particle. Typically, filamentous phage particles are flexible rods; being approximately 1μm in length and 6nm in diameter. The majority of the phage structure is composed of a tube of helically arranged molecules of the major coat protein pVIII (the single stranded phage DNA lies within this tube). At one tip of the particle there are five copies of each of the minor coat proteins pIII and pVI, and at the other tip are copies of the other minor coat proteins, pVII and pIX. Infection of *E.coli* strains, by filamentous phage particles, is mediated by attachment of the N-terminal domain of pIII to the tip of the bacterial F pilus. Upon penetration of the host cell membrane, the phage coat proteins dissolve into the surface envelope of the cell, and the single stranded phage DNA enters the hosts cytoplasm. On entry into the host cell, the host synthesises a complimentary DNA strand, thus forming a double stranded replicative form of the phage DNA (RF DNA). This RF DNA acts as the template for transcription and translation of the phage genes, and synthesis of progeny ssDNA. The progeny ssDNAs are extruded through the bacterial cell envelope, acquiring coat proteins which have been newly synthesised by the cell, and previously positioned in the cell membrane, in the process. Unlike infection by other types of bacteriophage, the

filamentous phages do not kill their host. Infected cells are able to multiply indefinitely, while continuing to secrete phage particles through their membranes.

Most phage display work has centred on fusions to three of the coat proteins (pIII, pVI and pVIII), exploiting the ability of the phage to incorporate foreign proteins into its coat, and package the DNA encoding it. For each of the coat proteins, three distinct display strategies have been devised [190] :

- The first type (type 3, 6 or 8 - depending on the phage gene of interest) has a single phage genome, bearing a foreign DNA insert within the relevant gene. Therefore, potentially, every copy of the particular protein, in the resulting phage particles, will display the recombinant protein.
- The second type (type 33, 66 or 88) again utilises a single phage genome, but with two copies of the relevant gene, one wild type form and one bearing the foreign DNA insert. Hence every copy of the resulting phage displays a mosaic of recombinant and wild type copies of the relevant protein.
- The third type (type 3+3, 6+6 or 8+8) has two copies of the relevant gene, but in this strategy, they are situated on different genomes. The wild type version is on a "helper" phage and the recombinant version is on a phagemid. The phagemid typically carries a specific resistance cassette, and can replicate as a plasmid, or on addition of the helper phage, can undergo phage replication. Hence resultant phage particles display a mixture of wild type and recombinant copies of the relevant protein.

Each of these methods has been used to produce numerous phage libraries, of either random peptides, or genomic sequences.

The most common method used to select phage particles from such libraries is affinity selection. Typically a potential ligand is tethered to a solid support, and the phage mixture is passed over the ligand, allowing phage particles bearing interacting proteins to attach to the support. Elution of the interacting phage particles, followed by amplification (by infection of *E.coli*), and subsequent repeated rounds of selection, identifies specific interacting phage particles. The protein domain responsible for the interaction can then be characterised by sequencing of the relevant region of the phage DNA. Of course, such selection is not as straightforward as it may seem. Attaining correct binding and elution conditions is far from simple. Alternative selection strategies have therefore been devised that do not require binding and elution of the phage particles from a specific support.

These alternative strategies utilise the unique characteristics of pIII, following a method similar to that of the yeast two-hybrid system [1, 90]. The pIII protein is a 406 amino acid protein. It is initially synthesised in a precursor form, of 420 amino acids, bearing an 18 amino acid signal peptide. The mature protein has a highly hydrophobic region, from amino acids 379 - 401, which is thought to anchor the protein in the bacterial membrane. Most of the protein is therefore positioned in the periplasm of the host cell. Extensive studies have shown pIII to consist of two completely separable domains, the N-terminal, (which can be further subdivided into domains N1 and N2 - 68 and 131 amino acids respectively) and the C-terminal (150 amino acids) [10]. Both of the domains are required for correct infectivity of the resulting phage particles. It has been shown that the N-terminus is required for docking of the phage particle onto the tip of the bacterial F pilus, and for subsequent penetration of the bacterial membrane [139]. The C-terminus however, forms part of the phage coat, and contributes greatly to the stability of the phage [51]. The different domains are joined together by two glycine-rich linker regions, of 18 and 39 amino acids. These are non-essential, but enhance the infectivity of the phage, most likely by conferring flexibility on the protein.

Display of a foreign protein, on a copy of pIII which lacks its N-terminus, produces non-infective phage particles. However, infectivity can be restored by joining the N-terminal domain of pIII, to a ligand that binds the protein displayed on the phage, thereby reforming the pIII protein. This strategy is therefore based on producing phage particles which only become infective when an interaction has occurred that restores the pIII protein, required for infectivity. Hence binding events are selected for, by coupling the event to infection of an *E. coli* strain, such strategies are therefore termed Selectively-Infective Phage (SIP) systems. Two classes of SIP system exist, "*in vivo* SIP" and "*in vitro* SIP" [196], which differ only in the means of producing the N-terminal fusion of gene III. In *in vivo* SIP experiments expression of the two potentially interacting domains occurs in one bacterium, and also possibly from one genetic package, hence interaction of the domains occurs within the periplasm of the bacterium. However, *in vitro* SIP requires the N-terminal fusion to be expressed from a second bacterium, it is then added to N-terminal deficient phage, and interaction occurs externally.

An example of *in vivo* SIP work, termed Direct Interaction Rescue (DIRE), was carried out by Gramatikoff *et al* [76]. Recombinant constructs of the two pIII domains were created, under the control of separate LacZ promoters, on a phagemid bearing a

specific resistance cassette. To identify interacting proteins, the phagemid was electroporated into a host *E. coli* strain, along with a gene III-mutant helper phage (i.e. a phage deleted for gene III). In the host cell, transcription and translation of both the phage and phagemid encoded genes occurred. This enabled potential interactions to occur (in the periplasm of the phage-producing cell) between the proteins linked to the two pIII domains. Phage particles were then packaged and extruded from the cell in the usual way. The extruded phage particles were isolated and used to infect a male *E. coli* host. Only those particles that contained a complete pIII (created by binding of interacting protein domains) were infective. In addition, infection by a phage particle containing the phagemid DNA, conferred the specific resistance of the phagemid, on the infected *E. coli* cells. Hence infectivity, and therefore protein interactions, were monitored by cfu (colony forming unit) count, following infection and plating on specific agar plates. Characterisation of the interacting protein domains was then achieved by sequencing of the relevant regions of the phagemid genome, as before.

The above system therefore represents a precise method of detecting protein interactions. However, it is not without complications. To function correctly, the gene III-mutant helper phage must not deliver any wild type pIII to the phage particles. The methodology required to achieve this requirement has proven to constitute a problem. Most methods have encountered a background level of infectivity, which does not derive from specific interaction between the proteins under investigation, hence effectively destroying the "selectivity" of the strategy. To overcome this problem Krebber *et al* [109] devised an *in vivo* SIP system that consisted of a single genetic package, and therefore that did not require a helper phage. In this work, initially, an antibiotic resistance cassette was inserted into the fd genome, thereby allowing simple detection of infection events. The wild type gene III was then replaced with an antibody-C-terminal fusion of pIII, and a N1N2-antigen fusion of pIII, each under the control of separate *lac* promoters. Experiments showed that phage particles displaying only the antibody (i.e. phage containing only a C-terminal fusion) were non-infectious, and these phage only acquired the ability to infect cells when an interaction occurred with an appropriate antigen connected to the N-terminal domain of pIII. It was also confirmed that restoration of infectivity only occurred when cognate antibody-antigen pairs were expressed. Similar work was conducted by Pedrazzi *et al* [154], utilising an *in vitro* SIP system, consisting of a phage with a recombinant C-terminal fusion of gene III, but no N-terminal. The N-terminal

fusion was supplied *in vitro* following expression from a specific vector. This method again allowed interacting protein domains to be detected.

Hence, in recent years a number of different SIP systems have been designed (for review see [196]). The methods described represent simple, yet precise, systems for use in detecting protein-protein interactions. With the increase in applications of the system, there have also been a number of studies directed at investigating the potential limits of the system, and in particular studying the tolerance of pIII to different sized inserts. To date the results obtained have been encouraging and have shown that pIII is able to tolerate large inserts in its structure without losing its native role [108].

Therefore, the functioning of the gene III protein, and the fact that it consists of two separable, but essential domains, make it of particular use in designing systems for testing protein-protein interactions. The aim of this work was to modify an already existing *in vivo* SIP [109], so that interactions between the chemotaxis proteins, and other proteins, could be investigated. The work described in this study is ultimately based on manipulation of the gene III protein (pIII) of fd.

The phage to be manipulated in this work is called fHAGHAG. It is a chloramphenicol resistant derivative of the filamentous phage fd (the differences between fd and fHAGHAG are shown in **Fig. 5.1**), which was designed to allow selection of cognate pairs of antibodies and antigens, as explained in the work by Krebber, above. The phage construct has a single chain antibody, which recognises a consensus of six histidine (H) residues, attached to the C-terminal domain of gene III. Hence, through the C-terminal domain of pIII, the phage presents the antibody on its surface, and only becomes infective when the N-terminal domain of pIII is attached. This only occurs when six H residues are attached to the N-terminal domain of pIII, hence enabling interaction to occur with the antibody. Interaction between the antibody and appropriate antigen therefore joins the N-terminal domain, to the C-terminal domain of pIII, and restores infectivity.

The system, described above, was to be modified by introduction of convenient restriction sites, adjacent to the gene III domains. This would allow introduction of a specific gene e.g. *cheA* or *vir*A, in-frame to the C-terminal domain of gene III, and either another known gene, or an *A. tumefaciens* library, to the N-terminal domain.

The novel gene III construct was to be made from two different sources; gene III from the originating phage, fHAGHAG, and that from the phagemid pAK200 [107] (see **Fig. 5.1**).

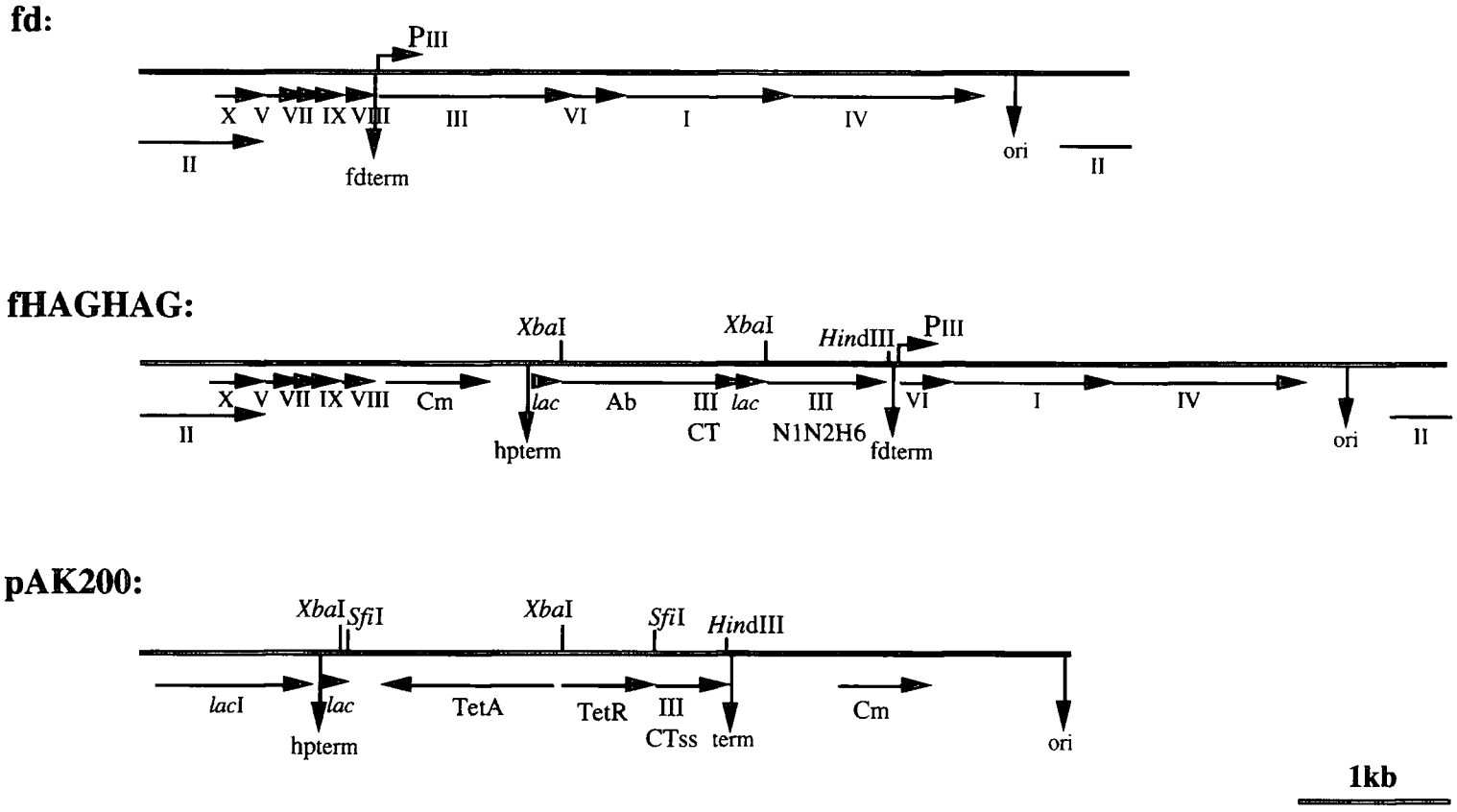

Fig. 5.1 Maps of fd, fHAGHAG and pAK200, showing the location of the phage genes, and the position of relevant restriction sites.
PIII = gene III promoter, fdterm = terminator of fd, ori = origin of replication, Cm = Chloramphenicol resistance, hpterm = hairpin terminator, *lac* = *lac* promoter/operator, Ab = antibody, IIICT = C-terminal of gene III, IIIN1N2H6 = N-terminal of gene III plus six H residues, TetA/TetR = Tetracycline resistance, IIICTss = supershort C-terminal of gene III (amino acids 250-406 of pIII).

5.2 Construction of the SIP.

Work began by removing the entire gene III, plus the attached antibody and six H residues, from fHAGHAG. fHAGHAG was digested with *Xba*I and *Hin*dIII, and the large *Xba*I-*Hin*dIII fragment produced, was isolated. A similar digest was carried out on pAK200. The resulting 1.1kb *Xba*I-*Hin*dIII fragment, and the 1.5kb *Xba*I fragment, together containing the C-terminal domain of gene III and a tetracycline resistance cassette, were isolated. The steps involved in construction of the new phage are outlined in **Fig. 5.2.1**, and given in more detail in the following text.

5.2.1 Introduction of the C-Terminal Domain of Gene III from pAK200, into the fHAGHAG Fragment.

Step 1 - The 1.1kb *Xba*I-*Hin*dIII fragment of pAK200 was ligated into the similarly cut fHAGHAG fragment, creating pH1.1. Correct insertion of the 1.1kb fragment was confirmed by restriction digests.

Step 2 - The 1.5kb *Xba*I fragment, from pAK200, was ligated into similarly cut pH1.1, creating pH1.1/1.5. Insertion of the fragment was selected for by plating transformants on 2xYT-agar plates, containing chloramphenicol and tetracycline. Correct orientation of the 1.5kb *Xba*I fragment was confirmed by digesting with *Sfi*I; positive clones gave a 2.1kb fragment, incorrect clones gave a 0.7kb fragment (as indicated by the position of the *Sfi*I sites in pAK200 shown in **Fig. 5.1**).

At this stage the construct pH1.1/1.5 contained only the C-terminal domain of gene III, attached to a Tet resistance gene (detailed structure of pH1.1/1.5 can be seen in **Fig. 5.4**). The Tet region of pH1.1/1.5 contained two *Sfi*I sites which, because of their construction (see below), would later allow introduction of new genes in-frame with the C-terminus of gene III.

The restriction enzyme *Sfi*I recognises a sequence of eight nucleotides, interrupted by five, non-recognised, nucleotides (5'GGCCNNNNNGGCC3'), and produces cohesive termini. The two *Sfi*I sites in pAK200 were designed with different cohesive termini, therefore allowing directional cloning of fragments into the phagemid. In addition, the different 3bp overhangs derived from the two *Sfi*I sites render it impossible for self dimerization to occur with either the insert or vector sequence. Finally, *Sfi*I is known to

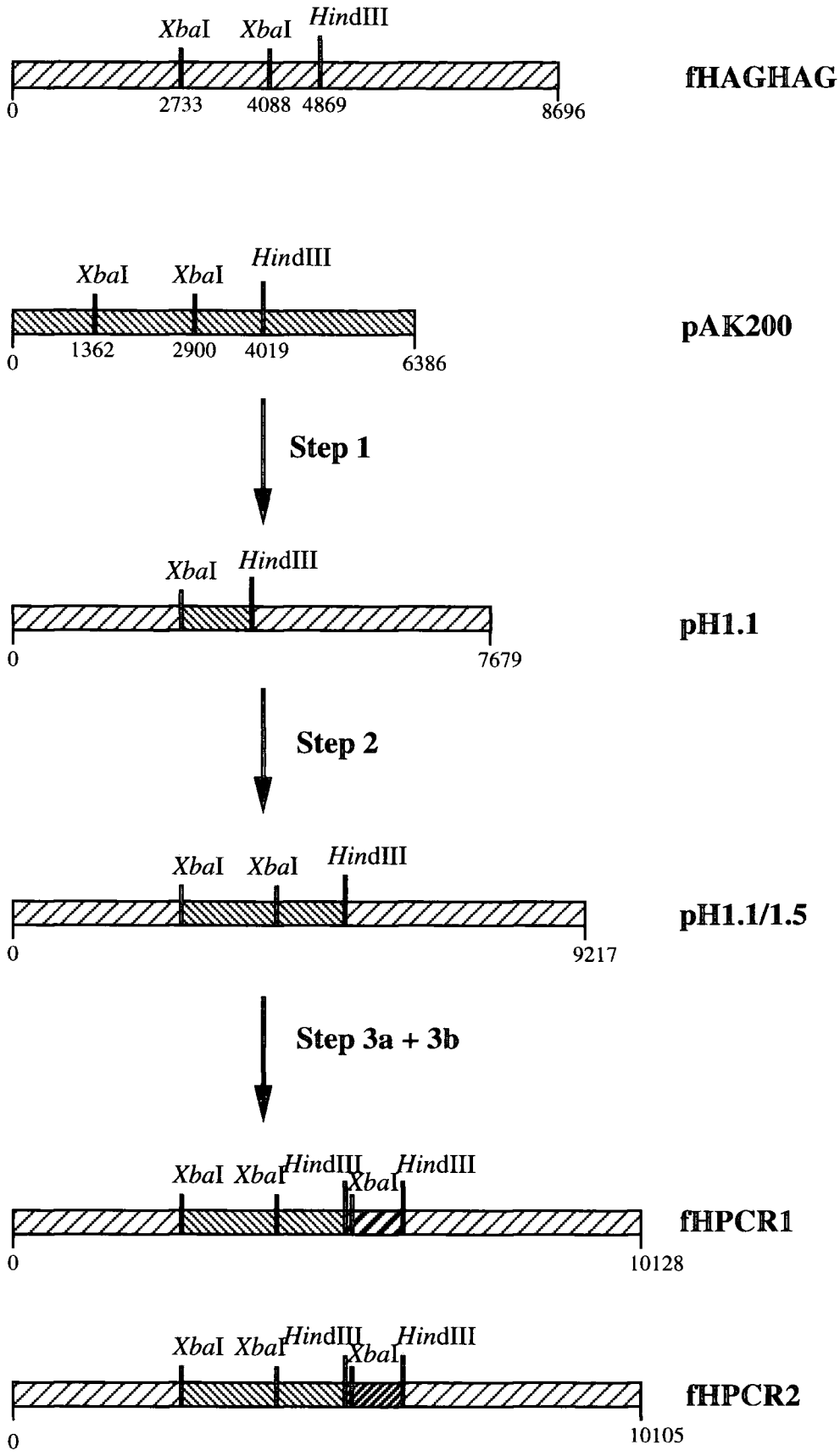

Fig. 5.2.1 Diagram outlining the steps involved in construction of the SIPs fHPCR1 and fHPCR2. (See text for further explanation.)

always cut two sites at once, therefore single cuts will not occur. Hence digestion of pH1.1/1.5 with *Sfi*I will remove the Tet resistance cassette, and permit cloning of specific *Sfi*I fragments, in a known orientation, into the phage sequence.

5.2.2 Reintroduction of the N-terminal Domain of Gene III from fHAGHAG into pH1.1/1.5.

The N-terminal domain of gene III for the SIP was derived, by PCR, from fHAGHAG. Two different constructs were created, fHPCR1 and fHPCR2. The construct fHPCR1 retained the six H residues required for recognition by the antibody used in fHAGHAG. Reintroduction of the antibody into fHPCR1 should therefore act as a positive control, and confirm that the manipulations carried out had not adversely affected phage function.

Step 3a - Construction of fHPCR1 - Primers were designed to amplify the *lac* promoter/operator sequence and the N-terminal of gene III, with the six attached H residues. The precise sequence for each primer is given below:

SIP3: **5'** *AATCAATCAAGCTT*GATATTAATGTGAGTTAGCTCACTC **3'**

3951

SIP4: **5'** GCTTGCTTTCGAGGTGAATTTCTCG **3'**

4899

Fig. 5.2.2.1 Primers used to amplify the N-terminal domain of gene III, plus the six H residues, from fHAGHAG.

Italicised bases are random additions, numbers beneath the primers indicate the position of the 5' terminus in fHAGHAG. The underlined sequence in SIP3 shows the introduction of a new *Hin*dIII site (AAGCTT).

Amplifications were carried out, using fHAGHAG as the template, according to the protocol given overleaf.

94°C	5mins	
94°C	1min	)
69°C	1min	) x30
72°C	1min 30secs	)
72°C	5mins	

As expected, a product of approximately 1.2kb was amplified. The fragment was therefore gel isolated and named PCR1. The product of SIP3/SIP4 (PCR1), contained two *Hin*dIII sites; a new site introduced at the 5' end of the fragment and a second site, from the fHAGHAG sequence, 30bp in from the 3' end of the product.

The PCR fragment would not cut directly with *Hin*dIII. It was therefore blunt-ended, ligated into *Sma*I cut SK+ and then re-isolated, by digestion with *Hin*dIII. Since the multiple cloning site of SK+ also contains a *Hin*dIII site, which may have cut in preference to one of the *Hin*dIII sites of the PCR fragment, the *Hin*dIII cut fragment was first ligated into similarly cut SK+. It was then sequenced, in both the forward and reverse directions, to check no additional sequence (from SK+) had been incorporated into the PCR fragment. Sequencing confirmed the DNA at the ends of PCR1 to be from fHAGHAG alone, and also verified that the PCR amplification had not introduced any mutations into the sequence. It was therefore isolated by digestion with *Hin*dIII and ligated into similarly cut pH1.1/1.5.

To identify positive transformants, a colony blot was carried out and probed with the PCR1 fragment. The blot also contained two positive controls (fHAGHAG and SK+/PCR1) and two negative controls (pH1.1/1.5 and DH5α - the *E.coli* strain used in the transformations). The result of the hybridisation can be seen in **Fig. 5.2.2.2**.

Positive colonies were restreaked on fresh 2xYTCmTet plates. Correct orientation of the PCR1 fragment was confirmed by digesting with *Xba*I. The inserted fragment contains an *Xba*I site approximately 130bp from the 5' end. Positive colonies therefore gave a 1.2kb fragment, whereas those with the incorrect orientation instead gave a 1.9kb fragment. Colony A1 was found to contain PCR1 in the correct orientation. The construct from A1 was therefore named fHPCR1 and used in subsequent work.

Step 3b - Construction of fHPCR2 - Primer SIP3 (used in construction of PCR1) was used for amplification of the second PCR fragment, along with a new primer, SIP5.

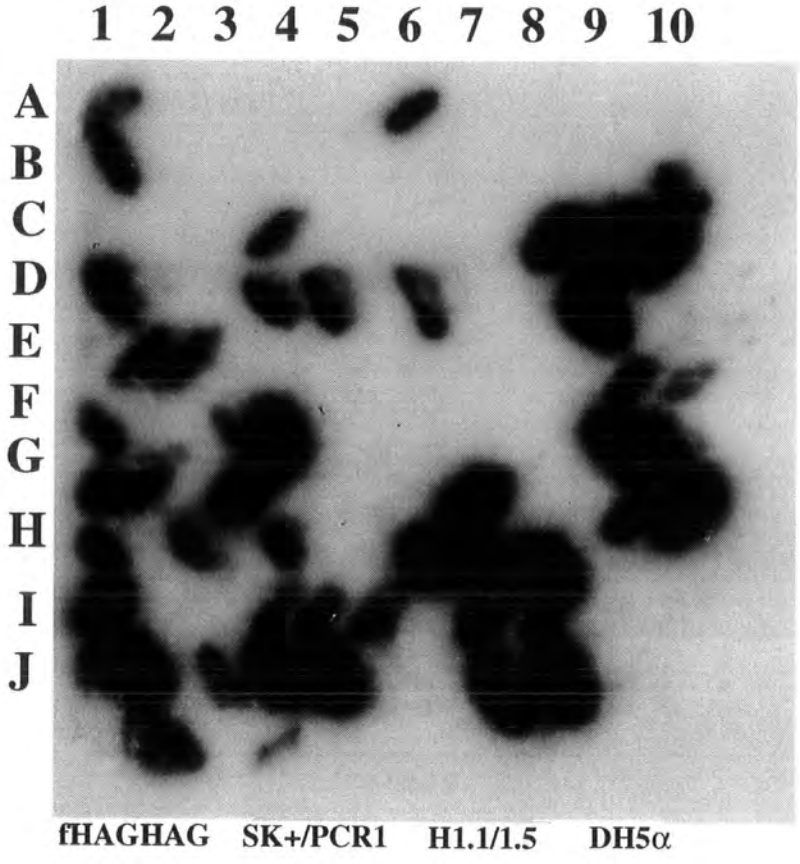

Fig. 5.2.2.2 Colony blot of possible positive transformants, probed with PCR1.

SIP5 was designed to amplify the N-terminal of gene III from fHAGHAG, without the attached H residues. The sequence of SIP5 is given in **Fig. 5.2.2.3**:

SIP5:

5' *AGTTATTT*<u>*AAGCTTGCGGCCGC*</u>AGGGAAGCGCGTAGTCTGGAACGTCGTAC
4845

GGG **3'**

Fig. 5.2.2.3 Primer used to amplify the N-terminal domain of gene III from fHAGHAG.

Italicised bases are additional to the fHAGHAG sequence, the figure beneath the primer indicates the position of the 5' terminus in fHAGHAG. The underlined bases show the introduction of two new restriction sites at the 3' end of the PCR product; *Hin*dIII (AAGCTT) and *Not*I (GCGGCCGC) sites.

Amplifications were carried out, using fHAGHAG as the template, according to the protocol used for amplification of PCR1. As expected, a fragment of approximately 1kb was amplified. The fragment was therefore gel isolated, and named PCR2. The SIP3/SIP5 PCR product (PCR2) contained two introduced *Hin*dIII sites, one at either end of the product, and an introduced *Not*I site at the 3' end.

As before, the PCR product was ligated into SK+ and the sequence confirmed, prior to ligation into pH1.1/1.5. In a similar manner to PCR1, PCR2 was incorporated into pH1.1/1.5 at the unique *Hin*dIII site. Positive transformants were checked by colony blotting and probing with PCR2, pH1.1/1.5 was used as the negative control and fHAGHAG was used as the positive control. The result of the hybridisation can be seen in **Fig. 5.2.2.4**.

Positive colonies were restreaked on fresh 2xYTCmTet plates. Correct orientation of the PCR product was, once again, checked by digestion with *Xba*I. Correct colonies gave a 1.2kb fragment, and those with the incorrect orientation instead gave a 1.8kb fragment. Colony A5 was found to contain PCR2 in the correct orientation. The construct from A5 was therefore named fHPCR2, and used in subsequent work.

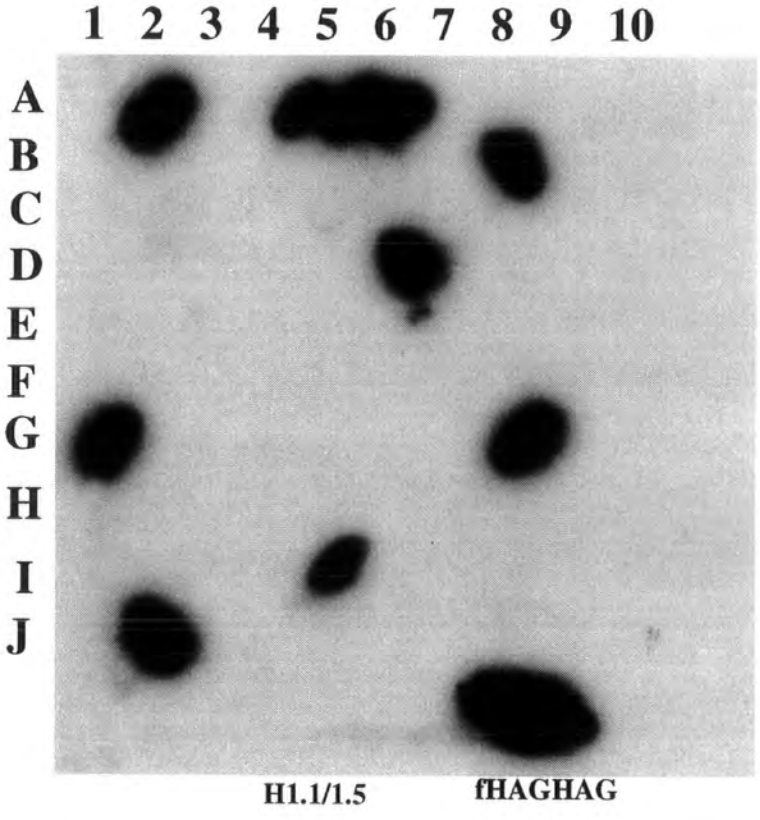

Fig. 5.2.2.4 Colony blot of possible positive transformants, probed with PCR2.

5.3 Construction of a Vector for Convenient Insertion of Fragments into the SIP fHPCR2.

fHPCR2 contains a unique *Not*I site, positioned adjacent to the N-terminal domain of gene III. This site was engineered into the SIP to allow easy and reliable introduction of sequences into the N-terminal domain of gene III. It was decided to construct a simple cloning vector that would allow a variety of restriction fragments to ultimately be cloned into the *Not*I site of fHPCR2.

Two complimentary oligonucleotides, containing primarily a *Hin*cII site and a *Bam*HI site, flanked by *Not*I sites, were designed (see **Fig 5.3**). These restriction sites would later permit two different cloning strategies to be employed. It was hoped to introduce an *A. tumefaciens* genomic library into the N-terminal domain of pIII. This could be achieved by shearing genomic DNA, therefore giving blunt ends, and ligating the fragments into the *Hin*cII site, or digesting genomic DNA with a frequent cutter e.g. *Sau*3AI, and ligating the fragments into the compatible *Bam*HI site. It should then be possible to use the *Not*I sites to isolate and ligate the fragments of genomic DNA, into the SIP construct fHPCR2. The restrction enzyme *Not*I was chosen for this purpose, as it is an infrequent cutter and therefore unlikely to cut in the insert sequence.

SIPA1:

5' ATC**GAATTC**GCGGCCGC**GTCGAC**GGATCCTAATAGTGAGCGGCCGC

*Eco*RI *Not*I *Hin*cII *Bam*HI *Not*I

AAGCTTATTCA **3'**

*Hin*dIII

SIPA2:

5' TGAAT**AAGCTT**GCGGCCGCTCACTATTAGGATCC**GTCGAC**GCGGCCG

*Hin*dIII *Not*I *Bam*HI *Hin*cII *Not*I

CGAATTCGAT **3'**

*Eco*RI

Fig. 5.3 Oligonucleotides used to create a new multiple cloning site, for use in introducing fragments into the SIP fHPCR2.

The restriction sites within each oligonucleotide are either shown in bold type or underlined, and are named at the 5' end of each site.

A 50µl solution, containing the two oligonucleotides, each at a final concentration of 20pmol/µl, was heated at 94°C for 5 minutes. It was then allowed to gradually cool down to room temperature, allowing the oligonucleotides to anneal to one another. The resulting fragment was digested with *Eco*RI and *Hin*dIII, and ligated into similarly cut pUC18, creating a new multiple cloning site in the vector.

Correct construction of the new vector (pUC18SIP) was confirmed by digesting with each of the enzymes in the new multiple cloning site. In addition, the sites were verified by sequencing.

5.4 Testing of the SIP Constructs.

Two SIP constructs were created, fHPCR1 and fHPCR2 (see **Fig. 5.4**), which differed only in the N-terminal region of gene III. Correct construction of the SIPs was confirmed by specific restriction digests and partial sequencing.

fHPCR1 contained six H residues attached to the N-terminal domain of gene III. It was constructed to act as a positive control of the signal sequence within the new hybrid phage construct, by reintroduction of the antibody gene from fHAGHAG. The antibody gene contained in fHAGHAG had also been subcloned into the phagemid pAK100, creating the phagemid pAK100Ab (pAK100 is essentially the same as pAK200 - see Krebber *et al* [107], originally created as an expression vector for use in phage display studies). The antibody gene had been ligated into pAK100 using the *Sfi*I sites (shown for pAK200, in **Fig. 5.1**). It was therefore possible to easily isolate the fragment from the pAK100Ab construct.

pAK100Ab and fHPCR1 were both digested with *Sfi*I. The large fHPCR1 fragment and the approximately 800bp antibody fragment were gel isolated, and the two fragments ligated together. Due to the formation of the *Sfi*I site, it was only possible for the antibody fragment to ligate into fHPCR1 in the correct orientation. Correct introduction of the fragment was confirmed by digesting possible positive colonies with *Sfi*I. The correct construct fHPCR1Ab was therefore identified.

Phage particles were isolated, and their infectivity checked, as described in section **2.15**. As a positive control, identical procedures were also carried out on fHAGHAG. Testing showed that fHAGHAG and fHPCR1Ab had equivalent levels of infectivity. This

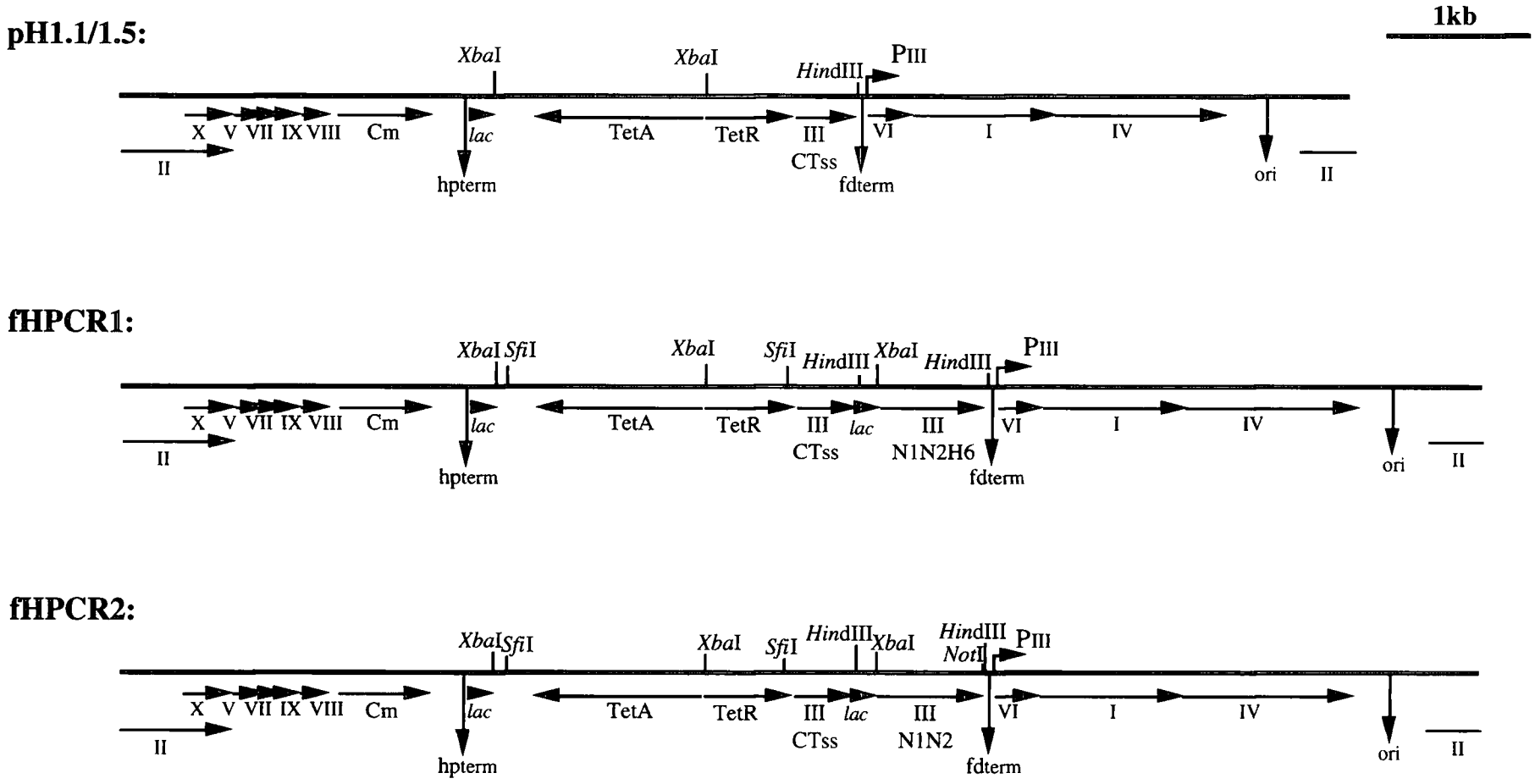

Fig. 5.4 Maps of pH1.1/1.5, fHPCR1 and fHPCR2, showing the location of the phage genes, and the position of relevant restriction sites. Cm = Chloramphenicol resistance, hpterm = hairpin terminator, *lac* = *lac* promoter/operator, TetA/TetR = Tetracycline resistance, IIICTss = supershort C-terminal of gene III (amino acids 250-406 of pIII), fdterm = terminator of fd, PIII = gene III promoter, ori = origin of replication, IIIN1N2H6 = N-terminal of gene III plus six H residues, IIIN1N2 = N-terminal of gene III.

was indicated by their cfu (colony forming unit) count, following phage isolation, and subsequent infection of XL1-Blue cells. Initial results therefore indicated that manipulation of the gene III domains had not adversely affected the overall functioning of the phage particles produced.

To test that the infectivity seen was due to interacting partners on the pIII domains, similar experiments were carried out using the two SIP constructs, fHPCR1 and fHPCR2, which should act as negative controls. It was found that the two SIP constructs produced a cfu count indistinguishable from that seen for fHAGHAG and fHPCR1Ab. The reason for this high level of infectivity, without interacting partners being attached to the two pIII domains, is unknown. The obvious answer would be that the phage preparations had, in some way, been contaminated with a wild type version of pIII, hence facilitating the production of infective phage particles. However, there could also be other explanations. It could be that expression from the *lac* promoters produced enough of the two pIII domains to allow reconstitution of wild type pIII, by a rudimentary interaction between the two regions, or alternatively a fusion could have occurred between the transcribed Tet region and the C-terminal, which then enabled interaction with the N-terminal domain. An alternative possibility would be that only one of the domains was sufficient to restore infectivity. However, extensive studies have shown that both domains are required for infectivity, this possibility can therefore be disregarded. A third possibility is that rearrangement of the gene III domains may have occurred in the SIP construct, hence reforming the wild type version of pIII. This was seen in the construction stages of the SIP fHAGHAG, however removal of the glycine rich linker regions, positioned between the domains, eliminated this problem. A further possibility is that some anomaly in the testing methodology allowed infective phage to be produced, however the methods used followed those given in a number of papers on SIP technology. In addition it seemed unlikely that it would be possible to "inadvertently" produce infective phage. At this stage therefore it was unclear how infective phage were being produced. The most obvious answer however was that cross-contamination of the non-infective phage DNA, with that from fHAGHAG, had occurred. Hence resulting in the production of infective phage particles when each construct was tested.

To test the theory that cross-contamination was the cause of the unusual results, it was decided to test the infectivity of the intermediate construct pH1.1/1.5. This construct only contained the C-terminal domain of gene III (see **Fig. 5.4**), under the control of a lac

promoter. It was therefore expected to produce non-infective phage particles, since extensive studies have previously shown that both domains of pIII are required for infectivity. It was found that pH1.1/1.5 also gave a cfu count similar to that for fHAGHAG. This therefore confirmed that the most likely reason for the unexpected results, was contamination of the phage preparations. The consequences of this will be discussed in more detail in section **5.5**.

5.5 Discussion.

The work described in this chapter details the preliminary work carried out in an attempt to study protein interactions within the *A. tumefaciens* chemosensory network. Due to the time constraints limiting the scope of the work possible in this section, it was decided to pursue the idea of using a SIP system to study biomolecular interactions. This constituted an easily accessible, straightforward, and yet novel way of studying such interactions.

A pre-existing, tested, SIP system was used as a template for creating a new SIP system, modified for the specific requirements of this work. It was hoped to design a system that could be used to investigate interactions between known proteins, but that should also allow identification of interacting proteins from a genomic library. The specific manipulations carried out to the existing SIP, altered the regions flanking the gene III domains. It was hoped that this would ultimately allow genes to be incorporated in-frame to either termini.

Two versions of the final SIP were created. Version 1 (fHPCR1) maintained the six H residues linked to the N-terminal of pIII. Version 2 (fHPCR2) did not have the six H residues, but had an introduced *Not*I site at the N-terminal domain. Introduction of the original antibody (from fHAGHAG) into fHPCR1 confirmed that the manipulations had not adversely affected the functioning of the phage, since infective phage particles were formed. However, further analysis seemed to suggest that a problem existed with the SIP constructs, since infective phage particles were produced without there being interacting partners connected to the two pIII domains, and indeed without both domains of pIII.

Although the work had to be halted at this stage, due to time constraints, there remains a great deal of scope for this work. Obviously the first item to be addressed would

be the seemingly non-selective production of infective phage particles. As stated previously, the most obvious explanation for this phenomenon is that a wild-type version of pIII was contaminating the experiments. For this to be true the phage preparations must have been contaminated with fHAGHAG (or possibly fHPCR1Ab), as this represents the only source of "wild type" pIII used in this work. Determining where the contamination occurred should aid in eliminating the problem. If contaminating DNA was present when expression of the pIII domains was induced with IPTG, then several forms of pIII would be produced. The different pIII domains would then be packaged into phage particles. Only those phage bearing the interacting domains from fHAGHAG, would subsequently be infective. However, the DNA packaged in the infective phage would either be that from the tested construct, or the contaminating DNA. Isolation and digestion of the phage DNA, from a sample of the colonies produced in the infectivity tests, should confirm this. It is also possible that the contamination occurred in the final step of testing, and hence was due to contaminating phage particles, rather than phage DNA. If this is true all of the resultant colonies would contain the contaminant DNA, rather than that of the tested construct. Isolation and digestion of the phage DNA, from the colonies produced in the infectivity tests, would again confirm if this had happened. Hence studying the phage particles, maintained within the colonies produced in the various infectivity tests, should give an indication of whether contamination had occurred, and if so at which step in the procedures it occurred.

The most likely cause of the contamination would be carry-over in the pipettes used. Although sterile technique was used throughout the procedures, there remains the possibility that contamination of the pipettes could have occurred, e.g. by passage of DNA, through the tip used, into the pipette barrel. Problems with carry-over contamination should be easily rectified by thoroughly cleaning and sterilising the pipettes used, and using filtered pipette tips in future work. Further testing of the SIPs could then be carried out. In addition to repeating the tests already performed, the antibody (from fHAGHAG) could be introduced into fHPCR2. If the constructs are correct, the resulting phage should not be infective, since fHPCR2 does not contain the six H motif recognised by the antibody.

Since DNA analysis suggested that the SIPs were correctly constructed, if repetition of the testing produced the expected results, they could be further checked by incorporating specific interacting, or non-interacting, proteins into the two pIII domains, and confirming subsequent infectivity / non-infectivity, as appropriate. This would then provide enough

evidence to confirm the correct functioning of the SIPs. Hence fHPCR2 could then be used, as planned, to study specific protein interactions within the chemosensory network. The results obtained could then be verified using more "established" techniques e.g. the yeast two-hybrid system, or traditional biochemical methods, such as affinity selection.

Although some problems were encountered in the latter stages of this work, and the study was prematurely curtailed by time constraints, the principle described still remains a viable option for studying protein interactions. If successfully constructed, the system represents a simple, yet highly sensitive method of investigating such interactions, which would provide rapid, reproducible results, and allow easy access to the relevant interacting domains.

6 Other Chemotaxis-Related Genes in *A. tumefaciens*.

6.1 *cheW.*

Sequencing of the *che* cluster, found in the cosmid pDUB1911, failed to identify a homologue of the chemotaxis gene *cheW* in *A. tumefaciens*. Similar chemosensory regions, in the related bacteria *S. meliloti* and *R. sphaeroides,* contain homologues of *cheW* [9]. Due to the presence of *cheW* in other bacterial species from the α-subgroup of proteobacteria, it was postulated that *A. tumefaciens* may also contain a homologue of *cheW.*

To try and identify a possible homologue, a heterologous probe was made from the *S. meliloti* plasmid pRmelW. The plasmid pRmelW consists of a 1.85kb *Xho*I fragment from the *S. meliloti che* operon (Accession no. U13166; bases 5560-7410), cloned into the vector pIC20R. A 0.45kb *Pst*I-*Sac*I fragment, which contains only *cheW* sequence, was isolated from the plasmid and radioactively labelled.

Initially the cosmids pDUB1900, pBUB1905 and pDUB1911 were hybridised with the *cheW* probe. No hybridising bands were seen. Therefore there did not appear to be a *cheW* homologue located close to any of the chemotaxis, flagellar or motility-related genes previously identified.

The *S. meliloti cheW* probe was then hybridised with Southern blots containing *A. tumefaciens* genomic DNA. Probing of several genomic blots identified faint, but definite, hybridising bands, indicating that a homologue of *cheW* existed in *A. tumefaciens.* It was decided to design primers that might amplify part of this homologue. Pile-up alignment of known CheW sequences (*S. meliloti, R. sphaeroides* & *E. coli*) identified regions of the protein that showed a high degree of conservation between all the species studied:

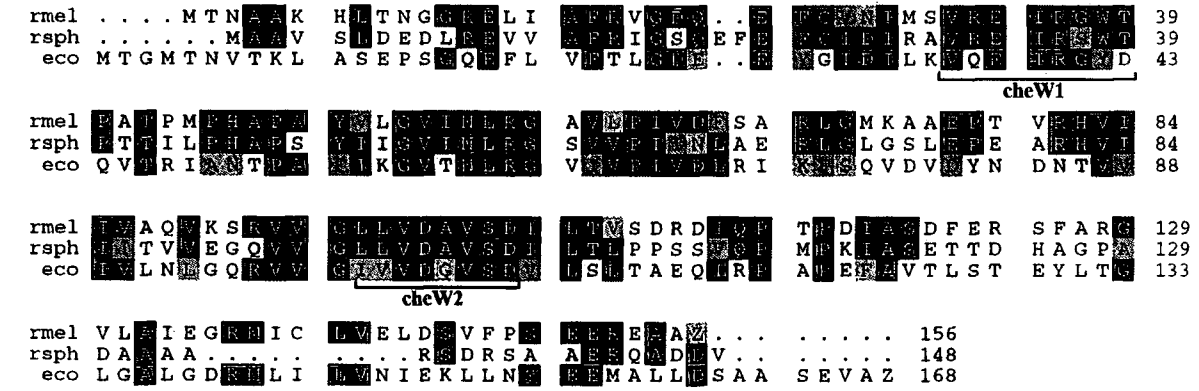

Fig. 6.1.1 Prettybox display, of a pileup alignment, of CheW from *S. meliloti*, *R. sphaeroides* and *E. coli.*

The sections underlined indicate the "conserved" regions used for primer design.

Primers were therefore designed from the identified regions, using the *S. meliloti cheW* sequence :

cheW1: 5' GTG CGA GAA ATT CGC GGA TG 3'
6490

cheW2: 5' AAT GTC GGA AAC GGC GTC GA 3'
6708

Fig. 6.1.2 Primers used to amplify *cheW* from *A. tumefaciens*.
Figures below each primer indicate the position of the 5' terminus in the *S. meliloti che* operon sequence (Accession no. U13166).

Amplifications were carried out on *A. tumefaciens* and *S. meliloti* genomic DNA, according to the following PCR protocol:

94°C 5 mins

94°C 1 min)
57°C 1 min) x30
72°C 1 min)

72°C 5 mins

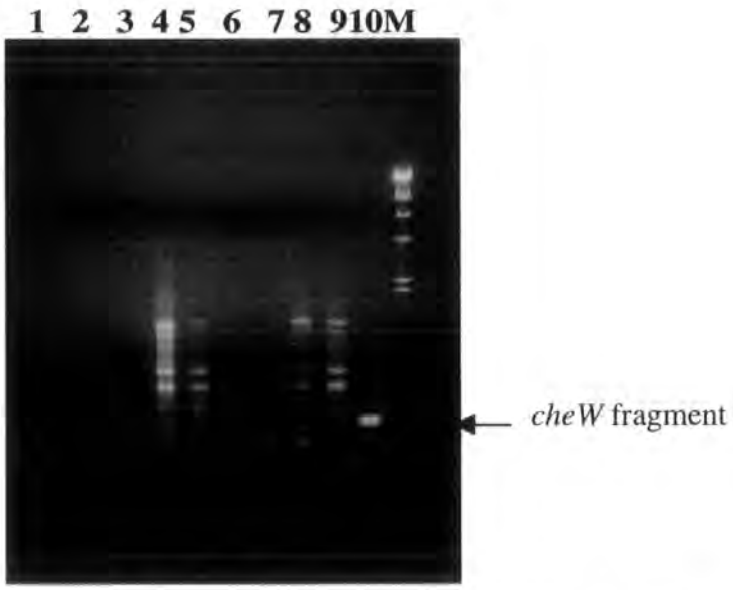

Fig. 6.1.3 PCR amplifications of *A. tumefaciens* genomic DNA using the primers cheW1 and cheW2.
1 = PCR blank, **2 – 5** = *A. tumefaciens* DNA, using 1mM - 4mM Mg^{2+}, **6 – 9** = repeat of lanes **2 – 5**, **10** = *S. meliloti* DNA, **M** = λ / *Hin*dIII.

The *S. meliloti* DNA acted as a positive control and produced a band of approximately 200bp, which was in accordance with the known product size of 216bp. As can be seen in **Fig. 6.1.3**, several non-specific bands were produced with the *A. tumefaciens* DNA. It was thought that this may have been because the primers and conditions used were too precise for the *S. meliloti* DNA and hence not specific enough for the *A. tumefaciens* sequence. The amplifications were repeated using a lower annealing temperature (50°C) to try and increase the specificity for the *A. tumefaciens* DNA, however again a large number of non-specific bands were produced. The amplifications were therefore repeated using the Hot-Start method (see section **2.5.7.1**), to try and increase the specificity of the reactions:

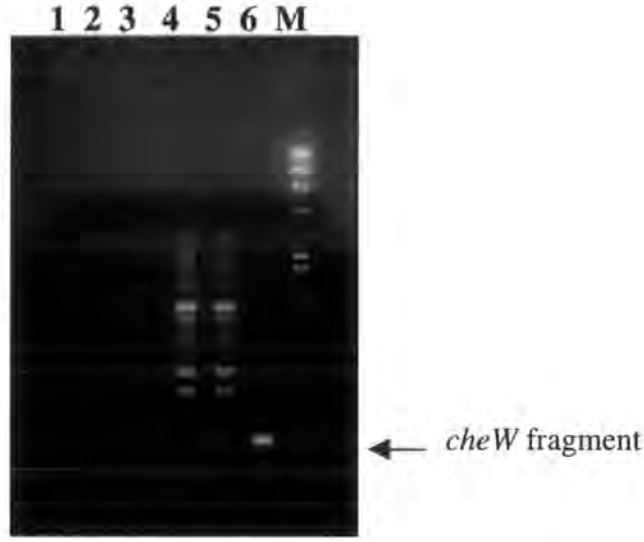

Fig 6.1.4 Hot-Start PCR amplifications of *A. tumefaciens* genomic DNA using the primers cheW1 and cheW2.
1 = PCR blank, **2 – 5** = *A. tumefaciens* DNA, using 1mM - 4mM Mg^{2+}, **6** = *S. meliloti* DNA, **M** = λ / *Hin*dIII.

Amplification using the Hot-Start method still resulted in the formation of several non-specific bands, however a faint band of a size equivalent to the positive control was also seen. Since the band produced was very faint, in order to increase the amount of product, a Band Stab PCR (see section **2.5.7.2**) was carried out from the band. (The band stab amplifications were carried out following the original PCR protocol.)

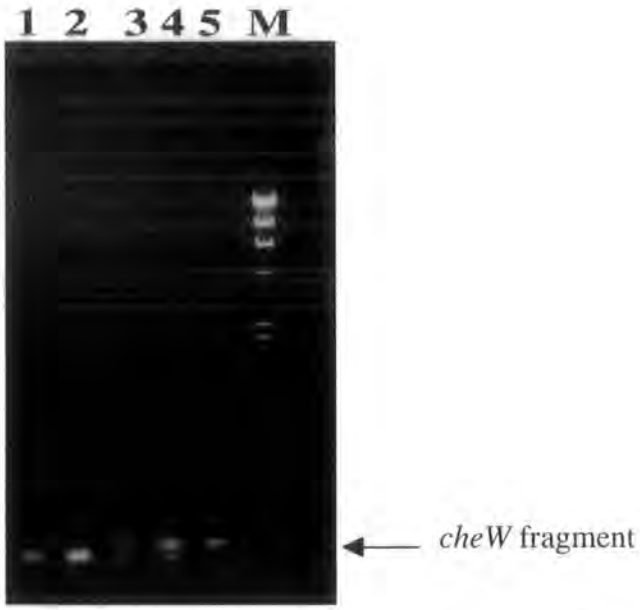

Fig. 6.1.5 Band Stab PCR amplifications of *A. tumefaciens* genomic DNA using the primers cheW1 and cheW2.
1 – 4 = Band Stab, using 1mM - 4mM Mg^{2+}, **5** = *S. meliloti* DNA, **M** = λ / *Hin*dIII.

At the highest Mg^{2+} concentration (lane **4**, **Fig. 6.1.5**) the band stab amplification produced a band approximately the same size as the *S. meliloti cheW* fragment, the fragment was therefore isolated, subcloned and sequenced.

DNA sequencing showed the *A. tumefaciens* fragment to be shorter than the *S. meliloti cheW* fragment (172bp compared to 216bp). At the amino acid level the *A. tumefaciens* sequence showed 49% similarity and 28% identity with CheW from *S. meliloti*. This level of homology is markedly lower than that seen between the other Che proteins of *A. tumefaciens* and *S. meliloti*. However, if in *A. tumefaciens cheW* does exist outside the main *che* region, it could have diverged quite substantially from *cheW* in *S. meliloti*, and therefore show this marked difference.

The fragment was radioactively labelled and used to probe a Southern blot containing *A. tumefaciens* and *S. meliloti* genomic DNA. A second copy of the blot was probed with the original *S. meliloti cheW* probe. Since only a low level of homology was seen between the putative *A. tumefaciens cheW* sequence, and that of *cheW* from *S. meliloti*, less stringent washes were used in the hybridisation procedure than were used previously i.e. washes were carried out at room temperature, rather than at 65°C.

As can be seen in **Fig. 6.1.6** and **Fig. 6.1.7** definite bands were seen in the genomic lanes hybridised with the corresponding (homologous) probe. Faint bands could also be

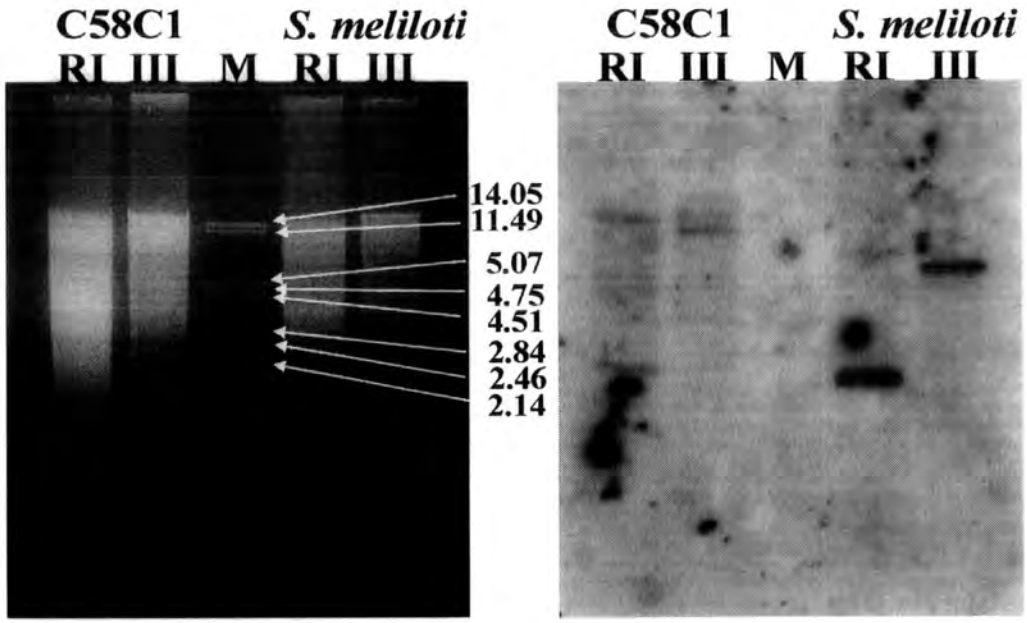

Fig. 6.1.6 0.7% agarose gel and subsequent Southern blot, showing the bands hybridising with the *S. meliloti cheW* probe.
RI = *Eco*RI, **III** = *Hin*dIII, **M** = λ / *Pst*I.

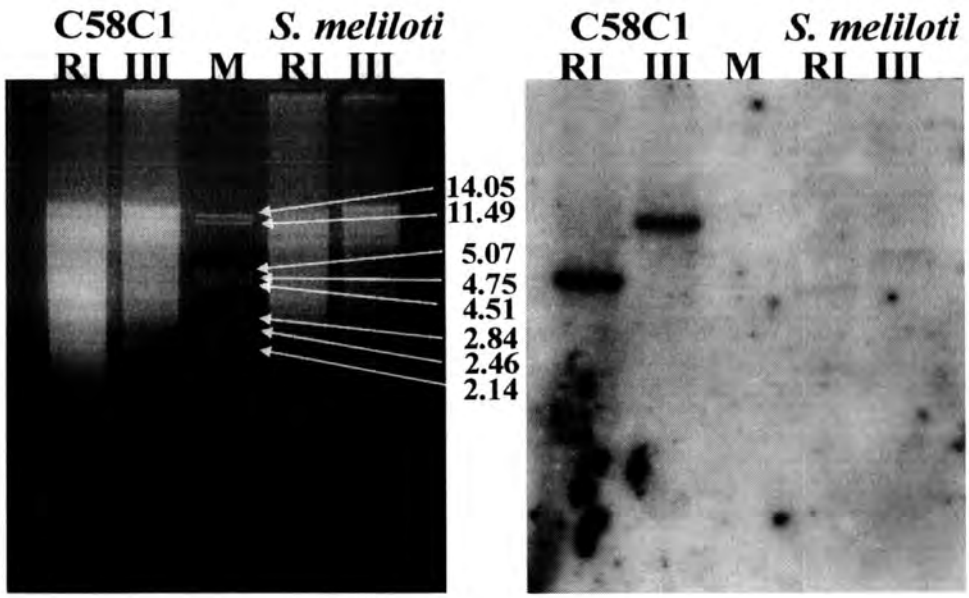

Fig. 6.1.7 0.7% agarose gel and subsequent Southern blot, showing the bands hybridising with the *A. tumefaciens* "*cheW*" PCR probe.
RI = *Eco*RI, **III** = *Hin*dIII, **M** = λ / *Pst*I.

seen when the opposite (heterologous) probe was used i.e. hybridising bands in the *A. tumefaciens* lanes when probed with the *S. meliloti* probe, and vice versa. A subset of the bands seen in both the *A. tumefaciens* and *S. meliloti* lanes, using the heterologous probes, appeared to correspond with the bands hybridising with the homologous probes.

	C58C1	***S. meliloti***
***Eco*RI**	4.6kb*	1.7kb
***Hin*dIII**	9.6kb*	5.8kb*

Table 6.1 Sizes of the C58C1 and *S. meliloti* genomic bands showing hybridisation with the homologous *cheW* probes.

Figures marked by a *, indicate those bands which also hybridised with the heterologous probes.

Evidence from the data collected to date, therefore suggests that *A. tumefaciens* does possess a homologue of the chemotaxis gene *cheW*, but that it is located distally to the other *che* genes identified. Unlike the other *che* genes, it appears to have diverged substantially from its homologue in *S. meliloti*.

6.2 Is There a Second Chemotaxis Cluster in *A. tumefaciens*?

Identification of a possible *cheW* homologue, presumably located in a region of the chromosome disparate to the other *che* genes thus far identified, implied that there could be a second *che* cluster in *A. tumefaciens* (as is true for the related bacterium *R. sphaeroides* [81]).

In order to begin investigations in to this possibility, the *che* deletion blot (**Fig. 4.4.2.4**) was hybridised with a probe containing *cheA/Y1*, identified in this work. The *cheA/Y1* probe was made by digesting the plasmid SK+/cheA (created during construction of the *cheA* in-frame deletion plasmid - see **Fig. 4.2.2.1**) with *Eco*RV and isolating the 2.7kb fragment produced.

Fig. 6.2 shows the results of the hybridisation. It can be seen that there were no hybridising bands in the lane containing the *che* deletion strain (**Fig 6.2**, track 1).

Obviously this initial hybridisation work can not, in any way, disprove the existence

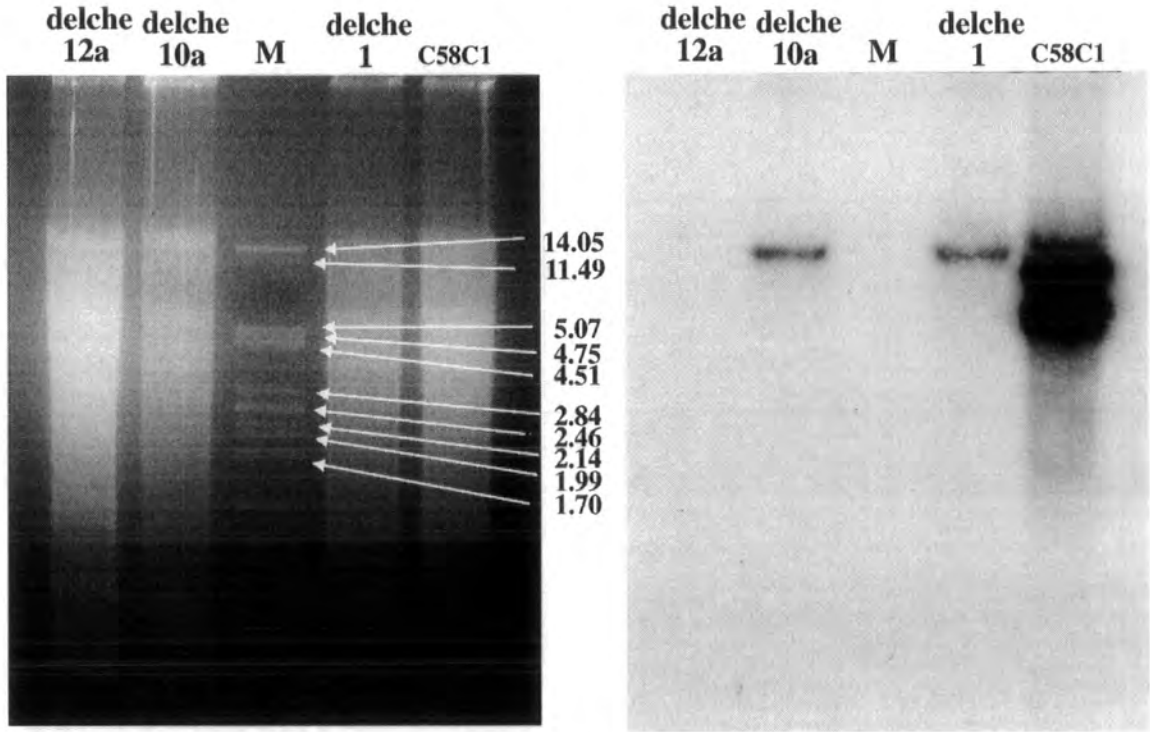

Fig. 6.2 0.7% agarose gel and subsequent Southern blot, showing the bands hybridising with the *cheA/Y1* probe.

delche12a = *che* deletion strain, **delche10a** = incorrect *che* deletion strain, **delche1** = integrated intermediate *che* deletion strain, **C58C1** = wild type strain, **M** = λ / *Pst*I.

of a second *che* cluster in *A. tumefaciens*. What can be concluded is that there does not appear to be any other, close, homologues of the chemotaxis genes *cheA* and *cheY1* in *A. tumefaciens*. However, it could be that further homologues of these genes do exist, but that they are sufficiently diverged from those previously identified so as not to be detected. Indeed, the levels of identity seen between the *R. sphaeroides* multiple homologues were between, approximately, 25% and 50%, depending on the specific genes studied [81]. CheA$_{II}$ from *R. sphaeroides* showed only 36% identity with its counterpart CheA. If this is set against the level of homology seen between the *S. meliloti* Che proteins and those identified in this work (see **Table 3**), it can be seen to be considerably lower. **Fig. 3.1.2** shows the degree of hybridisation seen between the *S. meliloti cheA* probe and *A. tumefaciens* genomic DNA. Even with the very high level of homology, subsequently shown to exist between the *S. meliloti* and *A. tumefaciens cheA* genes, the bands seen in **Fig 3.1.2** are not particularly strong. In addition, it should be noted that the *Hin*dIII and *Eco*RI bands seen in **Fig. 3.1.2** represent binding of the probe to two distinct fragments for both of the digests. Hence, if a second *che* region existed in *A. tumefaciens* which only showed a relatively low level of homology to the genes identified in this work, and which only spanned one *Eco*RI fragment, it would be very unlikely that it would be detected using the *cheA/Y1* probe used above. Whether or not *A. tumefaciens* contains a second *che* cluster therefore remains unresolved and requiring further investigation (see section **6.4**).

6.3 MCPs in *A. tumefaciens*.

Previous evidence (see section **1.8**), plus the identification of homologues of the chemotaxis genes *cheB*, *cheR* and *cheD* in this work, suggested that *A. tumefaciens* may possess MCP-like proteins.

In the preliminary stages of this work, sequencing data from the *che* cluster showed Orf1 to have a high level of sequence homology with several known MCPs (see section **3.5.1**). It was therefore decided to design primers that would amplify Orf1 (and most of Orf2), hence producing a preliminary "MCP" probe, for use against *A. tumefaciens* genomic DNA.

EW1 5' CGA TTT GCC ATC AGA TCA AGC 3'
1324

EW2 5' TGG TCG ATA TCG ACG CCT A 3'
3193

Fig. 6.3.1 Primers used to amplify *orf1* and *orf2* from pDUB1911.

Numbers below each primer indicate the position of the 5' terminus in the cosmid pDUB1911 (see section **3.9**).

Amplifications were carried out (using the plasmid pELW2 as the template) according to the following PCR protocol:

94°C 5 mins

94°C 1 min)
50°C 1 min) x30
72°C 2 min)

72°C 5 mins

As expected, a 1.8kb fragment was amplified. The fragment was gel isolated, radioactively labelled and used as a probe to blots containing digests of *A. tumefaciens* genomic and cosmid DNA.

The *A. tumefaciens* library cosmids pDUB1900 – 1905 gave no hybridising bands, indicating that none of the previously studied cosmids contained possible MCP-like sequence.

Hybridisation with blots containing *A. tumefaciens* genomic DNA and DNA from the cosmid pDUB1911, identified two *Eco*RI bands of approximately 8kb and 1.7kb, and two *Hin*dIII bands of approximately 4kb and 9kb. Orf1 and Orf2 from pDUB1911 were known to lie within a 4kb *Hin*dIII fragment and an approximately 8kb *Eco*RI fragment. These bands showed strongest binding of the probe; the small (1.7kb) *Eco*RI band and the large (9kb) *Hin*dIII band were much fainter in the pDUB1911 digests (see **Fig. 6.3.2**). Initial results therefore suggested that the cosmid pDUB1911 could contain another "MCP-like" protein, outside of the main *che* cluster (see **Fig. 3.3.3**, and later text).

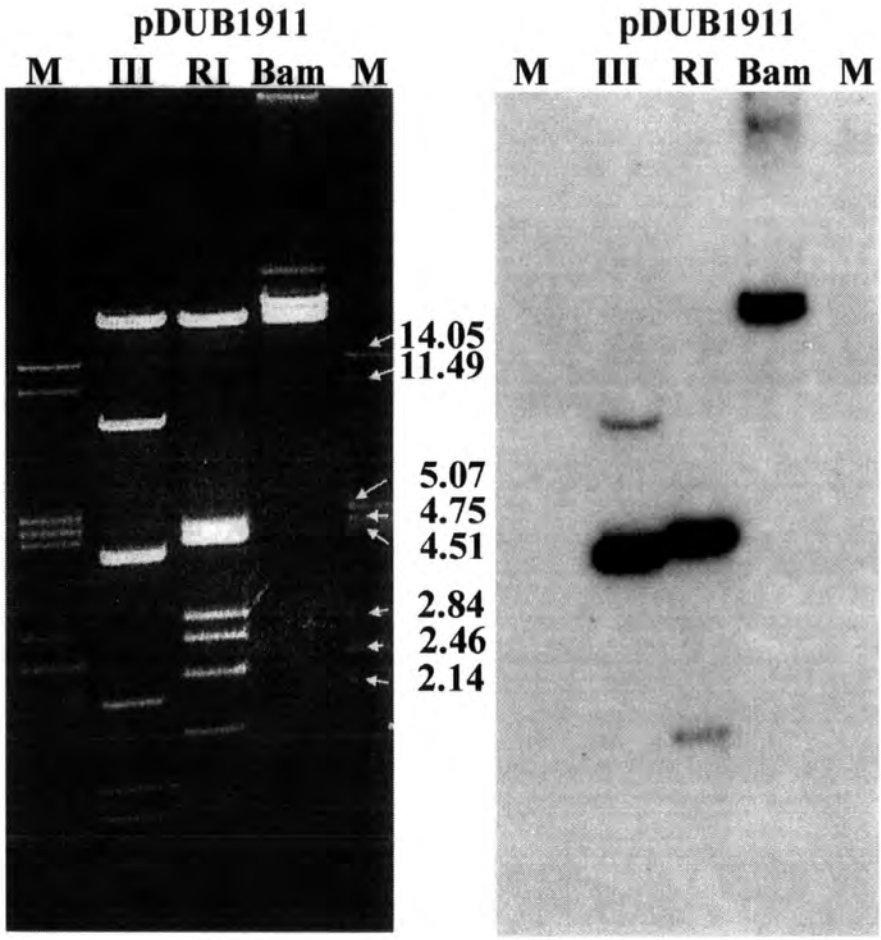

Fig. 6.3.2 0.7% agarose gel and subsequent Southern blot, showing the pDUB1911 fragments hybridising with the Orf1/Orf2 probe.
III = *Hin*dIII, **RI** = *Eco*RI, **Bam** = *Bam*HI, **M** = λ / *Pst*I.

Further sequencing of Orf1 showed that it only showed identity with the conserved signalling domain of the *E. coli* MCPs, hence effectively rendering a large majority of the 1.8kb fragment redundant in its role as an MCP probe. It was therefore decided to make an alternative, more precise MCP probe to reprobe the *A. tumefaciens* blots. The plasmid MCP3.2.7P (containing MCP3 from *R. leguminosarum* [228]) was digested with *Hin*dIII and *Pst*I, and the 0.7kb fragment (containing the first methylation domain and the highly conserved domain of MCP3) isolated and radioactively labelled. The probe was hybridised with Southern blots containing *A. tumefaciens* genomic DNA and DNA from pDUB1911.

All of the fragments in pDUB1911, identified by the first probe, showed very strong binding of the *R. leguminosarum* MCP probe. In addition, several of the lanes containing genomic DNA showed a number of hybridising bands, indicating the presence of other (approximately ten) possible MCPs elsewhere in the *A. tumefaciens* genome (see **Fig 6.3.3**).

The 1.7kb *Eco*RI fragment from pDUB1911, which hybridised to the MCP probes, was subcloned into pBluescriptSK+, forming the plasmid pELW6. Mapping of the cosmid pDUB1911 suggested that pELW6 lies some distance downstream of the identified *che* cluster (see **Fig. 3.3.3**). Preliminary sequencing of the plasmid showed that one end of the fragment contained considerable sequence homology, at both the DNA and protein level, to several known MCPs. The greatest homology seen was to the McpA homologue (Accession no. U60011) recently identified in the mannopine transport region of the *A. tumefaciens* Ti plasmid pTi15955 (63% identity and 80% similarity). The greatest homology seen to a better characterised MCP was to McpA from *C. crescentus* (38% identity and 57% similarity):

```
pELW6:     1 EFGNIARALVIFRENAIEKLAIEGKSAQERSAA--ESERHRNDAEKQELDGQIEFAVGEI 58
             E G I  AL +FR+N +    +  ++ QE+SAA    ER   +A       +    V  +
McpA :   249 ELGGIVTALKVFRDNQVHLEQL--RADQEKSAALTADERRSKEAAAAAAAQEASLVVSNL 306

pELW6:    59 ASGLGRLSRGDLSRTIETPFAGRLDRLRTDFNESLLNLRDALGQIRERTLIIQNSGIEIE 118
             A GL +L+ GDL+  +   F G   +L+ DFN ++ +L++ +  I   T  +     EI
McpA :   307 AEGLEKLASGDLTFRVTADFPGDYRKLKDDFNAAMGSLQETMKVIAASTDGLSTGADEIA 366

pELW6:   119 QSSVDLSKRTENQAASLEETAAAVEEITATVRSSAERAREQ---MSRTRHQA 167
              +S DLS+RTE QAASLEETAAA++E+TATVR +A  AR+     +S TR +A
McpA :   367 HASDDLSRRTEQQAASLEETAAALDELTATVRRTAAGARQASDVVSTTRGEA 418
```

Fig. 6.3.4 Alignment of the sequenced region of pELW6, with McpA from *C. crescentus*.

Putative methylation sites are shown in bold type.

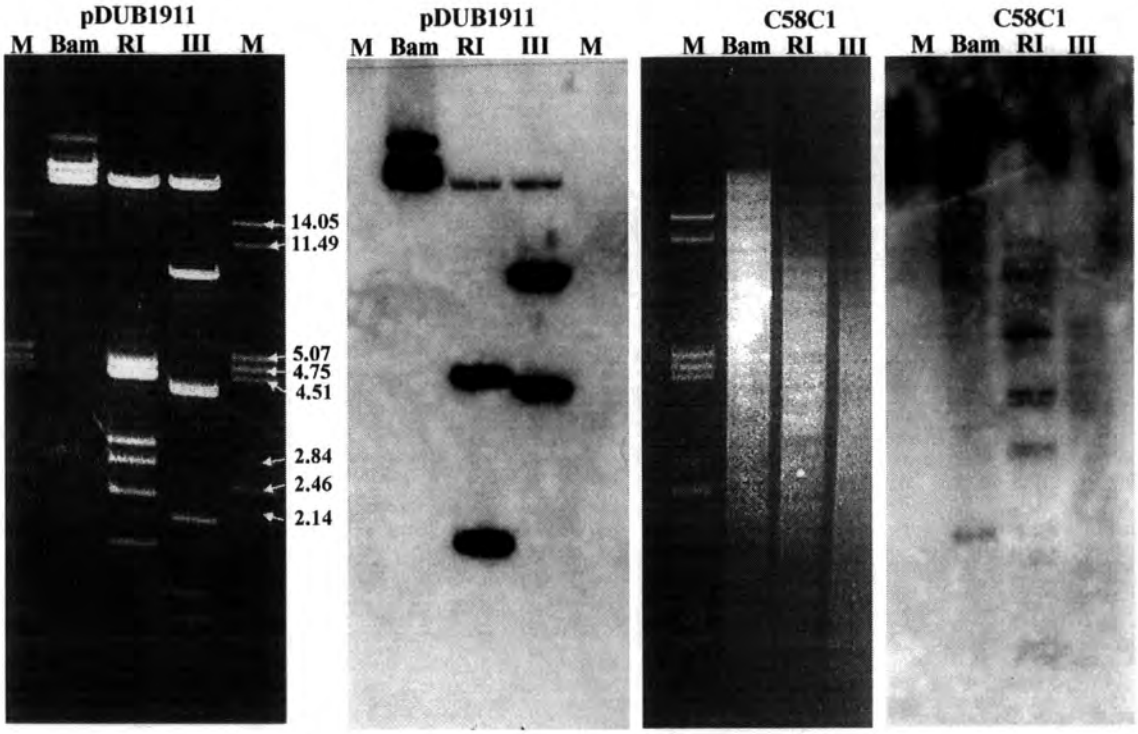

Fig. 6.3.3 0.7% agarose gel and subsequent Southern blot, showing the bands hybridising with the *R. leguminosarum* MCP probe.

Bam = *Bam*HI, **RI** = *Eco*RI, **III** = *Hin*dIII, **M** = λ / *Pst*I.

Alignment with McpA (see **Fig. 6.3.4**) showed that the putative MCP contained three possible methylation sites. Since only limited sequencing has been carried out on the plasmid pELW6, whether the putative MCP identified also contains the fourth conserved methylation site, and whether it has the transmembrane domains, indicative of the classical *E. coli* MCP, or bears greater resemblance to the cytoplasmic Tlps, requires further investigation. Pileup alignment of the sequence from pELW6, with Orf1 and Orf2 from the *che* cluster, showed that it had similarity with both proteins. It had 15% identity and 48% similarity with Orf2, plus 17% identity and 43% similarity with the C-terminal region of Orf1. Alignment with Orf1 showed the pELW6 sequence to be homologous to the putative highly conserved signalling domain. Further sequencing of the plasmid therefore needs to be carried out to establish the conformation of the putative MCP identified.

6.4 Discussion.

From the evidence gathered to date, it appears that *A. tumefaciens* possesses a homologue of the anchoring protein CheW. The presence of a *cheW* homologue correlates with the possible presence of MCPs in *A. tumefaciens*, and indeed with the possibility that *A. tumefaciens* contains a second *che* operon.

The recent wealth of evidence suggests that many bacteria utilise MCP-like proteins in their chemotactic responses. A large number of MCPs have recently been identified in *R. leguminosarum* [228] and *R. sphaeroides* [84]. Evidence from this work, and previous work on *A. tumefaciens* (see section **1.8**), suggests that there could also be a number of MCPs in *A. tumefaciens*, required for detecting, and responding to, specific chemical stimuli. Indeed an MCP homologue, showing the same structural characteristics as the *E. coli* MCPs, has already been discovered on the Ti plasmid pTiC58 [103].

It is known that, in *E. coli*, interaction of CheA with the MCPs requires the linking protein CheW. Hence the presence of MCPs in *A. tumefaciens* adds weight to the fact that there will also be a homologue of CheW, and vice versa. Since no precise functional domains have, as yet, been assigned to CheW, it is possible that it could be the one Che protein that could exhibit quite varied composition, without adversely affecting its role in the chemosensory pathway. This would therefore explain the low level of homology seen between the putative homologue identified in this work, and CheW from the highly related

bacterium *S. meliloti*. Indeed, low levels of identity were reported within the three CheW homologues from *R. sphaeroides,* and also between them and their counterparts from *S. meliloti* and *E. coli* [81]. It could be that CheW in *A. tumefaciens* has evolved to enable specific interactions with elements of the virulence system e.g. VirA, therefore causing it to be significantly diverged from CheW in related bacteria.

Whether *A. tumefaciens* has a second *che* cluster, and thus multiple copies of the *che* genes, is harder to clarify. If, as is thought, it contains a homologue of *cheW,* and presumably a number of MCPs, the genes encoding these proteins could be contained within a second *che* cluster, which could also contain copies of other *che* genes. However, it could be equally as likely that *cheW* and the MCPs are positioned in a region of the chromosome that does not contain any further copies of the other *che* genes.

Many MCPs are thought to be environmentally regulated [84], as such it would be expected that they would be transcribed separately from the *che* genes. In evolutionary terms, it is possible that the basic chemotaxis system existed first, and different MCP-type genes were then acquired, and added to this system. Therefore increasing the responses, and hence overall competitiveness, of the bacterium. If so, it would be expected that the MCPs could be positioned in other regions of the chromosome, distal to the main *che* system. The anchoring protein, CheW, could therefore be located with one or more of the MCPs to improve the response, or alternatively it could be situated in a separate region of the genome.

Since preliminary results suggest that neither *cheW*, nor the possible MCPs, are located on any of the library cosmids studied to date, the next stage in investigating their presence would be to try and identify the library clones containing their sequence. To locate *cheW*, the *A. tumefaciens* cosmid library could be probed using the *S. meliloti cheW* fragment and/or the putative *A. tumefaciens cheW* fragment, generated by PCR amplification in this work. Sequencing of possible positive clones should then identify *cheW* and confirm its location, relative to other chemotaxis-related genes i.e. confirm whether it is transcribed on its own, or with other genes from the chemosensory network. Similar work could also be carried out to identify possible MCP-like genes. Recent work by Yost *et al* [228] identified a number of MCPs in *R. leguminosarum*. Primers, designed from the highly conserved region of known MCPs, were used to amplify a fragment from *R. leguminosarum* genomic DNA. This fragment was then used to probe a genomic library and hence identify possible positive clones. Since both the Tlp and possible MCP,

identified in pDUB1911, showed homology at, what is presumed to be, a highly conserved signalling domain, similar work could be carried out on *A. tumefaciens* genomic DNA, in an attempt to identify library clones containing other possible MCPs.

The related bacterium *R. sphaeroides* shows a much greater diversity and hence complexity of life styles than does *A. tumefaciens*. As a result of this complexity *R. sphaeroides* is thought to potentially, utilise three versions of the basic chemosensory pathway. *S. meliloti* on the other hand, which exhibits a substantially "simpler" lifestyle than *R. sphaeroides*, is only thought to contain one chemosensory network. *A. tumefaciens* bears a greater resemblance to *S. meliloti* than *R. sphaeroides*, therefore, by association, it would seem that *A. tumefaciens* is likely to contain only one *che* region. However, it is also possible that *A. tumefaciens* could represent an intermediary position between the two extremes; having two *che* regions, with possible multiple copies of certain genes. Interestingly, recent work by Barak and Eisenbach [18] demonstrated that *che*$^-$ *E. coli* strains, containing overexpressed CheY, were able to exhibit chemotactic-like responses. It was proposed that this could indicate cross-talk between the chemotaxis system and other signal transduction pathways, or alternatively that an additional chemotactic pathway could exist in *E. coli*. Sequencing of the *E. coli* genome has shown that only one set of *che* genes exists in *E. coli*, however these results suggest that other, as yet unknown, cell components may also facilitate chemotaxis under certain circumstances. It is therefore possible that *A. tumefaciens* could contain only one set of *che* genes but, as is being suggested for other bacteria, control of chemotaxis could be further regulated by interaction with other cell components.

The results obtained in this work represent the starting point for further investigations to be made in to the peculiarities of the chemotactic responses exhibited by *A. tumefaciens*. However, as has recently been found in several other bacterial species, it appears that the chemotaxis system of *A. tumefaciens* will display a greater degree of complexity than is seen in the basic enteric system. The complex and unpredictable environments, in which bacterial species such as *A. tumefaciens* live, would seem to have dictated the need for a greater level of control of responses to environmental cues and hence subsequent motility, in order to ensure survival within a highly competitive environment.

7 Summary.

7 Summary.

Previous work has shown that *A. tumefaciens* exhibits chemotaxis to a defined set of attractants [118]. This study details experiments carried out in an attempt to identify and characterise the genes responsible for these responses.

Heterologous probing, using fragments from the *S. meliloti* chemotaxis operon [78], was used to identify possible chemotaxis genes in *A. tumefaciens*. The library cosmid pDUB1911 was identified (see chapter **3**). Sequencing of a 9.6kb region of the cosmid insert identified an approximately 8kb cluster of putative chemotaxis genes. The cluster contained nine genes with significant sequence homology, at both the DNA and protein level, to known chemotaxis-related genes from a number of bacterial species. In particular the cluster showed significant similarity, and a conservation of gene order, with the chemosensory regions identified in the related bacteria *S. meliloti* and *R. sphaeroides* [9]. The identified *che* cluster contained the genes *orf1*, *orf2*, *cheY1*, *cheA*, *cheR*, *cheB*, *cheY2*, *orf9* and *orf10*. In a manner similar to the arrangement of genes in *S. meliloti* [195], a homologue of the flagellar gene *fliF* was identified downstream of the *che* cluster.

Mutations were made in three of the nine genes identified in the *che* cluster. A neomycin cassette was inserted into *orf1* and *cheA*, in-frame deletions were made of *cheA* and *orf10* and the entire *che* cluster was deleted. In addition to the mutations made in the chemotaxis genes, a neomycin cassette was also inserted into the flagellar gene *fliF*. Analysis of the mutant strains showed each, except the deletion of *orf10*, to have a defined phenotype (as described in chapter **4**). The *orf1*, *cheA* and *che*$^-$ strains all had impaired chemotactic capabilities, but as far as could be ascertained, exhibited wild type patterns of flagellation and subsequent motility. The *fliF* mutant had a non-motile, non-flagellate phenotype. Under the conditions tested, the *orf10* mutant strain showed wild type patterns of chemotaxis, flagellation and motility.

As with *S. meliloti* and *R. sphaeroides*, no homologue of *cheZ* was identified in the *che* cluster, however unlike the related bacteria, there was also no homologue of the anchoring protein *cheW*. Subsequent Southern blotting and PCR, using primers designed to "conserved" regions of *cheW*, identified a possible homologue of *cheW* in *A. tumefaciens*. The location of the homologue requires further investigation, however it was found not to reside with any of the chemotaxis/flagellar/motility-related genes previously identified in *A. tumefaciens*. Previous evidence (see section **1.8**), plus the identification of homologues of

the chemotaxis genes *cheR*, *cheB* and *cheD* (*orf9*) in the *che* cluster, implied that *A. tumefaciens* could utilise MCPs in the chemotactic response. Probing with a fragment from the highly-conserved domain of an MCP recently identified in *R. leguminosarum*, identified a number of hybridising fragments (see chapter **6**). In particular a hybridising fragment was identified in pDUB1911 which was positioned downstream of the main *che* cluster. Preliminary sequencing of this fragment confirmed it had homology with known MCPs, however further analysis would be required to determine the precise conformation of the protein.

In addition to the work (outlined above) concerned with characterisation of the chemotactic genes in *A. tumefaciens*, preparatory work was also carried out on construction of a system to study biomolecular interactions within and between the chemotaxis and virulence systems of *A. tumefaciens*. Although only preliminary work was carried out, a selectively-infective phage vector was constructed (detailed in chapter **5**), which following further testing, should allow such investigations to begin.

The results described in this work therefore not only provide the groundwork for detailed analysis of the chemotactic responses of *A. tumefaciens*, but also give greater insight into the control of responses seen within members of the *Rhizobiaceae* and indeed within the α-subgroup of *Proteobacteria* as a whole.

Work on *R. sphaeroides* and *S. meliloti*, has shown that regulation of chemotaxis within members of the α-subgroup of *Proteobacteria*, involves a greater degree of complexity than is seen in the enteric bacteria. It has been postulated that this increased level of control is a consequence of the complex nature of the environments in which such bacteria live. The purple non-sulphur bacterium *R. sphaeroides* is able to survive in a diverse array of environments, which require it to respond to numerous different stimuli. To respond in this way it would be expected to contain highly evolved signal transduction mechanisms. Indeed in the bacterial species studied to date, *R. sphaeroides* appears to contain one of the most intricate chemosensory signal transduction networks. Two chemosensory regions have, thus far, been identified in *R. sphaeroides*, which contain numerous replicates of known chemotaxis genes. It is also thought that further copies may exist in a third region [165]. In contrast to *R. sphaeroides*, the related bacterium *S. meliloti* shows a much more directed lifestyle. This restriction in lifestyle again seems to be reflected in its signal transduction mechanisms. *S. meliloti* is thought to contain only one chemosensory region [9]. Of particular interest however is the high degree of conservation

of gene order, seen between this region and those in *R. sphaeroides*. In addition to this conservation, there are two significant differences in the genes identified in these bacteria, with those found in enteric bacteria. That is the lack of a *cheZ* homologue and the existence of at least two copies of *cheY*. The *che* region identified in this work also showed these attributes (see chapter **3**), it is therefore possible that they reflect a specific characteristic of these bacteria, possibly a feature of their predominantly unidirectional mode of flagella rotation.

Whether *A. tumefaciens* contains more than one chemosensory region and hence multiple copies of the *che* genes, requires further investigation. The generally high degree of homology seen between *A. tumefaciens* and *S. meliloti,* and the relatively simple lifestyle exhibited by *A. tumefaciens*, would seem to suggest that it contains only one chemosensory region. However, the presumed distal location of *cheW* could indicate the existence of a second region (see chapter **6**), although this appears unlikely based on the phenotype of the *che* deletion mutant.

The results obtained in this work have therefore confirmed a number of previously proposed principles on the chemosensory systems that exist within members of the α-subgroup of *Proteobacteria*. Of most importance however are the implications for future study of the specific chemotactic responses of *A. tumefaciens*. It should now be possible to study chemotaxis in *A. tumefaciens* in much more detail (see chapter **4**). In particular, the role of chemotaxis in the virulence response of *A. tumefaciens* could now be directly addressed (see chapters **4** and **5**). This should ultimately lead to a greater understanding of *A. tumefaciens* biology in general, thus increasing the pre-existing knowledge of the role of *A. tumefaciens* as both a genetic tool and a plant pathogen.

8 References.

1. Allen, J. B., M. W. Walberg, M. C. Edwards and S. J. Elledge. 1995. Finding Prospective Partners in the Library: the Two-Hybrid System and Phage Display Find a Match. TIBS. **20**: 511 - 516.

2. Alt-Morbe, J., J. L. Stryker, C. Fuqua, P. Li, S. K. Farrand and S. C. Winans. 1996. The Conjugal Transfer System of *Agrobacterium tumefaciens* Octopine-Type Ti Plasmids Is Closely Related to the Transfer System of an IncP Plasmid and Distantly Related to Ti Plasmid *vir* Genes. Journal of Bacteriology. **178**: 4248 - 4257.

3. Ankenbauer, R. G. and E. W. Nester. 1990. Sugar-Mediated Induction of *Agrobacterium tumefaciens* Virulence Genes: Structural Specificity and Activities of Monosaccharides. Journal of Bacteriology. **172**: 6442-6446.

4. Aoyama, T. and A. Oka. 1991. Cross Talk Between the Virulence and Pphosphate Regulons of *Agrobacterium tumefaciens* Caused by an Unusual Interaction of the Transcriptional Activator with a Regulatory DNA Element. Mol. Gen. Genet. **227**: 385-390.

5. Appleby, J. L. and R. B. Bourret. 1998. Proposed Signal Transduction Role for Conserved CheY Residue Thr87, a Member of the Response Regulator Active-Site Quintet. Journal of Bacteriology. **180**: 3563-3569.

6. Armitage, J. P. 1992. Behavioral Responses in Bacteria. Annu. Rev. Physiol. **54**: 683-714.

7. Armitage, J. P. 1993. Methylation-Independent Behavioural Responses in Bacteria, pp. 43-65. *In* Kurjan and Taylor (ed.), Signal Transduction: Prokaryotic and Simple Eukaryotic Systems. Academic Press, Inc., San Diego.

8. Armitage, J. P. 1997. Behavioural Responses of Bacteria to Light and Oxygen. Arch. Microbiol. **168**: 249 - 261.

9. Armitage, J. P. and R. Schmitt. 1997. Bacterial Chemotaxis: *Rhodobacter sphaeroides* and *Sinorhizobium meliloti* - Variations on a Theme. Microbiology. **143**: 3671 - 3682.

10. Armstrong, J., R. N. Perham and J. E. Walker. 1981. Domain Structure of Bacteriophage fd Adsorption Protein. FEBS Letters. **135**: 167-172.

11. Ashby, A. M., M. D. Watson, G. J. Loake and C. H. Shaw. 1988. Ti Plasmid-Specified Chemotaxis of *Agrobacterium tumefaciens* C58C1 Toward *vir*-Inducing Phenolic Compounds and Soluble Factors From Monocotyledonous and Dicotyledonous Plants. Journal of Bacteriology. **170**: 4181 - 4187.

12. Ashby, A. M., M. D. Watson and C. H. Shaw. 1987. A Ti-plasmid Determined Function is Rresponsible for Chemotaxis of *Agrobacterium tumefaciens* Towards the Plant Wound Product Acetosyringone. FEMS Microbiol. Letts. **41**: 189 -192.

13. Ballas and V. Citovsky. 1997. Nuclear Localization Signal Binding Protein from *Arabidopsis* Mediates Nuclear Import of *Agrobacterium* VirD2 Protein. Proc. Natl. Acad. Sci. USA. **94**: 10723 - 10728.

14. Banta, L. M., R. D. Joerger, V. R. Howitz, A. M. Campbell and A. N. Binns. 1994. Glu-225 Outside the Predicted ChvE Binding Site in VirA is Crucial for Sugar Enhancement of Acetosyringone Perception by *Agrobacterium tumefaciens*. Journal of Bacteriology. **176**: 3242 - 3249.

15. Barak, R., W. N. Abouhamad and M. Eisenbach. 1998. Both Acetate Kinase and Acetyl Coenzyme A Synthetase are Involved in Acetate-Stimulated Change in Direction of Flagellar Rotation in *Escherichia coli*. Journal of Bacteriology. **180**: 985 - 988.

16. Barak, R. and M. Eisenbach. 1992. Correlation Between Phosphorylation of the Chemotaxis Protein CheY and its Activity at the Flagellar Motor. Biochemistry. **31**: 1821-1826.

17. Barak, R. and M. Eisenbach. 1996. Regulation of Interaction Between Signaling Protein CheY and Flagellar Motor During Bacterial Chemotaxis., pp. 137-158. *In* Current Topics in Cellular Regulation. Academic Press, Inc.,

18. Barak, R. and M. Eisenbach. 1999. Chemotactic-like Response of *Escherichia coli* Cells Lacking the Known Chemotaxis Machinery but Containing Overexpressed CheY. Molecular Microbiology. **31**: 1125-1137.

19. Barnakov, A. N., L. A. Barnakov and G. L. Hazelbauer. 1998. Comparison In Vitro of a High- and a Low-Abundance Chemoreceptor of *Escherichia coli*: Similar Kinase Activation but Different Methyl-Accepting Activities. Journal of Bacteriology. **180**: 6713-6718.

20. Beijersbergen, A., A. Den Dulk-Ras, R. A. Schilperoort and P. J. J. Hooykaas. 1992. Conjugative Transfer by the Virulence System of *Agrobacterium tumefaciens*. Science. **256**: 1324-1327.

21. Belanger, C., I. Loubens, E. W. Nester and P. Dion. 1997. Variable Efficiency of a Ti Plasmid-Encoded VirA Protein in Different Agrobacterial Hosts. Journal of Bacteriology. **179**: 2305-2313.

22. Bellsolell, L., P. Cronet, M. Majplero, L. Serrano and M. Coll. 1996. The 3-Dimensional Structure of 2 Mutants of the Signal-Transduction Protein CheY Suggest its Molecular Activation Mechanism. Journal of Molecular Biology. **257**: 116 - 128.

23. Bischoff, D. S. and G. W. Ordal. 1992. *Bacillus subtillis* Chemotaxis: a Deviation from the *Escherichia coli* Paradigm. Molecular Microbiology. **6**: 23-28.

24. Bjourson, A. J. and J. E. Cooper. 1993. Band-Stab PCR: a Simple Technique for the Purification of Individual PCR Products. Nucleic Acids Research. **20**: 4675.

25. Blair, D. F. 1995. How Bacteria Sense and Swim. Annual Review of Microbiology. **49**: 489-522.

26. Blat, Y. and M. Eisenbach. 1994. Phosphorylation-Dependant Binding of the Chemotaxis Signal Molecule CheY to its Phosphatase, CheZ. Biochemistry. **33**: 902-906.

27. Blat, Y. and M. Eisenbach. 1996. Mutants with Defective Phosphatase Activity Show no Phosphorylation-Dependent Oligimerization of CheZ. Journal of Biological Chemistry. **271**: 1232-1236.

28. Blat, Y. and M. Eisenbach. 1996. Oligomerization of the Phosphatase CheZ upon Interaction with the Phosphorylated form of CheY. Journal of Biological Chemistry. **271**: 1226-1231.

29. Bourret, R. B., K. A. Borkovich and M. I. Simon. 1991. Signal Transduction Pathways Involving Protein Phosphorylation in Prokaryotes. Annu. Rev. Biochem. **60**: 401-444.

30. Bourret, R. B., J. Davagnino and M. I. Simon. 1993. The Carboxy-Terminal Portion of the CheA Kinase Mediates Regulation of Autophosphorylation by Transducer and CheW. Journal of Bacteriology. **175**: 2097-2101.

31. Bourret, R. B., J. F. Hess, K. A. Borkovich, A. A. Pakula and M. I. Simon. 1989. Protein Phosphorylation in Chemotaxis and Two Component Regulatory Systems of Bacteria. Journal of Biological Chemistry. **264**: 7085-7088.

32. Bravo-Angel, A. M., B. Hohn and B. Tinland. 1998. The Omega Sequence of VirD2 is Important but not Essential for efficient Transfer of T-DNA by *Agrobacterium tumefaciens*. Molecular Plant-Microbe Interactions. **11**: 57 - 63.

33. Bren, A., M. Welch, Y. Blat and M. Eisenbach. 1996. Signal Termination in Bacterial Chemotaxis: CheZ Mediates Dephosphorylation Of Free Rather Than Switch-Bound CheY. Proc. Natl. Acad. Sci. USA. **93**: 10090-10093.

34. Cangelosi, G. A., R. G. Ankenbauer and E. W. Nester. 1990. Sugars Induce the *Agrobacterium* Virulence Genes Through a Periplasmic Binding Protein and a Transmembrane Signal Protein. Proc. Natl. Acad. Sci. USA. **87**: 6708-6712.

35. Castro, O. A., A. Zorreguieta, V. Ielmini, G. Vega and L. Ielpi. 1996. Cyclic Beta-(1,2)-Glucan Synthesis in *Rhizobiaceae*: Roles of the 319-Kilodalton Protein Intermediate. Journal of Bacteriology. **178**: 6043-6048.

36. Chang, C. and R. C. Stewart. 1998. The Two Component System. Plant Physiology. **117**: 723-731.

37. Chang, C. and S. C. Winans. 1992. Functional Roles Assigned to the Periplasmic, Linker and Receiver Domains of the *Agrobacterium tumefaciens* VirA Pprotein. Journal of Bacteriology. **174**: 7033-7039.

38. Chervitz, S. A. and J. J. Falke. 1996. Molecular Mechanism of Transmemebrane Signaling by the Aspartate Receptor: A model. Proc. Natl. Acad. Sci. USA. **93**: 2545 - 2550.

39. Chesnokova, G. A., J. B. Coutinho, I. H. Khan, M. S. Mikhail and C. I. Kado. 1997. Characterization of Flagella Genes of *Agrobacterium tumefaciens*, and the Effect of a Bald Strain on Virulence. Molecular Microbiology. **23**: 579-590.

40. Chiang, P. K., R. K. Gordon, J. Tal, G. C. Zeng, B. P. Doctor, K. Pardhasaradhi and P. P. McCann. 1996. S-Adenosylmethionine and Methylation. FASEB Journal. **10**: 471-480.

41. Cho, K., C. Fuqua and S. C. Winans. 1997. Transcriptional Regulation and Locations of *Agrobacterium tumefaciens* Genes Required for Complete Catabolism of Octopine. Journal of Bacteriology. **179**: 1-8.

42. Chumakov, M. I. and I. V. Kurbanov. 1998. Localization of the Protein VirB1 Involved in Contact Formation During Conjugation Among *Agrobacterium* Cells. FEMS Microbiology Letters. **168**: 297-301.

43. Citovsky, V., D. Warnick and P. Zambryski. 1994. Nuclear Import of *Agrobacterium* VirD2 and VirE2 proteins in Maize and Tobacco. Proc. Natl. Acad. Sci. USA. **91**: 3210 - 3214.

44. Citovsky, V., J. Zupan, D. Warnick and P. Zambryski. 1992. Nuclear Localization of *Agrobacterium* VirE2 Protein in Plant Cells. Science. **256**: 1802 - 1805.

45. Cochran, A. G. and P. S. Kim. 1996. Imitation of *Escherichia coli* Aspartate Receptor Signaling in Engineered Dimers of the Cytoplasmic Domain. Science (Washington DC). **271**: 1113-1116.

46. Conley, M. P., A. J. Wolfe, D. F. Blair and H. C. Berg. 1989. Both CheA and CheW are Required for Reconstitution of Chemotactic Signalling in *Escherichia coli.* Journal of Bacteriology. **171**: 5190-5193.

47. Cook, D. M. and S. K. Farrand. 1992. The *oriT* Region of the *Agrobacterium tumefaciens* Ti Plasmid pTiC58 Shares DNA Sequence Identity with the Transfer Origins of RSF1010 and RK2/RP4 and with T-Region Borders. Journal of Bacteriology. **174**: 6238-6246.

48. Cook, D. M., P. Li, F. Ruchaud, S. Padden and S. K. Farrand. 1997. Ti Plasmid Conjugation is Independent of *vir*: Reconstitution of the *tra* Functions from pTiC58 as a Binary System. Journal of Bacteriology. **179**: 1291-1297.

49. Cooley, M. B., M. R. D'Souza and C. I. Kado. 1991. The *virC* and *virD* Operons of the *Agrobacterium* Ti-plasmid are Regulated by the *ros* Chromosomal Gene: Analysis of the Cloned *ros* Gene. Journal of Bacteriology. **173**: 2608-2616.

50. Cooley, M. B. and C. I. Kado. 1991. Mapping of the *ros* Virulence Regulatory Gene of *Agrobacterium tumefaciens*. Mol. Gen. Genet. **230**: 24-27.

51. Crissman, J. W. and G. P. Smith. 1984. Gene-III Protein of Filamentous Phages: Evidence for a Carboxy-Terminal Domain with a Role in Morphogenesis. Virology. **132**: 445-455.

52. D'Souza-Ault, M. R., M. B. Cooley and C. I. Kado. 1993. Analysis of the Ros Repressor of *Agrobacterium vir*C and *vir*D Operons: Molecular Intercommunication between Plasmid and Chromosomal Genes. Journal of Bacteriology. **175**: 3486 - 3490.

53. Davey, M. R., I. S. Curtis, K. M. A. Gartland and J. B. Power. 1994. *Agrobacterium*-Induced Crown Gall and Hairy Root Diseases: Their Biology and Application to Plant Genetic Engineering., pp. *In* Williams (ed.), Plant Galls. Clarendon Press, Oxford.

54. Deakin, W. J. 1994. Molecular Characterisation of Flagellar Genes from *Agrobacterium tumefaciens*. PhD Thesis, University of Durham.

55. Deakin, W. J., C. S. M. Furniss, V. E. Parker and C. H. Shaw. 1997. Isolation and Characterisation of a Linked Cluster of Genes From Agrobacterium tumefaciens Encoding Proteins Involved in Flagellar Basal-body Structure. Gene. **189**: 135-137.

56. Deakin, W. J., V. E. Parker, E. L. Wright, K. J. Ashcroft, G. J. Loake and C. H. Shaw. 1999. Agrobacterium tumefaciens possesses a Fourth Flagellin Gene Located in a Large Gene Cluster concerned with Flagellar Structure, Assembly and Motility. Microbiology. (In press)

57. Deakin, W. J., J. L. C. I. Sanderson, T. Goswami and C. H. Shaw. 1997. The *Agrobacterium tumefaciens* Motor Gene, *motA*, is in a Linked Cluster with the Flagellar Switch Protein Genes, *fliG*, *fliM* and *fliN*. Gene. **189**: 139-141.

58. Ditta, G., S. Stanfield, D. Corbin and D. R. Helsinki. 1980. A Broad Host Range DNA Cloning System for Gram-Negative Bacteria: Construction of a Gene Bank of *Rhizobium meliloti*. Proc. Natl. Acad. Sci. USA. **77**: 7347-7351.

59. Djordjevic, S., P. N. Goudreau, Q. Xu, A. K. Stock and A. H. West. 1998. Structural Basis for Methylesterase CheB Regulation by a Phosphorylation-Activated Domain. Proc. Natl. Acad. Sci. USA. **95**: 1381 - 1386.

60. Dombek, P. and W. Ream. 1997. Functional Domains of *Agrobacterium tumefaciens* Single-Stranded DNA-Binding Protein VirE2. Journal of Bacteriology. **179**: 1165 - 1173.

61. Doty, S. L., M. Chang and E. W. Nester. 1993. The Chromosomal Virulence Gene, *chvE*, of *Agrobacterium tumefaciens* is Regulated by a LysR Family Member. Journal of Bacteriology. **175**: 7880-7886.

62. Dowd, J. P. and P. Matsumura. 1997. The Use of Flash Photolysis for a High-Resolution Temporal and Spatial Analysis of Bacterial Chemotactic Behaviour: CheZ is Not Always Necessary for Chemotaxis. Molecular Microbiology. **25**: 295 - 302.

63. Duban, M. E., K. Lee and D. G. Lynn. 1993. Strategies in Pathogenesis: Mechanistic Specificity in the Detection of Generic Signals. Molecular Microbiology. **7**: 637-645.

64. Dunn, I. S. 1996. Phage Display of Proteins. Current Opinion in Biotechnology. **7**: 547-553.

65. Ellefson, D. D., U. Weber and A. J. Wolfe. 1997. Genetic Analysis of the Catalytic Domain of the Chemotaxis- Associated Histidine Kinase CheA. Journal of Bacteriology. **179**: 825 - 830.

66. Escudero, J. and B. Hohn. 1997. Transfer and Integration of T-DNA Without Cell Injury in the Host Plant. The Plant Cell. **9**: 2135-2142.

67. Estacio, W., S. Santa Anna-Arriola, M. Adedipe and L. M. Marquez-Magana. 1998. Dual Promoters are Responsible for Transcription Initiation of the *fla/che* Operon in *Bacillus subtilis*. Journal of Bacteriology. **180**: 3548-3555.

68. Falke, J. J., R. B. Bass, S. L. Butler, S. A. Chervitz and M. A. Danielson. 1997. The Two-Component Signalling Pathway of Bacterial Chemotaxis: A Molecular View of Signal Transduction by Receptors, Kinases, and Adaptation Enzymes., pp. 457-512. *In* Annual Review of Cell and Developmental Biology.

69. Farrand, S. K., I. Hwang and D. M. Cook. 1996. The *tra* Region of the Nopaline-Type Ti Plasmid Is a Chimera with Elements Related to the Transfer Systems of RSF1010, RP4 and F. Journal of Bacteriology. **178**: 4233 - 4247.

70. Fields, S. and O. Song. 1989. A Novel Genetic System to Detect Protein-Protein Interactions. Nature. **340**: 245.

71. Garrity, L. F., S. L. Schiel, R. Merrill, J. Reizer, M. H. Saier Jr and G. W. Ordal. 1998. Unique Regulation of Carbohydrate Chemotaxis in *Bacillus subtilis* by the Phosphoenolpyruvate-Dependent Phosphotransferase System and the Methyl-Accepting Chemotaxis Protein McpC. Journal of Bacteriology. **180**: 4475-4480.

72. Garzon, A. and J. S. Parkinson. 1996. Chemotactic Signalling by the P1 Phosphorylation Domain Liberated from the CheA Histidine Kinase of *Escherichia coli*. Journal of Bacteriology. **178**: 6752-6758.

73. Gegner, J. A. and F. W. Dahlquist. 1991. Signal Transduction in Bacteria: CheW Forms a Reversible Complex with the Protein Kinase CheA. Proc. Natl. Acad. Sci. USA. **88**: 750-754.

74. Gegner, J. A., D. R. Graham, A. F. Roth and F. W. Dahlquist. 1992. Assembly of an MCP receptor, CheW, and kinase CheA Complex in the Bacterial Chemotaxis Signal Transduction Pathway. Cell. **70**: 975-982.

75. Gelvin, S. B. 1998. *Agrobacterium* VirE2 Proteins Can Form a Complex with T Strands in the Plant Cytoplasm. Journal of Bacteriology. **180**: 4300-4302.

76. Gramatikoff, K., O. Georgiev and W. Schaffner. 1994. Direct Interaction Rescue, a Novel Filamentous Phage Technique to Study Protein-Protein Interactions. Nucleic Acids Research. **22**: 5761-5762.

77. Grebe, T. W. and J. Stock. 1998. Bacterial Chemotaxis: The Five Sensors of a Bacterium. Current Biology. **8**: R154 - R157.

78. Greck, M., J. Platzer, V. Sourjik and R. Schmitt. 1995. Analysis of a Chemotaxis Operon in *Rhizobium meliloti.* Molecular Microbiology. **15**: 989 - 1000.

79. Grishanin, R. N., D. E. Gauden and J. P. Armitage. 1997. Photoresponses in *Rhodobacter sphaeroides*: Role of Photosynthetic Electron Transport. Journal of Bacteriology. **179**: 24 - 30.

80. Hamblin, P. A., N. A. Bourne and J. P. Armitage. 1997. Characterization of the Chemotaxis Protein CheW from *Rhodobacter sphaeroides* and its Effect on the Behaviour of *Escherichia coli.* Molecular Microbiology. **24**: 41 - 51.

81. Hamblin, P. A., B. A. Maguire, R. N. Grishanin and J. P. Armitage. 1997. Evidence for two Chemosensory Pathways in *Rhodobacter sphaeroides.* Molecular Microbiology. **26**: 1083 - 1096.

82. Han, D. C. and S. C. Winans. 1994. A Mutation in the Receiver Domain of the *Agrobacterium tumefaciens* Transcriptional Regulator VirG Increases its Affinity for Operator DNA. Molecular Microbiology. **12**: 23-30.

83. Hanlon, D. W. and G. W. Ordal. 1994. Cloning and Characterization of Genes Encoding Methyl-Accepting Chemotaxis Proteins in *Bacillus subtilis.* The Journal of Biological Chemistry. **269**: 14038-14046.

84. Harrison, D. M., J. Skidmore, J. P. Armitage and J. R. Maddock. 1999. Localization and Environmental Regulation of MCP-like Proteins in *Rhodobacter sphaeroides*. Molecular Microbiology. **31**: 885-892.

85. Hawes, M. C. and L. Y. Smith. 1989. Requirement for Chemotaxis in Pathogenicity of *Agrobacterium tumefaciens* on Roots of Soil-Grown Pea Plants. Journal of Bacteriology. **171**: 5668-5671.

86. Hawes, M. C., L. Y. Smith and A. J. Howarth. 1988. *Agrobacterium tumefaciens* Mutants Deficient in Chemotaxis to Root Exudates. Molecular Plant-Microbe Interactions. **1**: 182-186.

87. Herrera-Estrella, A., M. Van Montagu and K. Wang. 1990. A Bacterial Peptide Acting as a Plant Nuclear Targeting Signal: the Amino-Terminal Portion of *Agrobacterium* VirD2 Protein Ddirects b-galactosidase Fusion Protein into Tobacco Nuclei. Proc. Natl. Acad. Sci. USA. **87**: 9534-9537.

88. Hooykaas, P. J. J. and A. G. M. Beijersbergen. 1994. The Virulence System of *Agrobacterium tumefaciens*. **32**: 157-179.

89. Howard, E. A., J. R. Zupan, V. Citovsky and P. C. Zambryski. 1992. The VirD2 Protein of *A.tumefaciens* Contains a C-Terminal Bipartite Nuclear Localization Signal: Implications for Nuclear Uptake of DNA in Plant Cells. Cell. **68**: 109-118.

90. Huang, M. W., G. A. Cangelosi, W. Halperin and E. W. Nester. 1990. A Chromosomal *Agrobacterium tumefaciens* Gene Required for Effective Plant Signal Transduction. J.ournal of Bacteriology. **172**: 1814-1824.

91. Jasper, F., C. Koncz, J. Schell and H. Steinbiss. 1994. *Agrobacterium* T-Strand Production *in vitro*: Sequence-specific Cleavage and 5' Protection of Single-Stranded DNA templates by Purified VirD2 Protein. Proc. Natl. Acad. Sci. USA. **91**: 694 - 698.

92. Jeziore-Sassoon, Y., P. A. Hamblin, C. A. Bootle-Wilbraham, P. S. Poole and J. P. Armitage. 1998. Metabolism is Required for Chemotaxis to Sugars in *Rhodobacter sphaeroides*. Microbiology. **144**: 229 - 239.

93. Jin, S., T. Roitsch, P. J. Christie and E. W. Nester. 1990. The Regulatory VirG Protein Specifically Binds to a *cis*-acting Regulatory Sequence Involved in Transcriptional Activation of *Agrobacterium tumefaciens* Virulence Genes. Journal of Bacteriology. **172**: 531-537.

94. Johnson, M. S., E. H. Rowsell and B. L. Taylor. 1995. Investigation of Transphosphorylation Between Chemotaxis Proteins and the Phosphoenolpyruvate : Sugar Phosphotransferase System. FEBS Letters. **374**: 161 - 164.

95. Jumas-Bilak, E., S. Michaux-Charachon, G. Bourg, M. Ramuz and A. Allardet-Servent. 1998. Unconventional Genomic Organization in the Alpha Subgroup of the *Proteobacteria*. Journal of Bacteriology. **180**: 2749-2755.

96. Kalogeraki, V. S. and S. C. Winans. 1995. The Octopine-Type Ti Plasmid pTiA6 of *Agrobacterium tumefaciens* Contains a Gene Homologous to the Chromosomal Virulence Gene *acvB*. Journal of Bacteriology. **177**: 892-897.

97. Kalogeraki, V. S. and S. C. Winans. 1998. Wound-Released Chemical Signals May Elicit Multiple Responses From an *Agrobacterium tumefaciens* Strain Containing an Octopine-Type Ti Plasmid. Journal of Bacteriology. **180**: 5660-5667.

98. Kemner, J. M., X. Liang and E. W. Nester. 1997. The *Agrobacterium tumefaciens* Virulence Gene *chv*E is Part of a Putative ABC-Type Sugar Transport Operon. Journal of Bacteriology. **179**: 2452-2458.

99. Kenney, L. J., M. D. Bauer and T. J. Silhavy. 1995. Phosphorylation-Dependent Conformational Changes in OmpR, an Osmoregulatory DNA-Binding Protein of *Escherichia coli*. Proc. Natl. Acad. Sci. USA. **92**: 8866 - 8870.

100. Kerr, A. 1969. Crown Gall of Stonefruit I: isolation of *Agrobacterium tumefaciens* and related species. Aust. J. Biol. Sci. **22**: 168 - 172.

101. Kihara, M., N. R. Francis, D. J. DeRosier and R. M. Macnab. 1996. Analysis of a FliM-FliN Flagellar Switch Fusion Mutant of *Salmonella typhimurium*. Journal of Bacteriology. **178**: 4582-4589.

102. Kim, H. and S. K. Farrand. 1997. Characterization of the *acc* Operon from the Nopaline-Type Ti Plasmid pTiC58, Which Encodes Utilization of Agrocinopines A and B and Susceptibility to Agrocin 84. Journal of Bacteriology. **179**: 7559-7572.

103. Kim, H. and S. K. Farrand. 1998. Opine Catabolic Loci from *Agrobacterium* Plasmids Confer Chemotaxis to Their Cognate Substrates. Molecular Plant-Microbe Interactions. **11**: 131-143.

104. Kirby, J. R., C. J. Kristich, S. L. Feinberg and G. W. Ordal. 1997. Methanol Production During Chemotaxis to Amino Acids in *Bacillus subtilis*. Molecular Microbiology. **24**: 869-878.

105. Koshland, D. E. 1988. Chemotaxis as a Model Second Messenger System. Biochemistry. **27**: 5829-5834.

106. Koukolikova-Nicola, Z., D. Raineri, K. Stephens, C. Ramos, B. Tinland, E. W. Nester and B. Hohn. 1993. Genetic Analysis of the *vir*D Operon of *Agrobacterium tumefaciens*: a Search for Functions Involved in Transport of T-DNA into the Plant Cell Nucleus and in T-DNA Integration. Journal of Bacteriology. **175**: 723 - 731.

107. Krebber, A., J. Bornhauser, J. Burmester, A. Honegger, J. Willuda, H. R. Bosshard and A. Pluckthun. 1997. Reliable Cloning of Functional Antibody Variable Domains from Hybridomas and Spleen Cell Repertoires Employing a Reengineered Phage Display System. Journal of Immunological Methods. **201**: 35-55.

108. Krebber, C., S. Spada, D. Desplancq, A. Krebber, L. Ge and A. Pluckthun. 1997. Selectively-Infective Phage (SIP): A Mechanistic Dissection of a Novel *in vivo* Selection for Protein-Ligand Interactions. Journal of Molecular Biology. **268**: 607-618.

109. Krebber, C., S. Spada, D. Desplancq and A. Pluckthun. 1995. Co-Selection of Cognate Antibody-Antigen Pairs by Selectively-Infective Phages. FEBS Letters. **377**: 227-231.

110. Lai, E. and C. I. Kado. 1998. Processed VirB2 Is the Major Subunit of the Promiscuous Pilus of *Agrobacterium tumefaciens*. Journal of Bacteriology. **180**: 2711-2717.

111. Lee, K., M. W. Dudley, K. M. Hess, D. G. Lynn, R. D. Joerger and A. N. Binns. 1992. Mechanism of Activation of *Agrobacterium* Virulence Genes: Identification of Phenol-Binding Proteins. Proc. Natl. Acad. Sci. USA. **89**: 8666-8670.

112. Lee, Y., U. Ha, W. Sim and E. W. Nester. 1998. Characterisation of an Unusual Sensor Gene (*vir*A) of *Agrobacterium*. Gene. **210**: 307 - 314.

113. Lee, Y., S. Jin, W. Sim and E. W. Nester. 1995. Genetic Evidence for Direct Sensing of Phenolic Compounds by the VirA Protein of *Agrobacterium tumefaciens*. Proc. Natl. Acad. Sci. USA. **92**: 12245-12249.

114. Lee, Y., S. Jin, W. Sim and E. W. Nester. 1996. The Sensing of Plant Signal Molecules by *Agrobacterium*: Genetic Evidence for Direct Recognition of Phenolic Inducers by the VirA Protein. Gene. **179**: 83-88.

115. Li, J., R. V. Swanson, M. I. Simon and R. M. Weis. 1995. The Response Regulators CheB and CheY Exhibit Competitive Binding to the Kinase CheA. Biochemistry. **34**: 14626 - 14636.

116. Lin, T. and C. I. Kado. 1993. The *virD4* Gene is Required for Virulence While *virD3* and *orf5* are not Required for Virulence of *Agrobacterium tumefaciens*. Molecular Microbiology. **9**: 803 - 812.

117. Liu, J. and J. S. Parkinson. 1991. Genetic Evidence for Interaction Between the CheW and Tsr Proteins During Chemoreceptor Signaling by *Escherichia coli*. Journal of Bacteriology. **173**: 4941-4951.

118. Loake, G. J., A. M. Ashby and C. H. Shaw. 1988. Attraction of *Agrobacterium tumefaciens* C58C1 Towards Sugars Involves a Highly Sensitive Chemotaxis System. J. Gen. Microbiol. **134**: 1427 - 1432.

119. Lukat, G. S., B. H. Lee, J. M. Mottonen, A. M. Stock and J. B. Stock. 1991. Roles of the Highly Conserved Aspartate and Lysine Residues in the Response Regulator of Bacterial Chemotaxis. The Journal of Biological Chemistry. **266**: 8348-8354.

120. Lux, R., K. Jahreis, K. Bettenbrock, J. S. Parkinson and J. W. Lengeler. 1995. Coupling the Phosphotransferase System and the Methyl-Accepting Chemotaxis Signaling Pathways of *Escherichia coli*. Proc. Natl. Acad. Sci. USA. **92**: 11583 - 11587.

121. Macnab, R. M. 1992. Genetics and Biogenesis of Bacterial Flagella. Annu. Rev. Genet. **26**: 131-158.

122. Maddock, J. R. and L. Shapiro. 1993. Polar Location of the Chemoreceptor Complex in the *Escherichia coli* Cell. Science. **259**: 1717-1723.

123. Manson, M. D., J. P. Armitage, J. A. Hoch and R. M. Macnab. 1998. Bacterial Locomotion and Signal Transduction. Journal of Bacteriology. **180**: 1009 - 1022.

124. Mantis, N. J. and S. C. Winans. 1992. The *Agrobacterium tumefaciens vir* Gene Transcriptional Activator *virG* is Transcriptionally Induced by Acid pH and Other Stress Stimuli. Journal of Bacteriology. **174**: 1189-1196.

125. Matthysse, A. G., D. L. Thomas and A. R. White. 1995. Mechanism of Cellulose Synthesis in *Agrobacterium tumefaciens*. Journal of Bacteriology. **177**: 1076-1081.

126. Matthysse, A. G., S. White and R. Lightfoot. 1995. Genes Required for Cellulose Synthesis in *Agrobacterium tumefaciens*. Journal of Bacteriology. **177**: 1069-1975.

127. McEvoy, M. M. and F. W. Dahlquist. 1997. Phosphohistidines in Bacterial Signaling. Current Opinion in Structural Biology. **7**: 793 - 797.

128. McEvoy, M. M., A. C. Hausrath, G. B. Randolph, S. J. Remington and F. W. Dahlquist. 1998. Two Binding Modes Reveal Flexibility in Kinase/Response Regulator Interactions in the Bacterial Chemotaxis Pathway. Proc. Natl. Acad. Sci. USA. **95**: 7333-7338.

129. McEvoy, M. M., D. R. Muhandiram, L. E. Kay and F. W. Dahlquist. 1996. Structure and Dynamics of a CheY-binding Domain of the Chemotaxis Kinase CheA Determined by Nuclear Magnetic Resonance. Biochemistry. **35**: 5633-5640.

130. McLean, B. G., E. A. Greene and P. C. Zambryski. 1994. Mutants of *Agrobacterium* VirA that Activate *vir* Gene Expression in the Absence of the Inducer Acetosyringone. The Journal of Biological Chemistry. **269**: 2645-2651.

131. McNally, D. F. and P. Matsumura. 1991. Bacterial Chemotaxis Signalling Complexes: Formation of a CheA/CheW Complex Enhances Autophosphorylation and Affinity for CheY. Proc. Natl. Acad. Sci. USA. **88**: 6269-6273.

132. Melchers, L. S., T. J. G. Regensburg-tuink, R. B. Bourret, N. J. A. Sedee, R. A. Schilperoot and P. J. J. Hooykaas. 1989. Membrane Topology and Functional Analysis of the Sensory Protein VirA of *Agrobacterium tumefaciens*. EMBO J. **8**: 1919-1925.

133. Miranda, A., G. Janssen, L. Hodges, E. G. Peralta and W. Ream. 1992. *Agrobacterium tumefaciens* Transfers Extremely Long T-DNAs by a Unidirectional Mechanism. Journal of Bacteriology. **174**: 2288-2297.

134. Mitchell, C. and V. R. Harley. 1997. Phage Display - A Powerful Genetic Probe of Biomolecular Interactions. Australasian Biotechnology. **7**: 218-222.

135. Montrone, M., M. Eisenbach, D. Oesterhelt and W. Marwan. 1998. Regulation of Switching Frequency and Bias of the Bacterial Flagellar Motor by CheY and Fumarate. Journal of Bacteriology. **180**: 3375-3380.

136. Montrone, M., D. Oesterhelt and W. Marwan. 1996. Phosphorylation-Independent Bacterial Chemoreponses Correlate with Changes in the Cytoplasmic Level of Fumarate. Journal of Bacteriology. **178**: 6882-6887.

137. Moreno, E. 1998. Genome Evolution Within the Alpha *Proteobacteria*: Why do Some Bacteria Possess Plasmids and Others Exhibit More Than One Different Chromosome? FEMS Micrbiology Reviews. **22**: 255-275.

138. Morrison, T. B. and J. S. Parkinson. 1994. Liberation of an Interaction Domain from the Phosphotransfer Region of CheA, a Signalling Kinase of *Escherichia coli*. Proc. Natl. Acad. Sci. USA. **91**: 5485-5489.

139. Nelson, F. K., S. M. Friedman and G. P. Smith. 1981. Filamentous Phage DNA Cloning Vectors: A Noninfective Mutant with a Nonpolar Deletion in Gene III. Virology. **108**: 338-350.

140. O'Neil, K. T. and R. H. Hoess. 1995. Phage Display: Protein Engineering by Directed Evolution. Current Biology. **5**: 443-449.

141. Oger, P., K. Kim, R. L. Sackett, K. Piper and S. K. Farrand. 1998. Octopine-Type Ti Plasmids Code For a Mannopine-Inducible Dominant-Negative Allele of *traR*, the Quorum-Sensing Activator that Regulates Ti Plasmid Conjugal Transfer. Molecular Microbiology. **27**: 277-288.

142. Okamoto, S., A. Toyoda-Yamamoto, K. Ito, I. Takebe and Y. Machida. 1991. Localisation and Orientation of the VirD4 Protein of *Agrobacterium tumefaciens* in the Cell Membrane. Mol. Gen. Genet. **228**: 24-32.

143. Okumura, H., S. Nishiyama, A. Sasaki, M. Homma and I. Kawagishi. 1998. Chemotactic Adaptation Is Altered by Changes in the Carboxy-Terminal Sequence Conserved Among the Major Methyl-Accepting Chemoreceptors. Journal of Bacteriology. **180**: 1862-1868.

144. Ordal, G. W., L. Màrquez-Magaña and M. J. Chamberlin. 1993. Motility and Chemotaxis, pp. 765-784. *In* Sonenshein, Hoch and Losick (ed.), *Bacillus subtilis* and other Gram-Positive Bacteria: Biochemistry, Physiology, and Molecular Genetics. American Society for Microbiology, Washington, D. C.

145. Packer, H. L. and J. P. Armitage. 1994. The Chemokinetic and Chemotactic Behaviour of *Rhodobacter sphaeroides*: Two Independent Responses. Journal of Bacteriology. **176**: 206-212.

146. Packer, H. L., H. Lawther and J. P. Armitage. 1997. The *Rhodobacter sphaeroides* Flagellar Motor is a Variable-Speed Rotor. FEBS Letters. **409**: 37 - 40.

147. Palmer, A. C. V. and C. H. Shaw. 1992. The Role of VirA and VirG Phosphorylation in Chemotaxis Towards Acetosyringone by *Agrobacterium tumefaciens*. J. Gen. Microbiol. **138**: 2509 - 2514.

148. Palumbo, J. D., C. I. Kado and D. A. Phillips. 1998. An Isoflavonoid-Inducible Efflux Pump in *Agrobacterium tumefaciens* Is Involved in Competitive Colonisation of Roots. Journal of Bacteriology. **180**: 3107-3113.

149. Pansegrau, W., F. Schoumacher, B. Hohn and E. Lanka. 1993. Site-Specific Cleavage and Joining of Single-stranded DNA by VirD2 Protein of *Agrobacterium tumefaciens* Ti Plasmids: Analogy to Bacterial Conjugation. Proc. Natl. Acad. Sci. USA. **90**: 11538 - 11542.

150. Parke, D., L. N. Ornston and E. W. Nester. 1987. Chemotaxis to Plant Phenolic Inducers of Virulence Genes is Constitutively Expressed in the Absence of the Ti-plasmid in *Agrobacterium tumefaciens*. Journal of Bacteriology. **169**: 5336-5338.

151. Parkinson, J. S. 1988. Protein Phosphorylation in Bacterial Chemotaxis. Cell. **53**: 1-2.

152. Parkinson, J. S. and E. C. Kofoid. 1992. Communication Modules in Bacterial Signaling Proteins. Annu. Rev. Genet. **26**: 71-112.

153. Pazour, G. J. and A. Das. 1990. Characterisation of the VirG binding site of *Agrobacterium tumefaciens*. Nucl. Acids Res. **18**: 6909-6913.

154. Pedrazzi, G., F. Schwesinger, A. Honegger, C. Krebber and A. Pluckthun. 1997. Affinity and Folding Properties Both Influence the Selection of Antibodies with the Selectively Infective Phage (SIP) Methodology. FEBS Letters. **415**: 289-293.

155. Piper, K. R., S. Beck von Bodman and S. K. Farrand. 1993. Conjugation Factor of *Agrobacterium tumefaciens* Regulates Ti Plasmid Transfer by Autoinduction. Nature. **362**: 448-450.

156. Pohlman, R. F., H. D. Genetti and S. C. Winans. 1994. Common Ancestry Between IncN Conjugal Transfer Genes and Macromolecular Export Systems of Plant and Animal Pathogens. Molecular Microbiology. **14**: 655-668.

157. Poole, P. S., M. J. Smith and J. P. Armitage. 1993. Chemotactic Signalling in *Rhodobacter sphaeroides* Requires Metabolism of Attractants. Journal of Bacteriology. **175**: 291-294.

158. Postma, P. W., J. W. Lengeler and G. R. Jacobson. 1993. Phosphoenolpyruvate: Carbohydrate Phosphotransferase Systems of Bacteria. Micobiol. Rev. **57**: 543-594.

159. Pratt, L. A. and T. J. Silhavy. 1995. Identification of Base-pairs Important for OmpR-DNA Interaction. Molecular Microbiology. **17**: 565-573.

160. Putnoky, P., A. Kereszt, T. Nakamura, G. Endre, E. Grosskopf, P. Kiss and A. Kondorosi. 1998. The *pha* Gene Cluster of *Rhizobium meliloti* Involved in pH Adaptation and Symbiosis Encodes a Novel Type of K+ Efflux System. Molecular Microbiology. **28**: 1091-1101.

161. Quandt, J. and M. F. Hynes. 1993. Versatile Suicide Vectors Which Allow Direct Selection for Gene Replacement in Gram-negative Bacteria. Gene. **127**: 15-21.

162. Quiocho, F. A. and P. S. Ledvina. 1996. Atomic Structure and Specificity of Bacterial Periplasmic Receptors for Active Transport and Chemotaxis - Variation of Common Themes. Molecular Microbiology. **20**: 17-25.

163. Ramakrishnan, R., M. Schuster and R. B. Bourret. 1998. Acetylation at Lys-92 Enhances Signaling by the Chemotaxis Response Regulator Protein CheY. Proc. Natl. Acad. Sci. USA. **95**: 4918-4923.

164. Roitsch, T., S. Jin and E. W. Nester. 1994. The Binding Site of the Transcriptional Activator VirG from *Agrobacterium* Comprises both Conserved and Specific Nonconserved Sequences. FEBS Letters. **338**: 127-132.

165. Romagnoli, S. and J. P. Armitage. 1999. Roles of Chemosensory Pathways in Transient Changes in Swimming Speed of *Rhodobacter sphaeroides* Induced by Changes in Photosynthetic Electron Transport. Journal of Bacteriology. **181**: 34-39.

166. Rosario, M. M. L. and G. W. Ordal. 1996. CheC and CheD Interact to Regulate Methylation of *Bacillus subtilis* Methyl-Accepting Chemotaxis Proteins. Molecular Microbiology. **21**: 511-518.

167. Rossi, L., B. Hohn and B. Tinland. 1993. The VirD2 Protein of *Agrobacterium tumefaciens* Carries Nuclear Localization Signals Important for Transfer of T-DNA to Plants. Mol. Gen. Genet. **239**: 345 - 353.

168. Rowsell, E. H., J. M. Smith, A. Wolfe and B. L. Taylor. 1995. CheA, CheW, and CheY are Required for Chemotaxis to Oxygen and Sugars of the Phosphotransferase System in *Escherichia coli*. Journal of Bacteriology. **177**: 6011-6014.

169. Sackett, M. J., J. P. Armitage, E. E. Sherwood and T. P. Pitta. 1997. Photoresponses of the Purple Nonsulfur Bacteria *Rhodospirillum centenum* and *Rhodobacter sphaeroides*. Journal of Bacteriology. **179**: 6764 - 6768.

170. Sambrook, J., E. F. Fritsch and T. Maniatis. 1989. Molecular Cloning: A Laboratory Manual. Cold Spring Harbour Laboratory Harbour Press, New York.

171. Sanna, M. G. and M. I. Simon. 1996. Isolation and *in-vitro* Characterization of CheZ Suppressors for the *Escherichia coli* Chemotactic Response Regulator Mutant CheYN23D. Journal of Biological Chemistry. **271**: 7357-7361.

172. Savka, M. A., R. C. Black, A. N. Binns and S. K. Farrand. 1996. Translocation and Exudation of Tumor Metabolites in Crown Galled Plants. Molecular Plant-Microbe Interactions. **9**: 310-313.

173. Schafer, A., A. Tauch, W. Jager, J. Kalinowski, G. Thierbach and A. Puhler. 1994. Small Mobilizable Multi-Purpose Cloning Vectors Derived From the *Escherichia coli* Plasmids pK18 and pK19:Selection of Defined Deletions in the Chromosome of *Corynebacterium glutamicum*. Gene. **145**: 69-73.

174. Scharf, B. E., K. A. Fahrner, L. Turner and H. C. Berg. 1998. Control of Direction of Flagellar Rotation in Bacterial Chemotaxis. Proc. Natl. Acad. Sci. USA. **95**: 201-206.

175. Schuster, M., W. N. Abouhamad, R. E. Silversmith and R. B. Bourret. 1998. Chemotactic Response Regulator Mutant CheY95IV Exhibits Enhanced Binding to the

Flagellar Switch and Phosphorylation-Dependent Constitutive Signaling. Molecular Microbiology. **27**: 1065 - 1075.

176. Shaw, C. H. 1990. Swimming Against the Tide: Chemotaxis in *Agrobacterium*. Bio-essays. **13**: 25-29.

177. Shaw, C. H. 1996. The Molecular Basis of Rhizosphere Competence in *Agrobacterium tumefaciens*., pp. 242-252. *In* Pickup, Saunders and Codd (ed.), Molecular Approaches to Environmental Microbiology. Ellis Harwood,

178. Shaw, C. H., A. M. Ashby, A. P. Brown, C. Royal, G. J. Loake and C. H. Shaw. 1988. VirA and VirG are the Ti-plasmid Encoded Functions Required for Chemotaxis of *Agrobacterium tumefaciens* Towards Acetosyringone. Molecular Microbiology **2**: 413-417.

179. Shaw, C. H., A. M. Ashby, G. J. Loake and M. D. Watson. 1988. One Small Step: The Missing Link in Crown Gall. Oxford Surveys of Plant Molecular & Cell Biology. **5**: 177-183.

180. Shaw, C. H., G. H. Carter and M. D. Watson. 1984. A Functional Map of the Nopaline Synthase Promoter. Nucleic Acids Research. **12**: 7831-7846.

181. Shaw, C. H., G. J. Loake, A. P. Brown, C. S. Garrett, W. Deakin, G. Alton, M. Hall, S. A. Jones, M. O'Leary and L. Primavesi. 1991. Isolation and Characterization of Behavioural Mutants and Genes of *Agrobacterium tumefaciens*. J. Gen. Microbiol. **137**: 1939-1953.

182. Sheng, J. and V. Citovsky. 1996. Agrobacterium-Plant Cell DNA Transport: Have Virulence Proteins, Will Travel. The Plant Cell. **8**: 1699 - 1710.

183. Shimoda, N., A. Toyoda-Yamamoto, J. Nagamine, M. Katayami, Y. Sakagami and Y. Machida. 1990. Control of Expression of *Agrobacterium vir* Genes by Synergistic Actions of Phenolic Signal Molecules and Monosaccharides. Proc. Natl. Acad. Sci. USA. **87**: 6684-6688.

184. Shin, S. and C. Park. 1995. Modulation of Flagellar Expression in *Escherichia coli* by Acetyl Phosphate and the Osmoregulator OmpR. Journal of Bacteriology. **177**: 4696 - 4702.

185. Shine, J. and L. Dalgarno. 1974. The 3'-Terminal Sequence of *Escherichia coli* 16s Ribosomal RNA: Complementarity To Nonsense Triplets and Ribosome Binding sites. Proc. Natl. Acad. Sci. USA. **71**: 1342-1346.

186. Shurvinton, C. E., L. Hodges and W. Ream. 1992. A Nuclear Localization Signal and the C-Terminal Omega Sequence in the *Agrobacterium tumefaciens* VirD2 Endonuclease are Important for Tumor Formation. Proc. Natl. Acad. Sci. USA. **89**: 11837 - 11841.

187. Silversmith, R. E., J. L. Appleby and R. B. Bourret. 1997. Catalytic Mechanism of Phosphorylation and Dephosphorylation of CheY: Kinetic Characterization of Imidazole Phosphates as Phosphodonors and the Role of Acid Catalysis. Biochemistry. **36**: 14965 - 14974.

188. Skidmore, J., B. P. McNamara, D. D. Ellefson, A. J. Wolfe and J. Maddock. 1996. Is *cheA* Function Required for the Polar Localization of the Chemoreceptor Complex? Abstracts of the General Meeting of the American Society for Microbiology. **96**: 313.

189. Smith, G. P. 1985. Filamentous Fusion Phage: Novel Expression Vectors That Display Cloned Antigens on the Virion Surface. Science. **228**: 1315-1317.

190. Smith, G. P. and V. A. Petrenko. 1997. Phage Display. Chem. Rev. **97**: 391-410.

191. Song, Y., M. Shibuya, Y. Ebizuka and U. Sankara. 1991. Synergistic Action of Phenolic Signal Compounds and Carbohydrates in the Induction of Virulence Gene Expression of *Agrobacterium tumefaciens*. Chem. Pharm. Bull. **39**: 2613-2616.

192. Song, Y., M. Shibuya, Y. Ebizuka and U. Sankawa. 1991. Identification of Plant Factors Inducing Virulence Gene Expression in *Agrobacterium tumefaciens*. Chem. Pharm. Bull. **39**: 2347-2350.

193. Sourjik, V. and R. Schmitt. 1996. Different Roles of CheY1 and CheY2 in the Chemotaxis of *Rhizobium meliloti*. Molecular Microbiology. **22**: 427-436.

194. Sourjik, V. and R. Schmitt. 1998. Phosphotransfer Between CheA, CheY1 and CheY2 in the Chemotaxis Signal Transduction Chain of *Rhizobium meliloti*. Biochemistry. **37**: 2327 - 2335.

195. Sourjik, V., W. Sterr, J. Platzer, I. Bos, M. Haslbeck and R. Schmitt. 1998. Mapping of 41 Chemotaxis, Flagellar and Motility Genes to a Single Region of the *Sinorhizobium meliloti* Chromosome. Gene. **223**: 283-290.

196. Spada, S., C. Krebber and A. Pluckthun. 1997. Selectively Infective Phages (SIP). Biological Chemistry. **378**:

197. Stachel, S. E., E. Messens, M. Van Montagu and P. Zambryski. 1985. Identification of The Signal Molecules Produced that Activate T-DNA Transfer in *Agrobacterium tumefaciens*. Nature. **318**: 624-629.

198. Stachel, S. E., E. W. Nester and P. C. Zambryski. 1986. A Plant Cell Factor Induces *Agrobacterium tumefaciens vir* Gene Expression. Proc. Natl. Acad. Sci. USA. **83**: 379-383.

199. Stachel, S. E. and P. C. Zambryski. 1986. *virA* and *G* Control the Plant Induced Activation of the T DNA Transfer Process of *Agrobacterium tumefaciens*. Cell. **46**: 325-333.

200. Steck, T. R. and C. I. Kado. 1990. Virulence Genes Promote Conjugative Transfer of the Ti Plasmid between *Agrobacterium* Strains. Journal of Bacteriology. **172**: 2191-2193.

201. Stock, A. M., E. Martinez-Hackert, B. F. Rasmussen, A. H. West, J. B. Stock, D. Ringe and G. A. Petsko. 1993. Structure of the Mg2+-Bound Form of CheY and Mechanism of Phosphoryl Transfer in Bacterial Chemotaxis. Biochemistry. **32**. 49: 13375-13380.

202. Stock, A. M. and S. L. Mowbray. 1995. Bacterial Chemotaxis - A Field in Motion. Current Opinion in Structural Biology. **5**: 744 - 751.

203. Stock, J. B., G. S. Lukat and A. M. Stock. 1991. Bacterial Chemotaxis and the Molecular Logic of Intracellular Signal Transduction Networks. Annu. Rev. Biophys. Biophys. Chem. **20**: 109-136.

204. Stock, J. B., A. M. Stock and J. M. Mottonen. 1990. Signal Transduction in Bacteria. Nature. **344**: 395-400.

205. Stock, J. B., M. G. Surette, W. R. McCleary and A. M. Stock. 1992. Signal Transduction in Bacterial Chemotaxis. Journal of Biological Chemistry. **267**: 19753-19756.

206. Surette, M. G., M. Levit, Y. Liu, G. Lukat, E. G. Ninfa, A. Ninfa and J. B. Stock. 1996. Dimerization is Required for the Activity of the Protein Histidine Kinase CheA that Mediates Signal Transduction in Bacterial Chemotaxis. Journal of Biological Chemistry. **271**: 939-945.

207. Swart, S., B. J. J. Lugtenberg, G. Smit and J. W. Wijne. 1994. Rhicadhesin-Mediated Attachment and Virulence of an *Agrobacterium tumefaciens chv*B Mutant can be Restored by Growth in a Highly Osmotic Medium. Journal of Bacteriology. **176**: 3816-3819.

208. Taylor, B. L., M. S. Johnson and J. M. Smith. 1988. Signalling Pathways in Bacterial Chemotaxis. B. Acta. **101**: 101-104.

209. Taylor, B. L. and J. W. Lengeler. 1990. Transductive Coupling by Methylated Transducing Proteins and Permeases of the Phosphotransferase System in Bacterial

Chemotaxis, pp. 69-90. *In* Aloia, Curtain and Gordon (ed.), Membrane Transport and Information Storage. Alan R. Liss Inc., New York.

210. Taylor, B. L. and I. B. Zhulin. 1998. In Search of Higher Energy: Metabolism-Dependent Behaviour in Bacteria. Molecular Microbiology. **28**: 683 - 690.

211. Tinland, B. 1996. The Integration of T-DNA into Plant Genomes. Trends in Plant Science. **1**: 178 - 184.

212. Tinland, B., B. Hohn and H. Puchta. 1994. *Agrobacterium tumefaciens* Transfers Single-Stranded Transferred DNA (T-DNA) into the Plant Cell Nucleus. Proc. Natl. Acad. Sci. USA. **91**: 8000-8004.

213. Tinland, B., Z. Koukolikova-Nicola, M. N. Hall and B. Hohn. 1992. The T-DNA-linked VirD2 Protein Contains Two Distinct Functional Nuclear Localization Signals. Proc. Natl. Acad. Sci. USA. **89**: 7442 - 7446.

214. Tisa, L. S. and J. Adler. 1992. Calcium Ions are Involved in *Escherichia coli* Chemotaxis. Proc. Natl. Acad. Sci. USA. **89**: 11804-11808.

215. Tisa, L. S., B. M. Olivera and J. Adler. 1993. Inhibition of *Escherichia coli* Chemotaxis by ω-Conotoxin, a Calcium Ion Channel Blocker. Journal of Bacteriology. **175**: 1235-1238.

216. Toker, A. S., M. Kihara and R. M. Macnab. 1996. Deletion Analysis of the FliM Flagellar Switch Protein of *Salmonella typhimurium*. Journal of Bacteriology. **178**: 7069-7079.

217. Toro, N., A. Datta, O. A. Carmi, C. Young, R. K. Prusti and E. W. Nester. 1989. The *Agrobacterium tumefaciens* VirC1 Gene Product Binds to Overdrive a T DNA Transfer Enhancer. Journal of Bacteriology. **171**: 6845-6849.

218. Turk, S. C. H. J., L. S. Melchers, H. den Dulk-Ras, A. J. G. Regensburg-Tuink and P. J. J. Hooykaas. 1991. Environmental Conditions Differentially Affect *vir* Gene Induction in Different *Agrobacterium* Strains. Role of the VirA Sensor Protein. Plant Molecular Biology **16**: 1051-1059.

219. Valdivia, R. H., L. Wang and S. C. Winans. 1991. Characterization of a Putative Periplasmic Transport System for Octopine Accumulation Encoded by *Agrobacterium tumefaciens* Ti Plasmid pTiA6. Journal of Bacteriology. **173**: 6398-6405.

220. Vaudequin-Dransart, V., A. Petit, C. Poncet, C. Ponsonnet, X. Nesme, J. B. Jones, H. Bouzar, W. S. Chilton and Y. Dessaux. 1995. Novel Ti Plasmids in *Agrobacterium* Strains Isolated from Fig Tree and Chrysanthemum Tumours and Their Opinelike Molecules. Molecular Plant-Microbe Interactions. **8**: 311-321.

221. Vogel, A. M. and A. Das. 1992. Mutational Analysis of *Agrobacterium tumefaciens virD2*: Tyrosine 29 is Essential for Endonuclease Activity. Journal of Bacteriology. **174**: 303-308.

222. VonLintig, J., D. Kreusch and J. Schroder. 1994. Opine-Regulated Promoters and LysR-Type regulators in the Nopaline (*noc*) and Octopine (*occ*) Catabolic Regions of Ti Plasmids of *Agrobacterium tumefaciens*. Journal of Bacteriology. **176**: 495-503.

223. Wang, H. and P. Matsumura. 1996. Characterisation of the CheA-S-CheZ Complex: A Specific Interaction Resulting in Enhanced Dephosphorylating Activity on CheY-Phosphate. Molecular Microbiology. **19**: 695 - 703.

224. Welch, M., N. Chinardet, L. Mourey, C. Birck and J. Samama. 1998. Structure of the CheY-Binding Domain of Histidine Kinase CheA in Complex with CheY. Nature Structural Biology. **5**: 25 - 29.

225. Wu, J., J. Li, G. Li, D. G. Long and R. M. Weis. 1996. The Chemotaxis Receptors from *Escherichia coli* Bind to the Methyltransferase (CheR) at a Site Distinct from the

Sites of Methylation. Abstracts of the General Meeting of the American Society for Microbiology. **96**: 313.

226. Wu, J. G., J. Y. Li, G. Y. Li, D. G. Long and R. M. Weis. 1996. The Receptor Binding Site for the Methyltransferase of Bacterial Chemotaxis is Distinct from the Sites of Methylation. Biochemistry. **35**: 4984-4993.

227. Yamamoto, K. and Y. Imae. 1993. Cloning and Characterization of the *Salmonella typhimurium*-Specific Chemoreceptor Tcp for Taxis to Citrate and From Phenol. Proc. Natl. Acad. Sci. USA. **90**: 217-221.

228. Yost, C. K., P. Rochepeau and M. F. Hynes. 1998. *Rhizobium leguminosarum* Contains a Group of Genes that Appear to Code for Methyl-Accepting Chemotaxis Proteins. Microbiology. **144**: 1945-1956.

229. Zanker, H., G. Lurz, U. Langridge, P. Langridge, D. Kreusch and J. Schroder. 1994. Octopine and Nopaline Oxidases from Ti Plasmids of *Agrobacterium tumefaciens*: Molecular Analysis, Relationship, and Functional Characterization. Journal of Bacteriology. **176**: 4511-4517.

230. Zanker, H., J. Von Lintig and J. Schroder. 1992. Opine Transport Genes in the Octopine (*occ*) and Nopaline (*noc*) Catabolic Regions in Ti Plasmids of *Agrobacterium tumefaciens*. Journal of Bacteriology. **174**: 841-849.

231. Zhang, L., P. J. Murphy, A. Kerr and M. E. Tate. 1993. *Agrobacterium* Conjugation and Gene Regulation by N-acyl-L-homoserine Lactones. Nature. **362**: 446-448.

232. Zhu, X., C. D. Amsler, K. Volz and P. Matsumura. 1996. Tyrosine 106 of CheY Plays an Important Role in Chemotaxis Signal Transduction in *Escherichia coli*. Journal of Bacteriology. **178**: 4208-4215.

233. Figurski, D. H. and D. R. Helinski. 1979. Replication of an Origin Containing Derivative of Plasmid RK2 Dependent on a Plasmid Function Provided in *trans*. Proc. Natl. Acad. Sci. USA. **76**: 1648-1652.

234. van Larebeke, N., G. Engler, M. Holsters, S. Van den Elsacker, I. Zaenen, R. A. Schilperoort and J. Schell. 1974. Large Plasmid in *Agrobacterium tumefaciens* Essential for Crown Gall Inducing Ability. Nature. **252**: 169-170.

235. Woodcock, D. M., P. J. Crowther, J. Doherty, S. Jefferson, E. DeCruz, M. Noyer-Weidner, S. S. Smith, M. Z. Michael and M. W. Graham. 1989. Quantitative Evaluation of *Escherichia coli* Host Strains for Tolerance to Cytosine Methylation in Plasmid and Phage Recombinants. Nucleic Acids Research. **17**: 3469-3478.